

**Development of Wildland Firefighters' Protective Clothing with Improved
Thermal Protection**

by

Elena Kosareva

A thesis submitted in partial fulfillment of the requirements for the degree of

Doctor of Philosophy

Department of Human Ecology
University of Alberta

© Elena Kosareva, 2024

ABSTRACT

This research was focused on the development of wildland firefighters' protective clothing with improved thermal protection properties. Specifically, a new shirt design was developed, and garments were constructed which incorporated a three-dimensional warp-knitted fabric in specific areas. These areas were the shoulders, upper front and upper back torso, neck, and wrists of the shirt where no air gap occurs between the clothing and the body of the wearer. Previous researchers had found that these areas are prone to second-degree burn injury when wildland firefighters' protective clothing was evaluated on an instrumented manikin in a simulated flash-fire test scenario. To determine whether the three-dimensional warp-knitted fabric in the newly designed shirt improved the thermal protection provided by the shirt, the following four interrelated studies were conducted.

In the *first study*, the heat and flame thermal performance of selected fabric systems representing the shirt that is currently worn by wildland firefighters in Alberta (control shirt) and the newly developed shirt prototype were assessed at the bench-scale level. Thermal performance was predicted by the values of thermal protective performance (TPP), radiant heat resistance (RHR), and cylinder heat transfer performance (CHTP). The *second study* was focused on the evaluation of the thermal comfort of selected fabric systems, also at the bench-scale level. Comfort properties were predicted using thermal resistance and evaporative resistance in a total heat loss (THL) calculation, together with air permeability. *Study three* was focused on the development of the design of the shirt prototype and its construction. The development of the new shirt design included reproduction of the control

garment, pattern editing for the development of the new shirt design, and three-dimensional simulation of both the control shirt and the new shirt prototype using CLO 3D software. The software allowed for visual simulation of the control shirt and prototype shirt on an avatar with the same dimensions as the instrumented manikin used for full-scale flash fire testing at the University of Alberta's Protective Clothing and Equipment Research Facility (PCERF). Three prototype shirts along with three control shirts were constructed to conduct study four. *Study four* was focused on the full-scale flash fire manikin testing of the shirts from study three worn as part of a wildland firefighters' protective clothing ensemble. Three control shirts and three prototype shirts were tested for 4 seconds of flame exposure. Percentage of the manikin surface reaching a predicted second- or third-degree skin burn injury was recorded for the control and prototype shirts.

Overall, the bench-scale test results showed that the incorporation of a three-dimensional warp-knitted fabric between the outer and base layers of a garment system substantially improved thermal protection over systems that included the outer and base layers alone. Test results showed: 1) an increase of TPP, RHR, and CHTP values with ~200% improvement in thermal protection; 2) a decrease of THL values by 41% to 56%; and 3) an increase in air permeability by 30% to 43%. A novel design for the shirt worn by wildland firefighters was successfully produced using CLO software and innovative construction techniques were implemented which allowed the inclusion of the inflexible three-dimensional warp-knit fabric into the garment. Control and prototype shirts were constructed for full-scale thermal protective performance assessment by the flash fire instrumented manikin test. The

prototype shirt design decreased the total burn area of the manikin surface by approximately 6% compared to the control shirt. The three-dimensional warp-knitted fabric specifically impeded thermal energy transfer in the areas of the upper front and back torso, upper arms, and neck during the full-scale flame engulfment test.

PREFACE

This thesis is an original work by Elena Kosareva. No part of this thesis has been previously published.

DEDICATION

This thesis is dedicated to my loving grandmother Nina Kosareva, and grandfather-in-law Guang Ren Lyu.

ACKNOWLEDGEMENTS

First and foremost, I would like to thank and gratefully acknowledge my supervisor Dr. Jane Batcheller for her great mentorship, support, and encouragement throughout my PhD program. I would also like to thank Vlada Blinova, Dr. Rachel McQueen, and Dr. David Torvi as the members of my supervisory committee for their help, insights, and guidance.

I wish to extend my gratitude to other people:

- Stephen Paskaluk who dedicated a lot of his time to setting testing equipment and shared his expertise in obtaining data in almost all testing procedures that have been used (particularly in Chapters 4, 5 and 7).
- Dr. Jane Batcheller, and Vlada Blinova for providing a teaching assistantship appointment for courses HECOL 270, HECOL 370, and HECOL 254 that contributed to my financial state and supported my graduate education and experience.
- Dr. Patricia Dolez, Dr. Rachel McQueen, and Dr. Jane Batcheller for providing a research assistantship appointment that also contributed to my financial state and supported my graduate education and experience.
- The Government of Alberta, the Department of Human Ecology, the Faculty of Graduate Studies and Research, the Graduate Students Association, and the Canadian Home Economics Foundation for selecting me to receive several scholarships and awards, such as the Alberta Graduate Excellence Scholarship, Betty Crown Scholarship in Textile and Apparel Science, Graduate Student Teaching Assistant Award, Graduate Student Research Assistant Award, two Graduate Student Teaching Awards, Verna M. Lefebvre Graduate Student Award, and Marilyn McNeil-Morin Graduate Research Scholarship in Textile Sciences. These awards supported my graduate education and experience as well.

- Companies and their representatives, such as Winner Garment Industries Ltd. (Tony Wong & Fanny Liao), Milliken & Company (James Cliver), Davey Textile Solutions (Dan King), Lincoln Fabrics (Gord McPhee), Heathcoat Fabrics Limited (Gemma Groves & Dawn Watts) who generously provided materials and other assistance for this research.
- My beloved husband Ziyi Lyu, and all my family for their unlimited support and encouragement, which helped me to finish my degree.
- My dear friends David Cooper, Lauren Degenstein, Jackie Fisher, Coleen Falk, Alfred Falk, Lucienne Gamache, Heather Waldie, Tammy Irwin and many other people who showed incredible hospitality, and support, and helped with lots of aspects of adapting to life in Canada.

TABLE OF CONTENTS

CHAPTER 1 GENERAL INTRODUCTION	1
1.1 Statement of problem.....	1
1.2 Definitions	3
1.3 Research question and purpose.....	5
1.4 Objectives	6
1.5 Null hypotheses	7
1.6 Dissertation Overview	8
1.7 Limitations and Delimitations	9
CHAPTER 2 REVIEW OF LITERATURE.....	10
2.1 Introduction.....	10
2.2 Protective clothing for wildland firefighters.....	11
2.2.1 Previous research	11
2.2.2 Standard requirements	14
2.2.3 Protective fabrics	30
2.2.4 Air gap role in thermal insulation properties of clothing system	31
2.2.5 Three-dimensional knitted fabrics	33
2.3 Thermal protection and skin burn predictions	35
2.3.1 Thermal protection assessment.....	35
2.3.2 Skin burns	36
2.3.4 Stoll criteria and bench-scale heat transfer testing	38
2.3.5 Henriques burn integral model and full-scale manikin testing.....	40
2.4 Comfort.....	41
2.4.1 Comfort in clothing systems	41
2.4.2 Thermal comfort	43
2.4.3 Tradeoffs between comfort and protection	45
2.5 Summary	46

CHAPTER 3 MATERIALS AND METHODS	47
3.1 Introduction.....	47
3.2 Materials	47
3.3 Fabric systems	50
3.4 Bench-scale tests for thermal protection assessment.....	52
3.4.1 Experimental design	52
3.4.2 Test methods and equipment	53
3.4.2.1 Exposure to a flame heat source	53
3.4.2.2 Exposure to a radiant heat source	56
3.4.2.3 Exposure to a combined radiant and flame heat source.....	58
3.5 Bench-scale tests for comfort assessment.....	62
3.5.1 Experimental design	62
3.5.2 Test methods and equipment	63
3.5.2.1 Total heat loss	63
3.5.2.2 Air permeability.....	67
3.6 Full-scale test for thermal protection assessment	69
3.6.1 Experimental design	69
3.6.2 Test method and equipment.....	71
CHAPTER 4 THERMAL PROTECTION PERFORMANCE OF FABRIC SYSTEMS AT BENCH-SCALE LEVEL.....	73
4.1 Introduction.....	73
4.2 Results and discussion	74
4.2.1 Effect of exposure to a flame heat source on fabric system performance	74
4.2.1.1 Summary of flame heat source exposure results	74
4.2.1.2 Analysis of planned pairwise comparison of two-way ANOVA of flame heat source exposure results.....	77
4.2.1.3 Analysis of thermocouple response during the flame heat source exposure.....	81

4.2.2	Effect of exposure to radiant heat source on fabric system performance	88
4.2.2.1	Summary of radiant heat source exposure results	88
4.2.2.2	Analysis of planned pairwise comparison of two-way ANOVA of radiant heat source exposure results	91
4.2.2.3	Analysis of thermocouple response during the radiant heat source exposure	95
4.2.3	Effect of exposure to a combined flame and radiant heat source on fabric system performance	102
4.2.3.1	Summary of combined flame and radiant heat source exposure results	102
4.2.3.2	Analysis of planned pairwise comparison of two-way ANOVA of combined flame and radiant heat source exposure results	105
4.2.4	Effect of moisture in a base layer on the thermal protection performance of fabric systems	111
4.3	Summary	111
CHAPTER 5 COMFORT EVALUATION OF FABRIC SYSTEMS AT BENCH-SCALE LEVEL		113
5.1	Introduction	113
5.2	Results and discussion	114
5.2.1	Total heat loss	114
5.2.1.1	Summary of total heat loss results	114
5.2.1.2	Analysis of planned pairwise comparison of one-way ANOVA	115
5.2.2	Air permeability	120
5.2.2.1	Summary of air permeability results	120
5.2.2.2	Analysis of planned pairwise comparison of one-way ANOVA	121
5.3	Summary	126

CHAPTER 6 DESIGN DEVELOPMENT AND CONSTRUCTION OF SHIRT PROTOTYPE	127
6.1 Introduction.....	127
6.2 Background.....	128
6.2.1 Standard requirements for design	128
6.2.2 Previous inventions.....	129
6.2.3 Control shirt design.....	133
6.3 Prototype shirt design development.....	135
6.3.1 Development of prototype shirt patterns in CLO	138
6.3.2 Construction of prototype shirt.....	141
6.4 Summary	146
CHAPTER 7 THERMAL PROTECTION PERFORMANCE OF SHIRT PROTOTYPE AT FULL-SCALE LEVEL	147
7.1 Introduction.....	147
7.2 Results and discussion	148
7.2.1 Performance of garment ensemble with control shirt.....	148
7.2.2 Performance of garment ensemble with prototype shirt.....	153
7.2.3 Comparison of thermal protection performance of garment ensembles with control and prototype shirts.....	158
7.2.3.1 Summary of instrumented manikin test results.....	159
7.2.3.2 Analysis of independent sample t-test	160
7.2.4 Analysis of individual sensor response.....	161
7.3 Summary.....	173
CHAPTER 8 SUMMARY, CONCLUSIONS, AND FUTURE WORK	174
8.1 Summary of research	174
8.2 Conclusions.....	175
8.3 Contributions and recommendations for future research.....	178
REFERENCES	181

APPENDICES	195
APPENDIX A: MATERIALS AND METHODS.....	196
Evaluation of fabric physical properties	196
Photomicrographs of fibres.....	197
Images of fabric surfaces	198
Instrumented manikin test settings	200
APPENDIX B: THERMAL PROTECTION TEST RESULTS.....	203
Raw data of thermal protection test results.....	203
Overall two-way ANOVA for thermal protection test results.....	206
Percentage of thermal protection increase	207
Pairwise comparisons of dry and wet thermal protection results	209
Complementary graphs with the thermocouple response	212
APPENDIX C: COMFORT TEST RESULTS.....	217
Raw data of comfort test results	217
Overall two-way ANOVA for comfort test results.....	219
APPENDIX D: DESIGN AND CONSTRUCTION OF SHIRTS	220
Pattern pieces of shirts	220
Construction of shirts.....	222
APPENDIX E: INSTRUMENTED MANIKIN TEST RESULTS	230
Shirt appearance before and after full-scale flame engulfment	230
Burn injury pattern.....	235
Individual sensor response.....	237

LIST OF TABLES

Table 2.1 Wildland firefighter's protective clothing textile performance requirements.	15
Table 2.2 Wildland firefighter's protective clothing design requirements.....	24
Table 3.1 Physical properties of fabrics.....	48
Table 3.2 Composition of the fabric systems.	50
Table 3.3 Factorial experimental design for assessment of differences in thermal protection properties of different fabric systems and base layer conditions.	52
Table 4.1 Summary table of mean values and standard deviation of TPP results for different fabric systems under dry and wet base layer conditions when exposed to a flame heat source.....	75
Table 4.2 Pairwise comparison of mean TPP ratings for different fabric systems under the dry and wet base layer conditions when exposed to a flame heat source.....	78
Table 4.3 Summary table of mean values and standard deviation of temperature of the copper calorimeter and thermocouples for different fabric systems under dry and wet base layer conditions when the Stoll criteria was reached under a flame heat source exposure.....	81
Table 4.4 Summary table of mean values and standard deviation of RHR results for different fabric systems under the dry and wet base layer conditions when exposed to a radiant heat source.....	88
Table 4.5 Pairwise comparison of mean RHR rating for different fabric systems under the dry and wet base layer conditions when exposed to a radiant heat source.....	92
Table 4.6 Summary table of mean values and standard deviation of temperature of the copper calorimeter and thermocouples for different fabric systems under dry and wet base layer conditions when the Stoll criteria was reached under a radiant heat source exposure.....	95

Table 4.7 Summary table of mean values and standard deviation of CHTP results for different fabric systems under the dry and wet base layer conditions when exposed to a combined flame and radiant heat source.	102
Table 4.8 Pairwise comparison of mean CHTP ratings for different fabric systems under the dry and wet base layer conditions when exposed to a combined flame and radiant heat source.	106
Table 5.1 Summary table of THL mean values of different fabric systems.	114
Table 5.2 Pairwise comparison of THL mean values among different fabric systems.	116
Table 5.3 Summary table of air permeability mean values of different fabric systems.	120
Table 5.4 Pairwise comparison of air permeability mean values among different fabric systems.	122
Table 7.1 Instrumented manikin test results of garment ensemble with control shirt after the full-scale flame engulfment for 4 seconds.	151
Table 7. 2. Instrumented manikin test results of garment ensemble with prototype shirt after the full-scale flame engulfment for 4 seconds.	157
Table 7.3 Summary table of the mean values of percentage of the manikin surface reaching the criteria for second or third degree burn when the garment ensembles were exposed to 4-seconds of flame engulfment.	159
Table 7.4 Comparison of mean values in percentage of burn area between garment ensembles with control and prototype shirts tested with instrumented manikin.	160
Table A.1 Body measurements of instrumented manikin (University of Alberta)...	200
Table B.1 Raw data of thermal energy and time to predicted second-degree burn for different fabric systems under dry and wet base layer conditions when exposed to a flame heat source.	203
Table B.2 Raw data of thermal energy and time to predicted second-degree burn for different fabric systems under dry and wet base layer conditions when exposed to a radiant heat source.	204

Table B.3 Raw data of thermal energy and time to predicted second-degree burn for different fabric systems under dry and wet base layer conditions when exposed to a combined flame and radiant heat source.	205
Table B.4 Overall two-way ANOVA test for TPP rating results.	206
Table B.5 Overall two-way ANOVA test for RHR rating results.	206
Table B.6 Table Summary table for overall two-way ANOVA test for CHTP rating results.	207
Table B.7 Summary of differences in TPP rating values in percentage among three-layer and two-layer fabric systems.	207
Table B.8 Summary of differences in RHR rating values in percentage among three-layer and two-layer fabric systems.	208
Table B.9 Summary of differences in CHTP rating values in percentage among three-layer and two-layer fabric systems.	208
Table B.10 Pairwise comparison of mean values of TPP rating for different fabric systems between dry and wet base layer conditions when exposed to a flame heat source.	209
Table B.11 Pairwise comparison of mean values of RHR rating for different fabric systems between dry and wet base layer conditions when exposed to a radiant heat source.	210
Table B.12 Pairwise comparison of mean values of CHTP rating for different fabric systems between dry and wet base layer conditions when exposed to a combined flame and radiant heat source.	211
Table C.1 Raw data of intrinsic thermal and evaporative resistance values of bare plate, and different fabric systems.	217
Table C.2 Raw data of air permeability values of different fabric systems.	218
Table C.3 Overall one-way ANOVA test for THL results.	219
Table C.4 Overall one-way ANOVA test for air permeability results.	219
Table D.1 Material consumption.	224
Table D.2 Prototype shirt construction sequence.	225

LIST OF FIGURES

Figure 2.1 Burn injury pattern generated by the instrumented manikin system when the wildland firefighter's garment ensemble was engulfed in flames for 4 seconds: (a) two-layer fabric system, (b) one-layer fabric system..	13
Figure 2. 2 Stoll curve: (a) temperature vs time, (b) thermal energy vs time.....	39
Figure 2.3 Comfort factors interaction schema.	42
Figure 3.1 Test apparatus for evaluation of the thermal protective performance of clothing systems.	54
Figure 3.2 Flat configuration non-conductive block with sensor (copper calorimeter): (a) top view, (b) bottom view.....	55
Figure 3.3 Fabric systems OL-BL and OL-BL-S mounted in the TPP specimen holder when tested (a) in contact with sensor, (b) with spacer between fabric system and sensor.....	55
Figure 3.4 Test apparatus for evaluation of the radiant heat resistance of clothing systems: (a) front view, (b) top view.....	56
Figure 3.5 Fabric systems OL-BL and OL-BL-S mounted in the RHR specimen holder when tested (a) in contact with sensor, (b) with spacer between fabric system and sensor.	58
Figure 3.6 Test apparatus for evaluation of the cylinder heat transfer performance of clothing systems.	59
Figure 3.7 Cylindrical configuration non-conductive block with sensor (copper calorimeter): (a) front view, (b) back view.	60
Figure 3.8 Additional thermocouple attached to (a) outer layer, (b) base layer.....	61
Figure 3.9 Sweating guarded hot plate.	63
Figure 3.10 Hot plate: (a) bare plate, (b) bare plate covered with ePTFE film.	66
Figure 3.11 High pressure differential air permeability testing apparatus.	68
Figure 3.12 Fabric system OL-3D1-BL mounted in clamps of air permeability testing apparatus.....	68
Figure 3.13 Instrumented manikin.....	72

Figure 4.1 Bar chart shows average thermal energy values supplied to different fabric systems under dry and wet base layer conditions over time of flame heat source exposure until reaching a second-degree burn as predicted by the Stoll criteria.	75
Figure 4.2 Average temperature of the copper calorimeter, and thermocouples positioned at the outer layer, and base layer of fabric system OL-BL during the flame exposure test under base layer conditions: (a) dry, and (b) wet.	82
Figure 4.3 Average temperature of the copper calorimeter, and thermal couples positioned at the outer layer, and base layer of fabric system OL-BL-S during the flame exposure test under base layer conditions: (a) dry, and (b) wet.	83
Figure 4.4 Average temperature of the copper calorimeter, and thermal couples positioned at the outer layer, and base layer of fabric system OL-S-BL during the flame exposure test under base layer conditions: (a) dry, and (b) wet.	84
Figure 4.5 Average temperature of the copper calorimeter, and thermal couples positioned at the outer layer, and base layer of fabric system OL-3D1-BL during the flame exposure test under base layer conditions: (a) dry, and (b) wet.	85
Figure 4.6 Average temperature of the copper calorimeter, and thermal couples positioned at the outer layer, and base layer of fabric system OL-3D2-BL during the flame exposure test under base layer conditions: (a) dry, and (b) wet.	86
Figure 4.7 Bar chart shows average thermal energy values supplied to different fabric systems under dry and wet base layer conditions over time of radiant heat source exposure until reaching a second-degree burn as predicted by the Stoll criteria.	89

Figure 4.8 Average temperature of the copper calorimeter, and thermocouples positioned at the outer layer, and base layer of fabric system OL-BL during the radiant exposure test under base layer conditions: (a) dry, and (b) wet.	96
Figure 4.9 Average temperature of the copper calorimeter, and thermal couples positioned at the outer layer, and base layer of fabric system OL-BL-S during the radiant exposure test under base layer conditions: (a) dry, and (b) wet.	97
Figure 4.10 Average temperature of the copper calorimeter, and thermal couples positioned at the outer layer, and base layer of fabric system OL-S-BL during the radiant exposure test under base layer conditions: (a) dry, and (b) wet.	98
Figure 4.11 Average temperature of the copper calorimeter, and thermal couples positioned at the outer layer, and base layer of fabric system OL-3D1-BL during the radiant exposure test under base layer conditions: (a) dry, and (b) wet.	99
Figure 4.12 Average temperature of the copper calorimeter, and thermal couples positioned at the outer layer, and base layer of fabric system OL-3D2-BL during the radiant exposure test under base layer conditions: (a) dry, and (b) wet.	100
Figure 4.13 Bar chart shows average thermal energy values supplied to different fabric systems under dry and wet base layer conditions over time of combined flame and radiant heat source exposure until reaching a second-degree burn as predicted by the Stoll criteria.	103
Figure 4.14 Fabric systems mounted in the CHTP specimen holder when tested (a) OL-BL-S, and (b) OL-S-BL.	110
Figure 5.1 Bar chart shows THL mean values for different fabric systems.	115
Figure 5.2 Bar chart shows air permeability mean values for different fabric systems.	121
Figure 5.3 Schematic drawing of airflow passing through the fabric system: (a) OL - BL, (b) OL-3D2-BL.	124

Figure 6.1 Wildland firefighter's shirt manufactured by Winner Garment Industries Ltd. (control shirt): (a) front view, (b) back view.	134
Figure 6.2 Technical drawing of control shirt design: (a) front view, (b) back view.	135
Figure 6.3 Technical drawing of prototype shirt design: (a) front view, (b) back view.	137
Figure 6.4 Simulation of control shirt fit in CLO: (a) front view, (b) back view.	139
Figure 6.5 Yoke joining the front and back yokes with a portion of the sleeve cap.	140
Figure 6.6 Top view of modified yoke in simulated prototype shirt.	140
Figure 6.7 Simulation of prototype shirt fit in CLO: (a) front view, (b) back view. .	141
Figure 6.8 Constructed wildland firefighter's prototype shirt: (a) front view, (b) back view.	142
Figure 6.9 Top view of modified yoke in constructed prototype shirt.	143
Figure 6.10 Schematic drawing of stand collar and yoke construction with incorporated layer of three-dimensional warp-knitted fabric.	144
Figure 6.11 Schematical drawing of cuff construction with incorporated layer of three-dimensional warp-knitted fabric.	145
Figure 7.1 Control shirt number 2 before the full-scale flame engulfment for 4 seconds: (a) front view, and (b) back view.	149
Figure 7.2 Control shirt number 2 after the full-scale flame engulfment for 4 seconds: (a) front view, and (b) back view.	149
Figure 7.3 Burn injury pattern generated by the instrumented manikin system when the garment ensemble with control shirt number 2 was engulfed in flames for 4 seconds.	150
Figure 7.4 Prototype shirt number 2 before the full-scale flame engulfment for 4 seconds: (a) front view, and (b) back view.	154
Figure 7.5 Prototype shirt number 2 after the full-scale flame engulfment for 4 seconds: (a) front view, and (b) back view.	154
Figure 7.6 Three-dimensional warp-knitted fabric in the yoke area: (a) before, (b) after the full-scale flame engulfment for 4 seconds (black areas are soot from the manikin surface).	155

Figure 7.7 Burn injury pattern generated by the instrumented manikin system when the garment ensemble with prototype shirt number 2 was engulfed in flames for 4 seconds.	156
Figure 7.8 Bar chart shows mean percentage of manikin surface reaching second and third-degree burn when garment ensembles with control and prototype shirts were exposed to 4-seconds of flame engulfment.	159
Figure 7.9 Location of sensors covered by the shirt and the areas prone to burn injury (shaded red) on the instrumented manikin: (a) front view, and (b) back view.	162
Figure 7.10 Average heat flux recorded by the skin simulant sensors caused by thermal energy passing through the garment ensemble with control and prototype shirts in different locations on the upper front torso area of the manikin: (a) left front, and (b) right front.	164
Figure 7.11 Average heat flux recorded by the skin simulant sensors caused by thermal energy passing through the garment ensemble with control and prototype shirts in different locations on the upper back torso area of the manikin: (a) left back, (b) centre back, and (c) right back.	165
Figure 7.12 Average heat flux recorded by the skin simulant sensors caused by thermal energy passing through the garment ensemble with the control and prototype shirts in different locations on the shoulder area of the manikin: (a) left shoulder, and (b) right shoulder.	167
Figure 7.13 Average heat flux recorded by the skin simulant sensors caused by thermal energy passing through the garment ensemble with the control and prototype shirts in different locations on the upper arm area of the manikin: (a) left side, and (b) right side.	169
Figure 7.14 Average heat flux recorded by the skin simulant sensors caused by thermal energy passing through the garment ensemble with the control and prototype shirts in different locations on the neck area of the manikin: (a) left, (b) centre, and (c) right.	170
Figure A.1 Photomicrographs of fibres: (a) meta-aramid fibre, (b) para-aramid fibre, (c) anti-static fibre. (scale bar 20 μm)	197

Figure A.2 Photomicrograph of cotton fibre. (scale bar 20 μm)	197
Figure A.3 Photomicrographs of fibres: (a) meta-aramid fibre, (b) monofilament PEEK fibre. (scale bar 20 μm)	198
Figure A.4 Surface light stereomicroscope images of the outer layer fabric: (a) front, (b) back. (scale bar 0.5 mm).....	198
Figure A.5 Surface light stereomicroscope images of the base layer fabric: (a) front, (b) back. (scale bar 0.5 mm).....	199
Figure A.6 Surface light stereomicroscope images of the three-dimensional warp- knitted fabric (type 1): (a) front, (b) back. (scale bar 1 mm)	199
Figure A.7 Surface light stereomicroscope images of the three-dimensional warp knitted fabric (type 2): (a) front, (b) back. (scale bar 1 mm)	199
Figure A.8 Simulated instrumented manikin in CLO software and sensor location in the area covered by shirts: (a) front view, (b) back view.	201
Figure A.9 Garment ensemble with the control shirt number 2: (a) front view, (b) back view.	201
Figure A.10 Garment ensemble with the prototype shirt number 2: (a) front view, (b) back view.	202
Figure A.11 Base layer comprised cotton t-shirt and briefs: (a) front view, (b) back view.	202
Figure B.1 Average temperature of the copper calorimeter, and thermocouples positioned at the base layer of fabric system OL-BL during the flame exposure test under dry and wet base layer condition: (a) copper calorimeter, and (b) thermocouple response.	212
Figure B.2 Average temperature of the copper calorimeter, and thermocouples positioned at the base layer of fabric system OL-BL-S during the flame exposure test under dry and wet base layer condition: (a) copper calorimeter, and (b) thermocouple response.	213
Figure B.3 Average temperature of the copper calorimeter, and thermocouples positioned at the base layer of fabric system OL-BL-S during the flame exposure test under dry and wet base layer condition: (a) copper calorimeter, and (b) thermocouple response.	214

Figure B.4 Average temperature of the copper calorimeter, and thermocouples positioned at the base layer of fabric system OL-3D1-BL during the flame exposure test under dry and wet base layer condition: (a) copper calorimeter, and (b) thermocouple response.	215
Figure B.5 Average temperature of the copper calorimeter, and thermocouples positioned at the base layer of fabric system OL-3D1-BL during the flame exposure test under dry and wet base layer condition: (a) copper calorimeter, and (b) thermocouple response.	216
Figure D.1 Pattern pieces of control shirt.	220
Figure D.2 Pattern pieces of prototype shirt.	221
Figure D.3 Garment mock-up of control shirt: (a) front view, (b) back view.	222
Figure D.4 Garment mock-up of prototype shirt: (a) front view, (b) back view.	222
Figure D.5 Detailed view of prototype shirt: (a) yoke back, (b) yoke inner side, (c) collar with front closure, (d) patch pocket with flap, and sleeve cuff (e) closed (f) open.	223
Figure E.1 Control shirt number 1 before the full-scale flame engulfment for 4 seconds: (a) front, and (b) back.	230
Figure E.2 Control shirt number 1 after the full-scale flame engulfment for 4 seconds: (a) front, and (b) back.	230
Figure E.3 Control shirt number 3 before the full-scale flame engulfment for 4 seconds: (a) front, and (b) back.	231
Figure E.4 Control shirt number 3 after the full-scale flame engulfment for 4 seconds: (a) front, and (b) back.	231
Figure E.5 Prototype shirt number 1 before the full-scale flame engulfment for 4 seconds: (a) front, and (b) back.	232
Figure E.6 Prototype shirt number 1 after the full-scale flame engulfment for 4 seconds: (a) front, and (b) back.	232
Figure E.7 Prototype shirt number 3 before the full-scale flame engulfment for 4 seconds: (a) front, and (b) back.	233
Figure E.8 Prototype shirt number 3 after the full-scale flame engulfment for 4 seconds: (a) front, and (b) back.	233

Figure E.9 Damage of the outer layer fabric of shirt after the full-scale flame engulfment for 4 seconds: (a) thermal shrinkage in the waist area, and (b) charring with broke open fabric on sleeve.	234
Figure E.10 Cuff hook and loop closure after the full-scale flame engulfment for 4 seconds: (a) control shirt, and (b) prototype shirt.....	234
Figure E.11 Three-dimensional knitted fabric appearance after the full-scale flame engulfment for 4 seconds under the outer layer fabric of shirt prototype: (a) cuff, and (b) front yoke.	234
Figure E.12 Burn injury pattern generated by the instrumented manikin system when the garment ensemble with control shirt number 1 was engulfed in flames for 4 seconds.....	235
Figure E.13 Burn injury pattern generated by the instrumented manikin system when the garment ensemble with control shirt number 3 was engulfed in flames for 4 seconds.....	235
Figure E.14 Burn injury pattern generated by the instrumented manikin system when the garment ensemble with prototype shirt number 1 was engulfed in flames for 4 seconds.....	236
Figure E.15 Burn injury pattern generated by the instrumented manikin system when the garment ensemble with prototype shirt number 3 was engulfed in flames for 4 seconds.....	236
Figure E.16 Heat flux recorded by the skin simulant sensors caused by thermal energy passing through each garment ensemble with the control and prototype shirts in different locations on the upper front torso area of the manikin: (a) left front, and (b) right front.	237
Figure E.17 Heat flux recorded by the skin simulant sensors caused by thermal energy passing through each garment ensemble with the control and prototype shirts in different locations on the upper back torso area of the manikin: (a) left side, (b) back centre, and (c) right side.	238

Figure E.18 Heat flux recorded by the skin simulant sensors caused by thermal energy passing through each garment ensemble with the control and prototype shirts in different locations on the shoulder area of the manikin: (a) left side, and (b) right side.	239
Figure E.19 Heat flux recorded by the skin simulant sensors caused by thermal energy passing through each garment ensemble with the control and prototype shirts in different locations on the upper arm areas of the manikin: (a) left side, and (b) right side.	240
Figure E.20 Heat flux recorded by the skin simulant sensors caused by thermal energy passing through each garment ensemble with the control and prototype shirts in different locations on the neck area of the manikin: (a) left side, (b) back centre, and (c) right side.	241
Figure E.21 Heat flux recorded by the skin simulant sensors caused by thermal energy passing through each garment ensemble with the control and prototype shirts in different locations on the right wrist area of the manikin: (a) front, (b) back, and (c) closure.	242
Figure E.22 Heat flux recorded by the skin simulant sensors caused by thermal energy passing through each garment ensemble with the control and prototype shirts in different locations on the left wrist area of the manikin: (a) front, (b) back, and (c) closure.	243
Figure E.23 Heat flux recorded by the skin simulant sensors caused by thermal energy passing through each garment ensemble with the control and prototype shirts in the location on the right chest area of the manikin. .	244
Figure E.24 Heat flux recorded by the skin simulant sensors caused by thermal energy passing through each garment ensemble with the control and prototype shirts in the location on the back neck-head centre area of the manikin.	244

LIST OF ABBREVIATIONS

ASTM:	American Society for Testing and Materials
CHTP:	Cylinder heat transfer performance
FR:	Flame resistant
NFPA	National Fire Protective Association
R_{ct} :	Fabric thermal insulation
R_{et} :	Fabric evaporative resistance
RH:	Relative humidity
RHR:	Radiant heat resistance
THL:	Total heat loss
TPP:	Thermal protective performance

CHAPTER 1 GENERAL INTRODUCTION

1.1 Statement of problem

Wildfires cause severe damage to natural resources, ecosystems, and communities around the world every year. The number of wildland fires has substantially increased during the last several decades (Tyukavina et al., 2022). There was a record-breaking wildfire season with approximately 15 million hectares burned across Canada in 2023 (Erni et al., 2024; Jain et al., 2024). There is a need for thousands of wildland firefighters to control these threats. Wildland firefighters risk their health to prevent such fires from spreading by performing fatiguing activities that lead to thermal strain (e.g., felling trees, removing brush, and digging barrier trenches) while facing hot weather, smoke, and open flame (Budd et al., 1997; Carballo-Leyenda et al., 2019; Reinhardt & Ottmar, 2004; Smith et al., 2013; Withen, 2015). The potential occupational hazards include exposure to high radiant heat, ultraviolet radiation, and contact with sharp objects (chainsaws and other tools). Work shifts can last up to 24 hours (Alberta ALIS, 2021). Although wildland firefighters are mostly exposed to radiant heat from the fire, they also can be engulfed in flames due to rapidly spreading fires and shifting wind directions (Butler, 2014; Dale et al., 2000). Additionally, wildland firefighters experience very high rates of metabolic heat production and may perspire heavily because of the natural cooling mechanisms of the human body (Das & Alagirusamy, 2010a). The thermal stress from the environmental conditions, and work activities can lead to physiological strain. There is also a risk of developing cardiovascular disease or lung cancer in the long run (Navarro et al., 2019).

Wildland firefighters' protective clothing is significantly different from the bulky protective gear of structural firefighters, that consists of multilayer jacket and pants (NFPA, 2018). According to 1) Canadian standard, CAN/CGSB-155.22 Fireline Workwear for Wildland Firefighters, and 2) US standard, NFPA 1977 Standard on Protective Clothing and Equipment for Wildland Firefighting, there are two options for wildland firefighters' protective clothing: a one-piece garment (coverall) or a two-piece garment (jacket/shirt and pants). The protective garment is

intended to provide protection against high thermal exposure as well as short-term engulfment by flames, while still allowing for ventilation and evaporation of perspiration to minimize physiological strain (Crown et al., 2002; Lawson et al., 2004). Essential requirements for the materials used in the protective garments such as flame- and heat-resistance, durability, including tearing and tensile strength of textile material and seams, and abrasion resistance are specified in regulatory standards in North America. Wildland firefighters' protective clothing is generally worn on top of undergarments and for this thesis, it is referred to as a two-layer fabric system since there are two layers of fabric between the skin and the hazardous environment. The outer garment which is a flame resistant material and undergarments (t-shirt and briefs) which are made of natural fibres or fibres with melt-resistant properties (Canadian General Standards Board [CGSB], 2014; Petrilli & Ackerman, 2008).

Air gaps play an essential role in all types of thermal protective clothing as the layer of air provides thermal insulation and helps prevent skin burn injury. According to previous work, it has been shown that the best performance of thermal insulation occurs when the air gap is approximately 7 mm thick (Song, 2007; He et al., 2012). Other researchers, who tested protective clothing in a simulated flash fire/instrumented manikin system that closely represented a life-like scenario of short-time full body engulfment in flames, have shown that personal protective clothing worn by wildland firefighters is not able to protect some areas of the body in direct contact with the garment fabric (e.g., neck, shoulders, upper torso of back and front, and wrists) (Rucker et al., 2000). They found that these areas showed more burn injuries than areas where an air gap between the fabric and skin was maintained.

Normally, it is not possible to maintain an evenly distributed air gap throughout all areas of a protective garment. The size of the air gap depends on the fit of the garment and is determined during product development. In all garment designs, there are areas where the fabric rests on the human body. The shoulders, upper front and upper back torso are among these areas of close contact with human skin. Because an air gap cannot be maintained, the protection that can be provided is

limited. Maintaining air gaps in these areas through garment design has not been addressed before. This research will investigate the possibility of incorporating three-dimensional warp-knitted fabrics (also known as 3D spacer material) into a shirt design for wildland firefighters' protective clothing to maintain an air gap and improve the thermal protection properties of the garment in problematic areas.

1.2 Definitions

For the purpose of this research the applicable terms are defined as follows:

Air permeability: is “the rate of airflow passing perpendicular through a known area under a prescribed air pressure differential between the two surfaces of a material, $L/m^2 \cdot s$ ” ASTM D 123 ([American Society for Testing and Materials \[ASTM\], 2019a, p. 3](#)).

Cylinder heat transfer performance (CHTP): in “testing of thermal protective materials with the use of a cylindrical specimen holder, the cumulative amount of thermal energy identified by the intersection of the measured time-dependent heat transfer response through the subject material to a time-dependent, empirical performance curve, expressed as a rating or value, J/cm^2 (cal/cm^2)” ASTM F3538 ([ASTM, 2022, p. 2](#)).

Evaporative resistance: is “the resistance to the flow of moisture vapour from a saturated surface (high vapour pressure) to an environment with a lower vapour pressure, $kPa \cdot m^2/W$ ” ASTM F1868 ([ASTM, 2017a, p. 1](#)).

Flame resistance: is “a property of a material whereby flaming combustion is slowed, terminated or prevented, afterflame (sec.), char length (mm)” CAN/CGSB-155.22 ([CGSB, 2014, p. 4](#)).

Heat flux: is “the thermal intensity indicated by the amount of energy transmitted divided by area and time, kW/m^2 ($cal/cm^2 s$)” ASTM F2700 ([ASTM, 2020a p. 2](#)).

Ignition temperature — the temperature of initiation of combustion of fibre, measured in degrees Celsius (Tesoro, 1978, p.287).

Radiant heat resistance performance (RHR): is “in testing of thermal protective materials, the cumulative amount of thermal exposure energy identified by the intersection of the measured time-dependent heat transfer response through the subject material to a time-dependent, empirical performance curve, kJ/m^2 (cal/cm^2)” ASTM 1939 (ASTM, 2020b, p. 2).

Spacer: is the aluminum frame that is mounted into the specimen holder for the TPP and RHR tests to create an air space between the sensor and tested fabric. The frame has 150 x 150 mm dimensions with 125 x 125 mm aperture in the center, and 6.4 mm thickness.

Thermal protective performance (TPP): is “the measurement of the thermal energy input from a flame source to a fabric specimen that is required to result in a heat transfer through the specimen sufficient to cause second-degree (partial-thickness) burn in human tissue, J/cm^2 (cal/cm^2)” CAN/CGSB-155.22 (CGSB, 2014, p. 7).

Thermal resistance: in measurements obtained by the sweating hot plate apparatus, it is “the resistance to the flow of heat from a heated surface to a cooler environment, $\text{K}\cdot\text{m}^2/\text{W}$ ” ASTM F1868 (ASTM, 2017a, p. 2).

Total heat loss (THL): is “the amount of heat transferred through a material or a composite by the combined dry and evaporative heat exchanges under specified conditions, W/m^2 ” ASTM F1868 (ASTM, 2017a, p. 2).

Three-layer fabric system: is a system of three layers of fabric between the skin and the hazardous environment that represents wildland firefighters’ protective clothing (e.g., shirt, pants, coverall) with the incorporation of three-dimensional warp-knitted fabric worn on top of undergarments (e.g., t-shirt, briefs).

Two-layer fabric system: is a system of two layers of fabric between the skin and the hazardous environment that represents wildland firefighters’ protective

clothing (e.g., shirt, pants, coverall) worn on top of undergarments (e.g., t-shirt, briefs).

1.3 Research question and purpose

The main research question of this study:

Is it possible to maintain an air gap and thereby improve thermal protection in the areas where the fabric of the shirt of wildland firefighters' protective clothing is in direct contact with the body by incorporating into the garment a three-dimensional warp-knitted fabric made of flame-resistant fibres?

The purpose of this research was to improve the thermal protection properties of the shirt of wildland firefighters' protective clothing without reducing comfort in areas where the fabric is in contact with the skin. In order to maintain an air gap between the fabric and skin in areas where contact occurs, the three-dimensional warp-knitted fabric was incorporated into the garment design. The performance of the garment was evaluated to determine if an improvement in thermal protection was achieved. The research was completed in the following four stages:

- 1) The thermal protective properties of three-layer fabric systems with three-dimensional knitted fabrics were determined through bench-scale testing and compared to the thermal protective properties of the original two-layer fabric systems of wildland firefighters' protective clothing.
- 2) Selected comfort properties of three-layer fabric systems with three-dimensional knitted fabrics were determined through bench-scale testing and compared to the comfort properties of the two-layer fabric systems of wildland firefighters' protective clothing.
- 3) A shirt (prototype shirt) was developed for wildland firefighters' protective clothing to incorporate three-dimensional warp-knitted fabric into contact areas of the garment. The prototype shirt was based on the design of the shirt currently worn by wildland firefighters in Alberta (control shirt). Control and prototype shirts were constructed for full-scale flash-fire testing.

- 4) The thermal protective performance of the prototype shirt designed for wildland firefighters' protective clothing was tested by a full-scale flash fire instrumented manikin test and compared to the thermal protective performance of the control shirt.

1.4 Objectives

The objectives of this research were to:

- 1) Assess the thermal protective performance of three-layer fabric systems compared with the two-layer fabric systems of the shirt of wildland firefighters' protective clothing at a bench-scale level by conducting the following test methods:
 - a) flame heat source test,
 - b) radiant heat source test,
 - c) combined flame and radiant heat source test.
- 2) Evaluate the comfort performance of three-layer fabric systems compared with the two-layer fabric system of the shirt of wildland firefighters' protective clothing at a bench-scale level by conducting the following test methods:
 - a) heat and moisture vapour transmission test,
 - b) air permeability test.
- 3) Design and produce a shirt prototype for wildland firefighters' protective clothing that incorporates selected three-dimensional warp-knitted fabric in areas of the garment that are close to the skin and prone to second-degree burn injuries by the following steps:
 - a) design sketching and pattern drafting of the control shirt,
 - b) design sketching and pattern editing of shirt prototype based on the control shirt,
 - c) final construction of the control and prototype shirts.

- 4) Assess the thermal protection performance of the control shirt of wildland firefighters' protective clothing and shirt prototype when tested by a flash fire instrumented manikin test system at the full-scale level by the following steps:
 - a) flash fire instrumented manikin testing of control shirts of wildland firefighters' protective clothing,
 - b) flash fire instrumented manikin testing of shirt prototypes of wildland firefighters' protective clothing.

1.5 Null hypotheses

The following null hypotheses were tested to meet objective 1:

H₀₁: There is no significant difference in mean values of TPP rating of the two-layer fabric systems and three-layer fabric systems when exposed to a flame heat source with a heat flux of $83 \pm 2 \text{ kW/m}^2$ at a bench-scale level.

H₀₂: There is no significant difference in mean values of RHR rating of the two-layer fabric systems and three-layer fabric systems when exposed to a radiant heat source with a heat flux of $21 \pm 2.1 \text{ kW/m}^2$ at a bench-scale level.

H₀₃: There is no significant difference in mean values of CHTP rating of the two-layer fabric systems and three-layer fabric systems when exposed to a flame heat source with a heat flux of $84 \pm 2 \text{ kW/m}^2$ at a bench-scale level.

The following null hypotheses were tested to meet objective 2:

H₀₄: There is no significant difference in air permeability mean values among all fabric systems, including two-layer systems and three-layer systems with three-dimensional warp-knitted fabrics at a bench-scale level.

H₀₅: There is no significant difference in mean values of total heat loss among all fabric systems, including two-layer systems and three-layer systems with three-dimensional warp-knitted fabrics at a bench-scale level.

The following null hypothesis was tested to meet objective 4:

H₀₆: There is no significant difference in thermal protective performance between the control shirt of wildland firefighters' protective clothing and the prototype shirt when tested by flash fire instrumented manikin system at the full-scale level.

1.6 Dissertation Overview

This doctoral thesis is divided into eight chapters. **Chapter 1** introduces the research and outlines the statement of the problem, research questions, objectives and null hypotheses. **Chapter 2** reviews the literature with background knowledge covering wildland firefighters' hazardous activities, protective clothing and materials, including three-dimensional warp-knitted fabrics (spacer material). The literature review also includes the role of an air gap in thermal protection, and the trade-off between protection and comfort in protective clothing. **Chapter 3** describes the materials and methods used to fulfill the objectives of this research. This chapter provides a detailed characterisation of the fabrics and fabric systems used. It also presents the experimental design and description of the test methods and equipment used to evaluate thermal protection and comfort performance of the fabric systems at the bench-scale and full-scale level. **Chapter 4** presents the results and discussion of Study One. It includes the TPP, RHR, and CHTP values. It shows significant increase in thermal protection of three-layer fabric systems over two-layer fabric systems when exposed to flame and radiant heat sources. **Chapter 5** presents the results and discussion of Study Two. It includes total heat loss and air permeability values. It shows that the incorporation of three-dimensional warp-knitted fabric between the outer and the base layer impedes the flow of heat and moisture vapour from the skin to the environment. However, it increases the air permeability of the fabric system and allows air movement through the clothing system. **Chapter 6** presents Study Three which is the design and construction of a new shirt for wildland firefighters. The novel design allows for the incorporation of a three-dimensional warp-knitted fabric into the garment areas in contact with the body that are prone to second-degree burn injuries as identified in the literature review. The chapter includes the steps

followed in the construction of the control and prototype shirts used for testing in Study Four. It also includes a review of the standard requirements for wildland firefighters' protective clothing and previous inventions related to clothing designs for improved thermal protection. **Chapter 7** presents the results and discussion of Study Four, the evaluation of the thermal performance of the wildland firefighters' prototype shirt in full-scale flash fire instrumented manikin tests. It shows a significant improvement in the thermal protective performance of the prototype shirt design over the control shirt design. **Chapter 8** presents the summary and conclusions of the research and the contributions of the research to the field of protective clothing. It also addresses recommendations for future research and suggestions for improvements to the proposed prototype shirt design for improved thermal protection of wildland firefighters.

1.7 Limitations and Delimitations

- The outer layer and base layer fabrics were limited to only one type. The outer layer fabric for shirts and pants was Nomex IIIA, and 100% cotton jersey knit was used as a base layer material.
- Only one garment design was developed since proof of concept was being investigated not the creation of an optimal shirt design.

CHAPTER 2 REVIEW OF LITERATURE

2.1 Introduction

The number of wildland fires has substantially increased during the last several decades (Tyukavina et al., 2022). There was a record-breaking wildfire season with approximately 18.5 mega hectares burned across Canada in 2023 (Erni et al., 2024). Wildland fires normally occur during the spring/summer period. They create hostile environmental conditions which are accompanied by smoke, toxic chemical release, high temperatures, low relative humidity (RH), and wind (Budd et al., 1997; Carballo-Leyenda et al., 2019; Reinhardt & Ottmar, 2004; Smith et al., 2013; Withen, 2015). The range of working conditions encountered by wildland firefighters are variable and there are no consistent findings reported by researchers regarding the specific temperature and relative humidity of the work environment. Radiant temperatures discovered by Budd et al. (1997) were approximately 33°C to 96°C with radiant heat fluxes between 0.4 and 8.6 kW/m². Sol et al. (2021) reported cooler working conditions with average temperatures of 29.5 ± 6.5°C, and RH of 28 ± 15%. Although wildland firefighters are mostly exposed to radiant heat from the fire, they also can be engulfed in flames due to rapidly spreading fires and shifting wind directions (Butler, 2014; Dale et al., 2000). Additionally, hazards for the human body are associated with the occupational duties of firefighting. In general, these occupational duties include: stooping and crouching, carrying heavy equipment, working quickly on steep and uneven surfaces, felling trees, burning dry grass with blow torches, and digging trenches to create fire barriers. They carry and use equipment such as chain saws, hand tools, water pumps and hoses, often for long periods of time, including shifts as long as 24 hours (Alberta ALIS, 2021). The thermal stress from the environmental conditions, and work activities can lead to physiological strain afterwards. There is also a risk of developing cardiovascular disease or lung cancer in the long run (Navarro et al., 2019).

2.2 Protective clothing for wildland firefighters

Many researchers have investigated the performance of different types of protective clothing, including protective clothing for wildland firefighters. These specialty garments can provide protection against harsh environments, impact, chemical exposure, radiation, extreme temperatures and flame.

2.2.1 Previous research

Protective clothing for firefighters aims to provide thermal protection against radiant heat and flames, and to prevent burn injuries. According to CAN/CGSB-155.22 and NFPA 1977, wildland firefighters' protective clothing in North America is a single-layer garment that may consist of two garments (shirt and pants) or one garment (coveralls) (CGSB, 2014; NFPA, 2016). It is significantly different from the bulky protective gear of structural firefighters, that consists of multilayer jacket and pants outlined in NFPA 1971 (NFPA, 2018). The majority of researchers in this field have focused on structural firefighters' protective clothing. However, protective clothing for wildland firefighters is also the focus of many research studies, a selection of which are included here.

Lawson et al. (2004) investigated the effect of external and internal moisture on the performance of clothing systems for wildland firefighters when exposed to flame and heat. The researchers used five different moisture settings of two-layer clothing systems (outer and base layer). Two options of outer layer fabrics (FR cotton and aramid) as well as two options of base layer (100% cotton jersey knit and aramid rib knit) were tested. The moisture saturation was as follows: both layers oven-dry, both layers conditioned in standard atmosphere, outer layer wet and base layer conditioned, outer layer conditioned and base layer wet, both layers saturated. To assess thermal protective performance at high heat flux (83 kW/m²) and radiant resistance at low heat flux (10 kW/m²) of selected clothing systems, the researchers conducted two tests CAN/CGSB-4.2 No.78.1 and NFPA 1977 (CGSB, 2013; NFPA, 2016). A spacer of 6.4 mm was applied in each test. Results showed heat transfer performance of clothing systems varies with fibre content of fabrics and moisture application. However, some patterns were revealed. It was concluded that external

moisture reduced heat transfer through the clothing system, while internal moisture increased heat transfer at high heat fluxes. The opposite behaviour was found at low heat fluxes. Similar results were obtained in other studies ([Mäkinen et al., 1988](#); [Rossi, & Zimmerli, 1996](#); [Stull, 2000](#)), where internal moisture reduced heat transfer through the clothing system, while external moisture showed inconclusive results.

[Carballo-Leyeda et al. \(2017\)](#) studied the influence of various wildland firefighters' protective clothing on physiological strain. Eight subjects (male wildland firefighters) were involved in the study. Test subjects had to carry a 20 kg backpack while walking on a treadmill. Room conditions were 30°C and 30% RH. Four types of protective clothing with different fibre contents were considered. Two types of protective clothing were made of fibre blends of flame-resistant (FR) viscose, Nomex and Kevlar, the third had the same fibre content but with the addition of antistatic carbon fibre, and the fourth was made of 100% FR cotton. All participants wore 100% cotton underwear. The heart rate and respiratory gas exchange, gastrointestinal temperature, blood lactate concentration, perceived exertion, and temperature and humidity underneath the protective clothing were measured throughout the test. Researchers stated that wearing protective clothing did not significantly increase physiological responses of wildland firefighters.

[Rucker et al., \(2000\)](#) compared the protective performance of their prototype with standard wildland firefighters' personal protective garments by performing full-scale flash fire instrumented manikin tests. The outer layer of protective jacket and pants consisted of a shirt composed of 98% aramid / 2% carbon. They tested garment ensembles with one-layer system and two-layer system. FR cotton sleeve liner and work under pants composed of 50% cotton / 50% polyester were added to some garment ensembles to give a two-layer protective garment system. Cotton t-shirts and briefs were used as a base layer in all tested garment ensembles. Figure 2.1 shows test results of the burn injury patterns obtained for their garment ensembles. The authors concluded that multi-layer fabric systems provide more protection from flash fires than one-layer fabric systems. They also found that heavier fabric did not provide the same level of protection as two-layer fabric systems. Since the authors were testing

their developed prototype, they provided some design recommendations, such as reducing or eliminating all the unsecured edges of the personal protective clothing (e.g. pocket flaps and open collar). The reason for this suggestion is because these parts of a garment tend to burn longer, and char compared to the rest of the garment. Additional suggestions regarding the design of wildland firefighters' protective clothing from patent disclosures are included in Chapter 6, section 6.2.2.

In addition to other findings, [Rucker et al., \(2000\)](#) noted that areas of the body where the skin is in close contact with the protective clothing, such as the neck, shoulders, and upper torso, are the most unprotected and tended to develop second-degree burning injuries in manikin testing, even with a two-layer clothing system.

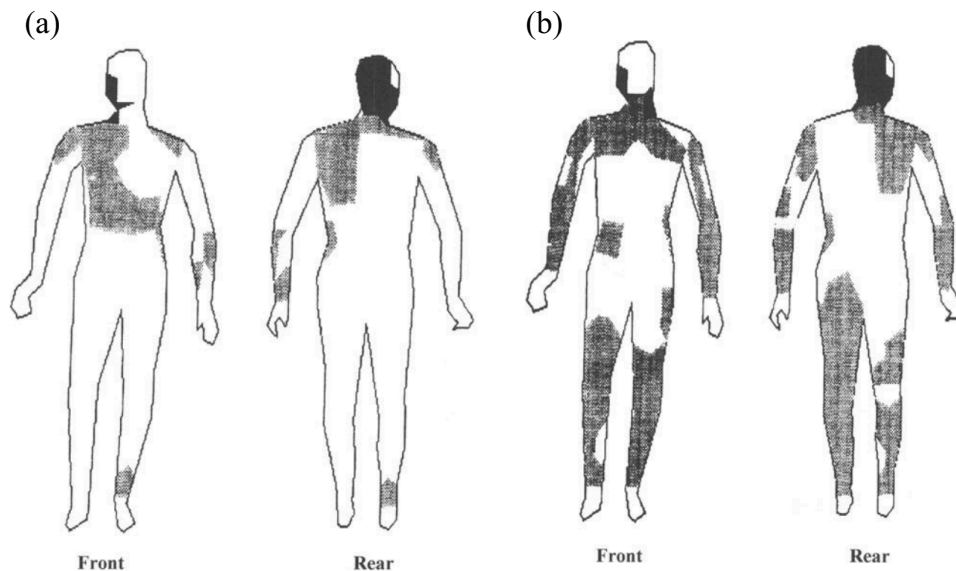


Figure 2.1 Burn injury pattern generated by the instrumented manikin system when the wildland firefighter's garment ensemble was engulfed in flames for 4 seconds:

(a) two-layer fabric system, (b) one-layer fabric system.

Note. From "Evaluation of standard and prototype protective garments for wildland firefighters," by M. Rucker, E. Anderson, and A. Kangas, 2000, *Performance of protective clothing: issues and priorities for the 21st century*, 7, p.553. Copyright 2000 by the American Society for Testing and Materials. Reprinted with permission.

Their work suggested that additional protection in selected garment locations was needed; however, this issue has not been addressed yet in wildland firefighters' protective clothing design. This dissertation research aims to address the need for improved thermal protection of wildland firefighters by developing and evaluating a new shirt design for their protective clothing.

2.2.2 Standard requirements

Three different standards for wildland protective garments were considered to gain an understanding of the current requirements for wildland firefighters protective clothing and the test methods used to assess fabric performance. These standards were compared by their fabric performance requirements. The following standards were included: 1) Canadian standard, CAN/CGSB-155.22 Fireline Workwear for Wildland Firefighters; 2) US standard, NFPA 1977 Standard on Protective Clothing and Equipment for Wildland Firefighting; and 3) ISO 15384 (CGSB, 2014; NFPA, 2016; International Organization for Standardization [ISO], 2018). They are summarised in Tables 2.1 and 2.2. The highlights from the North American Standards are presented in the paragraph that follow the tables.31

Table 2.1 Wildland firefighter's protective clothing textile performance requirements.

Property	CAN/CGSB-155.22 Fireline workwear for wildland firefighters	NFPA 1977 Standard on protective clothing and equipment for wildland fire fighting	ISO 15384 Laboratory test methods and performance requirements for wildland firefighting clothing	Comparison
Textile thermal requirements				
Flame resistance	CAN/CGSB-4.2 No. 27.10 <i>Textile test methods flame resistance - vertically oriented textile fabric or fabric assembly test</i> Garment textile fabrics shall have an average damaged length of not more than 100 mm in either direction and an average afterflame of not more than 2.0 s. There shall be no melting or dripping.	ASTM D6413 <i>Standard test method for flame resistance of textiles (vertical test)</i> Garment textile fabrics shall not have a char length of more than 100 mm average, shall not have an afterflame of more than 2 seconds average, and shall not melt or drip.	ISO 15025 <i>Protective clothing — protection against flame — method of test for limited flame spread</i> Bottom edge ignition No specimen shall permit any part of the lowest boundary of any flame to reach the upper or either vertical edge: no specimen shall give flaming or molten debris. Afterglow time shall be ≤ 2 s. Afterflame time shall be ≤ 100 mm.	<i>Same.</i> All standards (using bottom edge ignition) specify that textile specimens should not have: 1) char length of more than 100 mm, 2) afterflame time should not exceed 2 sec., 3) no melting or dipping. ISO 15384 also has an option of face ignition testing, which has slightly different requirements.

(continued)

Table 2.1 Wildland firefighter's protective clothing textile performance requirements (continued).

Property	CAN/CGSB-155.22	NFPA 1977	ISO 15384	Comparison
Fireline workwear for wildland firefighters	ASTM F1939 Standard	Standard on protective clothing and equipment for wildland fire fighting	Laboratory test methods and performance requirements for wildland firefighting clothing	
Radiant protective performance	ASTM F1939 Standard <i>test method for radiant heat resistance of flame resistant clothing materials with continuous heating</i> Exposure heat flux should be 21 W/m ² . The garment's outer textile fabric shall exhibit an average RHR value of 30 J/cm ² or greater, with no individual value less than 25 kJ/m ² . <i>*RHR - radiant heat resistance</i>	ASTM F1939 Standard <i>test method for radiant heat resistance of flame resistant clothing materials with continuous heating</i> Radiant heat exposure level should be 21 kW/m ² (0.5 cal/cm ²). Garment textile fabrics should have an average value of RPP not less than 7. <i>*RPP - radiant protective performance</i>	ISO 6942 Protective clothing —protection against heat and fire — <i>method of test: evaluation of materials and material assemblies when exposed to a source of radiant heat</i> A heat flux density should be 20 kW/m ² . The single layer shall have the minimum level as following: RHTI ₂₄ ≥ 11s; RHTI ₂₄ -RHTI ₁₂ ≥ 4s Mean Transmission Factor: T _F ≤ 70%. <i>*RHTI - radiant heat transfer index</i>	<i>Different.</i> Both CAN/CGSB-155.22 and NFPA 1977 have the same heat exposure level of 21 kW/m ² , but ISO 15384 has a slightly different value of 20 kW/m ² . All standards have their own measuring system of radiant protective performance. CAN/CGSB-155.22 has <i>RHR</i> not less than 30 kJ/m ² . NFPA 1977 has <i>RPP</i> not less than 7, and ISO 15384 has <i>RHTI</i> should have a minimum value of 11 sec.

(continued)

Table 2.1 Wildland firefighter's protective clothing textile performance requirements (continued).

Property	CAN/CGSB-155.22 Fireline workwear for wildland firefighters	NFPA 1977 Standard on protective clothing and equipment for wildland fire fighting	ISO 15384 Laboratory test methods and performance requirements for wildland firefighting clothing	Comparison
Heat resistance	CAN/CGSB-155.22 (section 6.1.1) <i>Heat resistance and thermal shrinkage tests</i> The garment's textile fabrics and other textile materials shall not melt, separate or ignite when individually tested at 260°C. Knitted fabrics shall not shrink more than 10% in any direction: other garment textile fabric shall not shrink more than 5% in any direction	ASTM F2894 <i>Standard Test method for evaluation of materials, protective clothing and equipment for heat resistance using a hot air circulating oven.</i> The test temperature shall be 260°C. Garment textile fabrics shall not shrink more than 10 percent in any direction. Garment textile fabrics should not melt, drip, separate, ignite or char.	ISO 17493 <i>Clothing and equipment for protection against heat — test method for convective heat resistance using a hot air circulating oven</i> At the temperature of (260 ± 5) °C, no material shall melt, drip, ignite or shrink >10 %.	<i>Slightly different.</i> All standards specify a test temperature of 260°C and textile garment materials should not melt, drip or ignite. NFPA1977 and ISO 15384 do not allow garment textiles to shrink more than 10%. However, CAN/CGSB-155.22 specified that knitted materials should not shrink more than 10%, but other more than 5%.

(continued)

Table 2.1 Wildland firefighter's protective clothing textile performance requirements (continued).

Property	CAN/CGSB-155.22 Fireline workwear for wildland firefighters	NFPA 1977 Standard on protective clothing and equipment for wildland fire fighting	ISO 15384 Laboratory test methods and performance requirements for wildland firefighting clothing	Comparison
Thermal protection	CAN/CGSB-4.2 No. 78.1 <i>Thermal protective performance of materials for clothing</i> The protective fabric should have an average TPP value of 6 or greater, with no individual value less than 5.5. <i>*TPP - thermal protective performance</i>	Not specified	Not specified	<i>Different.</i> Only CAN/ CGSB-155.22 used TPP apparatus for thermal resistance as protection from environmental conditions. The standard specifies average TPP value should not be greater than 6 and 5.5 for individual value.

(continued)

Table 2.1 Wildland firefighter's protective clothing textile performance requirements (continued).

Property	CAN/CGSB-155.22 Fireline workwear for wildland firefighters	NFPA 1977 Standard on protective clothing and equipment for wildland fire fighting	ISO 15384 Laboratory test methods and performance requirements for wildland firefighting clothing	Comparison
Thermal resistance & total heat loss	Not specified	ASTM F1868 <i>Standard test method for thermal and evaporative resistance of clothing materials using a sweating hot plate</i> Garment composite shall not have a total heat loss of not less than 450 W/m ² .	ISO 11092 <i>Textiles — Physiological effects — measurement of thermal and water-vapour resistance under steady-state conditions</i> The mean thermal resistance of the material or material combination shall give a thermal resistance: ≤0,055 m ² K/W. <i>The mean water vapour resistance of material or material combination shall give a water vapour resistance: ≤10 m² Pa/W.</i>	<i>Different.</i> Both NFPA 1977 and ISO 15384 used hotplate apparatus for thermal resistance performance (comfort assessment). However, the measuring system was different. NFPA 1977 specifies that garment composite should not have a total heat loss not less than 450 W/m ² and ISO 15384 specify thermal resistance of the material or material combination should not be less than 0,055 m ² K/W. In addition, the average value of water vapour resistance should not be less than 10 m ² Pa/W.
		Textile thermal comfort requirements		

(continued)

Table 2.1 Wildland firefighter's protective clothing textile performance requirements (continued).

Property	CAN/CGSB-155.22 Fireline workwear for wildland firefighters	NFPA 1977 Standard on protective clothing and equipment for wildland fire fighting	ISO 15384 Laboratory test methods and performance requirements for wildland firefighting clothing	Comparison
Textile mechanical requirements				
Tearing strength	CAN/CGSB-4.2 No. 12.2-M90 <i>Textile test methods: tearing strength - trapezoid method</i> The garment's outer textile fabric, as received, shall have a tearing strength of 45 N or greater in both the warp and the weft, with no single result being less than 42 N.	<i>ASTM D1424 Standard test method for the tear resistance of fabrics by falling pendulum (Elmendorf-type) Apparatus.</i> Woven garment- textile fabrics shall have a tear strength of not less than 22 N.	ISO 13937-2 <i>Determination of tear force of trouser-shaped test specimens (Single tear method)</i> The outer material shall give a tear strength in both machine and cross direction ≥ 25 N.	<i>Different.</i> The highest value of the minimal tearing strength requirement (45 N) is specified in CAN/CGSB-155.22. The lowest value of minimal tearing strength (22 N) is specified in NFPA 1977.

(continued)

Table 2.1 Wildland firefighter's protective clothing textile performance requirements (continued).

Property	CAN/CGSB-155.22 Fireline workwear for wildland firefighters	NFPA 1977 Standard on protective clothing and equipment for wildland fire fighting	ISO 15384 Laboratory test methods and performance requirements for wildland firefighting clothing	Comparison
Tensile strength	Not specified	Not specified	ISO 13934 <i>Determination of maximum force and elongation at maximum force using the strip method</i> The outer material shall give a breaking load in both machine and cross direction ≥ 600 N	<i>Different.</i> Only ISO 15384 specified the tensile strength requirement. The minimum tensile strength for the outer material should be not less than 600 N.
Burst strength	Not specified	ASTM D3787 <i>Standard test method for bursting strength of textiles — constant rate-of-traverse (CRT) ball burst test.</i> Garment textile fabrics shall have a burst strength of not less than 225 N.	Not specified	<i>Different.</i> Only NFPA 1977 specified burst strength requirement. The minimum burst strength for garment textile fabrics should be not less than 225 N.

(continued)

Table 2.1 Wildland firefighter's protective clothing textile performance requirements (continued).

Property	CAN/CGSB-155.22 Fireline workwear for wildland firefighters	NFPA 1977 Standard on protective clothing and equipment for wildland fire fighting	ISO 15384 Laboratory test methods and performance requirements for wildland firefighting clothing	Comparison
Seam strength	CAN/CGSB-4.2 No. 32.2-M89 <i>Textile test methods breaking strength of seams in woven fabrics</i> Major "A" seams shall have a minimum seam breaking strength of 315 N, either fabric or thread. Major "B" seams shall have a minimum seam breaking strength of 225 N, either fabric or thread.	ASTM D1683, <i>Standard test method for failure in sewn seams of woven fabrics</i> Woven material shall demonstrate a sewn seam strength equal to or greater than 315 N force for major seams and 225 N force for minor seams. All knit garment seam assemblies shall demonstrate a sewn seam strength equal to or greater than 180 N.	ISO 13935-2 <i>Textiles — seam tensile properties of fabrics and made-up textile articles — Part 2: Determination of maximum force to seam rupture using the grab method</i> Seams in the outer garment shall give a seam strength ≥ 300 N.	<i>Slightly different.</i> CAN/CGSB- 155.22 and NFPA 1977 both specified minimum breaking strength of 315 N for major seams and 225 N for minor seams of woven fabric. ISO 15384 determined minimum breaking strength for outer garment fabric of 300 N. Only NFPA 1977 has a minimum breaking strength value (180 N) specifically for knit garment seam.

(continued)

Table 2.1 Wildland firefighter’s protective clothing textile performance requirements (continued).

Property	CAN/CGSB-155.22 Fireline workwear for wildland firefighters	NFPA 1977 Standard on protective clothing and equipment for wildland fire fighting	ISO 15384 Laboratory test methods and performance requirements for wildland firefighting clothing	Comparison
Dimensional stability	Not specified	<p data-bbox="643 1203 675 1356"><i>AATCC 135</i></p> <p data-bbox="678 1050 786 1356"><i>Dimensional changes of fabrics after home laundry</i></p> <p data-bbox="789 1050 1146 1356">Specimens shall be tested using five cycles of Machine Cycle I, Wash Temperature IV and Drying Procedure A iii. Garment textile fabrics and shall not shrink more than 5% in any direction.</p>	<p data-bbox="643 680 675 1020">ISO 5077:2007 <i>Textiles — Determination of dimensional change in washing and drying</i></p> <p data-bbox="678 638 1146 1020">Note: dimensional change shall be measured before and after the samples have undergone five cleaning cycles. The dimensional change of woven material, in either length or width direction, shall not exceed 3 % and for knitted materials, the dimensional change shall not exceed 5 %.</p>	<p data-bbox="643 226 1040 611"><i>Slightly different.</i> NFPA 1977 and ISO 15384 both specified dimensional stability requirement, and the garment textile fabric should not shrink more than 5% (NFPA) and 3% (ISO). ISO 15384 mentioned knitted materials as well, the dimensional change shall not exceed 5 %.</p>
		Other requirements		

Table 2.2 Wildland firefighter's protective clothing design requirements.

Property	CAN/CGSB-155.22 Fireline workwear for wildland firefighters	NFPA 1977 Standard on protective clothing and equipment for wildland fire fighting	ISO 15384 Laboratory test methods and performance requirements for wildland firefighting clothing	Comparison
Overall appearance of garment	No specific section on overall appearance. Options of PPC for wildland firefighters are mentioned as one-piece garment (coverall) or jacket/shirt and pants. Standard refers to single-layer or multilayer protective garments that cover the body from the neckline to the wrists and ankles, and shall cover the neck when necessary.	No specific section on overall appearance. Options of PPC for wildland firefighters are mentioned as one-piece garments or upper torso garment (jacket/shirt) and lower torso garment (pants). Bottoms of upper torso protective garments shall be designed so that the bottom edge conforms to the respective front and back lengths. No portion of the bottom garment edge shall be less than the respective minimum front and back length measurement.	Personal protective garments for firefighters capable of satisfying the levels of performance specified in this document shall protect the wearer's body, except the head, hands, and feet. It may consist of 1) a coverall, 2) a protective suit provided with an interface overlap area, or 3) a number of inner and/or outer garments designed to be worn together. A protective suit shall be provided with an interface overlap area of at least 150 mm overlap between the jacket and the trousers.	<i>Same.</i> All standards specified two options of overall appearance of PPC for wildland firefighters, such as one-piece garment (coverall) and two-piece garment (jacket/shirt and pants). CAN/CGSB-155.22 and ISO 15384 mentioned that PPC can be a single-layer as well as a multi-layer garment. NFPA 1977 and ISO 15384 stressed that two-pieces garment should have an overlap between upper torso garment and lower torso garment.

(continued)

Table 2.2 Wildland firefighter's protective clothing design requirements (continued).

Property	CAN/CGSB-155.22 Fireline workwear for wildland firefighters	NFPA 1977 Standard on protective clothing and equipment for wildland fire fighting	ISO 15384 Laboratory test methods and performance requirements for wildland firefighting clothing	Comparison
Collar	All collars on protective garments shall remain upright after extension into a vertical position. When set upright, the collar shall encircle the neck and shall be affixed in such a manner using closures.	All collars on jackets, shirts, and one-piece protective garments shall remain upright after extension into a vertical position. All garments that encompass the neck area shall have a closure system at the neckline.	All protective clothing shall have a collar that encircles and protects the neck and have a closure system to keep the collar closed up the outer edge.	<i>Same.</i> The collar needs to protect the neck and remains upright, in the vertical position. The closure system should be used.
Sleeves	Protective garments shall not have sleeve vents. Sleeve cuffs shall have a closure system that can be adjusted to provide a snug and secure fit around the wrist, and may include wristlets.	Jackets, shirts, and one-piece protective garments shall not have turn-up cuffs. Sleeve cuffs shall have a closure system that can be adjusted to provide a snug and secure fit around the wrist while wearing a glove that is compliant with the glove requirements of this standard.	The protective coverall or protective suit shall not have turn-ups or cuffs. The end of the sleeves shall be designed to protect the wrist and shall have a closure system which allows the end of the sleeve to provide a protective interface overlap with gloves used for wildland firefighting.	<i>Slightly different.</i> Both CAN/CGSB-155.22 and NFPA 1977 specified that cuffs should have a closure system and provide secure fit around the wrist. Both NFPA 1977 and ISO 15384 prohibit turn-up cuffs. CAN/CGSB-155.22 specified that sleeve vents are not allowed.

(continued)

Table 2.2 Wildland firefighter's protective clothing design requirements (continued).

Property	CAN/CGSB-155.22 Fireline workwear for wildland firefighters	NFPA 1977 Standard on protective clothing and equipment for wildland fire fighting	ISO 15384 Laboratory test methods and performance requirements for wildland firefighting clothing	Comparison
Pockets	All pockets that open to the exterior of the garment, other than front waist pockets and pockets designed to carry a portable radio; shall have a cover or closure system.	Where provided, all pockets that open to the exterior of protective garments, other than front waist pockets, shall have a cover or closure system.	All pockets with external openings shall be constructed entirely of materials that have performance levels that are equal to or greater than the outer shell. Where fitted, pocket flaps shall overlap the pocket opening by no less than 10 mm on either side.	<i>Same.</i> All pockets, that are open to the exterior, should be constructed with an overlapping opening cover or closure system.
Hardware	Hardware shall not be directly exposed on the inside of the garment and shall not come in direct contact with the body.	Hardware of any garment shall not come into direct contact with the wearer's body. All garment hardware finish shall be free of rough spots, burrs, or sharp edges.	Hardware penetrating the outer material shall not be exposed on the innermost surface of component assembly. PPC shall be designed to ensure that the hardware shall not have sharp edges, roughness or projections which are likely to cause injury to the wearer.	<i>Same.</i> Hardware should not be in direct contact with the body. However, CAN/CGSB-155.22 does not specify that hardware design should not have roughness and sharp edges.

(continued)

Table 2.2 Wildland firefighter's protective clothing design requirements (continued).

Property	CAN/CGSB-155.22 Fireline workwear for wildland firefighters	NFPA 1977 Standard on protective clothing and equipment for wildland fire fighting	ISO 15384 Laboratory test methods and performance requirements for wildland firefighting clothing	Comparison
Pass- through openings	Pass-through openings of protective garments shall have a means of fastening them in a closed position. One-piece garment torso closure systems shall be continuous from the top of the crotch area to the top of the garment at the base of the neck.	Any pass-through openings in protective garments shall have a means of fastening them in a closed position. Closure systems shall not come into direct contact with the body. One-piece garment torso closure systems shall extend from the top of the crotch area to the top of the garment at the neck.	Closure systems shall be designed to not adversely affect the clothing's performance. All closure systems shall be designed to prevent the entry of burning debris.	<i>Same.</i> All three standards specified that PPC should have closure systems. CAN/CGSB- 155.22 stressed that closure system for coveralls should be continued from the top of crotch area to the top of garment (base of neck). NFPA 1977 does not permit the closure system to be in contact with the body. ISO 15384 pointed out that all closure systems should prevent the entry of burning debris.

(continued)

Table 2.2 Wildland firefighter’s protective clothing design requirements (continued).

Property	CAN/CGSB-155.22 Fireline workwear for wildland firefighters	NFPA 1977 Standard on protective clothing and equipment for wildland fire fighting	ISO 15384 Laboratory test methods and performance requirements for wildland firefighting clothing	Comparison
Retroreflective and/or fluorescent materials	Use of retroreflective or retroreflective/ fluorescent materials is an option in this standard. If used, the trim shall be attached to the outermost surface / layer of the protective clothing and provide for 360° visibility.	Where visibility markings are used on garments, the visibility markings shall be distributed over the exterior of the garment to provide 360-degree visibility of the wearer. This requirement shall not apply to names, organization identification, and heraldry.	Retroreflective and fluorescent material, or combined performance material, shall be attached to the outermost surface of the personal protective clothing and shall give all- round visibility by having at least one band encircling the arms, legs and torso regions of the garment(s).	<i>Same.</i> Retroreflective/ fluorescent materials or trims should be attached to the outermost surface or the PPC and provide 360- degree visibility. However, use of retroreflective/ fluorescent material is optional in CAN/CGSB- 155.22 and NFPA 1977.
Trousers	Not specified	Not specified	Trousers shall have a closure system which will be designed to provide a protective interface between the end of the trousers and any footwear that may be used for wildland firefighting.	<i>Different.</i> Only ISO 15384 standard specified this requirement. Trousers should have a protective interface (closure system) between the end and footwear.

Fabric thermal requirements included flame resistance, radiant protective performance, heat resistance, and thermal resistance of fabric to environmental conditions. The flame resistance requirement, using an edge ignition test, is the same for all standards. They specified that textile specimens should not have a char length of more than 100 mm. The afterflame time should not exceed 2 seconds, and there should not be melting, or dripping observed. Radiant protective performance is assessed with apparatus with similar radiant heat sources in both standards, however a different measuring system is used. Both CAN/CGSB-155.22 and NFPA 1977 have the same heat exposure level of 21 kW/m². CAN/CGSB-155.22 requires an average radiant heat resistance (RHR) of not less than 30 J/cm² on average, while NFPA 1977 requires an average rate of radiant protective performance (RHR) value of not less than 7 (measured in cal/cm² which is equal to 29.3 J/cm²).

Heat resistance is performed using a hot air circulating oven, which has a combination of convective and radiant heat. This requirement is slightly different in the two standards. All standards specify a test temperature of 260°C and that textile garment materials should not melt, drip or ignite. NFPA 1977 does not allow garment textiles to shrink more than 10%. However, CAN/CGSB-155.22 stressed that knitted materials should not shrink more than 10%, but other materials not more than 5%. Thermal resistance as a protection from open flame is evaluated by the thermal protective performance (TPP) apparatus and is a requirement only in CAN/CGSB-155.22. The average TPP value should be 6 cal/m² or greater, with no individual value less than 5.5 cal/m². Thermal resistance as a comfort assessment, is measured with a hotplate apparatus in NFPA 1977 which specifies that the garment composite should have a total heat loss of at least 450 W/m².

Textile mechanical requirements include: tearing, tensile and burst strength, as well as seam strength and dimensional change in laundering. Tearing strength requirements have different values in each standard. CAN/CGSB-155.22 specifies the minimum tearing strength requirement of 45 N, while NFPA 1977 specifies a lower value of 22 N. The minimum required tensile strength for the outer material should be not less than 600 N in all standards. NFPA 1977 also specifies the minimum burst

strength value for garment textile fabrics of not less than 225 N. Seam strength requirements have the same values in the North American standards. CAN/CGSB-155.22 and NFPA 1977 both specify a minimum breaking strength of 315 N for major seams and 225 N for minor seams of woven fabric. Other requirements such as dimensional change after laundering is specified in NFPA 1977. The garment textile fabric should not shrink more than 5%. Both CAN/CGSB-155.22 and NFPA 1977 standards also outline the requirements related to garment design. They are included in Chapter 6, section 6.2.1.

2.2.3 Protective fabrics

This section presents fabric trade names currently used for wildland firefighters' protective clothing and their fibre content. Fabrics that are used in protective clothing for wildland firefighters are commonly made of synthetic fibres with inherently flame-resistant properties or natural fibres treated with flame retardant finishes (Ackerman et al., 2015; Horrocks, 2016).

Synthetic fibres with inherently flame-resistant properties include meta-aramid, para-aramid, polyamide-imide fibres and modacrylic. Some common fabric brands made of aramid fibres include Nomex®, Nomex®IIIA, Teijinconex®, and Kermel®. Modacrylic fibres are found in fabric blends such as Tecasafe®Plus (modacrylic/lyocell/aramid). Nylon fibres are also found in fabric blends, but in small quantities because they are not inherently flame resistant (e.g. Westex Ultrasoft® 88% cotton/12% nylon). Natural fibres such as cotton or wool are also used when treated with flame retardant finishes (e.g. Westex Indura® cotton, and Zirpro®-treated wool).

According to researchers, the base layer (t-shirts) of wildland firefighters is commonly made of cotton (Lawson, 2002; Petrilli & Ackerman, 2008; Rucker et al., 2000). However, some researchers tested a base layer made of meta-aramid and a blend of modacrylic/FR lyocell (DenHartog et al., 2016; Lawson, 2002). The most important criteria for the base layer is that it must be made from fibres that do not melt when heated and contribute to burn injury. For example, CAN/CGSB-155.22

Fireline workwear for wildland firefighters, in Appendix B (par. B.3), specifies that “certain synthetic blend garments may not be appropriate for use under fireline workwear, as the transferred heat from a fire may cause them to melt. Any garment worn under the protective garment should have melt-resistant properties” (CGSB, 2014, p. 20).

2.2.4 Air gap role in thermal protection properties of clothing system

There are air gaps between the protective clothing layer and the human skin. The air gap plays an essential role in heat transfer and skin burn injuries (He et al., 2012). When heat transfers through the protective clothing, that represents a mixed medium of solid parts of fabric structure and gaseous air. The complex mechanisms of conduction, convection, and radiation take place at the same time (Kim et al., 2002). Kreith (1965) states that conduction happens through the contact points with the material (fabric). Convection and radiation occur through the air gap entrapped in the clothing system. Since the air has very low thermal conductivity properties, it acts as an efficient barrier against energy transfer (Song, 2007; Mah & Song, 2010).

The air gap distribution between the protective garment ensemble and human skin is not evenly distributed because of the complexity of the human body shape. Even with the loose fit of the garment, there are some body parts where the clothing rests on it and no air gap occurs, while the remaining areas have air gaps of different thicknesses between the human skin and clothing. The air gap size is crucial for the thermal barrier performance (Torvi et al., 1999). On one hand, if the gap is too small, heat passes easily through it. On the other hand, if the air gap is too big, energy transfer by convection may begin, which decreases the effectiveness of the thermal insulation. Many researchers investigated the most appropriate air gap size that provides the best thermal protection performance. Some examples of these studies, including full-scale and bench-scale tests, are presented below.

Kim et al. (2002) studied the air gap size and thermal protective properties of military thermal protective ensembles (jacket and pants, and coveralls) for aviators.

The fibre content of Nomex/Kevlar/P140 was the same for all protective ensembles. All ensembles were worn on top or cotton or Nomex base layer. The measurements of air gaps were conducted by 3D body scanning technology. The air gap distribution data was compared with the burn injury data from the full-scale flash fire test. The authors concluded that the presence of an air gap is a crucial factor that reduces heat injury.

[Song \(2007\)](#) conducted a similar study looking at the correlation between the distribution of an air layer under a single-layer garment (coverall) and its thermal protective performance at full-scale. Three different sizes of coveralls, made of Nomex® IIIA and Kevlar®/PBI fabric, were tested in the study. Air gap thickness was measured using 3D body scanning technology. The thermal protective performance of the garments was assessed by conducting full-scale flash fire manikin tests. The precise measurements of the air gaps were reported in this study. It was concluded that the optimal size of the air gap was in the range of 7 to 8 mm. The air gap of 8 mm is the upper level when a single-layer garment provides the best thermal protection. Anything beyond this range had a risk of convective currents developing and reducing the insulation properties.

[He et al. \(2012\)](#) studied the mechanism of heat transfer through the air gap between the layer of protective clothing for firefighters and human skin. A bench-scale test with low radiant heat exposure was conducted. Four-layer fabric systems that included an outer layer, moisture barrier, thermal liner and comfort layer were tested together along with the air gap. The tested air gap thickness varied from 0 mm to 10 mm with increments of 1 mm. The authors concluded that the critical air gap thickness was 7 mm. When the air gap thickness is more than 7 mm, the heat transfer by conduction gives way to convection.

[Wang et al. \(2012\)](#) investigated the effect of air gap on thermal protective performance of moist multilayer fabric system of firefighters' clothing. The bench-scale test with an intense combination of flame and radiant heat exposure was performed. The authors also tested a four-layer fabric system similar to what

He et al. (2012) used in their research. Wang et al. (2012) found that added moisture decreased the thermal protection performance of multilayer fabric systems, and almost eliminated the positive effect of the air gap when the air gap was positioned far from the heat source. The presence of moisture in multilayer fabric systems increased the thermal protection only when there is a small air gap between the outer shell fabric and the moisture barrier.

Lu et al. (2013) also investigated the mechanism of heat transfer at bench-scale through the air gap between the moist protective clothing and skin. The bench-scale test with an intense combination of flame and radiant heat exposure was also performed in this study. A single-layer Nomex® IIIA fabric system with different amounts of moisture was tested. The air gap size varied from 0 mm to 24 mm with increments of 3 mm. The authors found that the presence of moisture in fabric significantly increased thermal protection when the air gap size was less than 12 mm. This effect was not consistent when the air gap was greater than 12 mm. Also, this study showed that an air gap in the range of 9 to 12 mm between a single-layer fabric system and skin provides the maximum thermal protection under wet conditions.

Overall, the researchers found that the air gap plays an important role in the performance of protective garments. It significantly increases the thermal insulation of the protective ensemble whether it is single-layer or multilayer when it is tested under dry conditions and exposed to a heat source (Torvi et al., 1999). Based on the selected articles reviewed, the air gap thickness providing the best thermal insulation is approximately 7 mm (Song, 2007; He et al., 2012). Some of these studies showed that the presence of moisture can positively or negatively contribute to the heat transfer through the thermal protective fabric system with air gaps of various sizes (Wang et al., 2012; Lu et al., 2013).

2.2.5 Three-dimensional knitted fabrics

Three-dimensional warp-knitted fabrics (also known 3D spacer materials) possess superior compression and recovery properties and have wide applications in seats and backpacks for their cushioning effect, and some application in protective

clothing for their absorption of impact energy (Palani Rajan et al., 2016; Ye et al., 2008). Palani Rajan et al. (2016) showed that three-dimensional fabrics can also be used in body armour systems to improve their properties. Three layers of three-dimensional fabric, placed behind Kevlar® woven fabric, reduced the deformation depth in the area of projectile impact by 39%.

Three-dimensional warp-knitted fabrics are made on raschel double-needle warp knitting machines. They are composed of two knitted layers of fabrics that are joined by monofilament yarn to provide a pressure-tolerant space between the layers. Three-dimensional knitted fabrics can be made with large apertures and have very high air permeability properties. Commonly three-dimensional knitted fabrics are made of synthetic fibres such as polyester and have applications outside of thermal protection since they tend to melt when exposed to heat (Mao & Russel, 2007).

New technologies allow for the production of lightweight highly porous three-dimensional warp-knitted fabrics that can be made of inherently flame-resistant fibres. One such fabric consists of the meta-aramid top and bottom layers that are connected by polyether ether ketone (PEEK) monofilament fibres (Keitch, 2014). Thick monofilament PEEK fibres have good resiliency properties that maintain the fabric thickness allowing the entrapment of still air and serving as a thermal barrier as stated by the developers of this patent.

In this thesis, a flame-resistant three-dimensional warp-knitted fabric is used to improve the thermal protection of the wildland firefighters shirt in areas prone to burn injury (e.g., shoulder, upper front and back torso). The three-dimensional porous fabric structure entraps still air and acts as an artificial air gap in the contact areas of fabric with skin. Since the material is highly porous, it allows ventilation and moisture evaporation, while not adding significantly to the weight of the garment.

2.3 Thermal protection and skin burn predictions

2.3.1 Thermal protection assessment

The instrumented manikin in a simulated flash fire test, such as ASTM F1930, represents the most life-like scenario of heat and flame exposure and provides an extremely useful assessment of the performance of thermal protective clothing systems (ASTM, 2018c; Barker et al., 2020). Nevertheless, this test requires the construction of whole garments, making it more costly than bench scale tests.

There are several bench-scale test methods that can evaluate heat transfer performance of wildland firefighters' clothing systems also exposed to open flame and radiant heat but testing only a small amount of fabric. Some of the examples of these test methods are CAN/CGSB-4.2 No.78.1, ASTM F1939, and ASTM F2700 (CGSB, 2013; ASTM, 2020a; ASTM, 2020b). These tests can speed up the research and contribute to gaining an understanding of promising fabric performance before the full prototype construction and full-scale fire manikin test (Barker et al., 2020). All these test methods have a flat or planar configuration for the sensor and specimen holder and two options for fabric evaluation. The fabric may be tested in contact with the sensors or a 6.4 mm spacer may be positioned between the fabric and sensor to simulate an air gap between the clothing and the skin. Researchers have shown, in full-scale tests, that garments made of fabrics prone to thermal shrinkage reduce the air gap thickness, increase the heat transfer to the manikin surface and lead to more severe skin burn injury from the energy stored in the fabric during the flame exposure (Barker et al., 2020; Dale et al., 2000). At the bench-scale, the flat configuration of fabric specimen holder with a spacer did not allow such thermal shrinkage behaviour to occur. Moreover, it was shown that data of fabric thermal shrinkage using a flat sensor and specimen holder with 6.4 mm spacer did not correlate with the full-scale fire manikin test results (Barker et al., 2020; Crown et al., 2002; Dale et al., 2000; Wang et al., 2015).

Bench-scale cylindrical configuration of the sensor and specimen holder was developed at the University of Alberta and recently standardised as ASTM F3538 test

method (ASTM, 2022). Crown et al. (2002) found that the cylindrical configuration of the sensor and specimen holder captures the thermal shrinkage effect of tested fabrics at the bench-scale level. Barker et al. (2020) discovered that there is a strong correlation of fabric shrinkage measurements between the bench-scale cylindrical TPP test and the full-scale fire manikin test. The cylindrical specimen holder was designed so that it fits into the test frames of standard bench-scale heat transfer test methods mentioned above (Dale et al., 2000).

Both bench-scale and full-scale manikin tests were performed in this thesis. Bench-scale tests were conducted to gain an understanding of how the incorporation of the three-dimensional warp-knitted fabric in the protective garment would contribute to the thermal protection of the garment system. Also, the bench-scale tests were used to select the most suitable three-dimensional fabric for the construction of a new shirt design. The manikin tests were performed to assess the overall performance of the garment systems including the new shirt design.

2.3.2 Skin burns

Skin is the largest organ of the human body with a surface area of 1.7 m² for an average adult. It represents approximately 5.5% of the entire body mass (Edwards, & Marks, 1995). Human skin protects underlying tissues from thermal, chemical, and physical trauma; provides thermal regulation by sweating, and impermeability to environmental chemicals as well as tissue fluids; allows sensory perception of temperature, touch, and pain (Diller, 1985). Skin includes three main parallel layers which are the epidermis, dermis (or corium), and subcutaneous layer. The epidermis is the outermost layer that faces the environment. It is the thinnest layer (0.06 to 0.8 mm) and it is constantly wearing off and being replenished with new cells. The dermis is the next layer which is 20 to 30 times thicker than epidermis. This layer includes the vascular, nervous, lymphatic, and supporting structures of the skin. A basal layer is located between the epidermis and dermis layers, where most of the cell growth occurs. The final subcutaneous layer (adipose) contains lipocytes that produce and store large amounts of fat. This layer plays an important role in thermal

management of the internal body temperature as it functions as an insulator (ASTM, 2018c).

A skin burn occurs as the result of thermal exposure and elevation in temperature of the skin tissue above a threshold value for a limited time (Diller, 1985). Thermal exposure capable of causing a skin burn injury can include conduction, convection, radiation or a combination of these modes of energy transfer. Skin burn injuries are classified as first-, second-, third-, and fourth-degree burns depending on their severity. The description of each burn injury is provided below.

A first-degree burn injury causes only reddening of the tissue with minimal damage, such as slight edema with irritation of nerve endings at the outer layer of the epidermis. This burn injury leads to temporary discomfort, with fast healing and no permanent scarring or discolouration (Diller, 1985).

A second-degree burn injury or partial thickness burn leads to damage of the epidermis and dermis layers, causes capillary damage and blister formation. In deep second-degree burns, there are observations of basal layer loss, however, some elements like hair follicles and glands could remain present. For superficial second-degree burns, most of the basal cells of the dermis are not destroyed. Thus, healing from this type of injury may occur without scarring afterwards (Diller, 1985).

A third-degree burn injury leads to complete necrosis of the epidermis and dermis layers. This type of injury destroys blood flow in the microcirculation. As a result, the cells die in the location of full-thickness burn. This also leads to the loss of large volumes of extravascular fluid. Therefore, spontaneous healing is not possible, skin grafting would be required instead (Diller, 1985).

A fourth-degree burn injury leads to complete incineration of tissue. This type of injury affects the subcutaneous layer, muscle and bone. The healing process is similar to a third-degree burn; however, some greater complications can occur (Diller, 1985).

In textile test methods, there are two methods used to predict time to skin burn injury. These are the Stoll second-degree criterion and the Henriques burn integral model. The thermal protection performance assessment of protective fabric systems at the bench scale was based on the Stoll criteria and used in Chapter 4. The thermal insulation performance evaluation of protective garments at the full-scale were based on the Henriques burn integral model and used in Chapter 7.

2.3.4 Stoll criteria and bench-scale heat transfer testing

The work of [Stoll and Chianta \(1969\)](#) was focused on the estimation of the time required to reach a second-degree skin burn injury under a given thermal exposure. They discovered that a thermal burn injury depends on both the total energy of the thermal exposure and the duration of the exposure. In their studies with animal and human trials, they established a relationship between exposure levels with heat fluxes of 0.1 to 0.4 cal/cm²·s (4.2 to 16.8 kW/m²) and tolerance duration. Additional data were theoretically determined for higher heat fluxes of thermal exposure.

[Behnke \(1977\)](#) developed a test method for the evaluation of the thermal protective performance of fabrics or fabric systems. The work was based on the findings of [Stoll and Chianta \(1969\)](#). The test measured the transfer of heat through protective clothing which must be limited to prevent burn injuries. For the test, a second-degree burn injury or blister was set as the end point criteria as it is the most severe burn that the human body can heal from with no medical assistance. During the heat exposure in the test method, the fabrics are assessed by the amount of heat transfer just sufficient to obtain a second-degree burn as predicted by the Stoll criteria. Figure 2.1 represents the model curve based on the Stoll criteria using the units used in this research. The equations for the empirical performance Stoll curve with different units are also presented below (equations 2.1, 2.2, and 2.3) ([CGSB, 2013](#); [ASTM, 2022](#)).

$$^{\circ}\text{C} = 8.8715 \times t_i^{0.2905} \quad (2.1)$$

$$\text{J}/\text{cm}^2 = 5.0204 \times t_i^{0.2901} \quad (2.2)$$

$$\text{cal}/\text{cm}^2 = 1.1991 \times t_i^{0.2901} \quad (2.3)$$

where:

t_i the time value in seconds of the elapsed time since the initiation of the heat energy exposure.

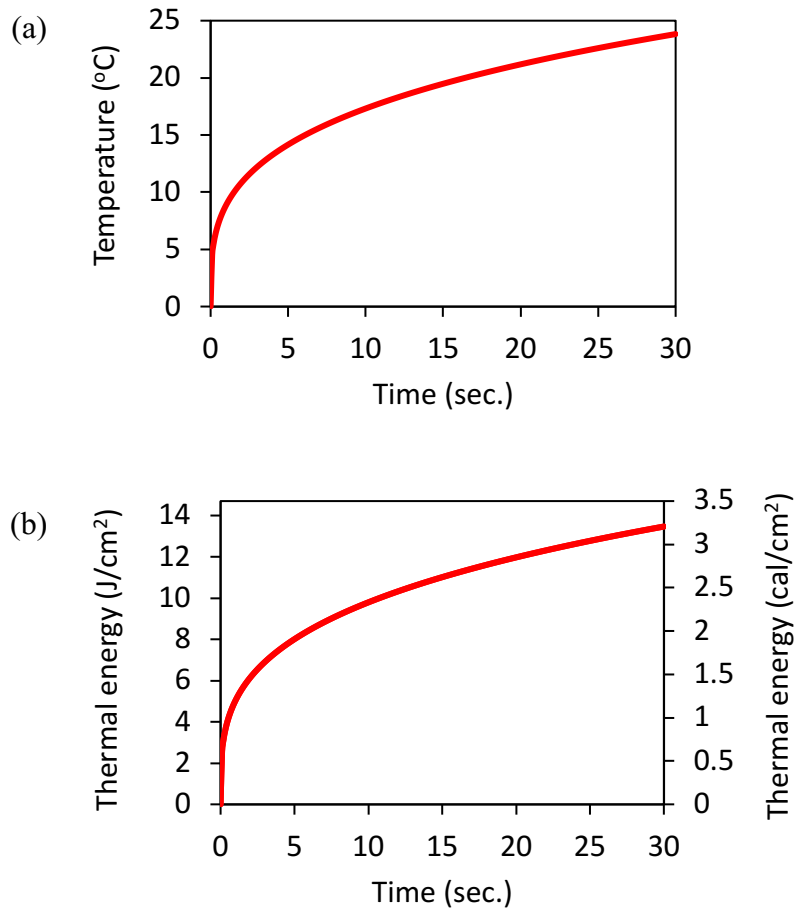


Figure 2. 2 Stoll curve: (a) temperature vs time, (b) thermal energy vs time.

Fabric heat transfer rating was calculated using equation 2.4 (CGSB, 2013; ASTM, 2020a; ASTM, 2022).

$$\text{Heat transfer rating} = \text{exposure heat flux} \times t_{\text{intersect}} \text{ seconds} \quad (2.4)$$

where:

$t_{\text{intersect}}$ time required to reach intersection of Stoll curve and time-dependent heat transfer response.

Materials with poor insulation properties transmit heat rapidly and a short-duration exposure can cause a second-degree burn injury. In contrast, materials with good insulation properties transmit heat slowly and a longer-duration exposure can be tolerated before a burn injury occurs. This test method is useful for fabric comparison, as well as for the development of improved materials and material combinations. The bench-scale heat transfer test methods (CAN/CGSB-4.2 No.78.1, ASTM F1939, and ASTM F3538), that are used in Chapter 4, are based on the Behnke (1977) approach to fabric testing.

2.3.5 Henriques burn integral model and full-scale manikin testing

Burn injury begins to occur when human skin reaches a temperature above 44 °C (Moritz and Henriques, 1947). The degree of burn injury (second or third) depends on the maximum depth within the skin layers to which tissue damage occurs. Second degree burn injury is a complete necrosis of the epidermis skin layer. Third degree burn injury is a complete necrosis of epidermis and dermis skin layers. The Henriques burn integral model (equation 2.5) predicts skin burn injury parameters that depend on the skin temperature values at each measurement time interval at skin model depths of 75×10^{-6} m epidermis (second-degree burn injury prediction), and 1200×10^{-6} m dermis (third-degree burn injury prediction) (Henriques, 1947).

$$\Omega = \int P e^{-(\Delta E/RT)} dt \quad (2.5)$$

where:

- Ω burn injury parameter; value, ≥ 1.0 indicates predicted burn injury,
- t time of exposure and data collection period, s,
- P pre-exponential term, dependent on depth and temperature, 1/s,
- ΔE activation energy, dependent on depth and temperature, J/kmol,
- R universal gas constant, 8314.5 J/mol · K, and
- T temperature at specified depth (in kelvin) K.

The integration according to equation 2.5 is calculated at each measured time interval for each of the sensors at 75×10^{-6} m skin depth and 1200×10^{-6} m skin depth when the temperature (T) is ≥ 44 °C. According to ASTM F1930, predicted second-degree burn injury occurs when the value of $\Omega \geq 1.0$ for depths greater than or equal to 75×10^{-6} m and less than 1200×10^{-6} m. And predicted third-degree burn injury occurs when the value of $\Omega \geq 1.0$ for depths greater than or equal to 1200×10^{-6} m. The full-scale flash fire manikin test method (ASTM F1930) is based on the Henriques burn integral model and was used in this dissertation research (ASTM, 2018c).

2.4 Comfort

Protection against hazardous environmental conditions, such as heat exposure for wildland firefighters, plays a critical role in protective garment design. Since the firefighter wears this clothing during long shifts, the comfort properties should not be underestimated. The garment should not contribute to discomfort and heat strain.

2.4.1 Comfort in clothing systems

The assessment of human comfort in clothing systems is complex in nature. Sontag (1985) in agreement with Das & Alagirusamy (2010a), identified comfort as a state of pleasant psychological, social, physiological and physical harmony between the human subject and their surrounding environment. Das & Alagirusamy (2010b) developed a schema more focused on the human-clothing level of comfort perception where they illustrated the steps of comfort assessment by humans. Figure 2.3 shows

the interaction of physiological, physical, and psychological factors, in the assessment of clothing comfort by the brain. For better understanding of the nature of these factors, a description of each factor in relation to comfort is provided below.

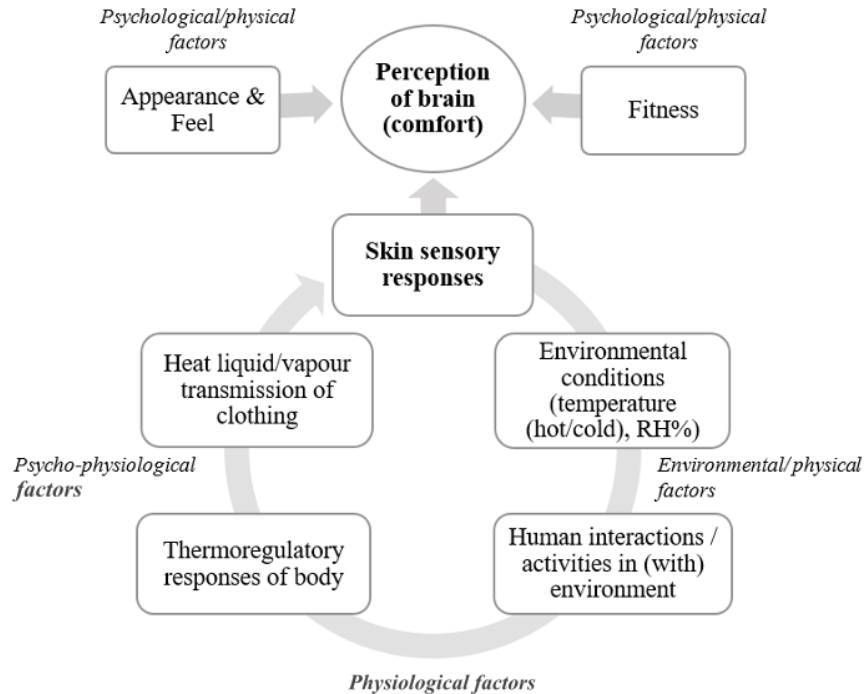


Figure 2.3 Comfort factors interaction schema.

Note. Adapted from “Science in clothing comfort” by A. Das & R. Alagirusamy , 2010, p. 14. Copyright 2010 by Woodhead Publishing India. Adapted with permission.

Physical comfort of human beings in a garment is related to their satisfaction with the physical attributes of the clothing, such as the moisture, air, and heat transfer properties of the fabric, and the weight, fit and mechanical properties (elasticity, flexibility) of clothing. Physical comfort includes subjective assessment of the feel of the fabric through touch and skin perception as well as negative sensation caused by restrictions to physical movement resulting from the weight or fit or flexibility of clothing (Sontag, 1985).

Sontag (1985) distinguished between psychological and social comfort, whereas Das & Alagirusamy (2010b) considered them as one (psychological). *Psychological comfort* is related to a state of mind which shows a balance of the

outfit and a self-concept of the wearer with the aesthetic characteristics of the clothing (Sontag, 1985). *Social comfort* is associated with relevance of a person's clothing to the occasion, as well as meeting the expectations of other participants of a social group.

Physiological comfort is related to the human body's thermoregulatory response mechanisms, such as metabolic heat production, respiratory responses, circulatory, heart rate etc.

According to Sontag (1985), most studies in clothing research are interested in physiological comfort, specifically, thermal comfort or the relationship of clothing comfort with the thermal environment. Therefore, they relate comfort with "thermal comfort", and define it as a state of mind which shows satisfaction with the thermal environment. The person is neither too warm nor too cold. Similarly, research in wildland firefighters' protective clothing also considers the relationship between human comfort and the thermal environment and aims to provide the best level of physiological comfort (Carballo-Leyeda et al., 2017).

2.4.2 Thermal comfort

This research includes the assessment of *thermal comfort* in wildland firefighters' protective clothing. Hazardous environmental conditions as well as the intensive occupational performance of wildland firefighters, that were mentioned in section 2.1, must be considered during the process of protective clothing development.

Generally, when the environmental temperatures are lower than the human body, the clothing releases metabolic body heat to the atmosphere because of the temperature differences (Das & Alagirusamy, 2010a). However, the wildland firefighters normally experience environmental temperatures that are higher than their body temperature as well as increased metabolic heat generation from high physical activity. The rate of metabolic heat production by humans performing low to moderate levels of activity ranges from 80 to 140 W/m²; but wildland firefighters' occupational activities create metabolic heat production rates ranging from of 290 to 400 W/m² (ISO, 2007). Consequently, firefighters' experience physiological strain as

heat is not released to the environment and the body's core temperature rises. Natural cooling mechanisms of human body come into action, such as sweating which allows some evaporative cooling of the skin. This and other physiological responses of the human body must be considered during clothing development to obtain an optimal level of comfort through a balanced heat exchange with the environment.

The heat exchange can be calculated using the general heat balance equation 2.6 specified in ISO11079 (ISO, 2007). The general heat balance equation consists of two parts. The left side of the equation represents internal heat production, while the right side represents the sum of heat exchange through the respiratory tract and skin and the heat storage accumulating in the body.

$$M - W = E_{\text{res}} + C_{\text{res}} + E + K + R + C + S \quad (2.6)$$

where:

M	metabolic rate, $\text{W}\cdot\text{m}^{-2}$
W	the effective mechanical power, $\text{W}\cdot\text{m}^{-2}$
E_{res}	respiratory evaporative heat flow (loss), $\text{W}\cdot\text{m}^{-2}$
C_{res}	respiratory convective heat flow (loss), $\text{W}\cdot\text{m}^{-2}$
E	evaporative heat flow (exchange) at the skin, $\text{W}\cdot\text{m}^{-2}$
K	conductive heat flow (exchange), $\text{W}\cdot\text{m}^{-2}$
R	radiative heat flow (exchange), $\text{W}\cdot\text{m}^{-2}$
C	convective heat flow (exchange), $\text{W}\cdot\text{m}^{-2}$
S	body heat storage rate, $\text{W}\cdot\text{m}^{-2}$.

Taking into consideration the work environment, occupational hazards, and the human body's response to these, clothing for wildland firefighters aims to protect the individual, while still allowing for heat exchange to prevent excessive physiological strain (Carballo-Leyenda et al., 2019). The personal protective clothing for wildland firefighters serves as the nearest environment, creating a microclimate between the human body and environment. In the case of wildland firefighters, the goal of the protective garment is to be fire resistant and strong, while still providing a sufficient level of ventilation to facilitate the natural cooling mechanisms of the

human body and not contribute to heat stress. Thus, this type of protective garment is usually lightweight (unlike structural firefighters' garments) and made of a single-layer of flame-resistant fabric, constructed into coveralls or shirts and pants.

2.4.3 Tradeoffs between comfort and protection

Protective clothing technology always progresses. It is very important to focus on providing sufficient environmental protection without diminishing thermal comfort properties when developing protective clothing for wildland firefighters. Researchers have shown that exercising in or exposure to extreme heat while wearing protective clothing will lead to heat strain (Cheung et al., 2010). The issue of thermal strain has been widely addressed in the research related to firefighting activities. The management of thermal strain through cooling mechanisms is presented below.

As described earlier, wildland firefighters perform very intense physical activities while being exposed to a hot environment. According to the metabolic rates generated by work activities presented by ISO 11079 – Ergonomics of the thermal environment, wildland firefighters on duty can experience a very high metabolic rate in the range of 290 to 400 W/m² (ISO, 2007). In addition to their metabolic heat generation, the wildland firefighters can also gain heat from their surroundings, and as a result, the human body can suffer from thermal physiological stress that can lead to reduced performance of working activities and increased risk of heat strain (Mokhtari, & Sheikhzadeh, 2014). To avoid heat strain, the human body has one of the most effective natural cooling mechanisms that carries produced metabolic heat to the skin and generates the necessary amount of sweat that should be effectively transmitted in liquid and vapour form through the clothing system (Das & Alagirusamy, 2010). Thus, it is very important to take not only protection into consideration when developing a new protective clothing design but also its thermal comfort properties. In other words, wildland firefighters' protective clothing design should provide sufficient thermal protective performance without dramatically diminishing its comfort properties.

2.5 Summary

The literature review revealed that wildland firefighters experience a very high rate of metabolic heat production with constant perspiration while facing hot weather, smoke, and open flame on duty. The protective clothing of wildland firefighters is a lightweight single-layer garment (coverall, or shirt and pants) that is worn on top of the base layer (t-shirt and briefs). The protective clothing must be able to protect against radiant heat exposure and possibly short-term engulfment in flames while still maintaining properties that will not contribute to heat strain.

Previous research has shown that areas of the human body (e.g. shoulders, upper arms, upper front and back torso areas) where the skin is in direct contact with fabric, and no air gap is present in a garment, are prone to skin burn injury in full-scale, flash fire instrumented manikin tests. This issue has not been addressed by other researchers yet. Recently developed, three-dimensional warp-knitted fabrics made of flame-resistant fibres can potentially improve the thermal protection properties of protective clothing of wildland firefighters in the problematic areas. This fabric is highly porous and possesses excellent compression-recovery properties, thus, it can be used to artificially create an air gap in clothing and potentially improve the thermal protection of garments. In this research, the idea that the thermal protection provided by a protective shirt worn by wildland firefighters can be improved through the incorporation of a three-dimensional warp-knitted fabric will be investigated. The influence of the added material on the thermal and evaporative resistance of the garment will also be evaluated. If the artificially created, and selectively positioned air gaps in a wildland firefighters' shirt improves protection, then the shirt design will have applications for other occupations where high heat, flame, and flash fire hazards exist.

CHAPTER 3 MATERIALS AND METHODS

3.1 Introduction

The first part of this chapter presents detailed information about the materials used in this research. It includes the physical properties of the fabrics selected to represent the current fabric systems worn by wildland firefighters in Alberta and two new fabric systems.

The second part of this chapter presents the test methods and apparatus used for the evaluation of fabric systems at a bench-scale level as well as the evaluation of wildland firefighters' protective clothing at a full-scale level used in this research.

3.2 Materials

Overall, four fabrics were used in the research: one outer layer fabric (OL), representing the main fabric of a protective shirt; one base layer fabric (BL), representing a t-shirt worn under the shirt; and two types of three-dimensional warp-knitted fabrics (3D1 and 3D2). Details of the fabrics are provided in Table 3.1. Physical properties of fabrics include the measurements of fabric mass, thickness, and fabric count. A description of the test methods used are provided in Appendix A. All fabrics were conditioned in accordance with ASTM D1776, prior to all testing by placing them on screens in a room with a standard atmosphere of $65\pm 5\%$ RH and $21\pm 1^\circ\text{C}$ for at least 24 hours to reach moisture and temperature equilibrium with the environment ([ASTM, 2020c](#)).

Table 3.1 Physical properties of fabrics.

Fabric Code	Fabric	Fibre Content	Yarn Structure	Fabric Structure	Finish	Physical Characteristics		
						Mass ^a (g/m ²)	Thickness ^b (mm)	Fabric Count ^c (yarns/cm)
OL	Outer layer	93% m-aramid/ 5%p-aramid/ 2%anti-static	s twist 2-ply staple spun	Plain	Moisture- wicking	212	0.6	25 x 20
BL	Base layer	100% cotton	z twist singles staple spun	Jersey knit	No finish	158	0.7	13 (wales) x 18 (courses)
3D1	Three- dimensional warp knitted fabric, type 1	100% m- aramid (face & back)/ 100% PEEK (spacer)	z twist singles staple spun/ monofilament	Raschel warp knit	No finish	555	5.9	Mesh: aperture size 3 x 4 mm Tricot: 9 (wales) x 10 (courses)
3D2	Three- dimensional warp knitted fabric, type 2	100% m- aramid (face & back)/ 100% PEEK (spacer)	z twist singles staple spun / monofilament	Raschel warp knit	Flame- retardant	380	5.3	Mesh: aperture size 2.5 x 4 mm

^aASTM D3776/ D3776M-20, option C.;

^bASTM D1777-96, option 1, measured with 1.0 kPa applied pressure;

^cASTM D3775-17e1 & ASTM D8007-15, measured per 1 cm distance.

Outer layer

A plain weave, Nomex® IIIA fabric was selected to represent the outer material of wildland firefighters' shirts. It is an inherently flame-resistant fibre blend of 93% m-aramid, 5% p-aramid, and 2% anti-static fibre (Figure A.1). Both the warp and weft yarns are 2-ply, spun staple yarns with zzS twist (Figure A.4). The physical properties of the fabric included a mass of 212 g/m², thickness of 0.6 mm, and fabric count of 25 warp x 20 weft yarns/cm. According to the supplier, Milliken & Company, the Nomex® IIIA fabric has a moisture-wicking finish.

Base layer

Knit fabric was obtained from commercially available t-shirts (Hanesbrands Inc.) to represent the base layer garment worn under wildland firefighters' shirts. The fabric is a single jersey knit comprised of 100% cotton fibres, and single, Z twist yarns (Figure A.2 & A.5). The physical properties of the base layer fabric included a mass of 158 g/m², thickness of 0.7 mm, and fabric count of 13 wales x 18 courses per cm. No specific finish was applied to the base layer fabric.

Insulation layer

Two types of three-dimensional warp-knitted fabrics were sourced from Heathcoat Fabrics and tested as potential insulation materials for wildland firefighters' shirts. One of these fabrics was added to specific areas of the shirt (shoulders, upper torso, neck and wrist) to create and maintain an air gap in these areas during full-scale flash-fire testing. The idea was to improve the thermal protection in these selected areas but without significantly decreasing the comfort of the shirt. Both of the three-dimensional warp-knitted fabrics had the same fibre content and yarn structure that included inherently flame-resistant meta-aramid staple fibre, Z-spun into singles yarns for both the face and back fabric, and monofilament polyetheretherketone (PEEK) fibre used for the spacer structure between the face and back fabrics (Figure A.3).

The three-dimensional warp-knitted fabric of Type 1 had a mesh with 3 x 4 mm apertures at the front and a solid tricot knit at the back (Figure A.6). The physical properties of the three-dimensional warp-knitted fabric of Type 1 included a

mass of 555 g/m², a thickness of 5.9 mm, and a fabric count of 9 wales x 10 courses per cm for the back. No specific finish was applied to the three-dimensional warp-knitted fabric Type 1.

The three-dimensional warp-knitted fabric of Type 2 has a mesh with 2.5 x 4 mm apertures at the front and back (Figure A.7). The physical properties of the three-dimensional warp-knitted fabric of Type 2 included a mass of 380 g/m², and thickness of 5.3 mm. A flame-retardant finish was applied by the manufacturer to the three-dimensional warp-knitted fabric Type 2.

3.3 Fabric systems

The composition of the fabric combinations with their assigned codes is shown in Table 3.2. The two-layer fabric systems, OL-BL, OL(2)-BL, OL-BL-S, and OL-S-BL, included one or two outer layers and one base layer fabric. The three-layer fabric systems, OL-3D1-BL, and OL-3D2-BL contained three-dimensional warp-knitted fabric between the outer layer and base layer. Each fabric system represents different areas of the protective shirt and t-shirt worn over the firefighter's body.

Table 3.2 Composition of the fabric systems.

Fabric system	Assembly description
<i>Two-layer system</i>	
OL-BL	Outer layer + Base layer
OL(2)-BL	Outer layer + Outer layer + Base layer
OL-BL-S	Outer layer + Base layer + Spacer (6.4mm)
OL-S-BL	Outer layer + Spacer (6.4mm) + Base layer
<i>Three-layer system</i>	
OL-3D1-BL	Outer layer + Three-dimensional warp-knitted fabric, Type 1 + Base layer
OL-3D2-BL	Outer layer + Three-dimensional warp-knitted fabric, Type 2 + Base layer

Fabric system OL-BL represents areas where the clothing rests on the human body and there is no space or air gap between the shirt, t-shirt, and skin when the garments are worn (e.g. the shoulder, upper front torso, and upper arm). Fabric system OL(2)-BL represents the upper back torso in the yoke area, and it has two outer layers of fabric and one base layer. Similar to the OL-BL fabric system, the OL(2)-BL fabric system rests on the body and there is no air gap between the shirt yoke, t-shirt, and skin when the garments are worn.

Fabric systems OL-BL-S and OL-S-BL represent areas where air gaps naturally form. Because the base layer t-shirt may be loose-fitting or tight-fitting, fabric system OL-BL-S has a spacer between the base layer and the sensor to represent a clothing system with a loose-fitting t-shirt, while fabric system OL-S-BL has a spacer between the outer layer and the base layer to represent a clothing system with a tight-fitting t-shirt.

The three-layer fabric systems OL-3D1-BL and OL-3D2-BL have two types of three-dimensional warp-knitted fabrics between the outer layer and the base layer. These fabric systems maintain an air gap within their knitted structures and are meant for areas of the garment where the clothing naturally rests on the human body. The fabric system OL-3D1-BL includes three-dimensional warp-knitted fabric Type 1, which has a solid tricot knit on one side, apertures on the other side, and a spacer yarn between. The fabric system OL-3D2-BL includes three-dimensional warp-knitted fabric Type 2, which has a flame-retardant finish and apertures on both sides of the fabric and a spacer yarn between.

3.4 Bench-scale tests for thermal protection assessment

Five different fabric systems OL-BL, OL-BL-S, OL-S-BL, OL-3D1-BL, and OL-3D2-BL were tested according to the following three standard test methods: (1) CAN/CGSB-4.2 No.78.1, (2) ASTM F1939, and (3) ASTM F3538 (CGSB, 2013; ASTM, 2020b; ASTM 2022). During the tests, fabric specimens were exposed to a flame heat source, radiant heat source, and a combined flame and radiant heat source. Data was collected to determine the thermal protective performance (TPP), radiant heat resistance (RHR), and cylinder heat transfer performance (CHTP) values for the fabric systems (CGSB, 2013; ASTM, 2020b; ASTM, 2022). Each fabric system was tested under dry and wet base layer conditions. The experimental design used for all three test methods and the description of each test apparatus are presented below.

3.4.1 Experimental design

A full two-way factorial experimental design was applied in the assessment of the thermal protection properties of the fabric systems. For all three tests there were two *independent variables*: 1) fabric system with five levels (OL-BL, OL-BL-S, OL - S- BL, OL-3D1-BL, OL-3D2-BL), and 2) base layer condition with two levels (dry and wet). The *dependent variable* was one for each test: thermal energy (J/cm^2) with recorded time to second-degree burn in seconds. All possible combinations of the independent variables and their levels are presented in Table 3.3. Based on the experimental design settings, a two-way ANOVA test with a follow-up pairwise comparison was used for statistical data analysis.

Table 3. 3 Factorial experimental design for assessment of differences in thermal protection properties of different fabric systems and base layer conditions.

Base layer cond.	Fabric system				
	OL-BL	OL-BL-S	OL-S-BL	OL-3D1-BL	OL-3D2-BL
D	OL-BL/D	OL-BL-S/D	OL-S-BL/D	OL-3D1-BL/D	OL-3D2-BL/D
W	OL-BL/W	OL-BL-S/W	OL-S-BL/W	OL-3D1-BL/W	OL-3D2-BL/W

Method of sampling

Five fabric systems (OL-BL, OL-BL-S, OL-S-BL, OL-3D1-BL, OL-3D2-BL) were tested under dry and wet base layer conditions and each fabric system and base layer condition had five replicates. Five specimens (samples) were systematically allocated on every fabric (outer layer, base layer, and two types of three-dimensional warp-knitted fabrics) for each fabric system such that the replicates for the same test contained different warp and weft yarns or wales and courses.

3.4.2 Test methods and equipment

This section contains a detailed description of each test apparatus for the standard test methods CAN/CGSB-4.2 No.78.1, ASTM F1939, and ASTM F3538, which measured the TPP, RHR, and CHTP values of the fabric systems (CGSB, 2013; ASTM, 2020b; ASTM, 2022). Additional thermocouples were attached to the outer and base layer fabrics during the CAN/CGSB-4.2 No.78.1 and ASTM F1939 tests. The mounting procedure for the additional thermocouples is presented in this chapter. Since each fabric system was tested under dry and wet base layer conditions, the description of the moisture application to the base layer is also included. Prior to all testing, the fabrics were conditioned in a standard atmosphere of $65 \pm 5\%$ RH and $21 \pm 1^\circ\text{C}$ for at least 24 hours to reach moisture and temperature equilibrium (ASTM, 2020c). The fabric specimens were placed in sealed plastic bags and tested within four hours of removal from the conditioned environment to ensure they remained conditioned at the point of testing

3.4.2.1 Exposure to a flame heat source

To establish TTP values for the fabric systems they were tested in accordance with CAN/CGSB - 4.2 No.78.1 - Thermal protective performance of materials for clothing, a test method specified in section 5.1.6 of CAN/CGSB - 155.22 (CGSB, 2013; CGSB, 2014). Figure 3.1 depicts the TPP test apparatus (built in-house). It consisted of a stand to support a specimen holder and a Meker-type burner with a handle for manual operation. A non-conductive block with a copper calorimeter sensor was placed horizontally on top of the specimen in the holder. In this test, the burner was a single-flame heat source. The flame heat flux was set to $83 \pm 2 \text{ kW/m}^2$

($\sim 2 \text{ cal/cm}^2\cdot\text{s}$). The burner was moved into position below the specimen and sensor at the start of each test. When the burner was in position, the outer layer of a fabric system specimen was exposed to the flame and the heat energy from the flame transferred through the specimen to the sensor.

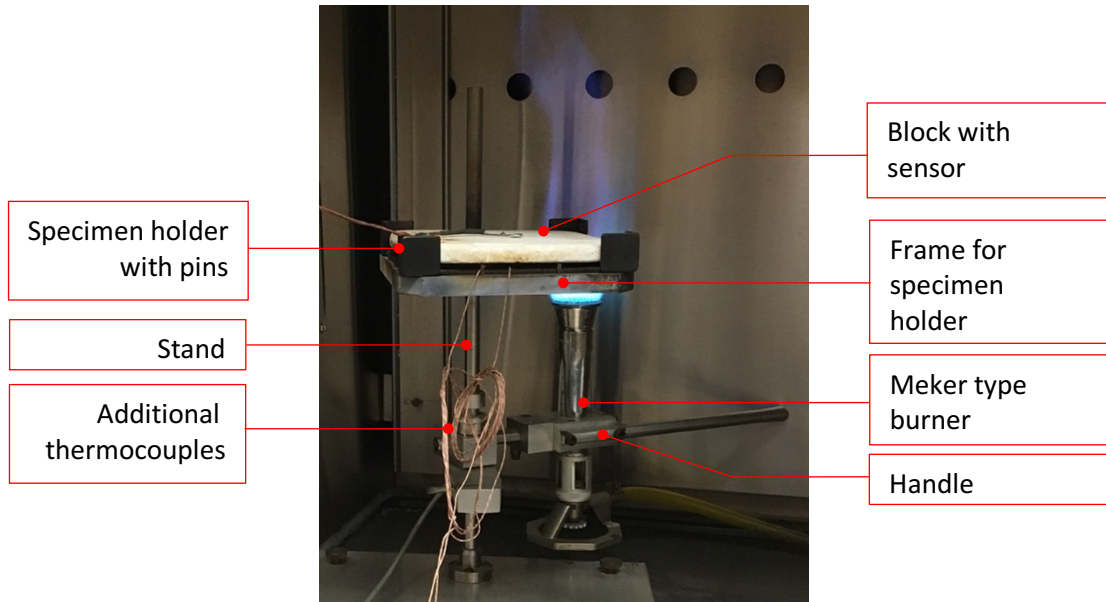


Figure 3.1 Test apparatus for evaluation of the thermal protective performance of clothing systems.

The burner positioning triggered the computer data acquisition system (software developed in-house) which recorded the temperature rise of the sensor and thermocouples over time (sampling rate 10 Hz). The temperature data from the sensor was converted to a time dependant thermal energy curve that was plotted against a Stoll curve representing second-degree burn injury. The time when the two curves intersected was the endpoint for the test. The burner was moved away from the test specimen. The data acquisition system continued to obtain temperature data from the sensor and additional thermocouples attached to the specimen layers until 30 seconds had elapsed. The initial temperature of the sensor was brought to an approximate skin temperature of $30^{\circ}\text{C} - 32^{\circ}\text{C}$ before the beginning of each test.

Figure 3.2 presents the top and bottom views of the flat configuration heat-resistant non-conductive block with the mounted sensor used in this test. It is a copper calorimeter ($18 \pm 0.05 \text{ g}$, 1.6 mm thick, 40 mm diameter) with a single

thermocouple. The surface of the sensor was coated with a thin layer of high temperature flat black spray paint (CGSB, 2013).

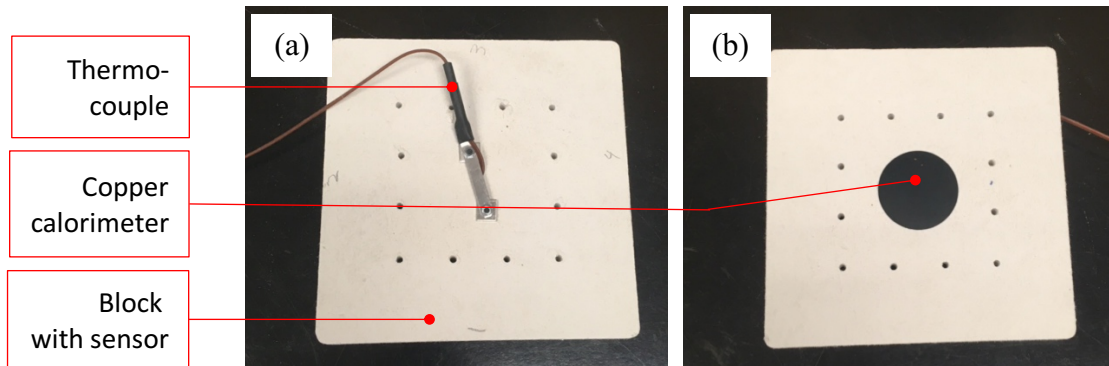


Figure 3.2 Flat configuration non-conductive block with sensor (copper calorimeter):
(a) top view, (b) bottom view.

Figure 3.3 depicts the examples of fabric systems OL-BL and OL-BL-S mounted in the TPP specimen holder with and without a spacer. The spacer is an aluminum frame that was mounted into the specimen holder to create an air gap between the sensor and tested fabric system. The frame dimensions are 150 x 150 mm with 125 x 125 mm aperture, and 6.4 mm thickness (CGSB, 2013). The specimen holder has a flat configuration with 12 stainless steel pins (1.5 mm diameter) positioned in 75 x 75 mm square around a 50 x 50 mm square opening. The pins are used to prevent the fabric specimen from moving due to thermal shrinkage during flame exposure (Day, 1988; Lawson et al, 2004).

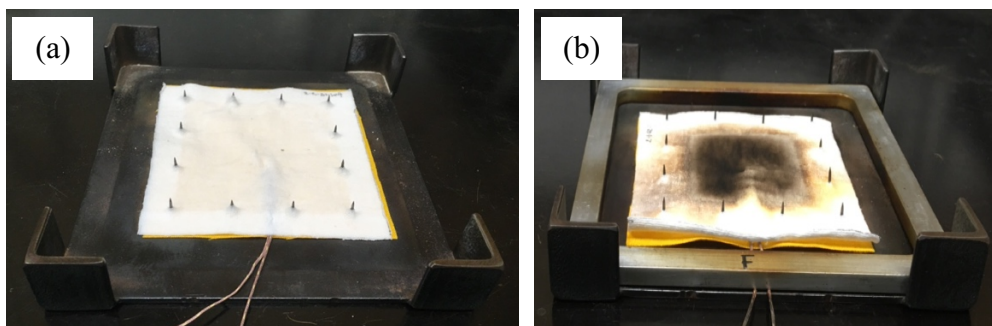


Figure 3.3 Fabric systems OL-BL and OL-BL-S mounted in the TPP specimen holder when tested (a) in contact with sensor, (b) with spacer between fabric system and sensor.

During the test, 100 x 100 mm fabric system specimens were centered over the opening of the specimen holder and pushed down onto the pins. The technical face of the outer layer fabric was exposed to the flame heat source from the Meker burner through the opening in the specimen holder. The sensor block was placed on top of the fabric system specimen with the base layer in contact with the sensor.

3.4.2.2 Exposure to a radiant heat source

To establish RHR values for the fabric systems they were tested in accordance with ASTM F 1939 - Standard Test Method for Radiant Heat Resistance of Flame-Resistant Clothing Materials with Continuous Heating, a test method specified in section 5.1.2 of CAN-CGSB - 155.22 (CGSB, 2014; ASTM, 2020b). Figure 3.4 depicts the RHR test apparatus (built in-house). It consisted of a vertically oriented radiant heat source, a manually operated protective shutter with cooling tubes, and a specimen holder.

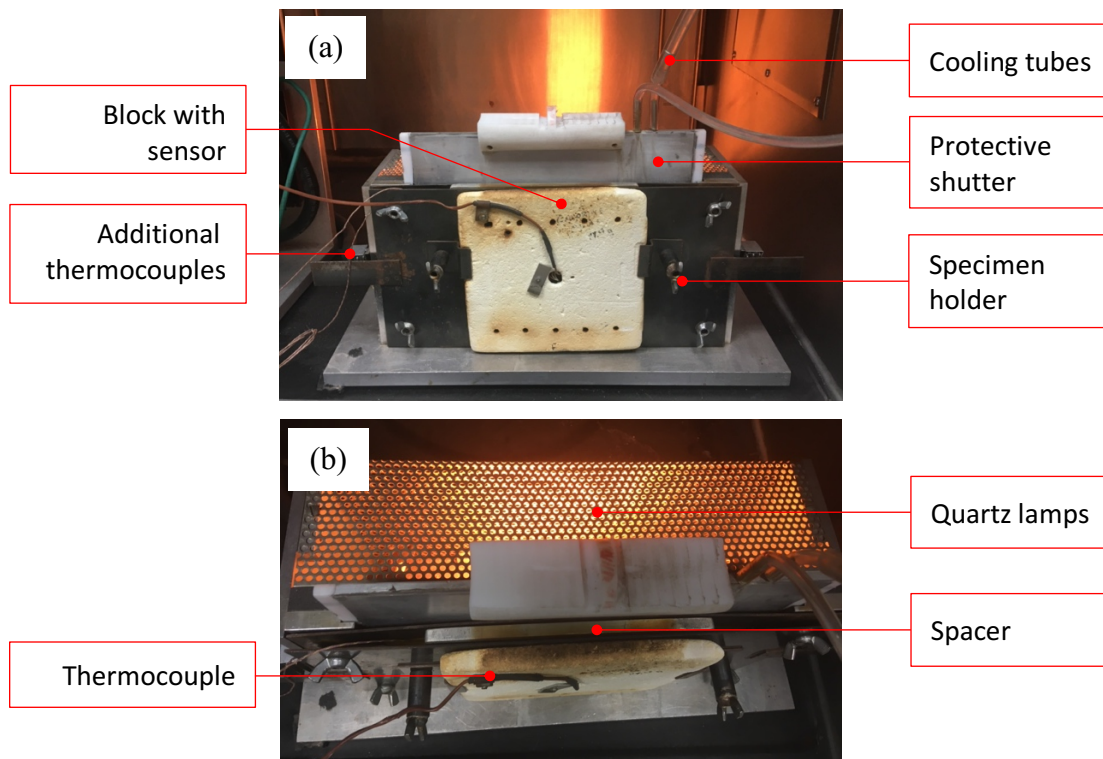


Figure 3.4 Test apparatus for evaluation of the radiant heat resistance of clothing systems: (a) front view, (b) top view.

In this test, a bank of five 500 W infrared, tubular, translucent quartz lamps were used as the single-radiant heat source. The radiant heat flux was set to $21 \pm 2 \text{ kW/m}^2$ ($\sim 0.5 \text{ cal/cm}^2\cdot\text{s}$). A fabric system specimen, attached to the specimen holder, was positioned in front of the lamps, and protected from the radiant heat by the water-cooled shutter before the test start. The same non-conductive block with the copper calorimeter sensor, as described previously and shown in Figure 3.2, was placed vertically in the specimen holder and in contact with the base layer of the fabric system. The test began when the protective shutter was lifted. The outer layer of the fabric system specimen was exposed to the radiant heat from the lamps and the radiant heat energy transferred through the specimen to the sensor.

The lifting of the shutter triggered the computer data acquisition system (software developed in-house) which recorded the temperature rise of the sensor and thermocouples over time (sampling rate 10 Hz). Similar to the TPP test, the temperature data from the sensor was converted to a time dependant thermal energy curve that was plotted against a Stoll curve representing second-degree burn injury. The time when the two curves intersect was the endpoint for the test. The shutter was replaced in its original position. The data acquisition system continued to obtain temperature data from the sensor and additional thermocouples attached to the specimen layers until 120 seconds had elapsed. The initial temperature of the sensor was brought to an approximate skin temperature of $30^\circ\text{C} - 32^\circ\text{C}$ before the beginning of each test.

Figure 3.5 illustrates examples of fabric systems OL-BL and OL-BL-S mounted in the RHR specimen holder with and without the spacer. The same spacer described in the TPP test was used to create a 6.4 mm air gap for fabric system OL-BL-S and OL-S-BL. The RHR specimen holder had a flat configuration with a rectangular opening (75 x 125 mm), but no pins to restrain the specimens as in the TPP holder. During the test, 100 x 200 mm specimens were centred over the opening in the specimen holder and held in place with clamps. The technical face of the outer layer fabric was exposed to the bank of lamps through the opening and the base layer was in contact with the sensor block.

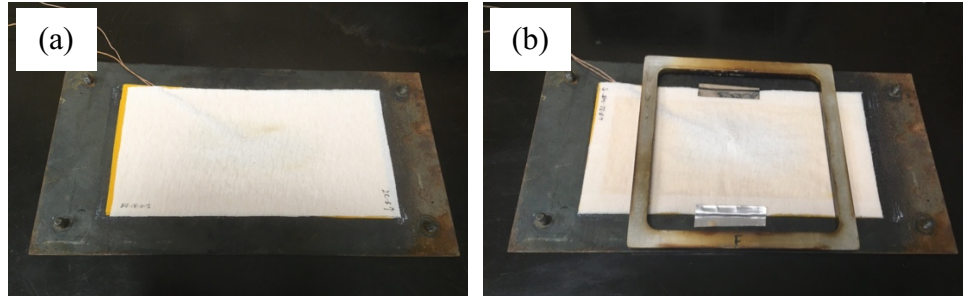


Figure 3.5 Fabric systems OL-BL and OL-BL-S mounted in the RHR specimen holder when tested (a) in contact with sensor, (b) with spacer between fabric system and sensor.

3.4.2.3 Exposure to a combined radiant and flame heat source

To establish CHTP values for the fabric systems they were tested in accordance with ASTM F 3538 - Standard Test Method for Measuring Heat Transmission Through Flame-Resistant Materials for Clothing in Flame Exposure Using a Cylindrical Specimen Holder (ASTM, 2022). Figure 3.6 depicts the CHTP test apparatus (MYAC Consulting Inc., Edmonton, AB). It consisted of a combined flame and radiant heat source, an automated protective shutter, and a cylindrical specimen holder with non-conductive block and copper calorimeter single-thermocouple sensor. Two Meker burners and the bank of nine 500 W infrared, tubular, translucent quartz lamps were used as the combination flame and radiant heat source. The combined flame and radiant heat flux was set to $84 \pm 2 \text{ kW/m}^2$ ($\sim 2 \text{ cal/cm}^2 \cdot \text{s}$). The CHTP test apparatus was equipped with a computer-controlled, moving specimen holder and a protective shutter. At the beginning of the test, the specimen holder and automated protective shutter are positioned over the heat source, The shutter blocked the fabric specimens and sensor from the burners and quartz lamps at the start of the test and precisely controlled the duration of thermal energy exposure during the test. The test began when the automated shutter was opened by the computer system. The outer layer of the fabric system specimen was exposed to the combined flame and radiant heat source and the heat energy transferred through the specimen to the sensor.

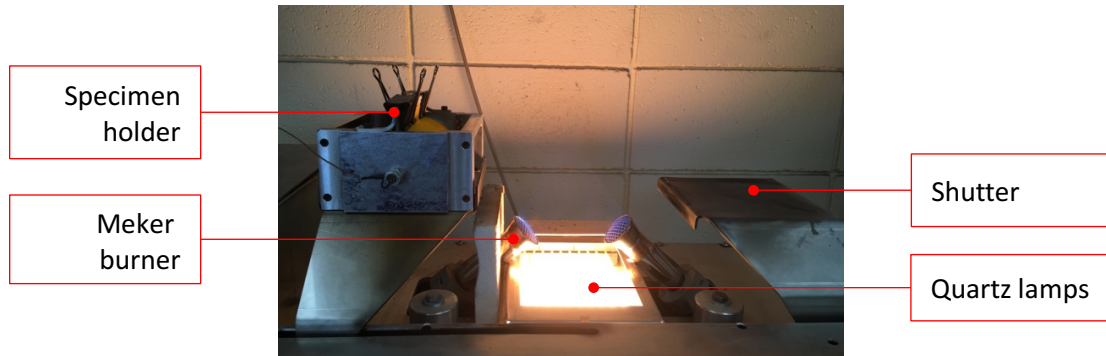


Figure 3.6 Test apparatus for evaluation of the cylinder heat transfer performance of clothing systems.

The opening of the shutter triggered the computer data acquisition system which recorded the temperature rise of the sensor over time (sampling rate 10 Hz). Similar to the TPP and RHR tests, the temperature data from the sensor was converted to a time dependant thermal energy curve that was plotted against a Stoll curve representing second-degree burn injury. The time when the two curves intersect was the endpoint for the test. The specimen holder and the shutter moved away from the heat source to their initial positions as shown in Figure 3.6. The initial temperature of the sensor was brought to an approximate skin temperature of 30°C – 32°C before the beginning of each test.

Figure 3.7 shows the cylindrical configuration heat-resistant non-conductive block – specimen holder with the aluminum support frame, mounted sensor and attached thermocouple for data acquisition used in this test. The curved copper calorimeter sensor has a mass of 18 g, thickness of 1.65 mm, and rectangular shape of 38.1 mm x 25.4 mm, fitting the cylindrical configuration of the sensor block (ASTM, 2022). With the base layer positioned closest to the sensor, the fabric system specimen was wrapped around the cylinder, covering the sensor, and was fixed in place with a clip.

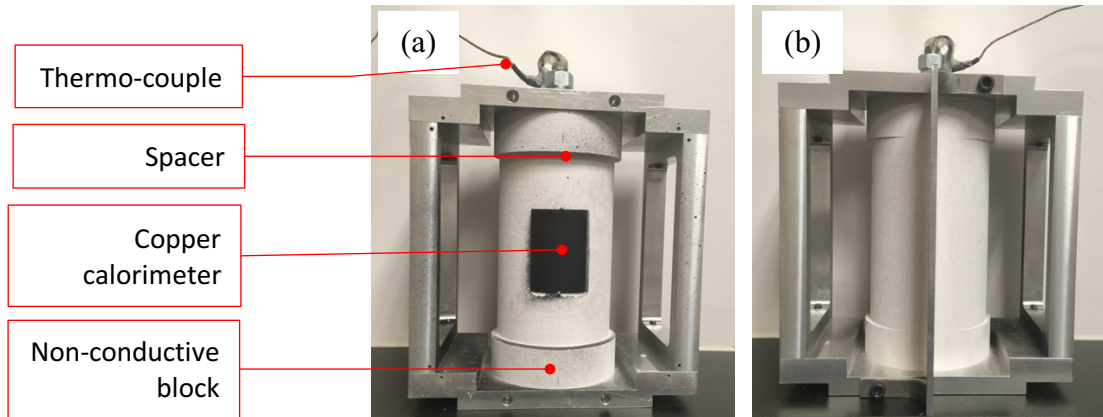


Figure 3.7 Cylindrical configuration non-conductive block with sensor (copper calorimeter): (a) front view, (b) back view.

There were two variations of fabric specimen size: narrow (100 x 280 mm) and wide (120 x 280 mm). The narrow specimens wrapped around the non-conductive block of the specimen holder and were used for the contact test. The wide specimens wrapped around the spacer portion of the non-conductive block and allowed for the setting of a 6.35 mm air gap between the sensor and the base layer of the fabric system when tested. The cylindrical shape of the specimen holder and sensor was similar to the instrumented manikin where many fabrics shrink tightly to the sensors and reduce the air gap thickness during heat exposure (Dale et al., 2000). It was important to track this fabric behaviour under heat exposure because decreases in the air gap in clothing systems can result in skin burn injuries. The flat specimen holder and sensor found in the TPP test does not show the effect of fabric thermal shrinkage on air gaps in fabric systems.

Thermocouple attachment

Two thermocouples (Omega, Calibration type K, 36 AWG) were used in each fabric system when flame heat exposure and radiant heat exposure bench-scale tests were conducted. One thermocouple was sewn to the centre of the inner side of the outer layer fabric using aramid threads so it could stay in place during the test. The second thermocouple was sewn in a similar way but to the outer side of the base layer fabric (Figure 3.8). The specimens with attached thermocouples were conditioned and stored in sealed plastic bags for no more than four hours prior testing. In the case of

testing the fabric systems under wet base layer conditions, the thermocouples were sewn to the base layer immediately after the moisture application procedure was completed. Additional thermocouples allowed tracking of the temperature change within the fabric systems throughout the tests.

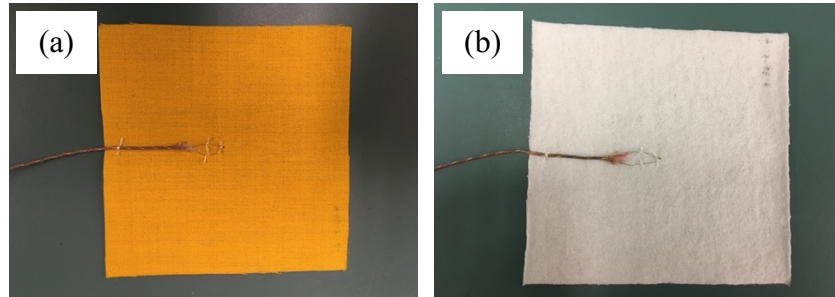


Figure 3.8 Additional thermocouple attached to (a) outer layer, (b) base layer.

Washing and drying procedure of the base layer

The base layer fabric was laundered once in accordance with CAN/GSB-4.2 No. 58 wash procedure 5 and drying procedure D1 (CGSB, 2019). The laundering was done to gain full relaxation of the fabric before testing, since the specimens for the base layer were cut from purchased cotton t-shirts with high relaxation shrinkage potential from garment finishing and packaging. The wash temperature was 50°C, wash time of 12 ± 1 minutes with moderate mechanical action and spin time of 6 ± 1 minutes. Sixty-six grams of AATCC 1993 Standard Reference Detergent in 72 ± 4 liters of water was used for the wash cycle. The drying procedure D1 was normal tumble dry with an exhaust temperature of $66 \pm 5^\circ\text{C}$, and 10 minutes of cooling down without heat at the end of the cycle.

Moisture application to the base layer

A method of moisture application from a previous study was followed (Lawson, 2002). Preconditioned base layer specimens were placed into a water bath with reverse osmosis water at approximately 22°C and remained saturated for at least 30 minutes. Just prior to testing, each base layer specimen was first placed between two sheets of blotting paper and rolled over twice with the 1 kg metal roller (forward and back) to remove the extra water, then weighed on the balance before mounting on

the fabric specimen holder. The weight of each base layer specimen was approximately the same, giving a saturated moisture content of $61 \pm 1\%$.

3.5 Bench-scale tests for comfort assessment

Comfort assessment was evaluated by testing heat and moisture vapour transmission in accordance with ASTM F 1868 and air permeability in accordance with ASTM D 737 (ASTM, 2017a; ASTM, 2018b). The data for the heat and moisture vapour transmission were collected as THL values calculated in W/m^2 , which were calculated as the sum of the thermal resistance measured in $K \cdot m^2/W$ and the evaporative resistance measured in $kPa \cdot m^2/W$. The data for the air permeability test were collected in $L/m^2 \cdot s$. A one-way factorial experimental research design used for both methods and the description of each test apparatus are presented below.

3.5.1 Experimental design

The one-way factorial experimental design was applied in the assessment of the comfort properties of the fabric systems. For both test methods, only one *independent variable* (fabric system) with four levels (OL-BL, OL(2)-BL, OL-3D1-BL, and OL-3D2-BL) was used. The *dependent variable* (measurement) was also one for each test: (1) THL value, W/m^2 , and (2) air permeability assessment, $L/m^2 \cdot s$. Based on the experimental design settings, a one-way ANOVA test with a follow-up pairwise comparison was used for statistical data analysis for both test methods.

Method of sampling

Similar to the sampling method used for bench-scale thermal protection assessment, a systematic sampling approach was used for the bench-scale comfort assessment tests. Four fabric systems (OL-BL, OL(2)-BL, OL-3D1-BL, and OL-3D2-BL) were tested for heat and moisture transmission and air permeability. Three replicates were needed for the heat and moisture transmission tests, and ten replicates for the air permeability tests. For thermal resistance and evaporative resistance, the same specimens were used for each test and the results used to

calculate the THL values used to compare the heat and moisture vapour transmission properties of the fabric systems.

3.5.2 Test methods and equipment

This section contains a detailed description of the test apparatus for the standard test methods, ASTM F 1868 and ASTM D 737, used to measure thermal and evaporative resistance and air permeability (ASTM, 2017a; ASTM, 2018b). Prior to testing the fabrics were conditioned in a standard atmosphere of $65 \pm 5\%$ RH and $21 \pm 1^\circ\text{C}$ for at least 24 hours to reach moisture and temperature equilibrium in accordance with ASTM D1776 (ASTM, 2020c).

3.5.2.1 Total heat loss

The total heat loss performance of each fabric system was tested in accordance with part C of ASTM F1868 - Standard Test Method for Thermal and Evaporative Resistance of Clothing Materials Using a Sweating Hot Plate (ASTM, 2017a). Figure 3.9 shows the sweating guarded hot plate 8.2 223-6 with mounted fabric system specimens (Measuring Technology NW Inc., Seattle, WA, US). The sweating hot plate was housed in a controlled atmosphere chamber that maintains the temperature and humidity of the ambient air during testing. The hot plate itself includes a test plate with temperature sensors and mounted nozzles for water supply, a guard section, and a bottom plate.

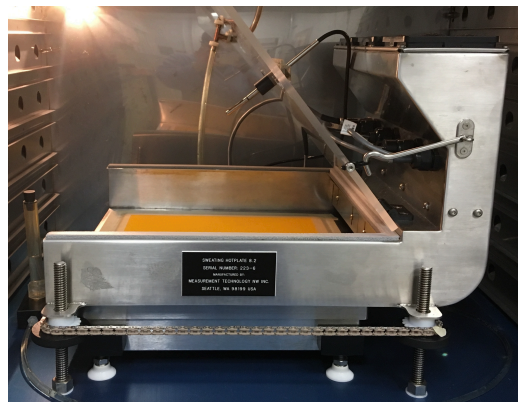


Figure 3.9 Sweating guarded hot plate.

Each plate was electrically maintained at a constant temperature of $35 \pm 0.1^\circ\text{C}$ to approximate human skin temperature. The chamber conditions were set to $25 \pm 0.1^\circ\text{C}$ and $65 \pm 4\%$ RH. The hotplate provided the measurement of thermal resistance and apparent evaporative resistance of each fabric system according to the following equations 3.1 and 3.2.

$$R_{ct} = (T_s - T_a) A / H_s \quad (3.1)$$

where:

R_{ct}	total resistance to dry heat transfer provided by the fabric system and air layer, $\text{K}\cdot\text{m}^2/\text{W}$,
T_s	surface temperature of the plate, $^\circ\text{C}$,
T_a	air temperature, $^\circ\text{C}$,
A	area of the plate test section, m^2 ,
H_s	power input, W .

$$R_{et}^A = [(P_s - P_a) A] / [H_T - (T_s - T_a) A / R_{ct}] \quad (3.2)$$

where:

R_{et}^A	apparent total evaporative resistance of the specimen and surface air layer, $\text{K}\cdot\text{m}^2/\text{W}$,
P_s	water vapour pressure at the plate surface, kPa ,
P_a	water vapour pressure in the air flowing over the specimen, kPa ,
A	area of the plate test section, m^2 ,
H_T	power input, W ,
T_s	temperature at the test plate surface, $^\circ\text{C}$,
T_a	temperature of the air flowing over the specimen, $^\circ\text{C}$,
R_{ct}	total thermal resistance of the specimen and surface air layer, $\text{K}\cdot\text{m}^2/\text{W}$.

Thermal resistance of a fabric system is the resistance to the flow of heat from the heated surface of the hot plate through the fabric system to the cooler environment of the chamber (ASTM, 2017a, p. 2). Thermal resistance assessment of each fabric system was conducted on the hot plate surface (Figure 3.10 (a)). During the test, the total thermal resistance of a fabric system and the boundary air layer at the outer surface of the fabric was measured. To obtain the intrinsic thermal resistance of the fabric system alone, the thermal resistance of the boundary air layer, found by testing the bare plate without a fabric covering, was subtracted from the average total thermal resistance of the fabric system (see equation 3.3). The assumption was made that the boundary air layer of the bare plate and the boundary air layer of the fabric test specimen are equal (ASTM, 2017a, p. 2).

$$R_{cf} = R_{ct} - R_{cbp} \quad (3.3)$$

where:

- R_{cf} intrinsic thermal resistance provided by the fabric alone, $K \cdot m^2/W$,
- R_{ct} total resistance to dry heat transfer provided by the fabric system and air layer, $K \cdot m^2/W$,
- R_{cbp} thermal resistance value measured for the air layer, $K \cdot m^2/W$.

Apparent evaporative resistance of a fabric system is the resistance to the flow of moisture vapour from the saturated surface of the hot plate, covered with a liquid barrier, through the fabric system specimens, to the lower vapour pressure environment of the test chamber when evaluated non-isothermally under similar conditions as were used for thermal resistance evaluation (ASTM, 2017a, pp. 1-2). Condensation may occur within the fabric system when apparent evaporative resistance is measured. During the test, the hot plate was covered with an expanded polytetrafluoroethylene (ePTFE) film (liquid barrier) so that water did not contact the fabric system specimens (Figure 3.10 (b)). The permeability index of the ePTFE film was calculated by equation 3.4 and exceeded 0.7 as required by the test method. The total apparent evaporative resistance of each fabric system and the boundary air layer at the outer surface of the fabric was measured first.

$$i_m = 0.060 (R_{cbp}/R_{ebp}) \quad (3.4)$$

where:

- i_m permeability index (dimensionless),
- R_{cbp} thermal resistance of bare plate, $K \cdot m^2/W$,
- R_{ebp} evaporative resistance of bare plate covered with liquid barrier, $kPa \cdot m^2/W$.

Similar to the measurement of thermal resistance, to obtain the apparent intrinsic evaporative resistance of the fabric system alone, the evaporative resistance of the boundary air layer, found by testing the bare plate covered with ePTFE film only, was subtracted from the average total apparent evaporative resistance of the fabric system (see equation 3.5).

$$R_{ef}^A = R_{et}^A - R_{ebp} \quad (3.5)$$

where:

- R_{ef}^A apparent intrinsic evaporative resistance of the sample alone, $K \cdot m^2/W$,
- R_{et}^A apparent total evaporative resistance of the specimen and surface air layer, $K \cdot m^2/W$,
- R_{ebp} evaporative resistance value measured for the air layer and liquid barrier, $kPa \cdot m^2/W$.

During the test, the 320 x 320 mm fabric system specimens were placed on the hot plate, secured with masking tape, and brought to equilibrium with the atmosphere of the test chamber. When a steady state was reached (temperature fluctuation no more than ± 0.1 °C, RH fluctuation not more than ± 4 %), the data acquisition system recorded the total thermal resistance values or apparent evaporative resistance values for 30 minutes.

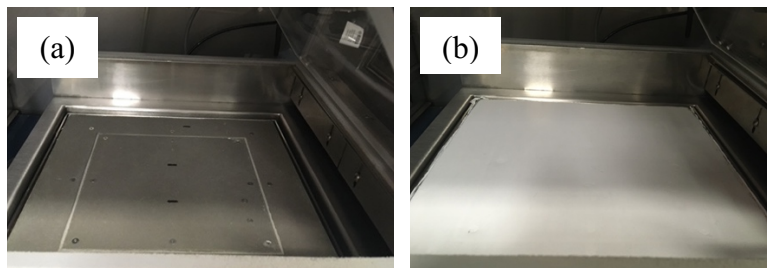


Figure 3.10 Hot plate: (a) bare plate, (b) bare plate covered with ePTFE film.

The performance of the fabric systems was evaluated by measuring thermal resistance and then apparent evaporative resistance. The THL was the amount of heat transferred through the fabric system by the combined dry and evaporative heat exchanges under the previously specified test conditions (ASTM, 2017a, p. 2). The THL value was determined by the following equation 3.6.

$$Q_t = \frac{10^\circ C}{R_{cf} + 0.04} + \frac{3.57 \text{ kPa}}{R_{ef}^A + 0.0035} \quad (3.6)$$

where:

Q_t	total heat loss, W/m ² ,
R_{cf}	average intrinsic thermal resistance of the fabric system, K·m ² /W,
R_{ef}^A	average apparent intrinsic evaporative resistance of fabric system, kPa·m ² /W,
10° C	difference between test plate surface temperature and ambient air temperature,
3.57 kPa	difference between water vapour pressure at the test plate surface and water vapour pressure in the ambient air flowing over test specimen.

3.5.2.2 Air permeability

Air permeability was determined for the fabric systems using a high-pressure differential air permeability testing apparatus (Frazier Precision Instrument Company, Hagerstown, MD, US) and following the test procedures of ASTM D 737 – Standard Test Method for Air Permeability of Textile Fabrics (ASTM, 2018b). The rate of perpendicular airflow passing through a known area under a prescribed air pressure differential between the two surfaces of the fabric system was measured (ASTM, 2019a, p.3). Figure 3.11 shows a schematic drawing of the air permeability testing apparatus. It comprises a suction fan with air discharge, two chambers with an air orifice between for controlling the amount of air flow, beveled ring mounted in the tabletop, clamps for fabric specimens, and oil reservoirs with monometers to track the air pressure.

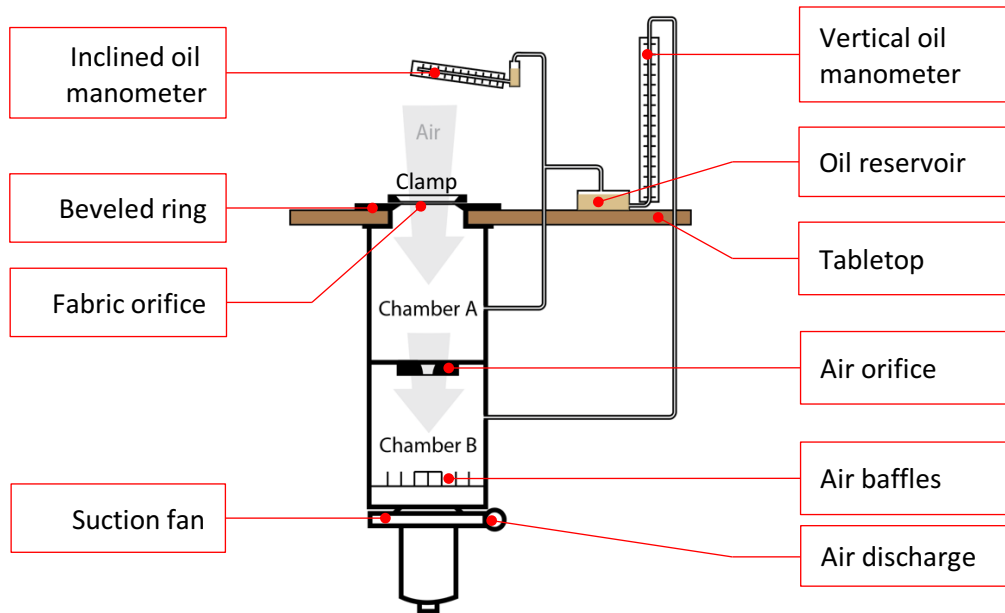


Figure 3.11 High pressure differential air permeability testing apparatus.

According to ASTM D 737, ten specimens with dimensions (140 x 140 mm) slightly greater than the clamping mechanism were taken from different locations of each fabric sample (ASTM, 2018b). Each fabric system specimen was tightly mounted between the beveled ring and the clamp before testing so that no air penetrated from the sides of the fabric system during the test (Figure 3.12). The air pressure was adjusted to provide a differential of 125 Pa (12.7 mm water gauge pressure). The volume of air passing through the specimen was measured by means of a calibrated orifice. The air permeability value for each test specimen was obtained in $\text{ft}^3/\text{ft}^2\cdot\text{min}$ and converted to $\text{L}/\text{m}^2\cdot\text{s}$.



Figure 3.12 Fabric system OL-3D1-BL mounted in clamps of air permeability testing apparatus.

3.6 Full-scale test for thermal protection assessment

The purpose of conducting a full-scale flash fire instrumented manikin test was to address the fourth research objective and assess whether the incorporation of a three-dimensional knitted fabric in the neck, shoulder, upper front and back torso, and wrist areas in the prototype shirt design of wildland firefighters' protective clothing can provide greater thermal protection from burn injuries as compared to the wildland firefighters' protective clothing shirt design that is currently in use.

3.6.1 Experimental design

Three shirts based on the design currently worn by wildland firefighters in Alberta (control shirt) and three prototype shirts were constructed for performance comparison in the full-scale flame engulfment instrumented manikin test. Garments were constructed to fit the size of the University of Alberta's instrumented manikin (Table A.1). Both control and prototype shirts were made of the same Nomex[®] IIIA fabric used as the outer layer (OL) in the bench-scale tests. A three-dimensional warp-knitted fabric Type 2 (3D2) was selected for incorporation in the areas prone to second-degree burn injury (e.g. upper front and back torso, neck, and wrists) in the construction of the prototype. The prototype shirt pattern design was developed on the basis of the pattern design of the control shirt. Both shirts had the same applied ease; thus, it is assumed that the air gap between the garment and the manikin was similar. Each shirt was tested with a whole garment ensemble, which included one shirt, one pair of pants, one t-shirt, and briefs (Figure A.9 and Figure A.10). To compare the performance of the control and prototype shirts, identical pants, t-shirts and briefs were used when the whole garment ensemble was tested.

Six identical pants in size L were supplied by Winner Garment Industries Ltd. (Edmonton, AB). They were made of Nomex[®] IIIA fabric and in the design style (GP.640) currently used by wildland firefighters. Shirts were tucked into the pants when tested on the instrumented manikin. Shirts and pants were worn on top of a cotton jersey t-shirt (BL used in all bench scale tests) and briefs (Figure A.11). Six identical cotton t-shirts from the Hanesbrands Inc. and cotton briefs from the Fruit of the Loom Inc. were purchased in size L. T-shirts were cut through the centre front to

be able to put them on the manikin, and then stapled together on the manikin before the shirts and pants were added. The control of variables such as fabric and applied ease of shirts, pants, t-shirts, and briefs eliminated the presence of confounding (extraneous) variables in the research. This approach allowed the comparison of the thermal protection between the two-layer fabric system in the control shirt design and the three-layer fabric system in the prototype shirt design in the areas prone to burn injury when the full garment ensemble was engulfed in flames during the full-scale instrumented manikin test.

Overall, there were three replicates of the garment ensemble with control shirts, and three replicates of the garment ensemble with the prototype shirts tested. The thermal protection performance of the garment ensembles was assessed and included the quantitative results and recorded qualitative observations. The quantitative results were presented as predicted percentage of total manikin body burn area (including predicted second-degree and third-degree burns). Those data were analysed by conducting one-sided independent samples t-tests. Additionally, the responses of individual sensors was recorded in absorbed heat flux and its variation with time in areas prone to second-degree burns. The afterflame was also recorded for each tested garment ensemble. The qualitative data included images taken before and after the test and recorded observations of each shirt's appearance after the test was conducted.

Before conducting the full-scale instrumented manikin test, all garments were washed, dried, and conditioned for at least 24 hours at $21 \pm 2^\circ\text{C}$ and $65 \pm 5\%$ relative humidity in accordance with ASTM D 1776 standard (ASTM, 2020c). Each garment ensemble was tested within 10 minutes of removal from the conditioning room. The washing and drying procedure are described below.

Washing and drying procedure of all garments

All garments (3 control shirts, 3 prototype shirts, 6 pants, 6 t-shirts and briefs) were washed before testing to remove any flammable residuals from mill finishes (e.g. sizing or softening agents) and to gain full relaxation shrinkage of the fabrics. They were laundered once in accordance with CAN/GSB-4.2 No.58, wash procedure 5 and drying procedure D1 equivalent to procedures IIIIE specified in CAN/CGSB-155.22 (CGSB, 2014, p.8; CGSB, 2019). The wash temperature was 50 °C, wash time 12 ± 1 minutes with moderate mechanical action and spin time of 6 ± 1 minutes. Sixty-six grams of AATCC 1993 Standard reference Detergent in 72 ± 4 liters of liquor was used for the wash cycle. The drying procedure D1 was normal tumble dry with an exhaust temperature of 66 ± 5 °C and 10 minutes of cooling down without heat at the end of the cycle.

3.6.2 Test method and equipment

The full-scale thermal protection performance of the garment ensembles that included the control and prototype shirts was assessed by the University of Alberta's flash fire instrumented manikin system in accordance with the ASTM F 1930 standard test (Dale et al., 1992; ASTM, 2018c). The instrumented manikin with 110 thermal energy sensors is designed and constructed to represent the adult-sized male human (Figure 3.13 and Table A.1). It is made from fibreglass and resin and is painted with high temperature flat black spray paint. The sensors are cylinders (1.9 cm diameter x 3.2 cm height) made from Colorceran. The feet and hands are unsensored and represent approximately 12% of the body surface that is not included in the test results. The manikin was placed in the chamber with six burner sets, each with two propane jet diffusion burners that generated the flames. The chamber had an ambient atmospheric temperature of 15 and 30 °C. It was isolated from any air movement other than the natural air flow required for the combustion process during the test. Each whole garment ensemble was exposed to propane-air diffusion flames with averaged incident heat flux of 84 kW/m² (2 cal/s·cm²) for a duration of 4 seconds. The exposure time was selected to match previous research on wildland firefighters' protective clothing (Rucker et al., 2000).



Figure 3.13 Instrumented manikin.

The data acquisition involves the thermal energy sensors, spread throughout the manikin body, and computer software. Each sensor is assigned a specific number (Figure A.8). Thermal energy transferred through and from the garment ensemble to the manikin was measured by each sensor during and after the 4-second flame exposure (120 seconds in total). Computer software collected this data, and then used it to calculate the incident heat flux and absorbed heat flux and their variations over time for each sensor. The calculated absorbed heat flux and its variation over time was used to determine the temperature within human skin and subcutaneous (body fat) layers as a function of time. The temperature history within the skin and subcutaneous layer was used to predict the beginning and severity of burn injury for each sensor. The sensor response and burn injury prediction was extrapolated to larger surroundings and represented a particular area on the manikin. The prediction of second-degree and third-degree injury after the exposure was calculated by the computer software for each area represented by the sensor. The overall percentage of predicted second-degree and third-degree injury, and total burn injury was calculated by dividing the total number of sensors with identified burn injury response by the total number of sensors on the manikin.

CHAPTER 4 THERMAL PROTECTION PERFORMANCE OF FABRIC SYSTEMS AT BENCH-SCALE LEVEL

4.1 Introduction

This chapter addresses the first objective of the research which focuses on the assessment of the thermal protection performance of three-layer fabric systems (OL-3D1-BL and OL-3D2-BL) compared to two-layer fabric systems (OL-BL, OL-BL-S, OL-S-BL) at a bench-scale level. Each fabric system was tested under dry and wet base layer conditions. Three bench-scale tests were conducted with the following variations of heat exposure: (a) flame heat source, (b) radiant heat source, and (c) combined flame and radiant heat source. The data was collected as TPP, RHR, and CHTP ratings of the fabric systems (Tables B.1, B.2, and B.3). These ratings represented the thermal energy that must be supplied to the fabric system over the time of the heat exposure until reaching a second-degree skin burn injury as predicted by the Stoll criteria. The greater the supplied thermal energy over time, the greater the thermal protection proved by the fabric system and base layer condition.

According to the CAN/CGSB-155.22 standard, fabric for wildland firefighters' protective clothing must have an average TPP value of 3 cal/cm^2 (12.5 J/cm^2) or greater in a contact test, and 6 cal/cm^2 (25.1 J/cm^2) or greater when tested with a spacer (CGSB, 2014); and an average RHR value of 30 J/cm^2 or greater (no individual value less than 25 J/cm^2) (CGSB, 2014). The NFPA 1977 standard has a similar minimum requirement for an average RHR value of the garment fabrics of not less than 7 cal/cm^2 (29.3 J/cm^2) (NFPA, 2016).

The ASTM F3538 standard test method was released recently, so there is no CHTP requirement in the CAN/CGSB-155.22 standard. However, wildland firefighters are normally exposed to a combination of flame and radiant heat and the cylindrical specimen holder is thought to represent more closely the configuration of a garment on the human body than the flat tests (Dale et al., 2000). Since the exposure heat flux for the TPP test is very similar to the heat flux for the CHTP test (approximately 84 kW/m^2), the requirement established for the TPP test may be used for the CHTP test results.

4.2 Results and discussion

A summary of the test results is presented in this chapter for each type of heat exposure. A planned pairwise comparison of the two-way ANOVA test was conducted to test the first, second, and the third null hypotheses. Additional thermocouples attached to the outer layer and the base layer of the fabric systems allowed for tracking the temperature change within the fabric systems during the flame heat exposure and the radiant heat exposure tests. Analysis of the thermocouple results is also presented.

4.2.1 Effect of exposure to a flame heat source on fabric system performance

This section addresses the first null hypothesis of the first objective of this research. It states that there is no significant difference in TPP rating between the two-layer fabric systems and three-layer fabric systems when exposed to a flame heat source with a heat flux of $83 \pm 2 \text{ kW/m}^2$ at a bench-scale level.

4.2.1.1 Summary of flame heat source exposure results

Table 4.1 and Figure 4.1 showed that all five fabric systems met the minimum requirement of average TPP ratings set by the CAN/CGSB-155.22 standard under both dry and wet base layer conditions. Fabric systems OL-3D1-BL, OL-3D2-BL, OL-BL-S, and OL-S-BL met the minimum requirement of an average TPP rating of 25.1 J/cm^2 for tests with a spacer. Despite the lowest thermal protection of the fabric system OL-BL, it also met the minimum requirement of an average TPP rating of 12.5 J/cm^2 for the contact test. The three-layer fabric systems OL-3D1-BL and OL-3D2-BL with incorporation of two types of three-dimensional warp-knitted fabrics have the greatest mean TPP ratings. The TPP rating of the two-layer fabric systems OL-BL-S and OL-S-BL tested with a 6.4 mm spacer are similar to each other and approximately half the value of the TPP ratings of three-layer systems. The lowest TPP rating was obtained for a two-layer system OL-BL in the contact test. In other words, three-layer fabric systems (OL-3D1-BL and OL-3D2-BL) provided the greatest thermal protection, and two-layer fabric system OL-BL showed the lowest

thermal protection under dry and wet base layer conditions when exposed to a flame heat source with a heat flux of $83 \pm 2 \text{ kW/m}^2$.

Table 4.1 Summary table of mean values and standard deviation of TPP results for different fabric systems under dry and wet base layer conditions when exposed to a flame heat source.

Base layer condition	Fabric system	Thermal energy (J/cm^2)	Time to 2 nd -degree burn (sec.)
Dry	OL-BL	42.7 ± 3.8	5.1 ± 0.5
	OL-BL-S	71.2 ± 1.6	8.5 ± 0.2
	OL-S-BL	74.3 ± 4.4	8.9 ± 0.5
	OL-3D1-BL	157.4 ± 7.8	18.8 ± 0.9
	OL-3D2-BL	116.0 ± 5.5	13.9 ± 0.7
Wet	OL-BL	38.0 ± 1.6	4.5 ± 0.2
	OL-BL-S	58.8 ± 1.9	7.0 ± 0.2
	OL-S-BL	64.8 ± 1.9	7.7 ± 0.2
	OL-3D1-BL	153.4 ± 5.3	18.3 ± 0.6
	OL-3D2-BL	114.0 ± 4.4	13.6 ± 0.5

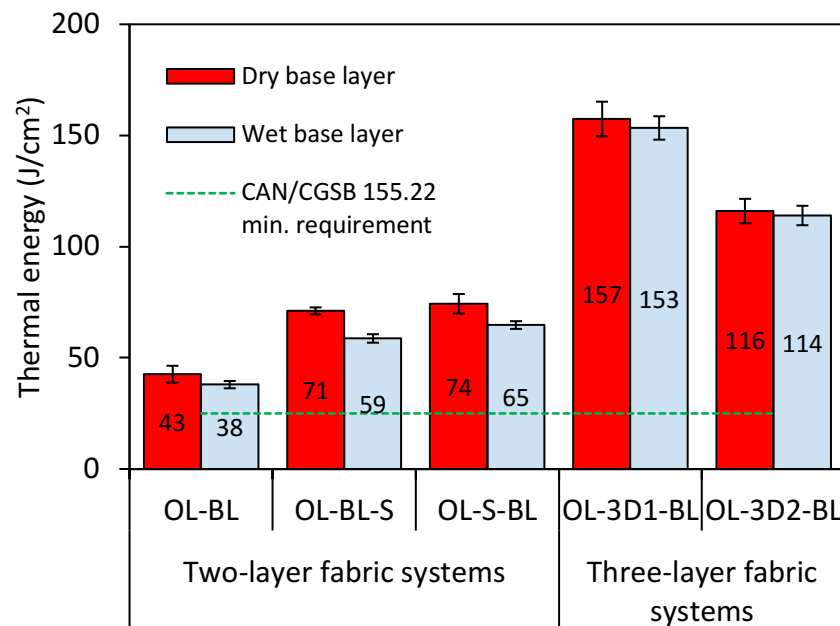


Figure 4.1 Bar chart shows average thermal energy values supplied to different fabric systems under dry and wet base layer conditions over time of flame heat source exposure until reaching a second-degree burn as predicted by the Stoll criteria.

When tested under the flame heat source, the three-layer fabric system OL-3D1-BL withstood an average thermal energy of $157.4 \pm 7.8 \text{ J/cm}^2$ over 18.8 ± 0.9 seconds under dry base layer conditions, and $153.4 \pm 5.3 \text{ J/cm}^2$ over 18.3 ± 0.6 seconds under wet base layer conditions when the predicted second-degree burn criteria was reached. The average TPP rating of the other three-layer fabric system OL-3D2-BL is slightly lower than OL-3D1-BL. Fabric system OL-3D2-BL withstood an average thermal energy of $116.0 \pm 5.5 \text{ J/cm}^2$ over 13.9 ± 0.7 seconds under dry base layer conditions, and $114.0 \pm 4.4 \text{ J/cm}^2$ over 13.6 ± 0.5 seconds under wet base layer conditions when the predicted second-degree burn criteria was reached.

When tested under the flame heat source, two-layer fabric system OL-BL-S withstood an average thermal energy of $71.2 \pm 1.6 \text{ J/cm}^2$ over 8.5 ± 0.2 seconds under dry base layer conditions, and $58.8 \pm 1.9 \text{ J/cm}^2$ over 7.0 ± 0.2 seconds under wet base layer conditions when the predicted second-degree burn criteria was reached. Fabric system OL-S-BL withstood an average thermal energy of $74.3 \pm 4.4 \text{ J/cm}^2$ over $8.9 \pm 0.5 \pm 0.7$ seconds under dry base layer conditions, and $64.8 \pm 1.9 \text{ J/cm}^2$ over 7.7 ± 0.2 seconds under wet base layer conditions when the predicted second-degree burn criteria was reached.

When tested under the flame heat source, two-layer fabric system OL-BL withstood an average thermal energy of $42.7 \pm 3.8 \text{ J/cm}^2$ over 5.1 ± 0.5 seconds under dry base layer conditions, and $38.0 \pm 1.6 \text{ J/cm}^2$ over 4.5 ± 0.2 seconds under wet base layer conditions when the predicted second-degree burn criteria was reached.

Overall, the incorporation of three-dimensional warp-knitted fabric into two-layer systems dramatically increased the mean TPP rating. Thus, it appeared that the thermal energy was impeded by still air entrapped in the three-dimensional warp-knitted fabrics in the three-layer fabric systems OL-3D1-BL and OL-3D2-BL when exposed to a flame heat source. These fabric systems required much more supplied thermal energy over a longer time of exposure to the flame heat source with a heat flux of $83 \pm 2 \text{ kW/m}^2$ before reaching a second-degree burn as predicted by the Stoll

criteria. The statistical data analysis of the differences in TPP ratings among five types of fabric systems is presented below.

4.2.1.2 Analysis of planned pairwise comparison of two-way ANOVA of flame heat source exposure results

A planned pairwise comparison of the two-way ANOVA test was used to test the first null hypotheses of the first objective of this research and showed whether the mean difference in TPP rating of the two-layer fabric systems and three-layer fabric systems is statistically significant when exposed to a flame heat source with a heat flux of $83 \pm 2 \text{ kW/m}^2$ at a bench-scale level.

The overall two-way ANOVA test showed no evidence ($F(4,40) = 2.511$; $p = .057$) that there was an interaction between the fabric system and base layer condition (Table B.4). The effect of the fabric system type on the TPP value did not depend on the base layer condition and vice versa. Thus, the main effects of the fabric systems and base layer conditions on the TPP values were considered separately. The test also showed significant difference ($F(4,40) = 1147.895$, $p < .001$) in TPP mean values among all five fabric systems. Table 4.2 presents the pairwise comparison of mean values of TPP ratings among five fabric systems. Considering more than two levels of factors, a Bonferroni correction was applied. Statistical significance (α) was set at 0.05.

Three-layer fabric systems OL-3D1-BL and OL-3D2-BL provide greater thermal protection than any of the two-layer fabric systems under the dry and wet base layer conditions when exposed to a flame heat source. There is strong evidence ($p < .001$) that the mean values of TPP ratings of the three-layer fabric systems and the two-layer fabric systems are different under the dry and wet base layer conditions.

Table 4.2 Pairwise comparison of mean TPP ratings for different fabric systems under the dry and wet base layer conditions when exposed to a flame heat source.

Base layer cond.	(I) Fabric system	(J) Fabric system	Mean difference (I-J)	Sig.	95% CI for Difference	
					Lower Bound	Upper Bound
Dry	OL-3D1-BL	OL-BL	114.7*	<.001	106.6	122.8
		OL-BL-S	86.2*	<.001	78.2	94.3
		OL-S-BL	83.1*	<.001	75.0	91.1
	OL-3D2-BL	OL-BL	73.3*	<.001	65.3	81.4
		OL-BL-S	44.9*	<.001	36.8	52.9
		OL-S-BL	41.7*	<.001	33.6	49.7
	OL-BL-S	OL-BL	28.5*	<.001	20.4	36.5
	OL-S-BL	OL-BL	31.6*	<.001	23.6	39.7
	OL-S-BL	OL-BL-S	3.2	1.000	-4.9	11.2
	Wet	OL-3D1-BL	OL-BL	115.4*	<.001	107.3
OL-BL-S			94.6*	<.001	86.6	102.7
OL-S-BL			88.6*	<.001	80.5	96.6
OL-3D2-BL		OL-BL	76.0*	<.001	68.0	84.1
		OL-BL-S	55.3*	<.001	47.2	63.3
		OL-S-BL	49.2*	<.001	41.2	57.3
OL-BL-S		OL-BL	20.8*	<.001	12.7	28.8
OL-S-BL		OL-BL	26.8*	<.001	18.7	34.8
OL-S-BL		OL-BL-S	6.0	.316	-2.0	14.1

* Means are significantly different between fabric systems under dry and wet base layer condition when subjected to a planned pairwise comparison of two-way ANOVA test ($p < .00125$).

Note. Bonferroni correction was used for the alpha value adjustment for multiple comparisons. In total 40 multiple comparisons were conducted. Only 18 comparisons of interests were reported.

Comparison between the mean TPP ratings of the fabric systems OL-3D1-BL and OL-BL showed a significant mean difference of 114.7 J/cm² with 95% CI (106.6, 122.8) under the dry base layer condition, and 115.4 J/cm² with 95% CI (107.3, 123.4) under the wet base layer condition. Comparison between the mean TPP ratings of fabric systems OL-3D1-BL and OL-BL-S showed a significant mean difference of 86.2 J/cm² with 95% CI (78.2, 94.3) under the dry base layer condition,

and 94.6 J/cm^2 with 95% CI (86.6, 102.7) under the wet base layer condition. Comparison between the mean TPP ratings of fabric systems OL-3D1-BL and OL-S-BL showed a significant mean difference of 83.1 J/cm^2 with 95% CI (75.0, 91.1) under the dry base layer condition, and 88.6 J/cm^2 with 95% CI (80.5, 96.6) under the wet base layer condition. Thus, there is strong evidence against the first null hypothesis when the mean TPP ratings of three-layer fabric systems OL-3D1-BL are compared with the mean TPP ratings of two-layer fabric systems OL-BL, OL-BL-S, and OL-S-BL.

Comparison between the mean TPP ratings of fabric system OL-3D2-BL and OL-BL showed a significant mean difference of 73.3 J/cm^2 with 95% CI (65.5, 81.4) under the dry base layer condition, and 76.0 J/cm^2 with 95% CI (65.5, 81.4) under the wet base layer condition. Comparison between the mean TPP ratings of fabric systems OL-3D2-BL and OL-BL-S showed a significant mean difference of 44.9 J/cm^2 with 95% CI (36.8, 52.9) under the dry base layer condition, and 55.3 J/cm^2 with 95% CI (47.2, 63.3) under the wet base layer condition. Comparison between the mean TPP ratings of fabric systems OL-3D2-BL and OL-S-BL showed a significant mean difference of 41.7 J/cm^2 with 95% CI (33.6, 49.7) under the dry base layer condition, and 49.2 J/cm^2 with 95% CI (41.2, 57.3) under the wet base layer condition. Thus, there is also strong evidence against the first null hypothesis when the mean TPP ratings of three-layer fabric systems OL-3D2-BL are compared with the mean TPP ratings of two-layer fabric systems OL-BL, OL-BL-S, and OL-S-BL.

In addition to testing the first null hypothesis, comparisons among the mean TPP ratings of two-layer fabric systems OL-BL, OL-BL-S, and OL-S-BL are also included in the Table 4.2. There is strong evidence ($p < .001$) that the mean TPP ratings of the fabric system OL-BL and fabric system OL-BL-S (or OL-S-BL) are different under the dry and wet base layer conditions. Comparison between the mean TPP ratings of fabric systems OL-BL-S and OL-BL showed a significant mean difference of 28.5 J/cm^2 with 95% CI (20.4, 36.5) under the dry base layer condition, and 20.8 J/cm^2 with 95% CI (12.7, 28.8) under the wet base layer condition. Comparison between the mean TPP ratings of fabric systems OL-S-BL and OL-BL

showed a significant mean difference of 31.6 J/cm^2 with 95% CI (23.6, 39.7) under the dry base layer condition, and 26.8 J/cm^2 with 95% CI (18.7, 34.8) under the wet base layer condition. However, there is no evidence ($p = 1, p = .316$) that the mean TPP ratings of the fabric system OL-BL-S and fabric system OL-S-BL are different under the dry and wet base layer conditions. Therefore, it can be concluded that the location of the air gap in a two-layer fabric system does not affect its thermal protection performance when tested in the flat specimen holder under the flame heat source with a heat flux of $83 \pm 2 \text{ kW/m}^2$.

Overall, the incorporated three-dimensional warp-knitted fabrics between the outer and base layers significantly increased TPP ratings, indicating an increase in the thermal protective properties of clothing systems with these materials. In other words, when tested under the flame heat source, the fabric systems OL-3D1-BL and OL-3D2-BL withstood significantly greater amounts of supplied thermal energy over longer time periods than any of two-layer fabric systems before reaching a predicted second-degree burn when tested under dry and wet base layer conditions.

The three-layer fabric system OL-3D1-BL and OL-3D2-BL provided 269% – 304% greater thermal protection than the two-layer fabric system OL-BL, and 112% – 161% greater thermal protection than the two-layer fabric systems with the air gaps, OL-BL-S and OL-S-BL in the TPP test. The three-layer fabric system OL-3D2-BL provided 172% – 200% greater thermal protection than the two-layer fabric system OL-BL, and 56% – 94% greater thermal protection than the two-layer fabric systems with the air gap OL-BL-S and OL-S-BL. Additionally, the two-layer fabric systems with the air gap provided 55% – 74% greater thermal protection than the two-layer fabric system without the air gap. For more detailed information on the differences in TPP rating values in percentage among three-layer and two-layer fabric systems see Table B.7.

4.2.1.3 Analysis of thermocouple response during the flame heat source exposure

This section introduces the analysis of the copper calorimeter and thermocouples response that were attached to the inner side of the outer layer and the outer side of the base layer in each fabric system during the flame heat exposure test. Table 4.3 shows the average temperature of the copper calorimeter and thermocouples recorded at the moment of reaching a predicted second-degree burn. The time needed to reach a second-degree burn is also presented in the table. Observations showed that since the outer layer fabric was the closest to the flame heat source, the average temperature of the thermocouple attached to the outer layer fabric was greater than the average temperature of thermocouples attached to the base layer fabric. The fabric systems with the wet base layer required lower temperatures and a shorter time to reach a predicted second-degree burn than the fabric systems with the dry base layer.

Table 4.3 Summary table of mean values and standard deviation of temperature of the copper calorimeter and thermocouples for different fabric systems under dry and wet base layer conditions when the Stoll criteria was reached under a flame heat source exposure.

Base layer cond.	Fabric system	Temperature (°C)			Time to 2 nd - degree burn (sec.)
		Outer layer	Base layer	Copper calorimeter	
Dry	OL-BL	414.6 ± 43.7	289.1 ± 26.7	45.3 ± 0.8	5.1 ± 0.5
	OL-BL-S	449.3 ± 58.8	370.3 ± 17.6	47.7 ± 0.7	8.5 ± 0.2
	OL-S-BL	531.4 ± 49.0	397.1 ± 47.2	48.1 ± 2.2	8.9 ± 0.5
	OL-3D1-BL	639.9 ± 71.2	196.6 ± 30.1	52.1 ± 1.4	18.8 ± 0.9
	OL-3D2-BL	640.8 ± 72.1	202.7 ± 48.4	50.3 ± 1.6	13.9 ± 0.7
Wet	OL-BL	295.4 ± 94.5	164.3 ± 49.4	45.0 ± 1.2	4.5 ± 0.2
	OL-BL-S	478.6 ± 53.8	116.9 ± 18.5	46.5 ± 1.1	7.0 ± 0.2
	OL-S-BL	515.1 ± 67.8	120.6 ± 25.2	46.8 ± 0.9	7.7 ± 0.2
	OL-3D1-BL	673.3 ± 50.0	101.8 ± 6.0	51.8 ± 2.1	18.3 ± 0.6
	OL-3D2-BL	655.5 ± 31.9	93.2 ± 8.8	50.1 ± 1.8	13.6 ± 0.5

Figure 4.2 shows the copper calorimeter and thermocouple response during the flame heat exposure test of the fabric system OL-BL. When tested with a dry base layer, the copper calorimeter needed an average time of 5.1 ± 0.5 seconds and an average temperature of $45.3 \pm 0.8^\circ\text{C}$ to reach a predicted second-degree burn. The thermocouples attached to the outer layer and base layer also reached an average temperature of $414.6 \pm 43.7^\circ\text{C}$ and $289.1 \pm 26.7^\circ\text{C}$ respectively. When tested with a wet base layer, the copper calorimeter needed an average time of 4.5 ± 0.2 seconds and an average temperature of $45.0 \pm 1.2^\circ\text{C}$ to reach a predicted second-degree burn. The thermocouples attached to the outer layer and base layer also reached an average temperature of $295.4 \pm 94.5^\circ\text{C}$ and $164.3 \pm 49.4^\circ\text{C}$ respectively.

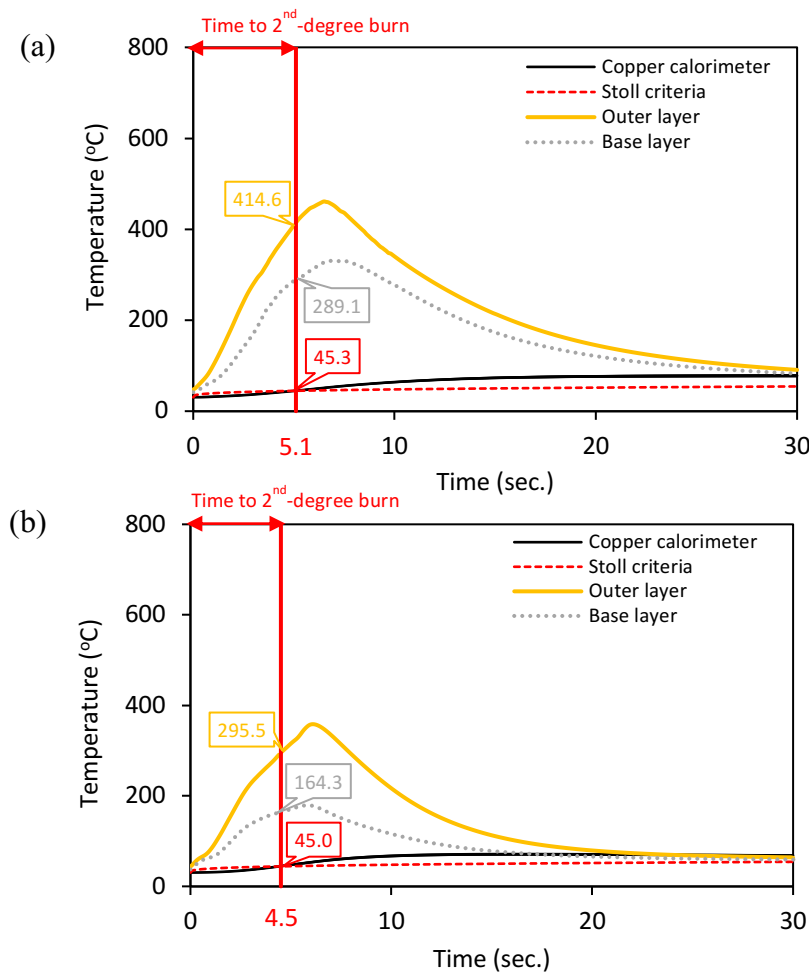


Figure 4.2 Average temperature of the copper calorimeter, and thermocouples positioned at the outer layer, and base layer of fabric system OL-BL during the flame exposure test under base layer conditions: (a) dry, and (b) wet.

Figure 4.3 shows the copper calorimeter and thermocouple response during the flame heat exposure test of the fabric system OL-BL-S. When tested with a dry base layer, the copper calorimeter needed an average time of 8.5 ± 0.2 seconds and an average temperature of $47.7 \pm 0.7^\circ\text{C}$ to reach a predicted second-degree burn. The thermocouples attached to the outer layer and base layer also reached an average temperature of $449.3 \pm 58.8^\circ\text{C}$ and $370.3 \pm 17.6^\circ\text{C}$ respectively. When tested with a wet base layer, the copper calorimeter needed an average time of 7.0 ± 0.2 seconds and an average temperature of $46.5 \pm 1.1^\circ\text{C}$ to reach a predicted second-degree burn. The thermocouples attached to the outer layer and base layer also reached an average temperature of $478.6 \pm 53.8^\circ\text{C}$ and $116.9 \pm 18.5^\circ\text{C}$ respectively.

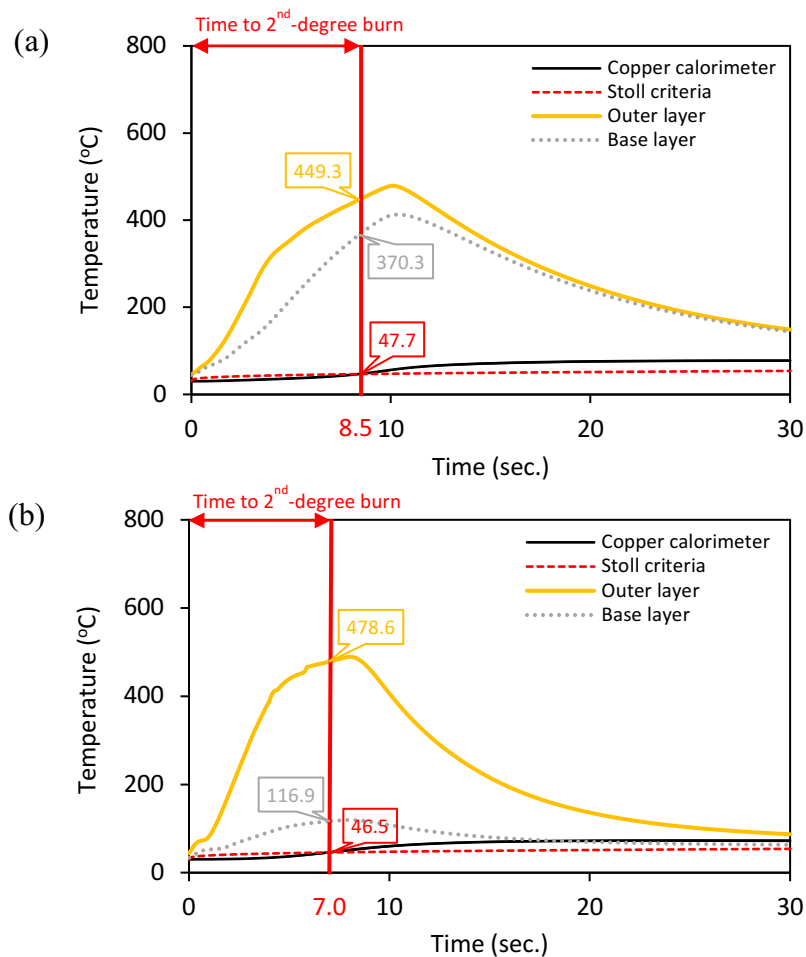


Figure 4.3 Average temperature of the copper calorimeter, and thermal couples positioned at the outer layer, and base layer of fabric system OL-BL-S during the flame exposure test under base layer conditions: (a) dry, and (b) wet.

Figure 4.4 shows the copper calorimeter and thermocouple response during the flame heat exposure test of the fabric system OL-S-BL. When tested with a dry base layer, the copper calorimeter needed an average time of 8.9 ± 0.5 seconds and an average temperature of $48.1 \pm 2.2^\circ\text{C}$ to reach a predicted second-degree burn. The thermocouples attached to the outer layer and base layer also reached an average temperature of $531.4 \pm 49.0^\circ\text{C}$ and $397.1 \pm 47.2^\circ\text{C}$ respectively. When tested with a wet base layer, the copper calorimeter needed an average time of 7.7 ± 0.2 seconds and an average temperature of $46.8 \pm 0.9^\circ\text{C}$ to reach a predicted second-degree burn. The thermocouples attached to the outer layer and base layer also reached an average temperature of $515 \pm 67.8^\circ\text{C}$ and $120.6 \pm 25.2^\circ\text{C}$ respectively.

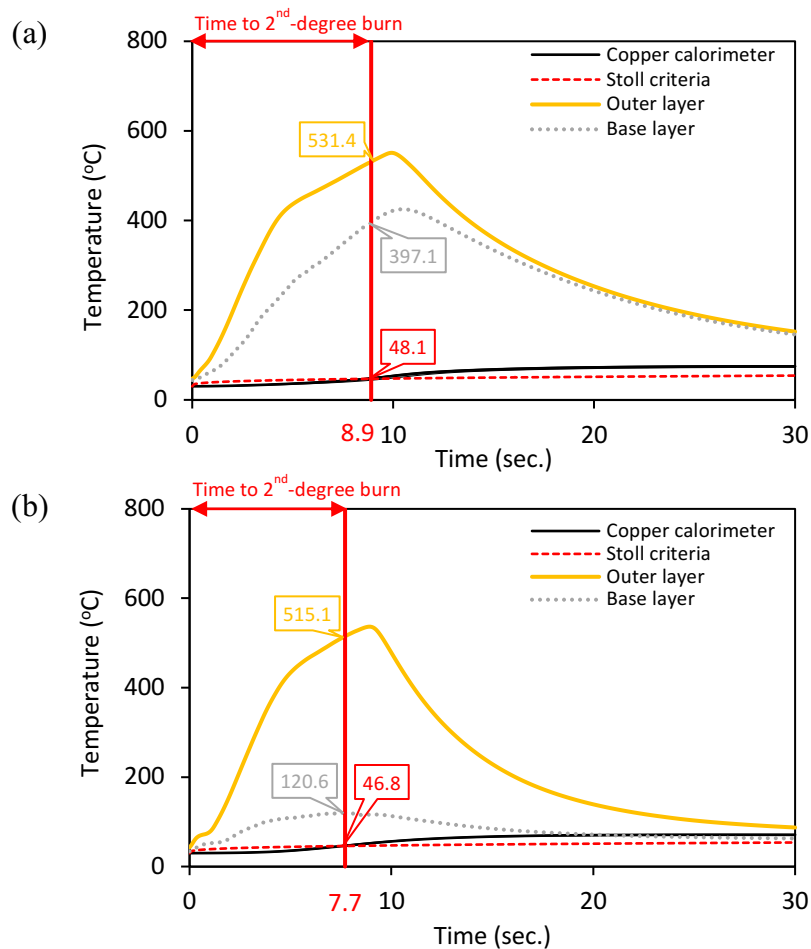


Figure 4.4 Average temperature of the copper calorimeter, and thermal couples positioned at the outer layer, and base layer of fabric system OL-S-BL during the flame exposure test under base layer conditions: (a) dry, and (b) wet.

Figure 4.5 shows the copper calorimeter and thermocouple response during the flame heat exposure test of the fabric system OL-3D1-BL. When tested with a dry base layer, the copper calorimeter needed an average time of 18.8 ± 0.9 seconds and an average temperature of $52.1 \pm 1.4^\circ\text{C}$ to reach a predicted second-degree burn. The thermocouples attached to the outer layer and base layer also reached an average temperature of $639.9 \pm 71.2^\circ\text{C}$ and $196.6 \pm 30.1^\circ\text{C}$ respectively. When tested with a wet base layer, the copper calorimeter needed an average time of 18.3 ± 0.6 seconds and an average temperature of $51.8 \pm 2.1^\circ\text{C}$ to reach a predicted second-degree burn. The thermocouples attached to the outer layer and base layer also reached an average temperature of $673.3 \pm 50.0^\circ\text{C}$ and $101.7 \pm 6.0^\circ\text{C}$ respectively.

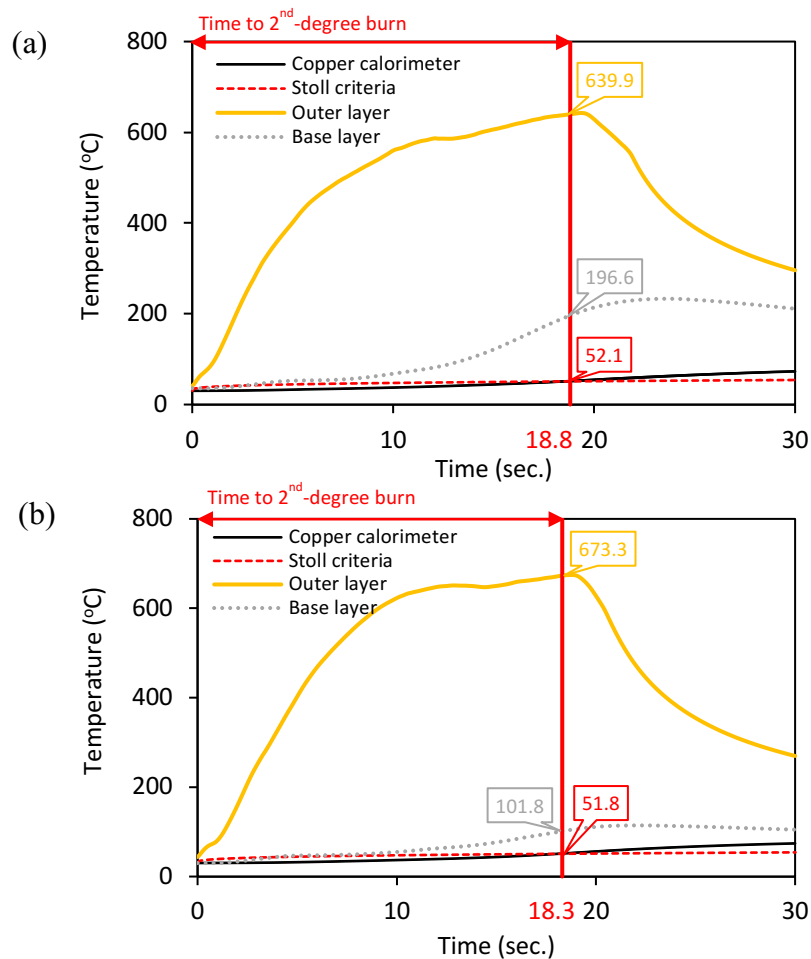


Figure 4.5 Average temperature of the copper calorimeter, and thermal couples positioned at the outer layer, and base layer of fabric system OL-3D1-BL during the flame exposure test under base layer conditions: (a) dry, and (b) wet.

Figure 4.6 shows the copper calorimeter and thermocouple response during the flame heat exposure test of the fabric system OL-3D2-BL. When tested with a dry base layer, the copper calorimeter needed an average time of 13.9 ± 0.7 seconds and an average temperature of $50.3 \pm 1.6^\circ\text{C}$ to reach a predicted second-degree burn. The thermocouples attached to the outer layer and base layer also reached an average temperature of $640.8 \pm 72.1^\circ\text{C}$ and $202.7 \pm 48.4^\circ\text{C}$ respectively. When tested with a wet base layer, the copper calorimeter needed an average time of 13.6 ± 0.5 seconds and an average temperature of $50.1 \pm 1.8^\circ\text{C}$ to reach a predicted second-degree burn. The thermocouples attached to the outer layer and base layer also reached an average temperature of $655.5 \pm 31.9^\circ\text{C}$ and $93.2 \pm 8.8^\circ\text{C}$ respectively.

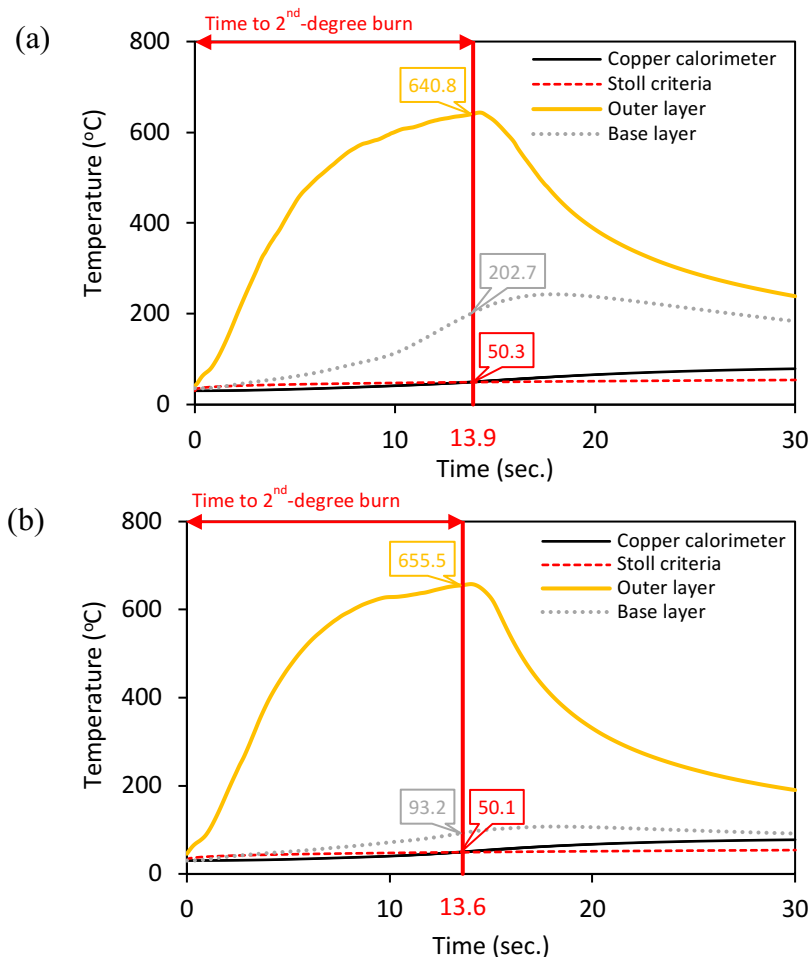


Figure 4.6 Average temperature of the copper calorimeter, and thermal couples positioned at the outer layer, and base layer of fabric system OL-3D2-BL during the flame exposure test under base layer conditions: (a) dry, and (b) wet.

Overall, when exposed to a flame heat source, the temperatures reached by the copper calorimeter ranged from 45.0°C – 52.1°C when a second-degree burn was predicted. Since the outer layer was always tested under dry conditions, the temperature required to reach a predicted second-degree burn was approximately the same within each fabric system when tested with dry or wet base layer condition. The thermocouple attached to the outer layer reached the temperature of more than 400°C for the two-layer system with no air gap OL-BL, more than 500°C for the two-layer systems with a 6.4 mm air gap OL-BL-S and OL-S-BL, and more than 600°C for the three-layer fabric systems OL-3D1-BL and OI-3D2-BL until a predicted second-degree burn occurred.

The temperatures required to reach a predicted second-degree burn were very different between the dry and wet base layer conditions of each fabric system. The thermocouple attached to the dry base layer reached the temperature of more than 250°C for the two-layer system with no air gap OL-BL, more than 350°C for the two-layer systems with a 6.4 mm air gap OL-BL-S and OL-S-BL. The temperature difference between the outer layer and dry base layer in two-layer fabric systems was approximately 150°C. Three-dimensional warp-knitted fabrics incorporated in the fabric systems OL-3D1-BL and OL-3D2-BL significantly increased thermal protection properties of these fabric systems. Thus, the thermocouple attached to the dry base layer reached the temperature of approximately 200°C for the three-layer fabric systems OL-3D1-BL and OL-3D2-BL until a predicted second-degree burn occurred. The temperature differences between the outer layer and dry base layer in three-layer fabric systems was approximately 400°C.

Interestingly, the fabric systems tested with the wet base layers tended to reach a predicted second-degree burn more quickly with much lower temperatures than the fabric systems tested with the wet base layers when exposed to flame heat source. The thermocouple attached to the wet base layer reached the temperature approximately 100°C for each fabric system until a predicted second-degree burn occurred. This phenomenon is described further in the section 4.2.4.

4.2.2 Effect of exposure to radiant heat source on fabric system performance

This section addresses the second null hypothesis of the first objective of this research. The second null hypothesis states that there is no significant difference in RHR rating between the two-layer fabric systems and three-layer fabric systems when exposed to a radiant heat source with a heat flux of $21 \pm 2.1 \text{ kW/m}^2$ at a bench-scale level.

4.2.2.1 Summary of radiant heat source exposure results

Obtained RHR results showed a similar trend as TPP results. Table 4.4 and Figure 4.7 showed that all five fabric systems also met the minimum requirement of average RHR rating of 30 J/cm^2 set by the CAN/CGSB-155.22 standard, and the minimum requirement of average RHR rating of 29.3 J/cm^2 set by NFPA 1977 standard.

Table 4.4 Summary table of mean values and standard deviation of RHR results for different fabric systems under the dry and wet base layer conditions when exposed to a radiant heat source.

Base layer condition	Fabric system	Thermal energy (J/cm^2)	Time to 2 nd -degree burn (sec.)
Dry	OL-BL	52.3 ± 2.4	24.4 ± 1.2
	OL-BL-S	86.6 ± 5.0	40.4 ± 2.3
	OL-S-BL	79.3 ± 4.5	37.0 ± 2.1
	OL-3D1-BL	157.1 ± 7.9	73.4 ± 4.3
	OL-3D2-BL	110.4 ± 3.3	51.6 ± 1.8
Wet	OL-BL	45.7 ± 1.2	21.3 ± 0.9
	OL-BL-S	82.5 ± 4.1	38.5 ± 2.5
	OL-S-BL	73.4 ± 7.1	34.3 ± 4.3
	OL-3D1-BL	142.7 ± 4.6	66.6 ± 2.6
	OL-3D2-BL	103.7 ± 4.1	48.3 ± 1.2

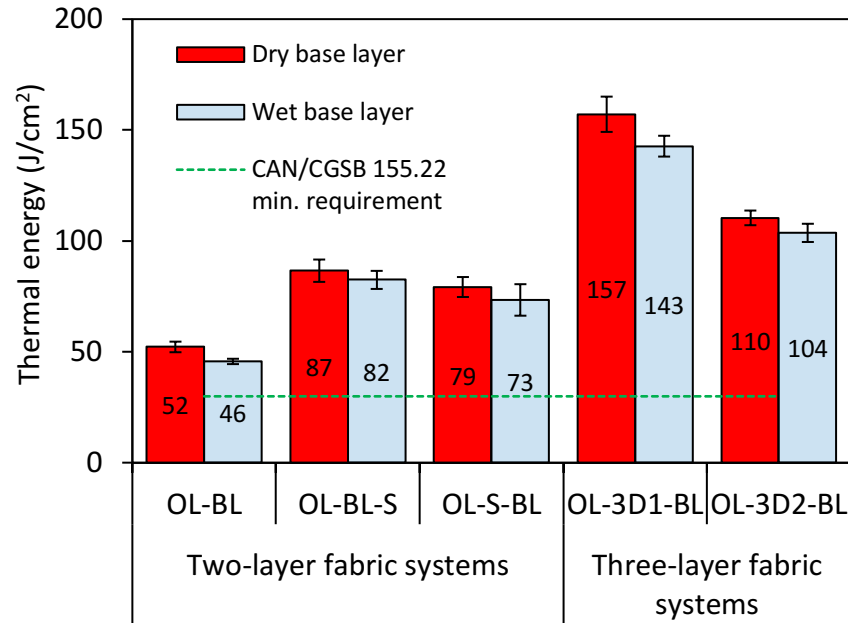


Figure 4.7 Bar chart shows average thermal energy values supplied to different fabric systems under dry and wet base layer conditions over time of radiant heat source exposure until reaching a second-degree burn as predicted by the Stoll criteria.

The three-layer fabric systems OL-3D1-BL and OL-3D2-BL with incorporation of two types of three-dimensional warp-knitted fabrics have the greatest mean values of RHR ratings. The RHR rating of two-layer fabric systems OL-BL-S and OL-S-BL tested with a 6.4 mm spacer are similar to each other and approximately half the value of the RHR ratings of the three-layer systems. The lowest RHR rating was obtained for a two-layer system OL-BL in the contact test. In other words, three-layer fabric systems (OL-3D1-BL and OL-3D2-BL) provided the greatest thermal protection, and two-layer fabric system OL-BL showed the lowest thermal protection under dry and wet base layer conditions when exposed to a radiant heat source with a heat flux of $21 \pm 2.1 \text{ kW/m}^2$.

When tested under the radiant heat source, the three-layer fabric system OL-3D1-BL withstood an average thermal energy of $157.1 \pm 7.9 \text{ J/cm}^2$ over 73.4 ± 4.3 seconds under dry base layer conditions, and $142.7 \pm 4.6 \text{ J/cm}^2$ over 66.6 ± 2.6 seconds under wet base layer conditions when the predicted second-degree burn criteria was reached. The average RHR rating of the other three-layer fabric

system OL-3D2-BL is slightly lower than OL-3D1-BL. Fabric system OL-3D2-BL withstood an average thermal energy of $110.4 \pm 3.3 \text{ J/cm}^2$ over 51.6 ± 1.8 seconds under dry base layer conditions, and $103.7 \pm 4.1 \text{ J/cm}^2$ over 48.3 ± 1.2 seconds under wet base layer conditions when the predicted second-degree burn criteria was reached.

When tested under the radiant heat source, two-layer fabric system OL-BL-S withstood an average thermal energy of $86.6 \pm 5.0 \text{ J/cm}^2$ over 40.4 ± 2.3 seconds under dry base layer conditions, and $82.5 \pm 4.1 \text{ J/cm}^2$ over 38.5 ± 2.5 seconds under wet base layer conditions when the predicted second-degree burn criteria was reached. Fabric system OL-S-BL withstands an average thermal energy of $79.3 \pm 4.5 \text{ J/cm}^2$ over 37.0 ± 2.1 seconds under dry base layer conditions, and $73.4 \pm 7.1 \text{ J/cm}^2$ over 34.3 ± 4.3 seconds under wet base layer conditions when the predicted second-degree burn criteria was reached.

When tested under the radiant heat source, two-layer fabric system OL-BL withstood an average thermal energy of $52.3 \pm 2.4 \text{ J/cm}^2$ over 24.4 ± 1.2 seconds under dry base layer conditions, and $45.7 \pm 1.2 \text{ J/cm}^2$ over 21.3 ± 0.9 seconds under wet base layer conditions when the predicted second-degree burn criteria was reached.

Overall, and similar to analysis of the TPP results, the incorporation of three-dimensional warp-knitted fabrics into two-layer systems dramatically increased the mean value of the RHR ratings. Thus, it appears that the thermal energy also is impeded by still air entrapped in three-dimensional warp-knitted fabrics in three-layer fabric systems OL-3D1-BL and OL-3D2-BL when exposed to a radiant heat source. These fabric systems required much more supplied thermal energy over a longer time of exposure to a radiant heat source with a heat flux of $21 \pm 2.1 \text{ kW/m}^2$ before the copper calorimeter reached a second-degree burn as predicted by the Stoll criteria. The statistical data analysis of the differences in RHR ratings among five types of fabric systems is presented below.

4.2.2.2 Analysis of planned pairwise comparison of two-way ANOVA of radiant heat source exposure results

A planned pairwise comparison of the two-way ANOVA test was used to test the second null hypotheses of the first objective of this research and showed whether the mean difference in RHR rating of the two-layer fabric systems and three-layer fabric systems is statistically significant when exposed to a radiant heat source with a heat flux of $21 \pm 2.1 \text{ kW/m}^2$ at a bench-scale level.

Similar to the statistical analysis in section 4.2.1.2, the overall two-way ANOVA test showed no evidence ($F(4,40) = 1.686, p = .172$) that there was an interaction between the fabric system and base layer condition when RHR values were analysed (Table B.5). The effect of the fabric system type on the RHR value did not depend on the base layer condition and vice versa. Thus, the main effects of the fabric systems and base layer conditions on the RHR values were considered separately. The test also showed significant difference ($F(4,40) = 614.162, p < .001$) in RHR mean values among all five fabric systems. Table 4.5 presents the pairwise comparison of mean values of RHR ratings among five fabric systems. Considering more than two levels of factors, a Bonferroni correction was applied. Statistical significance (α) was set at 0.05.

Three-layer fabric systems OL-3D1-BL and OL-3D2-BL provide greater thermal protection than any of the two-layer fabric systems under the dry and wet base layer conditions when exposed to a radiant heat source. Similar to the analysis of TPP results, there is strong evidence ($p < .001$) that the mean values of RHR ratings of the three-layer fabric systems and the two-layer fabric systems are different under the dry and wet base layer conditions.

Table 4.5 Pairwise comparison of mean RHR rating for different fabric systems under the dry and wet base layer conditions when exposed to a radiant heat source.

Base layer cond.	(I) Fabric system	(J) Fabric system	Mean difference (I-J)	Sig.	95% CI for Difference		
					Lower Bound	Upper Bound	
Dry	OL-3D1-BL	OL-BL	104.9*	<.001	95.8	113.9	
		OL-BL-S	70.5*	<.001	61.4	79.6	
		OL-S-BL	77.9*	<.001	68.8	86.9	
	OL-3D2-BL	OL-BL	58.2*	<.001	49.1	67.2	
		OL-BL-S	23.8*	<.001	14.7	32.9	
		OL-S-BL	31.2*	<.001	22.1	40.2	
		OL-BL-S	OL-BL	34.3*	<.001	25.3	43.4
		OL-S-BL	OL-BL	27.0*	<.001	17.9	36.1
		OL-BL-S	OL-S-BL	7.3	.208	-1.7	16.4
Wet	OL-3D1-BL	OL-BL	97.0*	<.001	87.9	106.1	
		OL-BL-S	60.3*	<.001	51.2	69.3	
		OL-S-BL	69.3*	<.001	60.2	78.4	
	OL-3D2-BL	OL-BL	57.9*	<.001	48.9	67.0	
		OL-BL-S	21.2*	<.001	12.1	30.3	
		OL-S-BL	30.2*	<.001	21.2	39.3	
		OL-BL-S	OL-BL	36.7*	<.001	27.7	45.8
		OL-S-BL	OL-BL	27.7*	<.001	18.6	36.8
		OL-BL-S	OL-S-BL	9.0	.052	-.038	18.1

* Means are significantly different between fabric systems under dry and wet base layer condition when subjected to pairwise comparison of two-way ANOVA test ($p < .00125$).

Note. Bonferroni correction was used for the alpha value adjustment for multiple comparisons. In total 40 multiple comparisons were conducted. Only 18 comparisons of interests were reported.

Comparison between the mean RHR ratings of fabric systems OL-3D1-BL and OL-BL showed a significant mean difference of 104.9 J/cm² with 95% CI (95.8, 113.9) under the dry base layer condition, and 97.0 J/cm² with 95% CI (87.9, 106.1) under the wet base layer condition. Comparison between the mean RHR ratings of fabric systems OL-3D1-BL and OL-BL-S showed a significant mean

difference of 70.5 J/cm² with 95% CI (61.4, 79.6) under the dry base layer condition, and 60.3 J/cm² with 95% CI (51.2, 69.3) under the wet base layer condition.

Comparison between the mean RHR ratings of fabric systems OL-3D1-BL and OL-S-BL showed a significant mean difference of 77.9 J/cm² with 95% CI (68.8, 86.9) under the dry base layer condition, and 69.3 J/cm² with 95% CI (60.2, 78.4) under the wet base layer condition. Thus, there is strong evidence against the second null hypothesis when the mean RHR rating of three-layer fabric system OL-3D2-BL compared with the mean RHR ratings of the two-layer fabric systems OL-BL, OL-BL-S, and OL-S-BL.

Comparison between the mean RHR ratings of fabric system OL-3D2-BL and OL-BL showed a significant mean difference of 58.2 J/cm² with 95% CI (49.1, 67.2) under the dry base layer condition, and 57.9 J/cm² with 95% CI (48.9, 67.0) under the wet base layer condition. Comparison between the mean RHR ratings of fabric systems OL-3D2-BL and OL-BL-S showed a significant mean difference of 23.8 J/cm² with 95% CI (14.7, 32.9) under the dry base layer condition, and 21.2 J/cm² with 95% CI (12.1, 30.3) under the wet base layer condition. Comparison between the mean RHR ratings of fabric systems OL-3D2-BL and OL-S-BL showed a significant mean difference of 31.2 J/cm² with 95% CI (22.1, 40.2) under the dry base layer condition, and 30.2 J/cm² with 95% CI (21.2, 39.3) under the wet base layer condition. Thus, there is also strong evidence against the second null hypothesis when the mean RHR rating of the three-layer fabric system OL-3D2-BL is compared with the mean RHR ratings of the two-layer fabric systems OL-BL, OL-BL-S, and OL-S-BL.

In addition to testing the second null hypotheses, comparisons among the mean RHR ratings of the two-layer fabric systems OL-BL, OL-BL-S, and OL-S-BL are also included in the Table 4.5. Similar to the analysis of the TPP results, there is strong evidence ($p < .001$) that the mean RHR ratings of the fabric system OL-BL and fabric system OL-BL-S (or OL-S-BL) are different under the dry and wet base layer conditions. Comparison between the mean RHR ratings of fabric systems OL-BL-S and OL-BL showed a significant mean difference of 34.3 J/cm² with

95% CI (25.3, 43.4) under the dry base layer condition, and 36.7 J/cm² with 95% CI (27.7, 45.8) under the wet base layer condition. Comparison between the mean RHR ratings of fabric systems OL-S-BL and OL-BL showed a significant mean difference of 27.0 J/cm² with 95% CI (17.9, 36.1) under the dry base layer condition, and 27.7 J/cm² with 95% CI (18.6, 36.8) under the wet base layer condition. However, there is no evidence ($p = .208$, $p = .052$) that the mean RHR ratings of the fabric system OL-BL-S and fabric system OL-BL-S are different under the dry and wet base layer conditions. Therefore, it can be concluded that the location of the air gap in two-layer fabric system does not affect its thermal protection when tested in the flat specimen holder under the radiant heat source with a heat flux of 21 ± 2.1 kW/m².

Overall, and similar to the analysis of the TPP results, the incorporated three-dimensional warp-knitted fabrics between the outer and base layers significantly increased the RHR ratings, therefore, it increased the thermal protective properties of clothing systems. In other words, when tested under the radiant heat source, the fabric systems OL-3D1-BL and OL-3D2-BL also withstood significantly greater amounts of supplied thermal energy over longer time periods than any of two-layer fabric systems before reaching a predicted second-degree burn when tested under dry and wet base layer conditions.

The three-layer fabric system OL-3D1-BL provided 200% – 212% greater thermal protection than the two-layer fabric system OL-BL with no air gap, and 73% – 98% greater thermal protection than the two-layer fabric systems OL-BL-S and OL-S-BL with a 6.4 mm air gap when tested in the flat specimen holder under the radiant heat source with a heat flux of 21 ± 2.1 kW/m². The three-layer fabric system OL-3D2-BL provided 111% – 127% greater thermal protection than the two-layer fabric system OL-BL with no air gap, and 26% – 41% greater thermal protection than the two-layer fabric systems OL-BL-S and OL-S-BL with a 6.4 mm spacer when tested in a flat specimen holder under the radiant heat source with a heat flux of 21 ± 2.1 kW/m². Additionally, the two-layer fabric systems OL-BL-S and OL-S-BL with a 6.4 mm air gap provided 52% – 80% greater thermal protection than the two-layer fabric system OL-BL with no air gap when tested in a flat specimen

holder under the radiant heat source with a heat flux of $21 \pm 2.1 \text{ kW/m}^2$. For more detailed information on the differences in RHR rating values in percentage among three-layer and two-layer fabric systems see Table B.8.

4.2.2.3 Analysis of thermocouple response during the radiant heat source exposure

This section introduces the analysis of the copper calorimeter and thermocouples response that were attached to the inner side of the outer layer and the outer side of the base layer in each fabric system during the radiant heat exposure test. Table 4.6 shows the average temperature of the copper calorimeter and thermocouples recorded at the moment of reaching a predicted second-degree burn. The time needed to reach a second-degree burn is also presented in the table. Observations showed that since the outer layer fabric was the closest to the radiant heat source, the average temperature of the thermocouple attached to the outer layer fabric was greater than the average temperature of thermocouples attached to the base layer fabric. The fabric systems with the wet base layer required lower temperatures and a shorter time to reach a predicted second-degree burn than the fabric systems with the dry base layer.

Table 4.6 Summary table of mean values and standard deviation of temperature of the copper calorimeter and thermocouples for different fabric systems under dry and wet base layer conditions when the Stoll criteria was reached under a radiant heat source exposure.

Base layer cond.	Fabric system	Temperature ($^{\circ}\text{C}$)			Time to 2 nd - degree burn (sec.)
		Outer layer	Base layer	Copper calorimeter	
Dry	OL-BL	333.0 ± 6.0	218.0 ± 29.1	53.4 ± 1.1	24.4 ± 1.2
	OL-BL-S	392.6 ± 8.5	300.4 ± 15.7	56.6 ± 1.3	40.4 ± 2.3
	OL-S-BL	374.1 ± 14.4	251.4 ± 18.1	55.3 ± 0.6	37.0 ± 2.1
	OL-3D1-BL	424.7 ± 7.4	153.9 ± 19.0	61.4 ± 1.2	73.4 ± 4.3
	OL-3D2-BL	401.2 ± 6.4	142.4 ± 17.1	58.6 ± 0.9	51.6 ± 1.8
Wet	OL-BL	270.7 ± 26.8	80.6 ± 3.5	52.2 ± 1.0	21.3 ± 0.9
	OL-BL-S	312.3 ± 8.8	85.2 ± 2.8	56.3 ± 1.2	38.5 ± 2.5
	OL-S-BL	320.3 ± 20.8	82.6 ± 6.3	55.6 ± 2.6	34.3 ± 4.3
	OL-3D1-BL	423.6 ± 11.7	77.1 ± 6.8	60.7 ± 1.0	66.6 ± 2.6
	OL-3D2-BL	389.8 ± 9.1	78.4 ± 7.2	57.9 ± 0.7	48.3 ± 1.2

Figure 4.8 shows the copper calorimeter and thermocouple response during the radiant heat exposure test of the fabric system OL-BL. When tested with a dry base layer, the copper calorimeter needed an average time of 24.4 ± 1.2 seconds and an average temperature of $53.4 \pm 1.1^\circ\text{C}$ to reach a predicted second-degree burn. The thermocouples attached to the outer layer and base layer also reached an average temperature of $333.0 \pm 6.0^\circ\text{C}$ and $218.0 \pm 29.1^\circ\text{C}$ respectively. When tested with a wet base layer, the copper calorimeter needed an average time of 21.3 ± 0.9 seconds and an average temperature of $52.2 \pm 1.0^\circ\text{C}$ to reach a predicted second-degree burn. The thermocouples attached to the outer layer and base layer also reached an average temperature of $270.7 \pm 26.8^\circ\text{C}$ and $80.6 \pm 3.5^\circ\text{C}$ respectively.

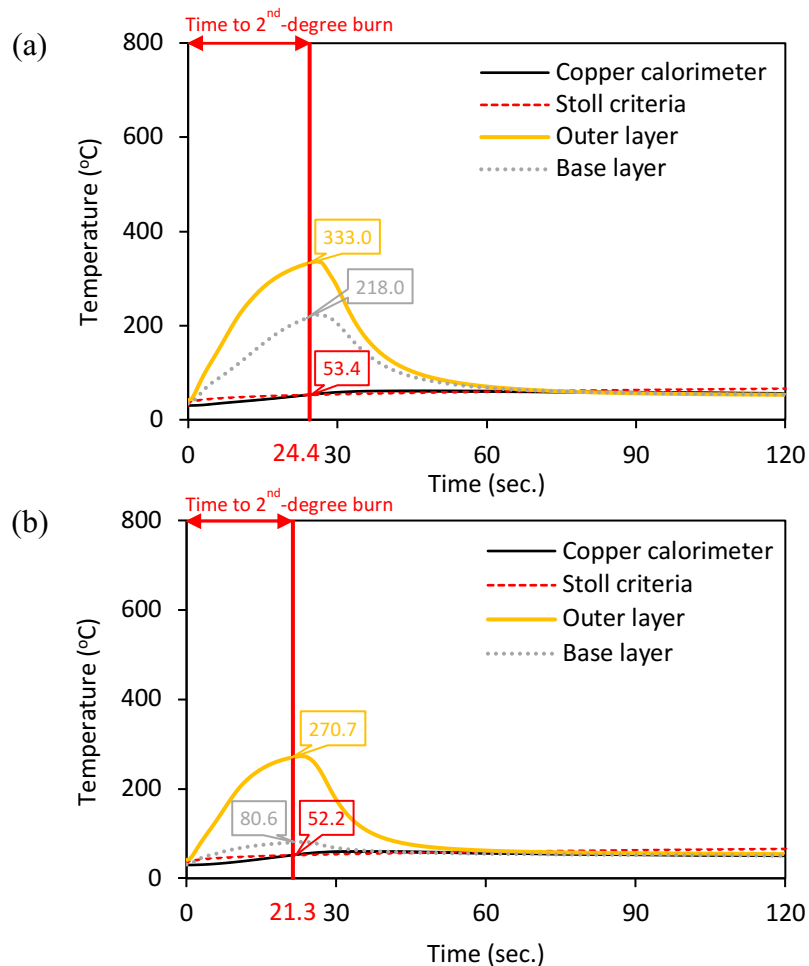


Figure 4.8 Average temperature of the copper calorimeter, and thermocouples positioned at the outer layer, and base layer of fabric system OL-BL during the radiant exposure test under base layer conditions: (a) dry, and (b) wet.

Figure 4.9 shows the copper calorimeter and thermocouple response during the radiant heat exposure test of the fabric system OL-BL-S. When tested with a dry base layer, the copper calorimeter needed an average time of 40.4 ± 2.3 seconds and an average temperature of $56.6 \pm 1.3^\circ\text{C}$ to reach a predicted second-degree burn. The thermocouples attached to the outer layer and base layer also reached an average temperature of $392.6 \pm 8.5^\circ\text{C}$ and $300.4 \pm 15.7^\circ\text{C}$ respectively. When tested with a wet base layer, the copper calorimeter needed an average time of 38.5 ± 2.5 seconds and an average temperature of $56.3 \pm 1.2^\circ\text{C}$ to reach a predicted second-degree burn. The thermocouples attached to the outer layer and base layer also reached an average temperature of $312.3 \pm 8.8^\circ\text{C}$ and $85.2 \pm 2.8^\circ\text{C}$ respectively.

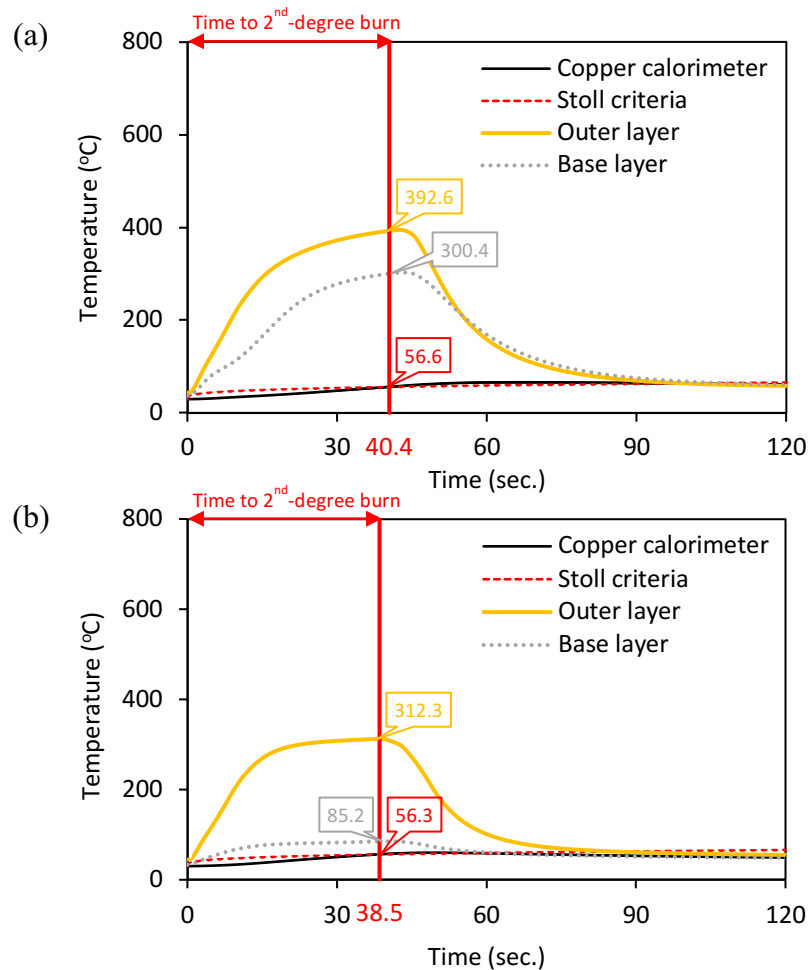


Figure 4.9 Average temperature of the copper calorimeter, and thermal couples positioned at the outer layer, and base layer of fabric system OL-BL-S during the radiant exposure test under base layer conditions: (a) dry, and (b) wet.

Figure 4.10 shows the copper calorimeter and thermocouple response during the radiant heat exposure test of the fabric system OL-S-BL. When tested with a dry base layer, the copper calorimeter needed an average time of 37.0 ± 2.1 seconds and an average temperature of $55.3 \pm 0.6^\circ\text{C}$ to reach a predicted second-degree burn. The thermocouples attached to the outer layer and base layer also reached an average temperature of $374.1 \pm 14.4^\circ\text{C}$ and $251.4 \pm 18.1^\circ\text{C}$ respectively. When tested with a wet base layer, the copper calorimeter needed an average time of 34.3 ± 4.3 seconds and an average temperature of $55.6 \pm 2.6^\circ\text{C}$ to reach a predicted second-degree burn. The thermocouples attached to the outer layer and base layer also reached an average temperature of $320.3 \pm 20.8^\circ\text{C}$ and $82.6 \pm 6.3^\circ\text{C}$ respectively.

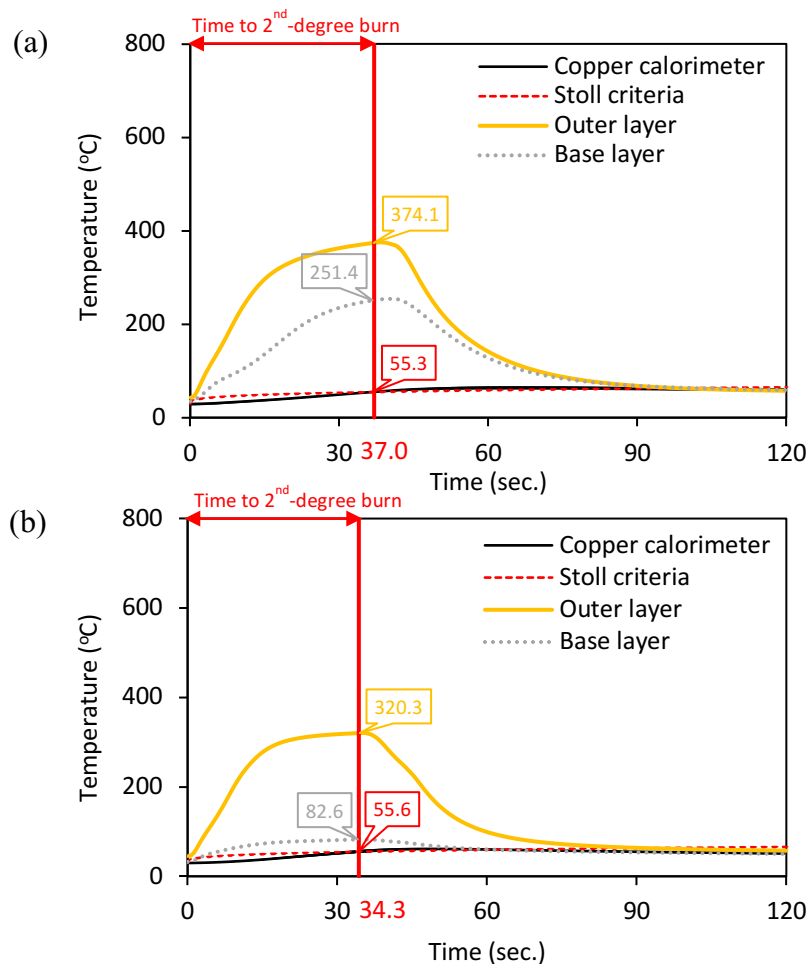


Figure 4.10 Average temperature of the copper calorimeter, and thermal couples positioned at the outer layer, and base layer of fabric system OL-S-BL during the radiant exposure test under base layer conditions: (a) dry, and (b) wet.

Figure 4.11 shows the copper calorimeter and thermocouple response during the radiant heat exposure test of the fabric system OL-3D1-BL. When tested with a dry base layer, the copper calorimeter needed an average time of 73.4 ± 4.3 seconds and an average temperature of $61.4 \pm 1.2^\circ\text{C}$ to reach a predicted second-degree burn. The thermocouples attached to the outer layer and base layer also reached an average temperature of $424.7 \pm 7.4^\circ\text{C}$ and $153.9 \pm 19.0^\circ\text{C}$ respectively. When tested with a wet base layer, the copper calorimeter needed an average time of 66.6 ± 2.6 seconds and an average temperature of $60.7 \pm 1.0^\circ\text{C}$ to reach a predicted second-degree burn. The thermocouples attached to the outer layer and base layer also reached an average temperature of $423.6 \pm 11.7^\circ\text{C}$ and $77.1 \pm 6.8^\circ\text{C}$ respectively.

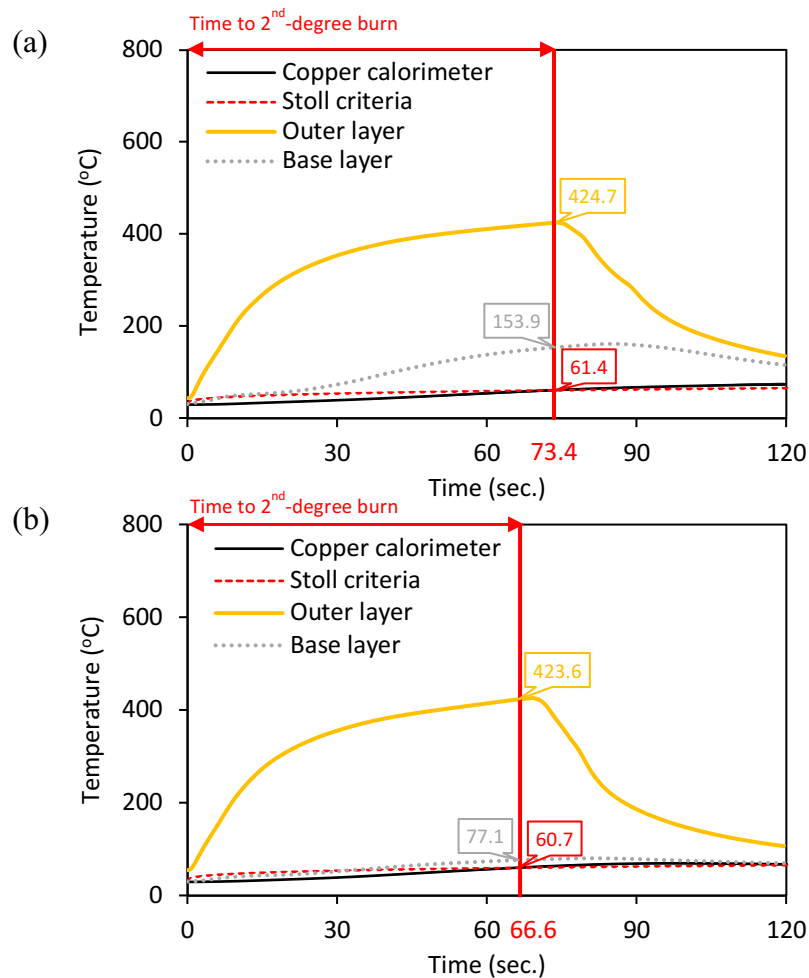


Figure 4.11 Average temperature of the copper calorimeter, and thermal couples positioned at the outer layer, and base layer of fabric system OL-3D1-BL during the radiant exposure test under base layer conditions: (a) dry, and (b) wet.

Figure 4.12 shows the copper calorimeter and thermocouple response during the radiant heat exposure test of the fabric system OL-3D2-BL. When tested with a dry base layer, the copper calorimeter needed an average time of 51.6 ± 1.8 seconds and an average temperature of $58.6 \pm 0.9^\circ\text{C}$ to reach a predicted second-degree burn. The thermocouples attached to the outer layer and base layer also reached an average temperature of $401.2 \pm 6.4^\circ\text{C}$ and $142.4 \pm 17.1^\circ\text{C}$ respectively. When tested with a wet base layer, the copper calorimeter needed an average time of 48.3 ± 1.2 seconds and an average temperature of $57.9 \pm 0.7^\circ\text{C}$ to reach a predicted second-degree burn. The thermocouples attached to the outer layer and base layer also reached an average temperature of $389.8 \pm 9.1^\circ\text{C}$ and $78.4 \pm 7.2^\circ\text{C}$ respectively.

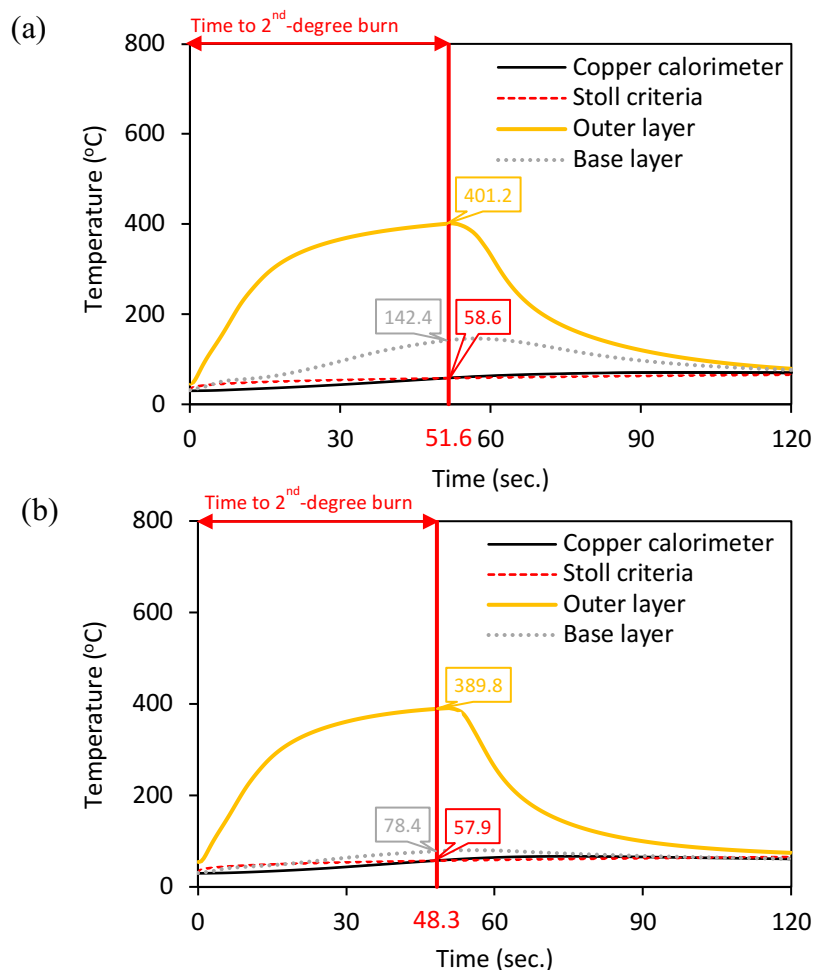


Figure 4.12 Average temperature of the copper calorimeter, and thermal couples positioned at the outer layer, and base layer of fabric system OL-3D2-BL during the radiant exposure test under base layer conditions: (a) dry, and (b) wet.

Overall, the analysis of the thermocouple response for the radiant heat exposure was similar to the response for the flame heat exposure. When exposed to a radiant heat source, the temperatures reached by the copper calorimeter range from 51.9°C to 60.9°C when a second-degree burn was predicted. Since the outer layer was always dry, the temperature required to reach a predicted second-degree burn was approximately the same within each fabric system when tested with dry or wet base layer conditions. The thermocouple attached to the outer layer reached the temperature of approximately 300°C for the two-layer system with no air gap OL-BL, approximately 350°C for the two-layer systems with a 6.4 mm air gap OL-BL-S and OL-S-BL, and approximately 400°C for the three-layer fabric systems OL-3D1-BL and OL-3D2-BL until a predicted second-degree burn occurred.

The temperatures they were reached when a predicted second-degree burn occurred were very different between the dry and wet base layer conditions of each fabric system. The thermocouple attached to the dry base layer reached the temperature of approximately 250°C for the two-layer system with no air gap OL-BL, approximately 150°C for the two-layer systems with a 6.4 mm air gap OL-BL-S and OL-S-BL. The temperature difference between the outer layer and dry base layer in two-layer fabric systems was approximately 100°C. Three-dimensional warp-knitted fabrics incorporated in the fabric systems OL-3D1-BL and OL-3D2-BL significantly increased thermal protection properties of these fabric systems. Thus, the thermocouple attached to the dry base layer reached the temperature of approximately 150°C for the three-layer fabric systems OL-3D1-BL and OL-3D2-BL when a predicted second-degree burn occurred. The temperature differences between the outer layer and dry base layer in the three-layer fabric systems was approximately 250°C. Interestingly, the fabric systems tested with the wet base layers also tended to reach a predicted second-degree burn faster at lower temperatures than the fabric systems tested with the wet base layers when exposed to a radiant heat source. The thermocouple attached to the wet base layer reached the temperature approximately 80°C for each fabric system until a predicted second-degree burn occurred.

4.2.3 Effect of exposure to a combined flame and radiant heat source on fabric system performance

This section addresses the third null hypothesis of the first objective of this research. It states that there is no significant difference in CHTP rating between the two-layer fabric systems and three-layer fabric systems when exposed to a combined flame and radiant heat source with a heat flux of $84 \pm 2 \text{ kW/m}^2$ at a bench-scale level.

4.2.3.1 Summary of combined flame and radiant heat source exposure results

The obtained CHTP results showed a similar trend as the TPP and RHR results. Table 4.7 and Figure 4.13 illustrate that similar to the TPP results, all five fabric systems with obtained CHTP ratings met the minimum requirement. The minimum requirement established for the TPP was also used for the CHTP test results.

Table 4.7 Summary table of mean values and standard deviation of CHTP results for different fabric systems under the dry and wet base layer conditions when exposed to a combined flame and radiant heat source.

Base layer condition	Fabric system	Thermal energy (J/cm^2)	Time to 2 nd -degree burn (sec.)
Dry	OL-BL	29.3 ± 1.0	3.4 ± 0.1
	OL-BL-S	54.1 ± 2.8	6.3 ± 0.3
	OL-S-BL	42.0 ± 0.8	4.9 ± 0.1
	OL-3D1-BL	125.9 ± 0.5	14.8 ± 0.1
	OL-3D2-BL	95.2 ± 1.5	11.2 ± 0.2
Wet	OL-BL	29.2 ± 1.1	3.4 ± 0.1
	OL-BL-S	49.6 ± 1.8	5.8 ± 0.2
	OL-S-BL	42.8 ± 1.1	5.0 ± 0.1
	OL-3D1-BL	117.8 ± 1.1	13.8 ± 0.1
	OL-3D2-BL	89.5 ± 1.0	10.5 ± 0.1

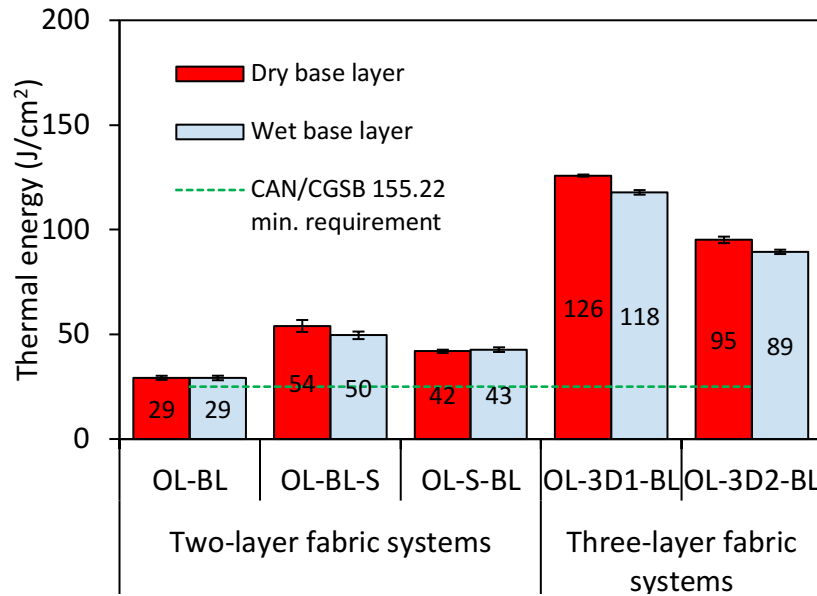


Figure 4.13 Bar chart shows average thermal energy values supplied to different fabric systems under dry and wet base layer conditions over time of combined flame and radiant heat source exposure until reaching a second-degree burn as predicted by the Stoll criteria.

Three-layer fabric systems OL-3D1-BL and OL-3D2-BL with incorporation of two types of three-dimensional warp-knitted fabrics have the greatest mean CHTP ratings. Unlike TPP and RHR ratings, the CHTP rating of two-layer fabric system OL-BL-S was slightly greater than the CHTP rating of fabric system OL-S-BL tested with a 6.35 mm air gap. However, the CHTP ratings of both systems were still very close and approximately half the value of the CHTP ratings of three-layer systems. The lowest CHTP rating was obtained for a two-layer system OL-BL in the contact test. In other words, three-layer fabric systems (OL-3D1-BL and OL-3D2-BL) provided the greatest thermal protection, and two-layer fabric system OL-BL showed the lowest thermal protection under dry and wet base layer conditions when exposed to a combined flame and radiant heat source with a heat flux of $84 \pm 2 \text{ kW/m}^2$.

When tested under the combined flame and radiant heat source, the three-layer fabric system OL-3D1-BL withstood an average thermal energy of $125.9 \pm 0.5 \text{ J/cm}^2$ over 14.8 ± 0.1 seconds under dry base layer conditions, and $117.8 \pm 1.1 \text{ J/cm}^2$ over 13.8 ± 0.1 seconds under wet base layer conditions when the

predicted second-degree burn criteria was reached. The average CHTP rating of the other three-layer fabric system OL-3D2-BL was lower than OL-3D1-BL. Fabric system OL-3D2-BL withstood an average thermal energy of $95.2 \pm 1.5 \text{ J/cm}^2$ over 11.2 ± 0.2 seconds under dry base layer conditions, and $89.5 \pm 1.0 \text{ J/cm}^2$ over 10.5 ± 0.1 seconds under wet base layer conditions when the predicted second-degree burn criteria was reached.

When tested under the combined flame and radiant heat source, two-layer fabric system OL-BL-S withstood an average thermal energy of $54.1 \pm 2.8 \text{ J/cm}^2$ over 6.3 ± 0.3 seconds under dry base layer conditions, and $49.6 \pm 1.8 \text{ J/cm}^2$ over 5.8 ± 0.2 seconds under wet base layer conditions when the predicted second-degree burn criteria was reached. Fabric system OL-S-BL withstands an average thermal energy of $42.0 \pm 0.8 \text{ J/cm}^2$ over 4.9 ± 0.1 seconds under dry base layer conditions, and $42.8 \pm 1.1 \text{ J/cm}^2$ over 5.0 ± 0.1 seconds under wet base layer conditions when the predicted second-degree burn criteria was reached.

When tested under the combined flame and radiant heat source, two-layer fabric system OL-BL withstood an average thermal energy of $29.3 \pm 1.0 \text{ J/cm}^2$ over 3.4 ± 0.1 seconds under dry base layer conditions, and $29.2 \pm 1.1 \text{ J/cm}^2$ over 3.4 ± 0.1 seconds under wet base layer conditions when the predicted second-degree burn criteria was reached.

Overall, and similar to the analysis of TPP and RHR results, the incorporation of three-dimensional warp-knitted fabric into the two-layer fabric systems substantially increased the mean CHTP ratings. Thus, it appeared that the thermal energy was impeded by still air entrapped in the three-dimensional warp-knitted fabrics in the three-layer fabric systems OL-3D1-BL and OL-3D2-BL when exposed to a combined flame and radiant heat source. These fabric systems required much more supplied thermal energy over a longer time of exposure before reaching a second-degree burn as predicted by the Stoll criteria. The statistical data analysis of the differences in CHTP ratings among five types of fabric systems is presented below.

4.2.3.2 Analysis of planned pairwise comparison of two-way ANOVA of combined flame and radiant heat source exposure results

A planned pairwise comparison of the two-way ANOVA test used to test the third null hypotheses of the first objective of this research showed that the mean difference in CTHP rating of the two-layer fabric systems and three-layer fabric systems was statistically significant when exposed to a combined flame and radiant heat source with a heat flux of $84 \pm 2 \text{ kW/m}^2$.

Unlike the statistical analyses in section 4.2.1.2 and 4.2.2.2, the overall two-way ANOVA test for CHTP rating results showed strong evidence ($F(4,40) = 17.352$, $p < .001$) that there was an interaction between the fabric system and the base layer condition when CHTP values were analysed (Table B.6). Meaning that the CHTP ratings obtained for dry and wet base layer conditions did not show consistent results among the five fabric systems like the previous tests, where TPP and RHR ratings of the dry base layer conditions were always higher than the wet conditions. Figure 4.13 and Table B.12 show that fabric system OL-S-BL has a CHTP rating for the wet base layer condition that is higher than for the dry condition. However, the difference between them was not statistically significant ($p = .376$). Conducting more tests for fabric system OL-S-BL could be suggested to clarify the interaction effect. Thus, in spite of significant interaction shown in by overall ANOVA test, the main effects of the fabric systems and base layer conditions on CHTP values were also considered separately. The test showed significant difference ($F(4,40) = 7257.614$, $p < .001$) in CHTP mean values among all five fabric systems. Table 4.8 presents the pairwise comparison of mean CHTP ratings among five fabric systems. Considering more than two levels of factors, a Bonferroni correction was applied. Statistical significance (α) was set at 0.05.

Three-layer fabric systems OL-3D1-BL and OL-3D2-BL provided greater thermal protection than any of the two-layer fabric systems under the dry and wet base layer conditions. Similar to the analysis of the TPP and RHR results, there was strong evidence ($p < .001$) that the mean CHTP ratings of the three-layer fabric

systems and the two-layer fabric systems are different under the dry and wet base layer conditions.

Table 4.8 Pairwise comparison of mean CHTP ratings for different fabric systems under the dry and wet base layer conditions when exposed to a combined flame and radiant heat source.

Base layer cond.	(I) Fabric system	(J) Fabric system	Mean difference (I-J)	Sig.	95% CI for Difference	
					Lower Bound	Upper Bound
Dry	OL-3D1-BL	OL-BL	96.5*	<.001	93.8	99.2
		OL-BL-S	71.8*	<.001	69.1	74.5
		OL-S-BL	83.9*	<.001	81.2	86.6
	OL-3D2-BL	OL-BL	65.8*	<.001	63.1	68.5
		OL-BL-S	41.1*	<.001	38.4	43.8
		OL-S-BL	53.2*	<.001	50.5	55.9
	OL-BL-S	OL-BL	24.7*	<.001	22.0	27.4
	OL-S-BL	OL-BL	12.6*	<.001	9.9	15.3
	OL-BL-S	OL-S-BL	12.1*	<.001	9.4	14.8
Wet	OL-3D1-BL	OL-BL	88.6*	<.001	85.9	91.3
		OL-BL-S	68.2*	<.001	65.6	70.9
		OL-S-BL	75.1*	<.001	72.4	77.7
	OL-3D2-BL	OL-BL	60.2*	<.001	57.5	62.8
		OL-BL-S	39.8*	<.001	37.2	42.5
		OL-S-BL	46.7*	<.001	44.0	49.4
	OL-BL-S	OL-BL	20.3*	<.001	17.7	23.0
	OL-S-BL	OL-BL	13.5*	<.001	10.8	16.2
	OL-BL-S	OL-S-BL	6.8*	<.001	4.2	9.5

* Means are significantly different between fabric systems under dry and wet base layer conditions when subjected to pairwise comparison of the two-way ANOVA test ($p < .00125$).

Note. Bonferroni correction was used for the alpha value adjustment for multiple comparisons. In total 40 multiple comparisons were conducted. Only 18 comparisons of interests were reported.

Comparison between the mean CHTP ratings of fabric system OL-3D1-BL and OL-BL showed a significant mean difference of 96.5 J/cm² with 95% CI

(93.8, 99.2) under the dry base layer condition, and 88.6 J/cm² with 95% CI (85.9, 91.3) under the wet base layer condition. Comparison between the mean CHTP ratings of fabric systems OL-3D1-BL and OL-BL-S showed a significant mean difference of 71.8 J/cm² with 95% CI (69.1, 74.5) under the dry base layer condition, and 68.2 J/cm² with 95% CI (65.6, 70.9) under the wet base layer condition. Comparison between the mean CHTP ratings of fabric systems OL-3D1-BL and OL-S-BL showed a significant mean difference of 83.9 J/cm² with 95% CI (81.2, 86.6) under the dry base layer condition, and 75.1 J/cm² with 95% CI (72.4, 77.7) under the wet base layer condition. Thus, there was strong evidence against the third null hypothesis when the mean CHTP rating of three-layer fabric system OL-3D2-BL was compared with the mean CHTP ratings of the two-layer fabric systems OL-BL, OL-BL-S, and OL-S-BL.

Comparison between the mean CHTP ratings of fabric system OL-3D2-BL and OL-BL showed a significant mean difference of 65.8 J/cm² with 95% CI (63.1, 68.5) under the dry base layer condition, and 60.2 J/cm² with 95% CI (57.5, 62.8) under the wet base layer condition. Comparison between the mean CHTP ratings of fabric systems OL-3D2-BL and OL-BL-S showed a significant mean difference of 41.1 J/cm² with 95% CI (38.4, 43.8) under the dry base layer condition, and 39.8 J/cm² with 95% CI (37.2, 42.5) under the wet base layer condition. Comparison between the mean CHTP ratings of fabric systems OL-3D2-BL and OL-S-BL showed a significant mean difference of 53.2 J/cm² with 95% CI (50.5, 55.9) under the dry base layer condition, and 46.7 J/cm² with 95% CI (44.9, 49.4) under the wet base layer condition. Thus, there was also strong evidence against the third null hypothesis when the mean CHTP rating of three-layer fabric system OL-3D2-BL was compared with the mean values of CHTP ratings of the two-layer fabric systems OL-BL, OL-BL-S, and OL-S-BL.

In addition to testing the third null hypotheses, comparisons among the mean CHTP ratings of the two-layer fabric systems OL-BL, OL-BL-S, and OL-S-BL are also included in the Table 4.9. Similar to the analysis of TPP and RHR results, there was strong evidence ($p < .001$) that the mean CHTP ratings of the fabric system OL-

BL and fabric system OL-BL-S (or OL-S-BL) are different under the dry and wet base layer conditions. Comparison between the mean CHTP ratings of fabric systems OL-BL-S and OL-BL showed a significant mean difference of 24.7 J/cm² with 95% CI (22.0, 27.4) under the dry base layer condition, and 20.3 J/cm² with 95% CI (17.7, 23.0) under the wet base layer condition. Comparison between the mean CHTP ratings of fabric systems OL-S-BL and OL-BL showed a significant mean difference of 12.6 J/cm² with 95% CI (9.9, 15.3) under the dry base layer condition, and 13.5 J/cm² with 95% CI (10.8, 16.2) under the wet base layer condition.

Unlike the analysis of the TPP and RHR results, there was strong evidence ($p < .001$) that the mean CHTP ratings of the fabric system OL-BL-S and fabric system OL-S-BL are different under the dry and wet base layer conditions. Comparison between the mean CHTP ratings of fabric systems OL-BL-S and OL-S-BL showed a significant mean difference of 12.1 J/cm² with 95% CI (9.4, 14.8) under the dry base layer condition, and 6.8 J/cm² with 95% CI (4.2, 9.5) under the wet base layer condition.

Overall, and similar to the analysis of TPP and RHR results, the incorporated three-dimensional warp-knitted fabrics between the outer and base layers significantly increased the CHTP ratings, therefore, it increased the thermal protective properties of the clothing systems. In other words, when tested under the combined flame and radiant heat source, the fabric systems OL-3D1-BL and OL-3D2-BL also withstood significantly greater amounts of supplied thermal energy over longer time periods than any of two-layer fabric systems before reaching a predicted second-degree burn when tested under dry and wet base layer conditions.

The three-layer fabric system OL-3D1-BL provided 303% – 329% greater thermal protection than the two-layer fabric system OL-BL with no air gap, and 133% – 200% greater thermal protection than the two-layer fabric systems OL-BL-S and OL-S-BL with a 6.35 mm air gap when tested in the cylindrical specimen holder under the combined flame and radiant heat source with a heat flux of 84 ± 2 kW/m². The three-layer fabric system OL-3D2-BL provided 206% – 225% greater thermal

protection than the two-layer fabric system OL-BL with no air gap, and 76% – 127% greater thermal protection than the two-layer fabric systems OL-BL-S and OL-S-BL with a 6.35 mm air gap when tested in the cylindrical specimen holder under the combined flame and radiant heat source with a heat flux of $84 \pm 2 \text{ kW/m}^2$.

The two-layer fabric systems OL-BL-S with a 6.35 mm air gap provided 69% – 84% greater thermal protection than the two-layer fabric system OL-BL with no air gap when tested in the cylindrical specimen holder under the combined flame and radiant heat source with a heat flux of $84 \pm 2 \text{ kW/m}^2$. The two-layer fabric systems OL-S-BL with a 6.35 mm air gap provided 43% – 46% greater thermal protection than the two-layer fabric system OL-BL with no air gap when tested in the cylindrical specimen holder under the combined flame and radiant heat source with a heat flux of $84 \pm 2 \text{ kW/m}^2$. The thermal protection of fabric system OL-BL-S was 15% – 29% greater than the thermal protection of fabric system OL-S-BL. Thus, the location of the air gap between the copper calorimeter and the base layer in two-layer fabric system provides greater thermal protection performance when tested in the cylindrical specimen holder under the combined flame and radiant heat source with a heat flux of $84 \pm 2 \text{ kW/m}^2$. For more detailed information on the differences in the CHTP ratings in percentage among the three-layer and two-layer fabric systems see Table B.12.

The difference in the CHTP performance of OL-S-BL and OL-BL-S fabric systems occurs due to different behaviour of the thermal shrinkage of the aramid outer layer in different fabric systems during the heat exposure. Figure 4.14 shows the example of the latter fabric systems mounted in the in the CHTP specimen holder after exposure by combined flame and radiant heat.

In the fabric system OL-BL-S, the cotton base layer was mounted in contact with the aramid outer layer, and the air gap was located between the base layer and the copper calorimeter. When the fabric system was exposed to a heat source, the air gap was slightly reduced because of the thermal shrinkage of the aramid outer layer fabric. Since the cotton base layer behind did not shrink, it prevented the aramid outer layer fabric from fully shrinking and reducing the air gap (Figure 4.14(a)).

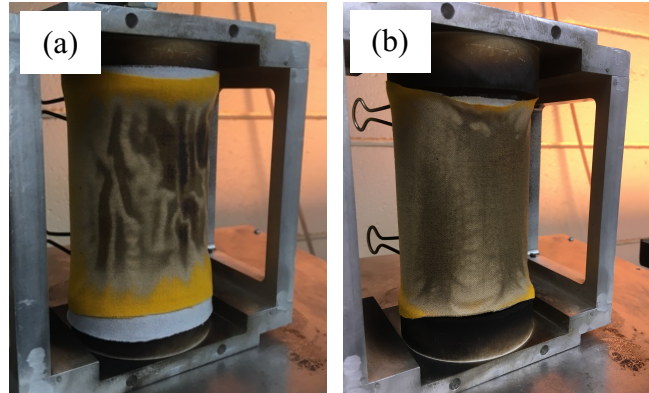


Figure 4.14 Fabric systems mounted in the CHTP specimen holder when tested (a) OL-BL-S, and (b) OL-S-BL.

In the fabric system OL-S-BL, the cotton base layer was mounted in contact with the copper calorimeter, and the air gap was located between the base layer and the outer layer. When the fabric system was exposed to a heat source in that case, the air gap rapidly was reduced because of the thermal shrinkage of the aramid outer layer fabric. Nothing prevented this fabric layer from shrinking fully (Figure 4.14(b)). It decreased the thermal protection properties of the two-layer fabric system OL-S-BL compared to OL-BL-S. Interestingly, the flat specimen holder and sensor does not show any effect of fabric thermal shrinkage on the air gap. Therefore, unlike the analysis of TPP and RHR results, it can be concluded that the location of the air gap in the two-layer fabric system affected its thermal protection performance when tested in the cylindrical specimen holder under the radiant heat source with a heat flux of $84 \pm 2 \text{ kW/m}^2$.

According to the findings of previous researchers, the cylindrical specimen holder and sensor closely represent the configuration of the fabric on the instrumented manikin where many fabrics are pulled tightly to the sensors and a reduction in the air gap thickness occurs because of thermal shrinkage during the heat exposure (Dale et al., 2000). It is important to note this fabric behaviour under heat exposure because a decrease in the air gap in the clothing system can lead to more severe skin burn injuries.

4.2.4 Effect of moisture in a base layer on the thermal protection performance of fabric systems

Table B.10, Table B.11, and Table B.12 show that each fabric system tended to provide greater thermal protection when tested with the dry base layer than when tested with the wet base layer. The findings of [Lawson et al. \(2004\)](#), which agree with the findings of this research, showed that the fabric systems with internal moisture tended to increase heat transfer, therefore, decrease thermal protection when exposed to a flame heat source with 83 kW/m² heat flux. However, it should be noted that in most cases in this research, the differences in TPP, RHR, and CHTP ratings between the fabric systems with wet and dry base layer conditions were very small and not statistically significant.

[Lee and Barker \(1986\)](#) state that moisture changes a fabric's response to heat, specifically, it changes the heat capacity of the fabric and the rate of fabric heating. In this research, the additional data obtained from the thermocouples illustrates this trend as well (Figure 4.2 – Figure 4.6, and Figure 4.8 – Figure 4.12). Since the outer layer was tested only under dry conditions, its temperature rates were approximately the same during all tests. However, the base layer temperature rises were considerably different when tested under dry and wet conditions. Where the dry base layer reached approximately 300°C for two-layer fabric systems, and approximately 200°C for the three-layer fabric systems, the wet base layer reached a temperature of approximately 100°C for all fabric systems when a predicted second-degree burn injury occurred (Figure B.1 – Figure B.5). Also because of the high heat capacity of water, the presence of moisture in protective clothing system increases the amount of thermal energy absorbed if the water is still present after exposure to the heat source ([Lawson et al., 2004](#)).

[Lawson et al. \(2004\)](#) concluded that if all layers of fabric system are wet, the moisture can store energy, but it is able to evaporate out of the clothing system when heated. However, if the fabric system is only internally wet, as in this research, moisture vapour is unable to escape from the fabric system and condenses on the

copper calorimeter. As a result, the overall thermal protection of fabric system tends to decrease. This research also showed that when exposed to the flame heat source and radiant heat source, the fabric systems tested with the wet base layers reach a predicted second-degree burn faster and the wet base layer reached a much lower temperature than the fabric systems tested with the dry base layers.

4.3 Summary

To sum up, three bench-scale tests were conducted to assess the thermal protection properties of three-layer fabric systems compared to two-layer systems. The results showed that the inclusion of a three-dimensional warp-knitted fabric (Type 1 or Type 2) between the outer layer and base layer in a fabric system, significantly improved the thermal protection in all three tests. The three-layer fabric systems withstood significantly more thermal energy than the two-layer fabric systems (up to 329% more) and over longer periods of time before reaching predicted second-degree burn injuries when exposed to heat sources that included flame, radiant heat, and combined flame and radiant heat. The same trend was seen when the base layer condition was wet or dry.

It was noted that three-dimensional warp-knitted fabric incorporated between the outer layer and base layer in fabric systems OL-3D1-BL and OL-3D2-BL showed less thermal protection improvement when exposed to the radiant heat source in comparison to the exposure to the flame heat and combined flame and radiant heat sources. The thermal radiation was not blocked by the still air in the knit fabric as effectively as the convective energy from the flame exposure.

The three-dimensional warp-knitted fabric Type 1 provided greater thermal protection than Type 2, although both showed improvement over the two-layer fabric systems with or without a spacer in the fabric system. Three-dimensional warp-knitted fabric Type 2 is slightly thinner with a more open structure than Type 1 which could account for the differences in the performance. The selection of a three-dimensional warp-knitted fabric for use in the prototype shirt was based on these test results together with the thermal comfort properties assessed in Chapter 5.

CHAPTER 5 COMFORT EVALUATION OF FABRIC SYSTEMS AT BENCH-SCALE LEVEL

5.1 Introduction

This chapter addresses the second objective of the research which focuses on the assessment of thermal comfort properties of three-layer fabric systems compared to two-layer fabric systems. As described in Chapter 3, four different fabric systems including OL-BL, OL(2)-BL, OL-3D1-BL, and OL-3D2-BL were tested. The thermal comfort assessment of the fabric systems was based on total heat loss (THL) values obtained from thermal and evaporative resistance tests (ASTM, 2017a) and air permeability values obtained from air permeability tests (ASTM, 2018b) (Table C.1 and C.2).

THL values help to predict the comfort properties of clothing systems when the flow of heat and moisture from the human body to the environment is impeded by clothing (ASTM, 2017a). Because three-dimensional warp-knitted fabrics trap still air, the addition of this type of fabric are expected to reduce the THL values of the fabric systems and could contribute to the heat strain experienced by the wearer. Measuring the air permeability values of the fabric systems provides the rate of air flow passing through the fabric system, an indication of the overall “breathability” of the clothing system (ASTM, 2018b). The addition of one more layer (three-dimensional warp-knitted fabric) to the two-layer system may reduce the air permeability rate. The fabric system may partially block the flow of air from the environment into the clothing and prevent cooling of the human body. This would decrease the comfort properties of the garment and also contribute to the heat strain experienced by the wearer.

According to the standard requirements for wildland firefighters’ protective clothing NFPA 1977, the clothing system should be tested for thermal and evaporative heat resistance and the calculated total heat loss value should not be less than 450 W/m^2 (NFPA, 2016). However, there is no minimum requirement for air permeability set in the standards for wildland firefighters’ protective clothing.

5.2 Results and discussion

5.2.1 Total heat loss

This section addresses the fourth null hypothesis of the second research objective, which states that there is no significant difference in THL mean values among the fabric systems, including two-layer systems and three-layer systems with three-dimensional warp-knitted fabrics.

5.2.1.1 Summary of total heat loss results

The test results included the analysis of four fabric systems and showed whether the incorporation of three-dimensional warp-knitted fabrics in the three-layer systems decreased the THL mean values compared with the two-layer systems. The total heat loss value of each fabric is comprised of approximately 25% dry heat loss and 75% evaporative heat loss. It can be seen from Table 5.1 and Figure 5.1 that only the two-layer fabric system OL-BL met the NFPA 1977 minimum required THL value for fabric composites of 450 W/m². Fabric system OL-BL had the greatest THL mean value of 485 ± 16.4 W/m². Fabric system OL(2)-BL had a slightly lower THL mean value of 414 ± 2.0 W/m². The three-layer systems OL-3D1-BL and OL-3D2-BL showed similar and much lower THL mean values of 216 ± 5.3 W/m² and 244 ± 9.6 W/m², respectively.

Table 5.1 Summary table of THL mean values of different fabric systems.

Fabric system	Mean values and standard deviation of heat loss, (W/m ²)		
	Dry heat loss	Evaporative heat loss	Total heat loss
OL-BL	120 ± 2.5	365 ± 14	485 ± 16
OL(2)-BL	99 ± 2.6	315 ± 1.0	414 ± 2.0
OL-3D1-BL	60 ± 0.6	156 ± 5.5	216 ± 5.3
OL-3D2-BL	67 ± 1.7	176 ± 11	244 ± 9.6

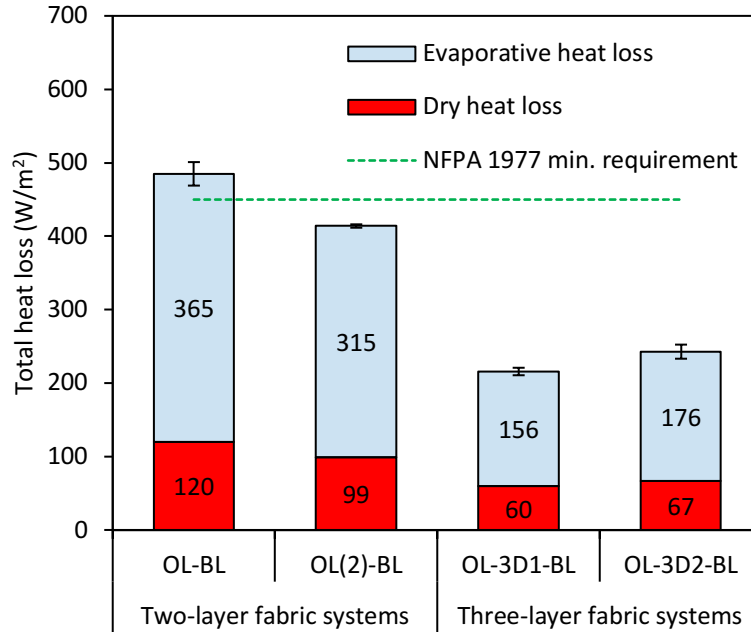


Figure 5.1 Bar chart shows THL mean values for different fabric systems.

The test results showed that the incorporation of the three-dimensional warp-knitted fabrics into the two-layer fabric systems dramatically decreased the THL mean values. The flow of heat and moisture vapour from human skin to the environment through the fabric systems is impeded by the three-dimensional warp-knitted fabrics used in fabric systems OL-3D1-BL and OL-3D1-BL when compared to the two-layer fabric systems OL-BL and OL(2)-BL. The planned pairwise comparison of the one-way ANOVA test showing a detailed analysis of the differences in THL mean values among four fabric systems is presented below.

5.2.1.2 Analysis of planned pairwise comparison of one-way ANOVA

A planned pairwise comparison of the one-way ANOVA tested the fourth null hypothesis of the second objective of this research and showed whether the mean difference in THL values of the three-layer systems and two-layer systems was statistically significant.

The overall one-way ANOVA test showed significant difference ($F(3,8) = 524.534, p < .001$) in THL mean values among all four fabric systems (Table C.3). Table 5.2 presents the pairwise comparison of THL mean values among these four fabric systems. Statistical significance (α) was set at 0.05.

Table 5.2 Pairwise comparison of THL mean values among different fabric systems.

(I) Fabric system	(J) Fabric system	Mean difference (I-J)	Sig.	95% CI for Difference	
				Lower Bound	Upper Bound
OL-3D1-BL	OL-BL	-270*	<.001	-298.1	-241.9
	OL(2)-BL	-198*	<.001	-226.1	-169.9
OL-3D2-BL	OL-BL	-242*	<.001	-270.5	-214.2
	OL(2)-BL	-170*	<.001	-198.5	-142.2
OL-3D2-BL	OL-3D1-BL	28	.054	-0.5	55.8
OL-BL	OL(2)-BL	72*	<.001	43.9	100.1

* Means are significantly different between fabric systems when subjected to a planned pairwise comparison of ANOVA test ($p < .05$).

The pairwise comparison of the three-layer fabric system OL-3D1-BL with the two-layer fabric systems showed that there was strong evidence ($p < .001$) that the THL mean values of the fabric system OL-3D1-BL were lower than the THL mean values of the fabric systems OL-BL and OL(2)-BL. There was a significant mean difference in THL mean values of 270 W/m² with 95% CI (241.9, 298.1) between the fabric systems OL-BL and OL-3D1-BL. There was also a significant mean difference in THL mean values of 198 W/m² with 95% CI (169.9, 226.1) between the fabric systems OL(2)-BL and OL-3D1-BL. Thus, there was strong evidence against the fourth null hypothesis when the THL mean values of the three-layer fabric system OL-3D1-BL compared with the THL mean values of two-layer fabric systems OL-BL and OL(2)-BL.

Similarly, the pairwise comparison of the three-layer fabric system OL-3D2-BL with the two-layer fabric systems showed that there was strong evidence ($p < .001$) that the THL mean value of the fabric system OL-3D2-BL was lower than the THL mean values of fabric systems OL-BL and OL(2)-BL. There was a significant mean difference in THL mean values of 242 W/m² with 95% CI (214.2, 270.5) between the fabric systems OL-BL and OL-3D2-BL. There was also a significant mean difference in THL mean values of 170 W/m² with 95% CI (142.2, 198.5) between the fabric systems OL(2)-BL and OL-3D2-BL. Thus, there was also strong evidence against the fourth null hypothesis when the THL mean value of the three-layer fabric system OL-3D2-BL was compared with the THL mean values of the two-layer fabric systems OL-BL and OL(2)-BL.

Additionally, a pairwise comparison was conducted between the three-layer fabric systems OL-3D2-BL and OL-3D1-BL, and the two-layer fabrics OL-BL and OL(2)-BL. There was no evidence ($p = .054$) that the THL mean values of the fabric systems OL-3D1-BL and OL-3D2-BL were different. The insignificant difference in their THL mean value was only 28 W/m² with 95% CI (-0.5, 55.8). On the other hand, there was strong evidence ($p < .001$) that the THL mean value of the fabric system OL-BL was lower than the THL mean value of fabric systems OL(2)-BL. There was a significant mean difference in THL mean values of 72 W/m² with 95% CI (43.9, 100.1) between the fabric systems OL-BL and OL(2)-BL.

Overall, statistical analysis of data in THL mean values showed that the incorporation of three-dimensional warp-knitted fabric between the outer and base layers impeded the flow of heat and moisture vapour passing from the hotplate surface through the clothing systems to the environment. The average THL value of the three-layer fabric system OL-3D1-BL was 216 W/m². The flow of heat and moisture vapour that can pass through the fabric system OL-3D1-BL dramatically decreased by 56% compared to the two-layer fabric system OL-BL, and by 48% compared to OL(2)-BL. The average THL value of the three-layer fabric system OL-3D2-BL was 244 W/m², which was 28 W/m² greater than the THL value of the fabric system OL-3D1-BL but not statistically significant. The flow of heat and

moisture vapour that can pass through the fabric system OL-3D2-BL dramatically decreased by 50% compared to the two-layer fabric system OL-BL, and by 41% compared to OL(2)-BL. Both three-layer fabric systems OL-3D1-BL and OL-3D2-BL did not meet the NFPA 1977 minimum required THL value for fabric composites of 450 W/m^2 . The THL mean value of fabric system OL(2)-BL also did not meet the NFPA 1977 standard requirement. The additional outer layer in the yoke area of fabric system OL(2)-BL decreased the flow of heat and moisture vapour through the fabric system by 15% compared to fabric system OL-BL. According to the test results, it can be assumed that the air entrapped in the three-dimensional fabrics not only contributed to insulation against the heat sources from the environment, as was investigated in Chapter 4, but also partially prevented heat and moisture vapour transmission from the hotplate to the environment. This is the trade-off that often takes place between comfort and thermal protection. As protection increases, comfort is reduced as illustrated by the THL results of the three-layer fabric systems.

The obtained measurements of thermal and evaporative resistance and analysed THL data are important in thermal comfort assessment of clothing systems. As described in Chapter 2 (section 2.1), wildland firefighters perform very intense physical activities while being exposed to a hot environment that leads to heavy perspiration rate. [Weiner \(1945\)](#) found the following sweat distribution: 50% from the trunk, 25% from the lower limbs, and 25% from the head and the upper limbs. [Smith & Havenith \(2011\)](#) conducted more detailed investigation of the body mapping of sweating patterns. They found that the central upper and lower back torso, along with the forehead have the highest intensity sweat rates, and as a result are areas that lose the most heat. The chest area of the upper torso and shoulder areas have medium intensity sweat rates. And the lowest sweat rates are observed on the extremities (hands and feet).

The clothing system of wildland firefighters should have a sufficient THL value that it does not impede the flow of heat and moisture passing from the human skin through the clothing systems to the environment, especially in the areas of body

with the most intensive heat loss. As mentioned earlier NFPA 1977 require a minimum THL value of 450 W/m^2 for wildland firefighters' clothing system when measured on the sweating guarded hotplate. This may be higher than the workload of wildland firefighters which likely reaches 400 W/m^2 which is equivalent to sustained high intensity work with high metabolic rate according to ISO11079 (ISO, 2007, p.18). DenHartog et al. (2016) noted that if the THL measurement of the fabric system meets that level, metabolic heat generated will be completely released through clothing into the atmosphere during work and there should be minimal heat buildup. The researchers stated that the minimum requirement for the THL value set by NFPA 1977 was overestimated and did not represent the actual heat loss in humans (DenHartog et al., 2016). Their human trial research showed that the clothing system, similar to the fabric system OL-BL used in this research, had a THL value of 453 W/m^2 when tested on the sweating-guarded hot plate, and a THL value of 263 W/m^2 when a human subject performed activities leading to a human body metabolic heat production of 290 W/m^2 for 130 min to induce heat strain. Similarly, in this research, fabric system OL-BL showed the THL value of 485 W/m^2 when tested on the sweating guarded hotplate. The calculated THL value of the bare hotplate for that test was 721 W/m^2 (see the note for Table C.1, Appendix C) which is 2.5 times greater than the actual wildland firefighters metabolic heat production rate of approximately 290 W/m^2 while on duty. DenHartog et al. (2016), in addition to human trials and sweating guarded hotplate tests, also conducted sweating manikin test, that showed closer, but lower THL values compared to human trial results. The researchers concluded that the development of a new manikin test method with simulated wildland firefighters working conditions is needed and it would greatly help to predict the actual THL of humans in clothing systems and more realistically assess the thermal comfort of garments. Therefore, the NFPA 1977 minimum requirement of the THL value of the clothing system for wildland firefighters may need to be re-evaluated based on this research.

5.2.2 Air permeability

This section addresses the fifth null hypothesis of the second research objective, which states that there is no significant difference in the air permeability mean values among the fabric systems, including two-layer systems and three-layer systems with three-dimensional warp-knitted fabrics.

5.2.2.1 Summary of air permeability results

The test results included the analysis of four fabric systems for air permeability and showed whether the incorporation of three-dimensional warp-knitted fabrics in the three-layer systems decreased the mean values of air permeability compared with the two-layer systems. Table 5.3 and Figure 5.2 show that the three-layer system OL-3D2-BL has the greatest air permeability of 293 ± 7.31 L/m²·s and the fabric system OL(2)-BL has the lowest air permeability of 168 ± 6.57 L/m²·s. The three-layer system OL-3D1-BL and two-layer system OL-BL have approximately the same air permeability with mean values of 248 ± 8.46 L/m²·s and 256 ± 7.66 L/m²·s, respectively.

Table 5.3 Summary table of air permeability mean values of different fabric systems.

Fabric system	Mean values and standard deviation of air permeability, (L/m ² ·s)
OL-BL	256 ± 7.66
OL(2)-BL	168 ± 6.57
OL-3D1-BL	248 ± 8.46
OL-3D2-BL	293 ± 7.31

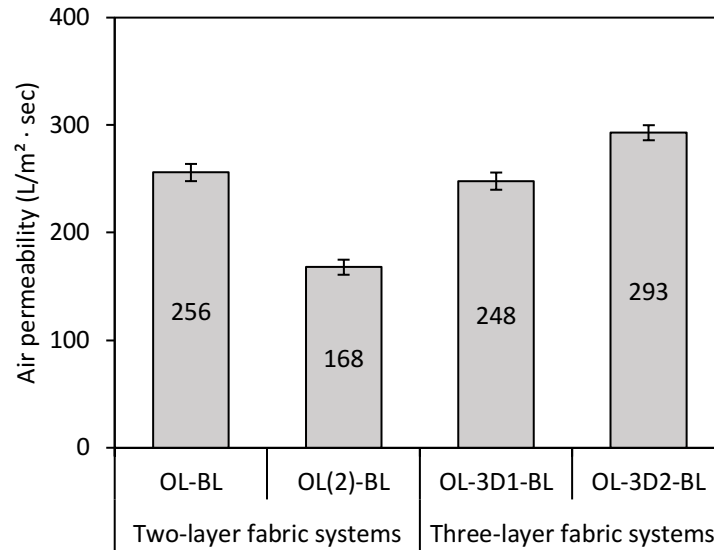


Figure 5.2 Bar chart shows air permeability mean values for different fabric systems.

The incorporation of three-dimensional warp-knitted fabrics into two-layer fabric systems did not decrease the air permeability mean values. The rate of airflow through fabric systems OL-3D1-BL and OL-3D2-BL was similar to, or greater than the rate through the two-layer fabric systems OL-BL and OL(2)-BL. A planned pairwise comparison of the one-way ANOVA test showed the differences in air permeability mean values among four fabric systems and is presented below.

5.2.2.2 Analysis of planned pairwise comparison of one-way ANOVA

A planned pairwise comparison of the one-way ANOVA tested the fifth null hypothesis of the second objective of this research and showed whether the mean difference in air permeability of the three-layer systems and two-layer systems was statistically significant.

The overall one-way ANOVA test showed significant difference ($F(3,36) = 489.540, p < .001$) in air permeability mean values among all four fabric systems (Table C.4). Table 5.4 presents the pairwise comparison of air permeability mean values among the four fabric systems. Statistical significance (α) was set at 0.05.

Table 5.4 Pairwise comparison of air permeability mean values among different fabric systems.

(I) Fabric system	(J) Fabric system	Mean difference (I-J)	Sig.	95% CI for Difference	
				Lower Bound	Upper Bound
OL-3D1-BL	OL-BL	-8	.127	-17.5	1.2
	OL(2)-BL	80*	<.001	70.5	89.4
OL-3D2-BL	OL-BL	37*	<.001	27.8	46.6
	OL(2)-BL	125*	<.001	115.8	134.7
OL-3D2-BL	OL-3D1-BL	45*	<.001	35.9	54.7
OL-BL	OL(2)-BL	88*	<.001	78.7	97.5

* Means are significantly different between fabric systems when subjected to a planned pairwise comparison of ANOVA test ($p < .05$).

The pairwise comparison of three-layer fabric system OL-3D1-BL with two-layer fabric system OL-BL shows that there is no evidence ($p = .127$) that the air permeability mean values of these two fabric systems are different. Their mean difference in air permeability is only 8 L/m²·s with 95% CI (-1.2, 17.5) which is not statistically significant. Therefore, there is no evidence against the fifth null hypothesis when the air permeability mean values of the three-layer fabric system OL-3D1-BL and the two-layer fabric system OL-BL are compared. On the other hand, there is strong evidence ($p < .001$) that the air permeability mean value of fabric system OL-3D1-BL is greater than the air permeability mean value of fabric system OL(2)-BL with the significant mean difference in air permeability of 80 L/m²·s with 95% CI (70.5, 89.4). Therefore, there is strong evidence against the fifth null hypothesis when the air permeability mean values of the three-layer fabric system OL-3D1-BL and the two-layer fabric system OL(2)-BL are compared.

The pairwise comparison of the three-layer fabric system OL-3D2-BL with two-layer fabric systems shows that there is strong evidence ($p < .001$) that the air permeability mean value of the fabric system OL-3D2-BL is greater than the air permeability mean value of fabric systems OL-BL and OL(2)-BL. There is a significant mean difference in air permeability of 37 L/m²·s with 95% CI (27.8, 46.6) between the fabric systems OL-3D2-BL and OL-BL. There is also a significant mean difference in air permeability of 125 L/m²·s with 95% CI (115.8, 134.7) between the fabric systems OL-3D2-BL and OL(2)-BL, which makes the rate of airflow through the fabric system OL-3D2-BL almost two times greater than the rate through fabric system OL(2)-BL. Thus, there is no evidence against the fifth null hypothesis when the air permeability mean value of the three-layer fabric system OL-3D2-BL is compared with the air permeability mean values of the two-layer fabric systems OL - BL and OL(2)-BL.

Additionally, the pairwise comparison was conducted between the three-layer fabric systems OL-3D2-BL and OL-3D1-BL, and the two-layer fabrics OL-BL and OL(2)-BL. The air permeability mean value of fabric system OL-3D2-BL with the incorporation of three-dimensional warp-knitted fabric Type 2 is significantly greater ($p < .001$) than the air permeability mean value of fabric system OL-3D1-BL with the incorporation of three-dimensional warp-knitted fabric Type 1. Their difference in air permeability mean value is 45 L/m²·s with 95% CI (35.9, 54.7). The use of two outer layers in the yoke area in fabric system OL(2)-BL significantly decreased ($p < .001$) the air permeability mean value by 88 L/m²·s with 95% CI (78.7, 97.5) in comparison with fabric system OL-BL that has only one outer layer and base layer.

Statistical analysis of the air permeability mean values showed that the incorporation of three-dimensional warp-knitted fabric between the outer and base layers does not diminish the rate of airflow passing from the environment through the clothing system to human skin and in some cases it even increased the air flow. The schematic drawing of the airflow passing through the fabric systems OL-BL and OL - 3D2 - BL can explain this phenomenon (Figure 5.3).

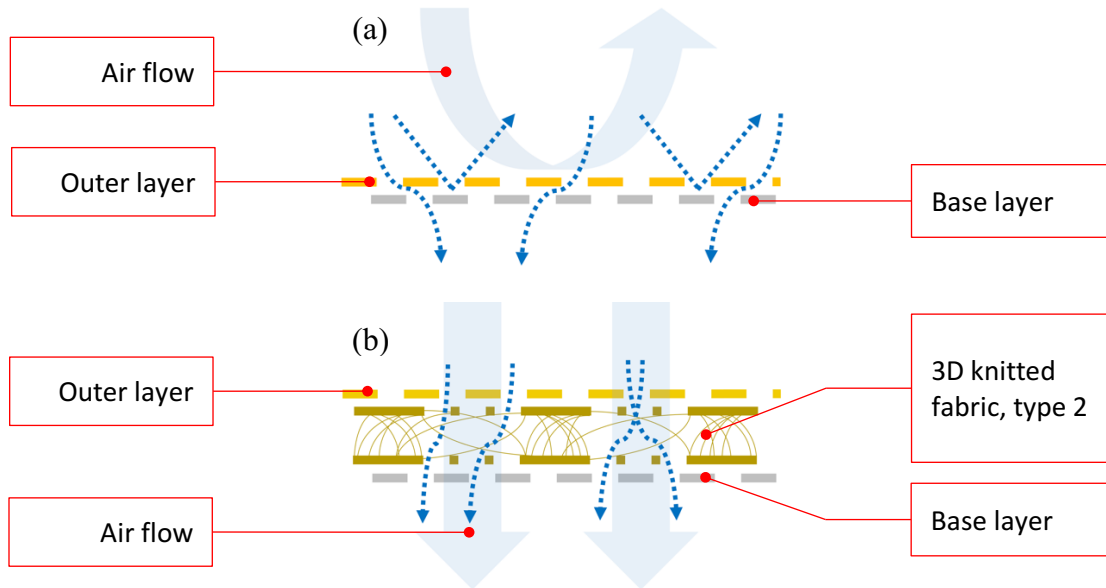


Figure 5.3 Schematic drawing of airflow passing through the fabric system:
(a) OL - BL, (b) OL-3D2-BL.

Figure 5.3 (a) illustrates the fabric system OL-BL which comprises one outer layer and one base layer. Both fabric layers are very close to each other in this fabric system and the location of pores between the yarns in each fabric cannot be perfectly aligned. The yarns of the outer layer fabrics would partially block the pores of the base layer fabric. Therefore, the air does not flow easily through fabric system OL - BL and decreases even more in fabric system OL(2)-BL with the additional outer layer.

Figure 5.3 (b) depicts the fabric system OL-3D2-BL which comprises one outer layer, one base layer, and one layer of three-dimensional warp-knitted fabric Type 2. As described in Chapter 3, the three-dimensional warp-knitted fabric has a mesh with 2.5 x 4 mm apertures at the front and back, it is 5.3 mm thick and resilient to compression because of the PEEK monofilament fibre used for the spacer structure between the face and back fabrics. This structure is highly permeable and allows the air to flow freely through the fabric. The incorporation of the three-dimensional warp-knitted fabric separates the outer and base layers so their pores are not blocked by the yarns of each other. The apertures of the three-dimensional warp-knitted fabric opens the access to the pores in outer and base layer fabric structures for more air to pass through the whole fabric system.

Overall, the incorporation of three-dimensional warp-knitted fabrics between the outer and base layers did not decrease the rate of airflow through the clothing system. For thermal protection, high air flow may not be desirable and is a trade off to increase comfort. The rate of the airflow through the three-layer fabric system OL - 3D1 - BL is the same as that of the two-layer fabric system OL-BL and 30% greater than that of OL(2)-BL. The rate of the airflow through the three-layer fabric system OL-3D2-BL is 13% greater than that of the two-layer fabric system OL-BL, and 43% greater than that of OL(2)-BL. The additional outer layer in the yoke area of fabric system OL(2)-BL decreased the airflow through the fabric system by 34% compared to fabric system OL-BL.

The obtained measurements of the fabric system air permeability values are also very important in the thermal comfort assessment of the clothing systems. Wind or air blowing from the environment can assist the thermal regulation mechanisms of the human body. [Barwood et al. \(2009\)](#) studied different cooling techniques for the human body after subjects exercised in a chamber with a hot and humid environment of 31°C and 70% RH. Their findings showed that a whole-body blowing technique by a fan was most effective in reducing core body temperature. [Reffeltrath \(2006\)](#), in his study on ventilated vests for helicopter crew, also found that ventilation significantly reduced the increase in core temperature and improved the thermal comfort of the subject under chamber conditions of 35°C and 50% RH. Similar to these studies, wildland firefighters perform activities with high metabolic heat production. But in the wildfire scenario, the environmental conditions mentioned in Chapter 2 (section 2.1) are slightly different from the ones presented in the laboratory test performed by [Barwood et al. \(2009\)](#) and [Reffeltrath \(2006\)](#). The work conditions of wildland firefighters could have higher temperatures, lower RH, but similar or higher wind speed. As stated by [Xavier Viegas \(1998\)](#), wind is recognised as the single most important factor in the propagation of wildfires. Thus, considering that the main focus of wildland firefighters is to prevent forest fire from spreading by the wind, the use of three-dimensional warp-knitted fabrics in the new prototype design will potentially increase the rate of airflow through the clothing system by approximately 30%–43% over the current shirt design with two layers of outer fabric in the yoke areas. Wind or

air flow from the environment can more easily pass through the proposed clothing system, and potentially help to cool the human body.

5.3 Summary

To sum up, two bench-scale tests were conducted to assess the thermal physiological comfort properties of three-layer fabric systems compared to two-layer systems. The results showed that the inclusion of a three-dimensional warp-knitted fabric (Type 1 or Type 2) between the outer layer and base layer in a fabric system, had some negative and positive effects. It negatively influenced thermal comfort by impeding the flow of heat and moisture vapour from the skin (hotplate) to the environment by 41%–56%. In the proposed garment design (section 6.3), only 25% of the shirt area includes the three-layer fabric system. Thus, the increase in thermal and evaporative resistance will mainly affect a small portion of the upper back torso which has a high sweat rate (Smith & Havenith, 2011), as well as areas of the upper front torso, shoulders, and upper arms which have a medium sweat rate. The lower back area which also has a high sweat rate will be covered with only one outer layer and base layer of fabric and this two-layer system provided good heat and moisture vapour transmission in testing. The inclusion of the three-dimensional warp-knitted fabric between the outer and base layers positively influenced air permeability making the three-layer fabric systems 30%–43% more air permeable than two-layer fabric systems with either one or two outer layers and the base layer. In the proposed garment design, the inclusion of a three-dimensional warp-knitted fabric will allow wind from the environment to penetrate through the clothing system and may have a positive effect on thermal comfort.

Based on the bench-scale thermal protection and thermal comfort performance assessment conducted in Chapters 4 and 5, the three-dimensional warp-knitted fabric Type 2 was selected for the shirt prototype design rather than Type 1. Type 2 showed sufficient thermal protection properties and better air permeability and better total heat loss values than Type 1. Type 2 also has an FR finish and is slightly thinner and more easily stitched into a sewn garment than Type 1.

CHAPTER 6 DESIGN DEVELOPMENT AND CONSTRUCTION OF SHIRT PROTOTYPE

6.1 Introduction

This chapter addresses the fourth objective of the research which focuses on the design development and construction of a prototype shirt for wildland firefighters that incorporates three-dimensional warp-knitted fabric in areas of the garment that are in contact with the skin and prone to burn injuries. The design process included two main steps: the background exploration (e.g. standard requirements, existing inventions), and the development of the prototype shirt for further full-scale flash fire instrumented manikin testing.

Prior to the design development of the prototype shirt, the design requirements for wildland firefighters' protective clothing outlined in the CAN/CGSB-155.22 and NFPA 1977 standards were summarised ([CGSB, 2014](#); [NFPA, 2016](#)) Review of existing patents included inventions among wildland firefighters' protective clothing and other thermal insulation or protection solutions used in protective clothing.

The prototype shirt design that was developed in this research is based on the design of the protective shirt manufactured at Winner Garment Industries Ltd. that is currently used by wildland firefighters in Alberta. Reproduced pattern pieces of this shirt were developed in CLO 3D fashion design software (CLO Virtual Fashion Inc., Seoul, South Korea). These pattern pieces were then edited and manipulated to develop the prototype shirt pattern pieces. The fitting process of the prototype shirt to the manikin body included simulated garment visualisation in CLO software and construction of a mock-up garment. The full prototype shirt construction sequence and specific sewing techniques selected to make the shirt are also presented in this chapter. All applied types of seams and stitches were used in accordance with the ASTM D 6193 standard ([ASTM, 2020e](#)).

6.2 Background

6.2.1 Standard requirements for design

Protective clothing system design for wildland firefighters in North America should meet the minimal requirements outlined in CAN/CGSB-155.22 and NFPA 1977 standards (CGSB, 2014; NFPA, 2016). According to these standards, protective clothing could be two-piece garment (shirt or jacket, and pants), or one-piece garment (coverall). Collars should remain upright after being extended to the vertical position. Sleeves should not have turn-up cuffs. The cuffs should have a closure that can provide tight and secure fit around the wrists. All pockets that open to the exterior should have a cover (flaps) of other closure system. This requirement does not apply to the front waist pockets. Pass through openings must have a means of fastening them in a closed position. In case of one-piece garments, the closure should be continuous from the top of the crotch area to the top of the garment in the neck area. Closure systems and hardware cannot come into direct contact with body.

Additionally, NFPA 1977 specifies that garment hardware finish must be free of any rough or sharp edges (NFPA, 2016). All threads used in garment construction should be made of inherently flame-resistant fibres. Visibility markings are applied on the exterior of the garments and should provide 360-degree visibility of the wearer.

CAN/CGSB-155.22 specifies that the use of high visibility trim in wildland firefighters' protective clothing is optional (CGSB, 2014). Sleeve vents are prohibited. In addition, any garment worn under the protective garment should have melt-resistant properties. Thus, some synthetic and synthetic blends are not suitable to be used as a base layer.

6.2.2 Previous inventions

This section includes the review of previous inventions that are specifically related to wildland firefighters protective clothing design and thermal insulation solutions in protective clothing overall. There are several present inventions specifically related to wildland firefighters' protective clothing. [Pan et al. \(2023\)](#) in China patent No. 115569314B, assigned to Fuzhou Chunhui Clothing Co, Ltd., disclosed a high-strength forest fireproof garment and its protection method. The invention reinforced existing protective clothing with an additional vest worn on top of it. The additional vest can improve the protection of the body trunk from the impact force of branches, leaves, and other sharp objects in the surroundings. [Li et al. \(2021\)](#) in China patent No. 213220621U disclosed a multifunctional emergency protective clothing for wildland firefighters. This invention is a multilayer coverall that can be turned into a bag for carrying tools. [Yin et al. \(2020\)](#) in China patent No. 211132764U disclosed a novel forest fire prevention clothing that also consists of several layers. The lining layer of this invention has a cooling system with water tubes placed throughout the whole ensemble for increasing comfort properties. In addition, this protective clothing system has a GPS device in case the firefighter is lost and needs to be rescued. [Shu et al. \(2012\)](#) in China patent No. 201220221345, assigned to Northeast Forestry University, disclosed a forest firefighting protective clothing that is partially made of polysulfonamide material in the leg and arm areas for lowering the cost of the garment. Also, this invention is equipped with illumination for visibility in the waist area. None of these inventions related to wildland firefighters clothing design were focused on the improvement of thermal protection and comfort properties specifically in the areas of the upper torso and upper arms of the protective shirt for wildland firefighters.

However, various inventions were focused on the improvement of the thermal insulation layer in the protective clothing system for structural firefighters. The conventional structural firefighter garment consists of a flame resistant and abrasion resistant outer shell, moisture barrier and thermal liner or barrier ([Barbeau et al., 2019](#)). The most heavy and bulky layer is the thermal liner. It is

normally made of an insulating layer of batting or non-woven fabric quilted or laminated to woven fabric. The thermal barrier plays the most important role in the resistance to the transmission of heat from the external environment to the body of the firefighter. Inventors aim to create protective clothing that allows for protection from heat transmission while also minimize heat stress on the wearer, so that the firefighter is able to work more efficiently than in the conventional protective clothing systems.

[Flay et al. \(2007\)](#) in U.S. patent No. 2007/0284558A1 disclosed a fire insulating barrier material for a firefighter's protective garment. This material consists of two fabric layers that are connected by the pile yarns that create a space between. This space contains an insulating substance. The fabric layers can have woven or knitted structures that are made of fire-resistant fibres (e.g. aramid, polyacrylate, phenolic, polybenzole, or melamine). The insulating substance between the fabric layers can be air, aerogel, or phase change materials. An additional laminated layer can be applied to provide a moisture repellent property. The thickness range of the fabric can be from 1 to 8 mm. This invention replaces the traditional thick, needle-punched batt used as an insulator in the thermal liner layer of structural firefighters' protective clothing.

[Keitch \(2014\)](#) in European patent No. 2707529B1, assigned to Heathcoat Fabrics Limited, disclosed spacer textiles. Generally, spacer textiles are produced from polyester or nylon on raschel warp-knitting machines. But this invention has two layers of fabric, knitted from meta-aramid yarns. Both fabric layers are connected by relatively thick (0.05 to 0.25 mm diameter) monofilament polyetheretherketone (PEEK) yarn. These monofilaments provide the three-dimensional quality to the textile. The thickness range can be varied, and it depends on the final use. These fabric structures can be highly porous and lightweight. At the same time, they provide sufficient resilience without being too stiff in use. The inherently flame-resistant fibre content of this fabric along with entrapped air in the fabric allows this invention to be implemented as a thermal barrier in protective clothing.

[Bibeau \(2016\)](#) in Canadian patent No. 2919104C, assigned to Logistik Unicorp Inc., disclosed an insulating garment for firefighters' bunker gear. The invention is worn under the main outer shell of firefighters and serves as a moisture repellent and thermal barrier. This garment is made of fabric similar to the one that was disclosed by [Flay et al. \(2007\)](#) in U.S. patent No. 2007/0284558A1 and [Keitch \(2014\)](#) in European patent No. 2707529B1. It also has two layers of fire-resistant fabric that are interconnected by a yarn and laminated with a moisture repellent breathable membrane. The method of connecting the two fabric layers is similar to the construction of a double-weave velvet, but without the separation of the two fabrics after weaving. [Flay et al. \(2007\)](#) failed to identify the overall essential function of the connecting yarn. However, [Bibeau \(2016\)](#) similarly to [Keitch \(2014\)](#) specified that this yarn should be a monofilament with good compression resilience, possibly made of polyphenylene sulphate (PPS), polyetheretherketone (PEEK), or polyetherimide. [Bibeau \(2016\)](#) emphasized that normally firefighters carry heavy loads that cause high compression of the shoulder area. This leads to compression of the thermal barrier and loss of its thermal insulation properties. Therefore, the resilient monofilament in the new thermal barrier fabric developed by [Bibeau \(2016\)](#) can resist compression, entrap a large quantity of air and can potentially improve the properties of the thermal liners.

There were also other attempts to improve the thermal insulation layer of structural firefighters' protective clothing. [Taylor and Aldridge \(1999\)](#) in U.S. patent No. 5924134A, assigned to Lion Apparel Inc., disclosed a protective garment with an apertured closed-cell foam liner. The invention is focused on the improvement of the thermal liner in protective clothing for structural firefighters. The thermal liner is made of flame and heat resistant apertured closed-cell foam material. This material is placed between and bonded to two substrates of woven aramid materials. The invention is non-moisture absorbent, light weight, and provides high thermal insulation. The apertures formed in the foam layer promote moisture vapour transfer from the skin through the clothing system. [Grilliot and Grilliot \(1991\)](#) in U.S. patent No. 5001783A, assigned to Norcross Safety Products LLC, disclosed firefighter's garments having minimum weight and excellent protective qualities.

The thermal liner in this invention is provided by creating dead air space. The inventors describe one of the preferred options of maintaining dead air space is incorporation of corrugated mesh material. This method provides good thermal insulation, while maintaining minimum weight and resistance to compression forces.

Some inventions were related to improvement of comfort properties of the thermal insulation layer of structural firefighters' protective clothing.

[Barbeau et al. \(2019\)](#) in U.S. patent No. 10245454B2, assigned to Innotex Inc., disclosed a firefighter's protective garment having a thermal barrier with spacers to increase dissipation of metabolic heat. The inventors modified the thermal liner by attaching spacer elements to the innermost surface. The spacer elements were strategically spread in the areas of back and waist with the highest metabolic heat production and rates of perspiration. This arrangement redistributes metabolic heat over the surface area, facilitates evaporative cooling, and increases thermal comfort properties of the garment.

Interestingly, there was one invention that aimed to provide thermal protection to the areas of upper front, upper back torso, and upper arms by wearing an additional garment over the standard protective clothing for structural firefighters. [Butzer and Coombs \(1995\)](#) in U.S. patent No. 5406648A, assigned to Cairns and Brother Inc., disclosed a thermal protective overjacket. This invention was an additional improvement to the invention of a multilayer protective garment for structural firefighters disclosed by [Coombs \(1985\)](#) in the U.S. patent No. 4507806. Since the heat is concentrated closer to the ceiling and reaches 430 to 530°C in residential or commercial structures, the thermal protective overjacket was invented to provide additional flame and thermal protection in the areas of the upper torso and upper arms when the structural firefighters stand upright while on duty within a fire. The thermal protective overjacket is worn on top of the outer protective shell and thermal liner. It consists of a short front and back that covers the chest and upper back, short set-in type sleeves that cover only the upper arms, and a stand-up collar that also has the same multilayer system of shell and thermal liner as the protective garment. The

firefighters can remove the thermal protective overjacket when in lower heat release conditions, or when tasks outside a fire are performed (e.g. vehicle fires).

The prototype shirt design developed in this research, similarly to [Butzer and Coombs \(1995\)](#) in their protective overjacket invention for structural firefighter protective clothing ensembles, aimed to provide thermal protection to the upper front, upper back torso, and upper arms areas. The additional areas of wrists and neck were also provided with additional thermal protection in the prototype shirt. However, unlike the protective overjacket invention, the prototype shirt is a one-piece garment that has additional thermal protection provided through the localized incorporation of a three-dimensional warp-knitted fabric into the garment. Also, the prototype shirt is an invention for the wildland firefighters' protective clothing ensemble. The three-dimensional warp-knitted fabric used in the prototype shirt design is a spacer textile disclosed by [Keitch \(2014\)](#) earlier. As [Bibeau \(2016\)](#) and [Keitch \(2014\)](#) specify, the monofilament yarn made of PEEK fibre in the spacer fabrics provides good compression resilience. Thus, this fabric can entrap a large quantity of air and act as a thermal barrier. Additionally, it provides cushioning in the shoulder area when wildland firefighters carry heavy loads that cause high compression of the shoulder area. The invention of the prototype shirt design with the aforementioned features has never before been developed as part of the wildland firefighters' protective clothing ensemble. The shirt design currently worn by wildland firefighters in Alberta was the starting point for the design of the prototype garment. The current shirt is the control shirt in this research and the design of this shirt is described below.

6.2.3 Control shirt design

Protective clothing for wildland firefighters in Alberta consists of a protective shirt and pants. The prototype shirt design that was developed in this research is based on the design of the shirt (style GS. 640) provided by Winner Garment Industries Ltd. (Figure 6.1). Reproduction of this shirt is further called the control shirt. A detailed description of the control shirt design is provided below.



Figure 6.1 Wildland firefighter's shirt manufactured by Winner Garment Industries Ltd. (control shirt): (a) front view, (b) back view.

Description of the control shirt

The control shirt is the protective shirt for male wildland firefighters (Figure 6.2). The shirt has a regular fit and low hip length. The front has a placket closure with sewn-on stainless steel hidden snaps. Two patch pockets with flaps and flame-resistant hook-and-loop closure are attached to the shirt front pieces in the chest area. The back of the shirt has two action pleats and a double shirt yoke. The stand collar has a flame-resistant hook-and-loop closure. Each of the two long sleeves are set-in and consist of one-piece of fabric with a single lengthwise seam and continuous sleeve placket. There are two pleats in the sleeve at the cuff. The cuff has a flame-resistant hook-and-loop closure. The double top stitched seam (two parallel straight stitches) is applied on the edge of the pocket, pocket flap, shoulder, yoke, and armhole seams. A single top-stitched seam (one straight stitch) is applied on the edges of the collar, cuffs, and bottom hem. The shirt is made of plain weave Nomex[®] IIIA fabric. Segmented adhesive reflective trim, 3M[™] Scotchlite[™], is applied horizontally at the chest level of the shirt front and back, and on each sleeve slightly below the elbow.

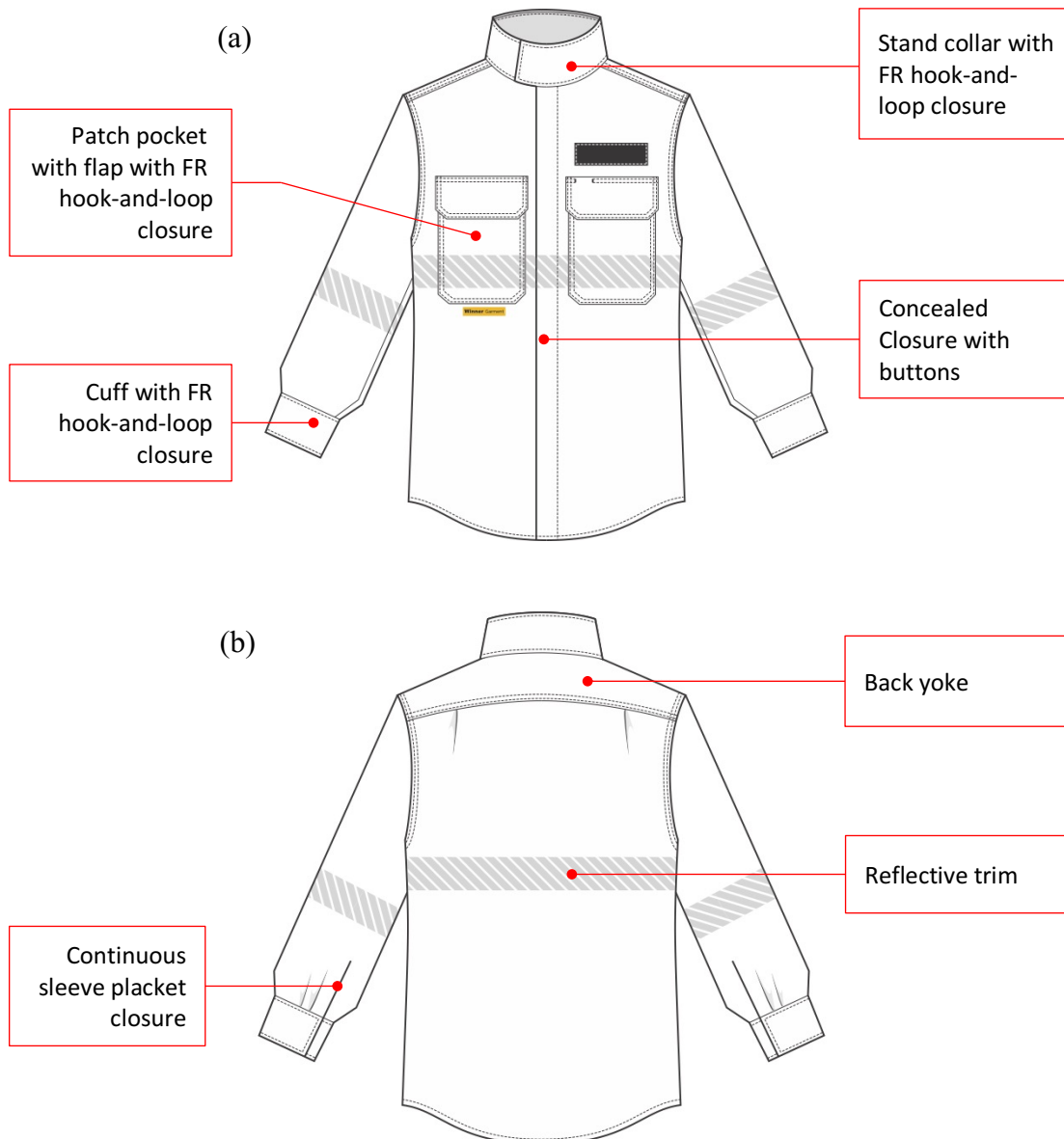


Figure 6.2 Technical drawing of control shirt design: (a) front view, (b) back view.

6.3 Prototype shirt design development

Summary of the invention

The prototype shirt is a wildland firefighter's protective shirt with incorporated highly porous, lightweight, compression-resilient, and flame-resistant three-dimensional raschel warp-knitted fabric in specific areas for improvement of the thermal protection performance and comfort properties of the garment. Three-dimensional warp-knitted fabric was incorporated in areas of the upper front and back

torso, upper arms, shoulders, neck, and wrists. These areas normally do not have an air gap between the garment and body. As a result, these areas of the body do not have sufficient thermal protection and are prone to skin burn injury in short-duration flame engulfment tests. The three-dimensional warp-knitted fabric Type 2 (code 3D2) entraps still air and impedes thermal energy transfer through the garment system while increasing air permeability and improving thermal comfort. Thus, the protective shirt provides sufficient thermal protection to prevent skin burn injury in specific areas of the garment. Additionally, the resiliency of the three-dimensional warp-knitted fabric provides good resistance to compression and cushioning in the shoulder area when wildland firefighters carry heavy loads on their shoulders.

Description of the prototype shirt

The prototype shirt is a protective shirt for male wildland firefighters (Figure 6.3). The shirt has a regular fit and low hip length. The shirt has a yoke that covers the shoulders, upper front, upper back and upper arm areas. The yoke consists of two pieces that are sewn together by a centre back seam. Each left and right piece combines the front and back yoke with a portion of the sleeve cap. The shirt front has a placket closure with the stainless steel sewn-on hidden snaps. Two patch pockets and flaps with flame-resistant hook-and-loop closure are attached to the shirt front pieces in the chest area below the yoke seam. The shirt back has two action pleats in the yoke seam. The stand collar has a flame-resistant hook-and-loop closure. The sleeves are comprised of three pieces, including the upper sleeve that is attached to the extended yoke above the elbow level, the front under-sleeve, and the back under-sleeve. Each of the two sleeves has an in-seam placket at the cuff location, and two pleats on the back under-sleeve at the cuff. The cuff has a flame-resistant hook-and-loop closure. A double top-stitched seam (two parallel straight stitches) is placed at the edge of the pockets, and pocket flaps. A single top-stitched seam (one straight stitch) is applied on the edge of the bottom hem. The shirt is made of plain weave Nomex[®] IIIA fabric (OL) and flame-resistant three-dimensional warp-knitted fabric Type 2, Spacetec[®]. The outer layers of the yoke, collar, and sleeve cuffs were stitched together in evenly spaced parallel lines to a layer of three-dimensional warp-knitted fabric. Segmented adhesive reflective trim, 3M[™] Scotchlite[™], is applied

horizontally at the chest level of the shirt front and back, and on each sleeve slightly below the elbow.

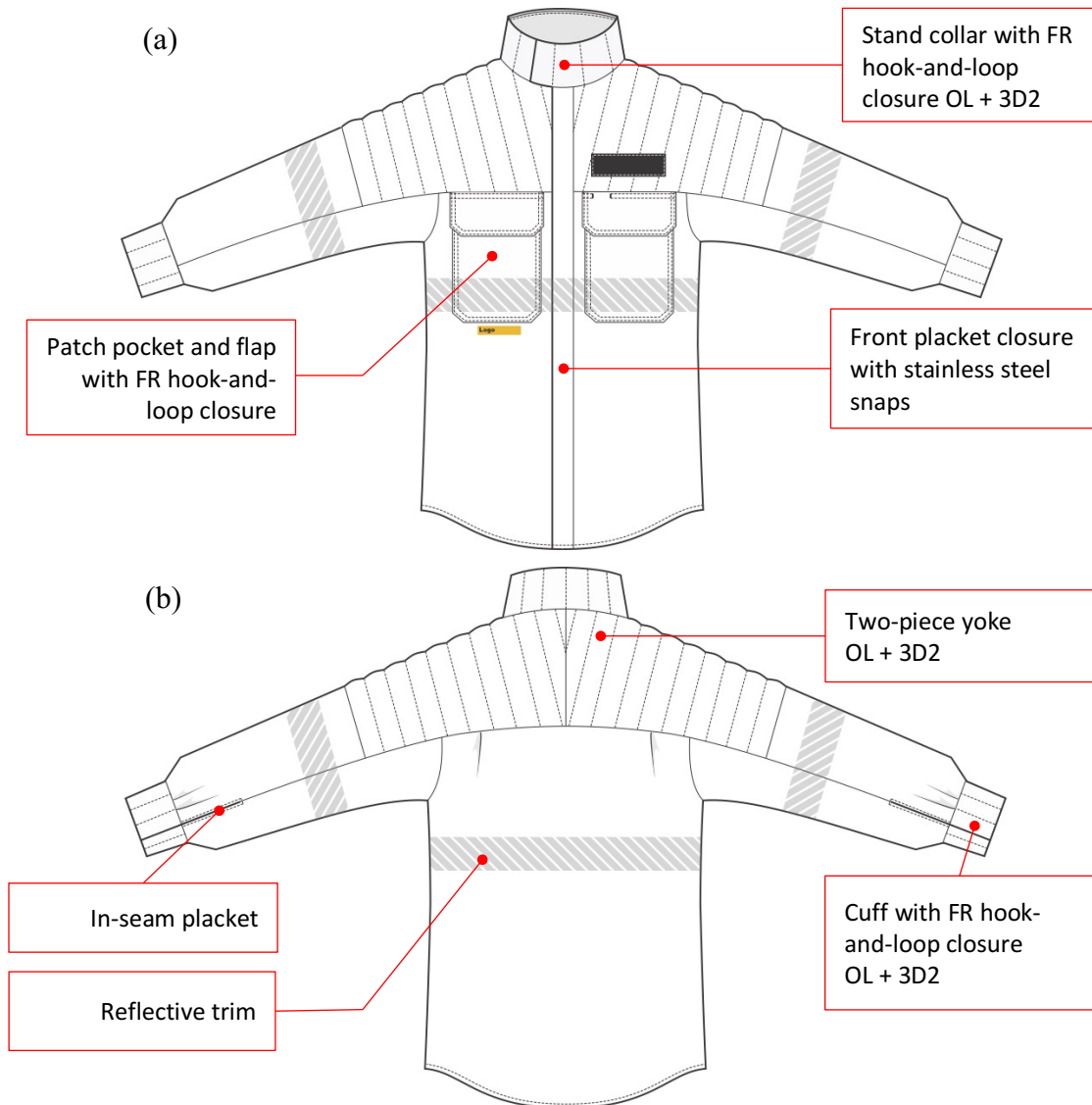


Figure 6.3 Technical drawing of prototype shirt design: (a) front view, (b) back view.

6.3.1 Development of prototype shirt patterns in CLO

Development of prototype shirt patterns was conducted in CLO software. It comprised several steps, such as adjustment of simulated mannequin size, development of pattern pieces of the control shirt, manipulating existing pattern pieces of the control shirt to develop new pattern pieces of the prototype shirt and garment fit simulation.

Prior to any pattern development, the simulated mannequin (avatar) was created in the CLO software and accurately adjusted to be the same dimensions as the flash fire instrumented manikin used for testing. These dimensions included a height of 177 cm, chest circumference of 101 cm, waist of 85 cm and hip of 99.5 cm. The CLO software allows for working in two windows (2D and 3D) simultaneously. The 2D window allows for flat pattern pieces to be developed, edited, and manipulated. The 3D window is for garment seam application and fitting simulation on the avatar. As a result, the software enables the visualization of the final garment fit and allows for pattern adjustments without sewing multiple mock-up garments.

Development of the control shirt pattern

Once the size of the simulated mannequin was adjusted, the next step was to develop pattern pieces of the control shirt. The wildland firefighters' protective shirt provided by Winner Garment Industries Ltd. was measured and almost identical pattern pieces were developed in the CLO software (Figure D.1). The pattern pieces included the shirt front (2), back (1), set-in sleeve (2), back yoke (2), cuff (4), collar (2), patch pocket (2), pocket flap (4) and front placket (2). The front placket closure of the control shirt was slightly different from the shirt of Winner Garment Industries Ltd. It had stainless steel sewn-on hidden snaps instead of a concealed closure with buttons. The simulated garment and mock-up garment showed a very good fit on the avatar and manikin, meaning there was no excess material forming folds or improper drape or restrictions on the body (Figure 6.4, and Figure D.3). Only the stand collar pattern was slightly changed to ensure a tighter fit of the collar to the neck. Once all these steps were completed, the pattern pieces were ready to use for the prototype shirt development.

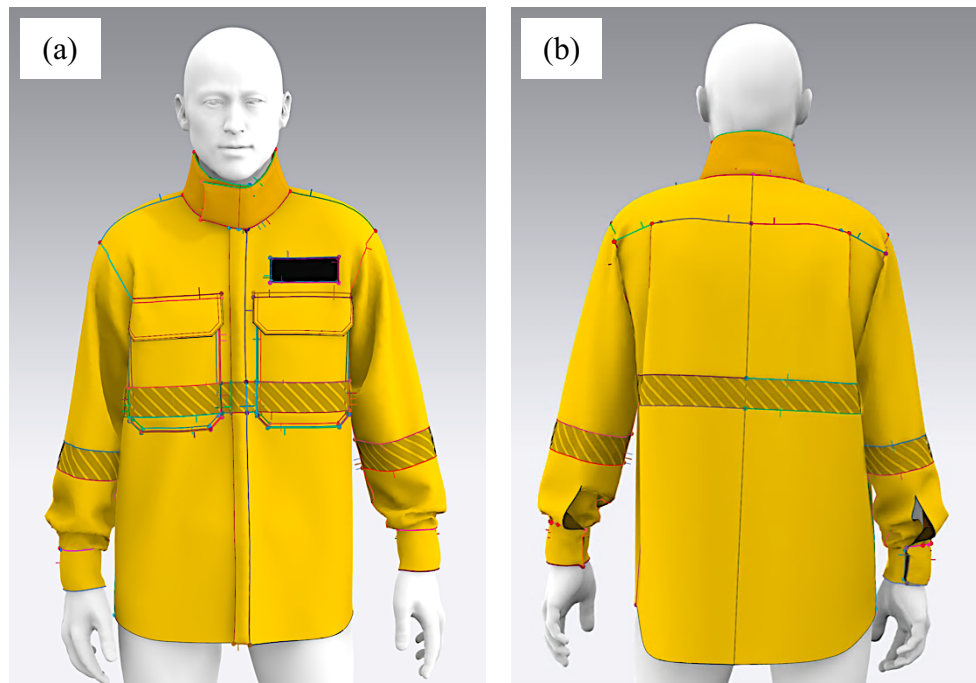


Figure 6.4 Simulation of control shirt fit in CLO: (a) front view, (b) back view.

Development of the prototype shirt pattern

The new pattern pieces of the prototype shirt were developed by manipulating and editing previously developed pattern pieces for the control shirt. The prototype shirt pattern design included editing of the back yoke, front, back and sleeve patterns (Figure 6.5). The back yoke was lowered by 5.5 cm to cover most of the upper back area that has no air gap between the garment and skin. A front yoke was also created to cover most of the front upper torso area that also has no air gap. The front, back, and sleeves of the control shirt were joined by the shoulder, armhole, and sleeve cap seams. The bottom seams of the front and back yokes were extended throughout the sleeve. Thus, the sleeve was divided into three pattern pieces including back under-sleeve, upper-sleeve, and front under-sleeve. The part of the upper-sleeve that covers the upper arm area was cut and joined with the modified back and front yoke. As a result, a one-piece yoke was developed for each side of the shirt (left and right) that seamlessly covers the upper front and back torso and the upper arm area (shaded in red). This pattern manipulation allowed the incorporation of the three-dimensional warp-knitted fabric into a modified yoke that covers the areas (excluding wrist and

neck areas) that are prone to burn injuries in short-duration flame-engulfment tests (Figure 6.6). The three-dimensional warp-knitted fabric was separately incorporated into the collar and cuffs. Smaller-sized pattern pieces for the yoke, collar, and cuffs were developed specifically for the three-dimensional warp-knitted fabric. In this way, the extra fabric was not included in the construction seams of the shirt. Instead, it was quilted together with the outer fabric.

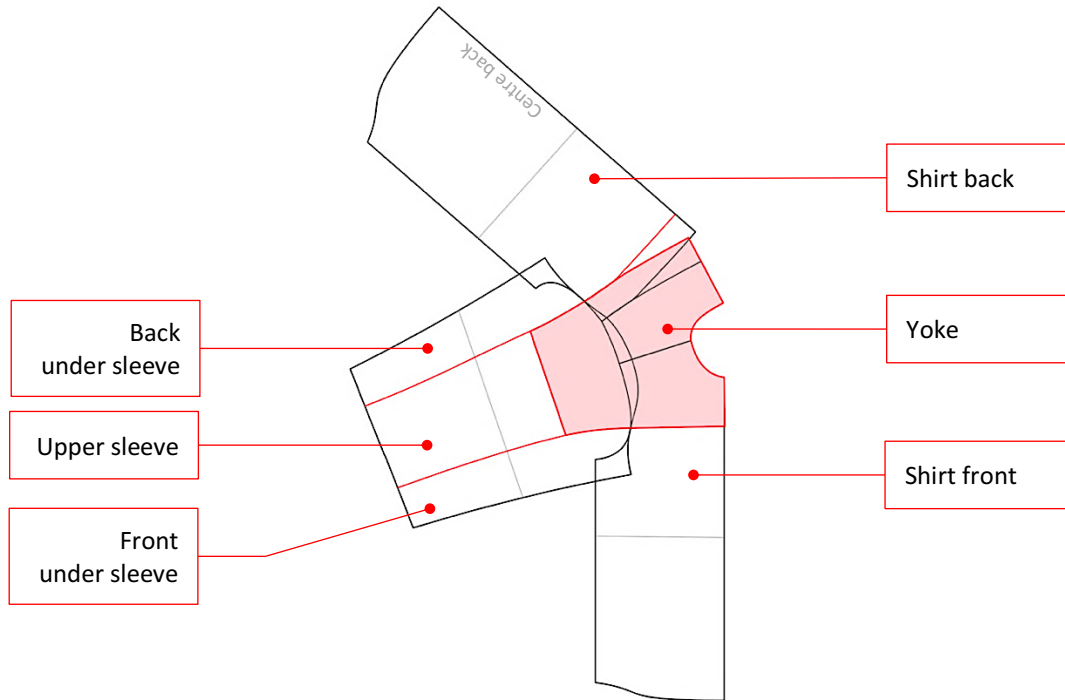


Figure 6.5 Yoke joining the front and back yokes with a portion of the sleeve cap.



Figure 6.6 Top view of modified yoke in simulated prototype shirt.

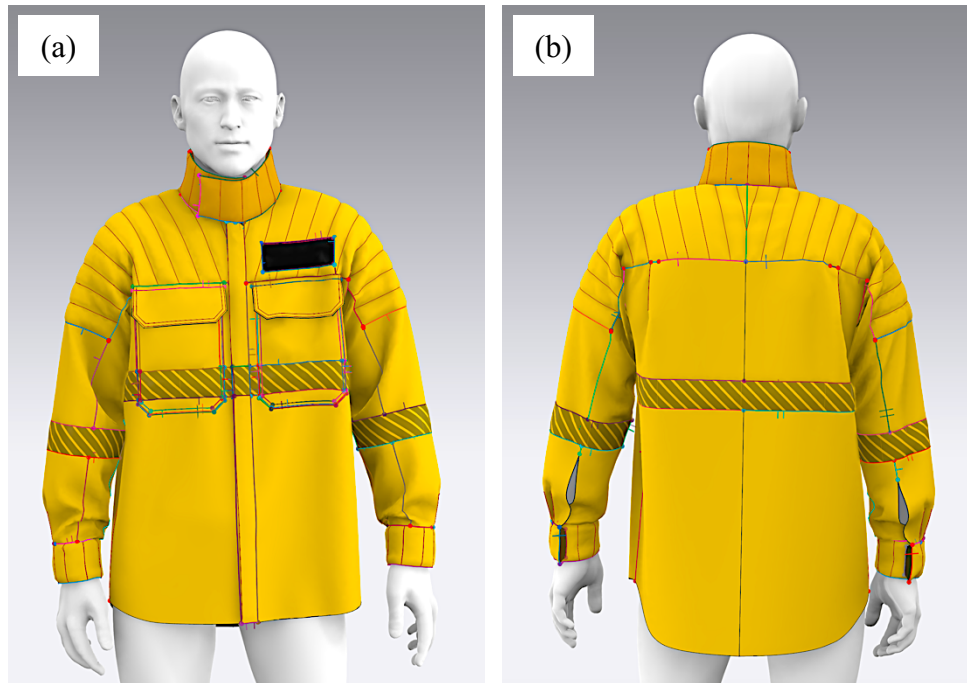


Figure 6.7 Simulation of prototype shirt fit in CLO: (a) front view, (b) back view.

Overall, the prototype shirt contained pattern pieces for the front (2), back (1), upper-sleeve (2), front under-sleeve (2), back under-sleeve (2), yoke (2), cuff (4), collar (2), patch pocket (2), pocket flap (4), and front placket (2) (Figure D.2). The simulated garment showed excellent fit on the avatar (Figure 6.7).

6.3.2 Construction of prototype shirt

The construction of wildland firefighters' protective clothing does not require any specialized equipment for special purpose seams (e.g. welded seams). A two-thread lockstitch sewing machine and a four-thread overlock sewing machine were used for the prototype construction. All types of seams and stitches in the prototype shirt construction were applied in accordance with the ASTM D 6193 standard (ASTM, 2020e). The garment mock-up fitting, and prototype shirt construction process are presented below.

As described previously, the 3D simulation of the prototype shirt in CLO software demonstrated an overall good fit of the garment. However, some fabric properties, specifically fabric stiffness, were not accurately visualized in the software. Thus, a mock-up garment made from a fabric with similar thickness and stiffness to

the OL fabric was sewn before the final construction of the prototype shirt. The mock-up garment showed excellent fit, meaning there was no excess material forming folds or improper drape or restrictions on the body and no further adjustments were needed before the final prototype shirt was constructed (Figure D.4).

Figure 6.8 shows the front and back views of a fully constructed prototype shirt. The materials used in the garment construction included Nomex[®] IIIA fabric used for the outer layer, flame-resistant three-dimensional warp-knitted fabric Spacetec[®], flame-resistant hook-and-loop fastener (50 mm wide strip), segmented adhesive reflective trim (50 mm wide strip, 3M[™] Scotchlite[™]), stainless steel sew-on snaps, and aramid threads. Additional information regarding the material consumption is provided in Table D.1.

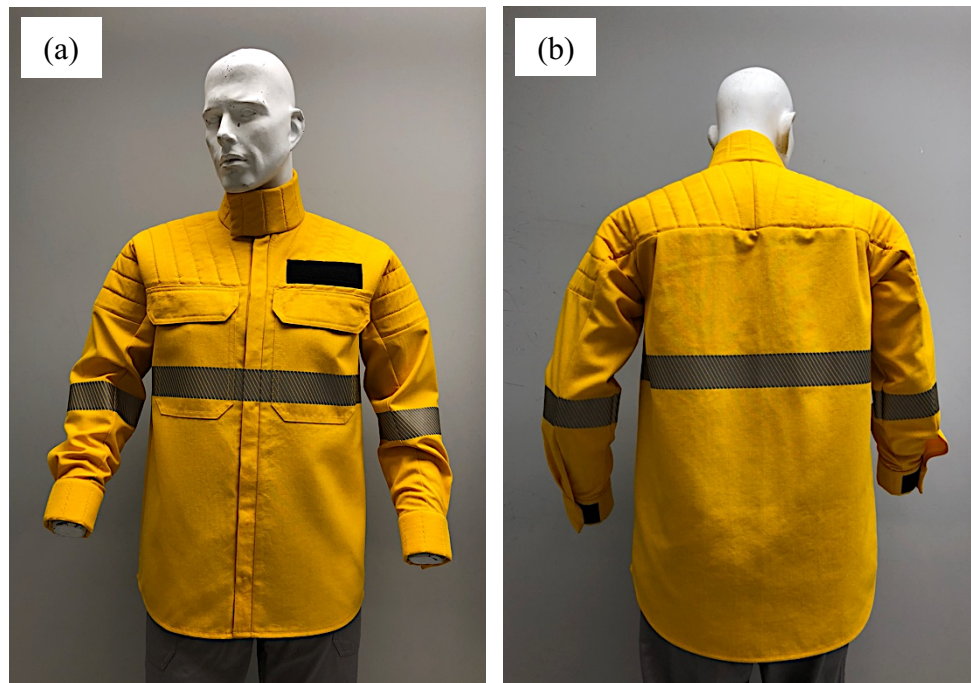


Figure 6.8 Constructed wildland firefighter's prototype shirt: (a) front view, (b) back view.

The construction sequence included preparing the separate pieces of yoke, front, back, cuffs, and collar, and joining all prepared pieces together. Figure E.8 shows a detailed view of the main parts of the constructed prototype shirt. The full construction sequence, including the types of seams and the stitches used, is provided in Table D.2.

Figure 6.9 shows the top view of the prototype shirt yoke. As previously described, the yoke has no shoulder seam or armhole-sleeve cap seam. The outer layer of the yoke was quilted together with the three-dimensional warp-knitted fabric. This design solution which joined the front and back yokes along with a portion of the upper-sleeve eliminated any possible seam bulk from sewing two layers of the outerlayer fabric with the three-dimensional warp-knitted fabric. It also simplified the garment construction and improved the overall range of motion of this area of the garment. Since wildland firefighters carry heavy backpacks on duty, eliminating the seams and providing additional cushioning from the three-dimensional knitted fabric in the shoulder, upper front and back torso areas may also improve the physical comfort properties of the garment.



Figure 6.9 Top view of modified yoke in constructed prototype shirt.

Construction of the yoke included attachment of bias binding along the three-dimensional warp-knitted fabric (seam SSaa, LSq; stitch 301) and stitching the outer layer fabric with three-dimensional warp-knitted fabric following evenly spaced 30 mm distant stitch lines (seam SSv; stitch 301). The pattern piece for the three-

dimensional warp-knitted fabric is smaller than the piece for the outer layer fabric, so bias binding was attached to compensate for the initial dimensions. This approach allows the exclusion of three-dimensional warp-knitted fabric from any seam allowances and makes the seams thinner and more flexible. Figure 6.10 presents schematic drawings of this construction technique and Figure D.5(b) presents a detailed view of the inner side of the yoke.

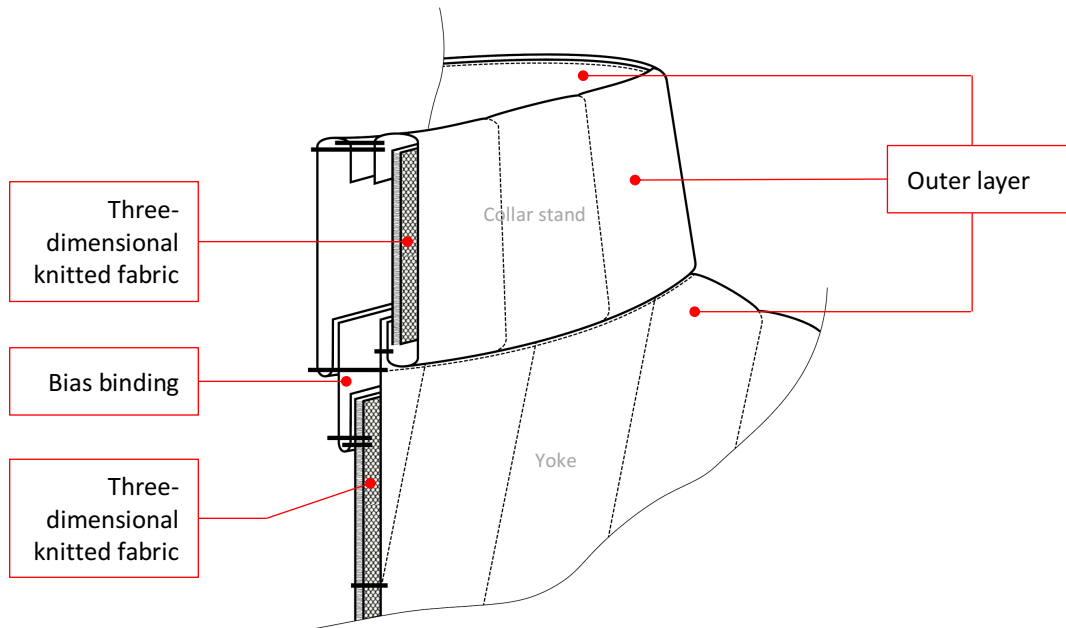


Figure 6.10 Schematic drawing of stand collar and yoke construction with incorporated layer of three-dimensional warp-knitted fabric.

Cuffs and collar construction included similar operations. Like the yoke construction, the pattern pieces for the three-dimensional warp-knitted fabric of the cuffs and collar are smaller than the pieces for the outer layer fabric. However, these pieces were directly stitched to the outer layer fabric of the cuffs or collar following evenly spaced 30 mm distant parallel lines (seam SSv; stitch 301). Eventually, the three-dimensional warp-knitted fabric was positioned between the outer layer fabric forming the outer and inner surfaces of the cuffs and collar (seam LScg-2; stitch 301). Figure 6.11 shows a schematic drawing of this construction technique and Figure D.5 shows a detailed view of collar and cuff.

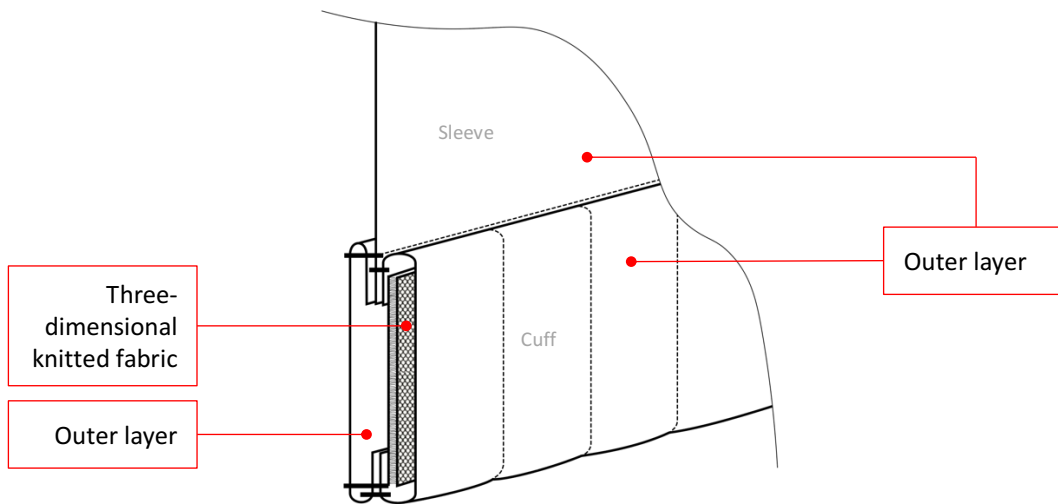


Figure 6.11 Schematical drawing of cuff construction with incorporated layer of three-dimensional warp-knitted fabric.

The yoke, collar, and cuffs that are padded with the three-dimensional warp-knitted fabric cover approximately 25% of the whole prototype shirt area. Construction of the shirt front included preparation and attachment of patch pockets and flaps, also attachment of snaps to the front plackets (seam LSbj, LSd-2, SSa-1, SSe-3; stitch 301, 506). The action pleats of the shirt back were pressed and basted before joining all pieces together. The final step was to join all sections of the garment together, serge the edges, and finish the hem (seam SSa-2, EFs; stitch 301, 506).

6.4 Summary

The design requirements for wildland firefighters' protective clothing outlined in the CAN/CGSB-155.22 and NFPA 1977 standards were identified and taken into consideration for the development of the prototype shirt. As well, a review of existing patented inventions showed that there are no wildland firefighters' protective shirt designs that focus on improving thermal protection in the selected contact areas known to be susceptible to burn injuries in flash fire tests. However, one patent of [Butzer and Coombs \(1995\)](#) disclosed a short thermal protective overjacket worn on top of structural firefighters' protective clothing. It aimed to provide additional thermal protection to similar areas as the prototype shirt of this research.

Innovative garment production techniques were developed that allowed for the successful incorporation of a three-dimensional raschel warp-knitted fabric made of inherently flame-resistant fibres (patented by [Keitch \(2014\)](#)) into the yoke, collar, and cuffs of the prototype shirt constructed for this research.

Although the garments were constructed by the researcher, the final patterns, construction sequence, and sewing techniques were sufficiently developed to be used for industrial garment production. Modern design tools such as CLO software allowed for computer visualisation of the garment on the manikin, and ensured an excellent fit of the final garments without requiring additional adjustments.

Development of the novel prototype shirt design and construction of the control and prototype shirts allowed for the next level of the research which was performing the full-scale flash fire instrumented manikin tests.

CHAPTER 7 THERMAL PROTECTION PERFORMANCE OF SHIRT PROTOTYPE AT FULL-SCALE LEVEL

7.1 Introduction

Thermal protection is a function of garment design and total garment assembly as well as fabric structure and fibre properties, therefore, it is important to conduct not only bench-scale tests of fabric and fabric systems but also follow-up with full-scale tests of garment systems (Crown et al., 1998). This chapter addresses the fourth objective of the research which is focused on the thermal protection assessment of the control shirt of wildland firefighters' protective clothing and shirt prototype when tested by a flash fire instrumented manikin test system (ASTM, 2018c). Each shirt was tested as part of a whole garment ensemble. Data was obtained as the percentage of the predicted total manikin body surface area (including predicted second-degree and third-degree burn injury), and the analysis of individual sensor response in absorbed heat flux and its variation with time in areas prone to second-degree burns. The obtained absorbed heat flux values were used to assess whether the incorporated three-dimensional knitted fabrics in the areas of neck, shoulders, upper arms, upper front and back torso, and wrists in the prototype shirt design of wildland firefighters' protective clothing can provide greater thermal protection when compared with the wildland firefighters' protective clothing shirt design that is currently in use. Additionally, the observations of each shirt's appearance after 4-second flame exposure were recorded.

As described in Chapter 3, three replicates of the garment ensemble with control shirts, and three replicates of the garment ensemble with the prototype shirts tested. Each garment ensemble included a shirt and pants worn on top of a cotton t-shirt and briefs. All garments were prewashed and dried to remove any flammable residuals from mill finishes in accordance with CAN/GSB-4.2 No.58 as specified in CAN/GSB-155.22 (CGSB, 2014, p.8; CGSB, 2019).

7.2 Results and discussion

This section presents a description of the appearance of the control and prototype shirts after 4 seconds of flame engulfment. As well, the thermal protection performance of each type of shirt, and statistical analysis of the independent sample t-test comparison of this performance measured in total percentage of predicted second-degree and third-degree burn injury is presented. An analysis of the response of individual sensors from areas of interest is also presented as absorbed heat flux and its variation with time.

7.2.1 Performance of garment ensemble with control shirt

Control shirts made of Nomex[®] IIIA fabric were worn on top of cotton t-shirts and tucked into the pants when tested (Figure 7.1, also Figure E.1 and Figure E.3). The air gap between the garment ensemble with control shirt and the manikin was distributed unevenly. The maximum air gap was at the waist and arm area, and minimal to no air gap at the areas of the neck, shoulders, upper arms, upper front and back torso, and wrists.

The torso and upper arm areas of the manikin were covered with two layers of fabric including the outer layer fabric of the shirt and t-shirt fabric underneath with various air gap locations (fabric systems OL-BL, OL-BL-S, OL-S-BL). The yoke and front patch pockets with flaps of the control shirt comprised two outer layers, and a t-shirt (fabric system OL(2)-BL). The arms were covered with long sleeves that had only one outer layer of OL. Neck and wrists were covered with a stand collar and cuffs that comprise two layers of outer layer fabric OL(2). The collar stand, pocket flaps and cuffs had FR hook and loop closures.

Figure 7.2, also Figure E.2 and Figure E.4 show the appearance of each control shirt after the full-scale 4-second flame engulfment of the whole garment ensemble on the instrumented manikin. More detailed observations for control shirt appearance after testing were recorded: discolouration (colour change from yellow to gray and brown) of the major portion of the fabric; thermal shrinkage of the fabric that notably decreased the air gap between the garment and manikin surface in the

waist and arm areas; degradation and char formation led to some break-open of the fabric at folds and creases; also melting of the hook and loop closures on the cuffs (Figure E.9 and Figure E.10(a)).

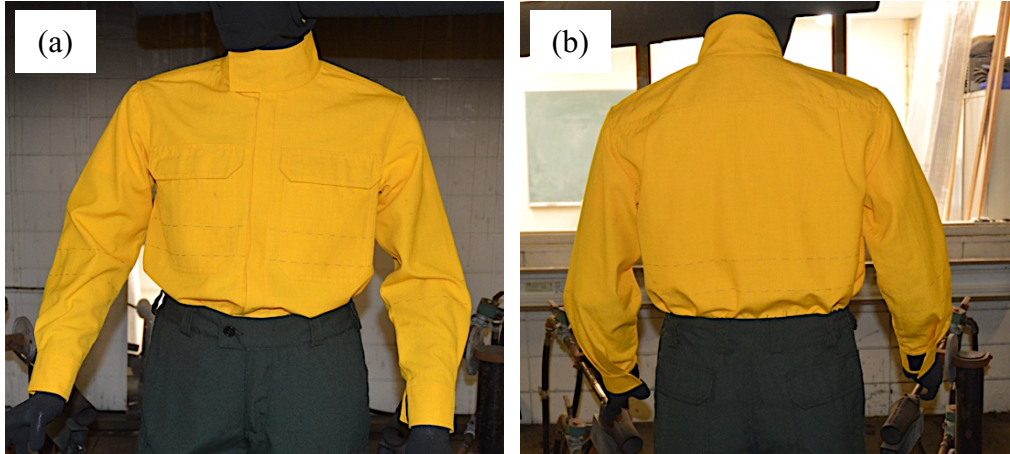


Figure 7.1 Control shirt number 2 before the full-scale flame engulfment for 4 seconds: (a) front view, and (b) back view.



Figure 7.2 Control shirt number 2 after the full-scale flame engulfment for 4 seconds: (a) front view, and (b) back view.

Figure 7.3, also Figure E.12 and Figure E.13 show the burn injury pattern spread throughout the manikin surface after full-scale 4-second flame engulfment of the garment ensemble with the control shirt. These computer-generated images of the manikin surface indicate predicted second-degree burn areas with yellow and predicted third-degree burn areas with red. The sensors of the manikin's head were not covered by the garment ensembles, and in each test, the skin simulant sensors of the head generated predicted third-degree burns as indicated by the red colour. Burn injuries were mainly concentrated on the legs, and arms where the garment ensemble had only one layer of fabric. Also, burns were predicted in the upper arms, neck, and upper front and back torso. These areas did not have an air gap between the garment system and skin simulant sensors mounted at the manikin surface. Thus, despite the presence of two layers of fabric covering the manikin surface in those areas, the lack of air gap allowed sufficient thermal energy transfer during the testing to cause burns. Additionally, second-degree, and third-degree burns were predicted in the wrist and cuff closure areas. And in some cases, the upper arm area reached third-degree burns.

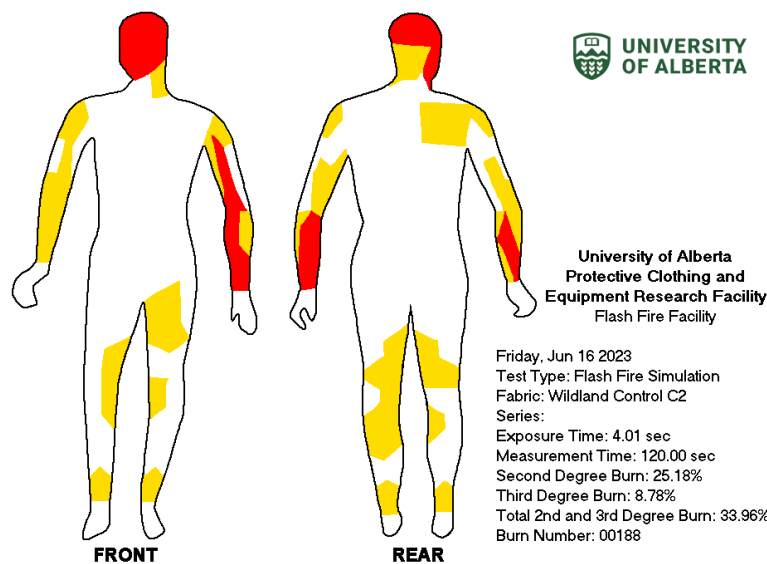


Figure 7.3 Burn injury pattern generated by the instrumented manikin system when the garment ensemble with control shirt number 2 was engulfed in flames for 4 seconds.

Table 7.1 summarises the instrumented manikin test results for each garment ensemble tested with the control shirt. It shows the percentage of second-degree, third-degree, and total burn area for each garment ensemble with the control shirt. Also, it includes the after-flame data for each garment ensemble and for the control shirt alone. Skin simulant sensors showed an average prediction of second and third-degree burn injury of $22.38 \pm 2.99\%$ and $8.59 \pm 0.41\%$ of the manikin surface area, respectively. The 4-second flame engulfment instrumented manikin test of the garment ensemble with the control shirt predicted an average total burn injury of $30.97 \pm 2.94\%$ of the manikin surface area. The average after-flame time of the whole garment ensemble was 3.9 ± 0.5 seconds, and the average after-flame time of the control shirt alone was 2.4 ± 0.3 second.

Table 7.1 Instrumented manikin test results of garment ensemble with control shirt after the full-scale flame engulfment for 4 seconds.

Garment ensemble with shirt	Percent of burn area (%)			After-flame (sec.)	
	Second-degree	Third-degree	Total	Garment ensemble	Shirt
Control 1	19.22	8.87	28.09	3.8	2.7
Control 2	25.18	8.78	33.96	4.5	2.5
Control 3	22.75	8.12	27.66	3.5	2.1
Mean value and standard deviation	22.38 ± 2.99	8.59 ± 0.41	30.97 ± 2.94	3.9 ± 0.5	2.4 ± 0.3

Overall, after the full 4-second flame engulfment of the garment ensemble, the control shirt had major areas of discoloured fabric, notable thermal shrinkage of fabric in the areas of waist and arms, degraded fabric and char formation with some broken open parts, and melted hook and loop closures. The after-flame of the whole garment ensemble was 3.9 seconds, and 2.4 seconds of the control shirt alone on average. The test results generated by the instrumented manikin system, showed second-degree burn of 22.38%, third-degree burn of 8.59%, for a total burn of 30.97% of the whole manikin surface on average. The total burn area of the manikin surface under the control garment ensemble was 26.52%.

Rucker et al. (2000) also tested various wildland firefighters protective clothing using an instrumented manikin system and 4-second flame exposure. As mentioned in Chapter 2, during the experiment, the authors also used protective jackets and pants of various designs that are made of aramid. Some of them were two-layer garment systems and one was a one-layer garment system. The two-layer garment systems were worn over work pants and also had jackets with sleeve liners. The one-layer garment system was tested without sleeve liners and work pants. All garment systems were tested over cotton t-shirts and briefs. Two-layer systems showed 9.6% - 15.87% total burn area of the manikin surface under the garment system. A one-layer garment system in Rucker et al. (2000), was similar to the garment ensemble with control shirt tested in this research. It showed 52.67% total burn area of the manikin surface under the garment system, which is two times more than the results obtained in this research.

Rucker et al. (2000), similarly to Crown et al. (1993), concluded that a multilayer system provides significantly higher thermal protection from flames with a much lower percentage of burn area. Rucker et al. (2000) also found that lining the sleeves with FR cotton fabric improved the thermal protection of the arms and decreased the burn areas of arms. The areas of the upper front and back torso, upper arms, shoulders, neck and wrists for one-layer and two-layer garment systems indicated burns after 4-second flame exposure which is consistent with the data obtained in this research. Also, the researchers recorded similar outer layer fabric observations after flame exposure, such as discolouration, shrinkage, and charring with broken-open areas.

It is important to note that manikin testing is not required in the CAN/CGSB-155.22 and NFPA 1977 standards for wildland firefighters' protective clothing. However, the design of protective clothing for industrial personnel is similar to protective clothing of wildland firefighters. CAN/CGSB-155.20 and NFPA 2112 is a standard for flame-resistant clothing for the protection of industrial personnel against short-duration thermal exposures from fire (CGSB, 2017; NFPA, 2023). According to NFPA 2112 standard requirements, the results for a 6 oz (~200 g/m²) garment should

fall within the range of 16% to 24% predicted body burn following a 3-second flame exposure. There are no requirements for a 4-second exposure in the NFPA 2112 standard.

7.2.2 Performance of garment ensemble with prototype shirt

Prototype shirts were made of Nomex[®] IIIA fabric and three-dimensional warp-knitted fabric type 2 that was sewn (quilted) together with the outer layer of the yoke, collar and cuffs. The prototype shirts were worn on top of cotton t-shirts and tucked into pants when tested (Figure 7.4, also Figure E.6 and Figure E.8). The air gap between the garment ensemble with prototype shirt and the manikin was also distributed unevenly. Similar to the control shirt, the maximum air gap under prototype shirt was at the waist and arm area. However, in contrast to the control shirt, three-dimensional warp-knitted fabric entrapped still air and artificially created an air gap (approximately 6 mm) in the areas of the neck, shoulders, upper arms, upper front and back torso, and wrists of the manikin.

The central and lower torso of the manikin was covered with two layers of fabric including the outer layer fabric of the shirt and t-shirt underneath with various air gap locations (fabric system OL-BL, OL-BL-S, OL-S-BL). The upper front and back torso, and upper arms areas were covered with the one-piece yoke consisting of the outer layer sewn together with the three-dimensional warp-knitted fabric with the t-shirt underneath (fabric system OL-3D1-BL). The neck and wrists were covered with the collar and cuffs that comprised two outer layers with the three-dimensional warp-knitted fabric placed between (OL-3D1-OL). Similar to the control shirt, the front patch pockets with flaps also comprise two outer layers over the t-shirt (fabric system OL(2)-BL). The arms were covered with long sleeves that had only one outer layer of OL. The pocket flaps, collar and cuffs had FR hook and loop closures.

Figure 7.5, also Figure E.6 and Figure E.8 show the appearance of each prototype shirt after the full-scale 4-second flame engulfment of the whole garment ensemble on the instrumented manikin. Recorded observations for the appearance of the prototype shirt after testing were similar to the control shirt observations:

discolouration (colour change from yellow to gray and brown) of the major portion of the fabric; thermal shrinkage of the fabric that notably decreased the air gap between the garment and manikin surface in the waist and arm areas; degradation and char formation led to some break-open of the fabric along some folds and creases; also melting of the hook and loop closures on cuffs. The appearance of the three-dimensional warp-knitted fabric incorporated into the prototype shirt was also examined and the condition recorded after the 4-second flame exposure (Figure 7.6, and Figure E.11).



Figure 7.4 Prototype shirt number 2 before the full-scale flame engulfment for 4 seconds: (a) front view, and (b) back view.

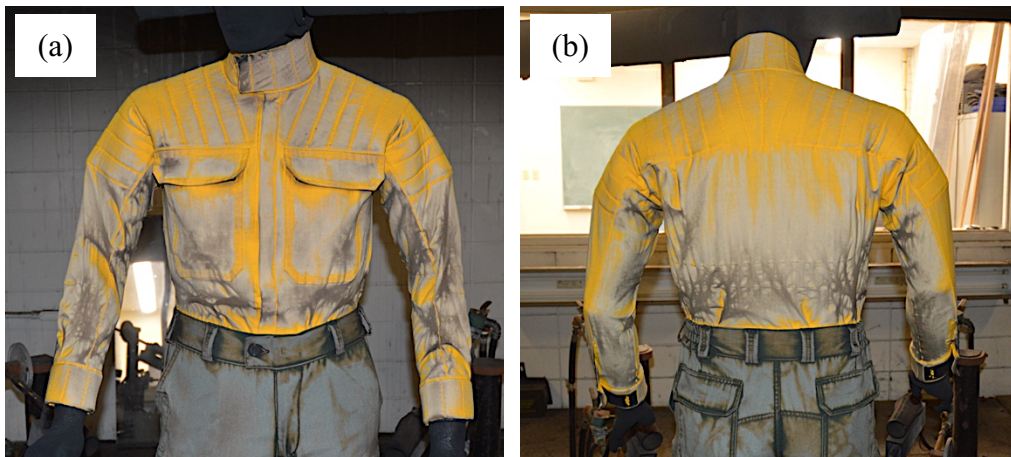


Figure 7.5 Prototype shirt number 2 after the full-scale flame engulfment for 4 seconds: (a) front view, and (b) back view.

Figure 7.6 shows no damage to the inner side of three-dimensional warp-knitted fabrics in the yoke area. It should be noted that the black marks on the collar and yoke are from soot that transferred from the manikin surface and are not charred or burned areas of fabric. The yoke, collar, and cuffs were cut open from the flame exposed side to observe the three-dimensional warp-knitted fabric directly underneath the outer fabric after testing. Figure E.11 shows that there was no visible damage to the three-dimensional warp-knitted fabrics, even within the cuffs at the wrist area that received the highest thermal energy heat flux exposure, and where third-degree burns were predicted (Figure 7.7).

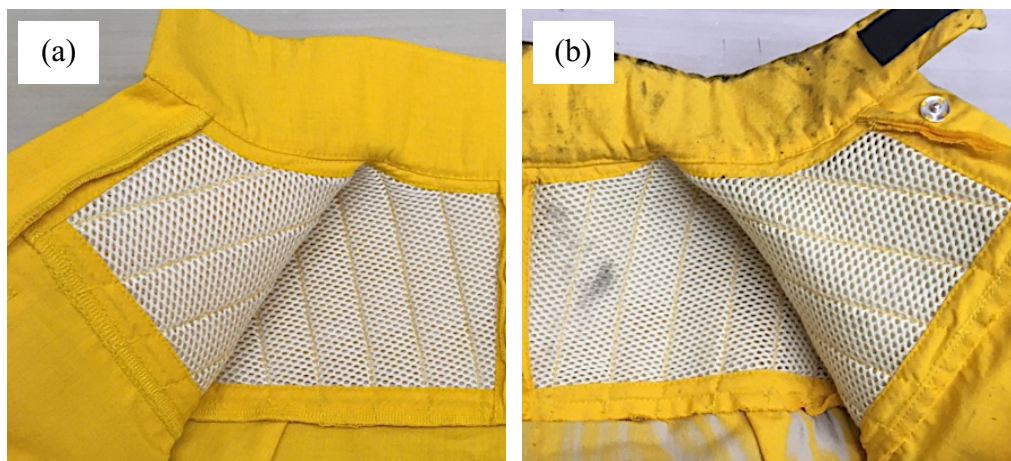


Figure 7.6 Three-dimensional warp-knitted fabric in the yoke area: (a) before, (b) after the full-scale flame engulfment for 4 seconds (black areas are soot from the manikin surface).

Figure 7.7, also Figure E.14 and Figure E.15 show the burn injury pattern spread throughout the manikin surface after full-scale 4-second flame engulfment of garment ensemble with prototype shirt. Similar to the testing of the garment ensemble with the control shirt, burn injuries were mainly concentrated in the legs, and arms where the garment ensemble with the prototype shirt had only one layer of fabric. In contrast to the garment ensemble with the control shirt, the areas of the upper arms, neck, and upper front and back torso did not indicate predicted burn injuries. Therefore, it would appear that these areas were insulated with still air entrapped in the incorporated three-dimensional warp-knitted fabrics during the test. Noticeably

fewer third-degree burns were indicated in the arm, and specifically wrist area under the tested prototype shirt compared to the control shirt. However, despite of presence of the three-dimensional warp-knitted fabrics within the cuffs, the wrists areas still showed some predicted second and third-degree burns. Thus, the new cuff design in the prototype shirt did not improve the thermal protection performance in those areas. The exact reason is thought to be a combination of factors. The cuffs may not have fully covered the sensors on the wrists or they were not closed tightly enough around the wrists. Also, the in-seam placket on the sleeves (Figure D. 5 (e and f)) did not completely seal that area and allowed access for direct thermal energy to reach the manikin sensor in the wrist area. Further improvement of the cuff and closure design is needed.

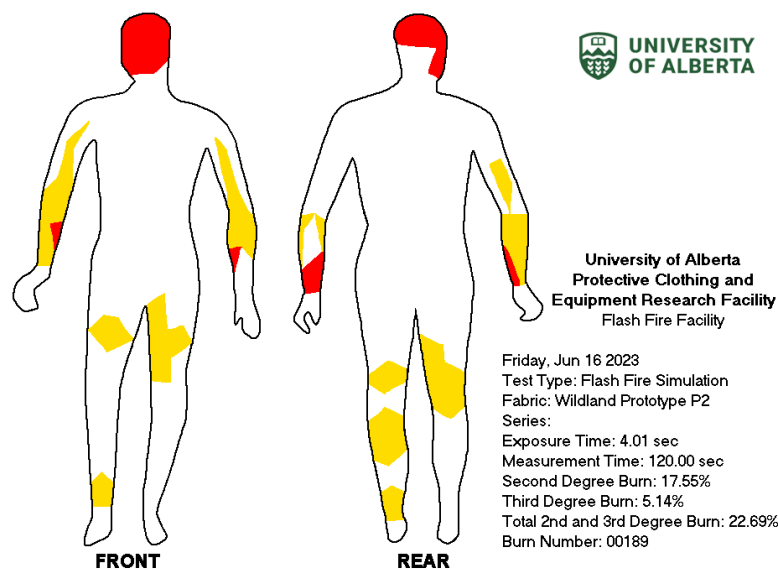


Figure 7.7 Burn injury pattern generated by the instrumented manikin system when the garment ensemble with prototype shirt number 2 was engulfed in flames for 4 seconds.

Table 7.2 summarises the instrumented manikin test results for each garment ensemble tested with the prototype shirt. It shows the percentage of second-degree, third-degree, and total burn area for each garment ensemble with the prototype shirt. Also, it includes the after-flame data for each garment ensemble and for the prototype

shirt alone. Skin simulant sensors showed an average prediction of second and third-degree burn injury of 18.86 ± 1.98 % and 5.86 ± 0.69 % of the manikin surface area, respectively. The 4-second flame engulfment instrumented manikin test of the garment ensemble with the prototype shirt predicted an average total burn injury of 24.72 ± 2.61 % of the manikin surface area. Total burn area of the manikin surface under the prototype garment ensemble was 19.7 %. The average after-flame time of the whole garment ensemble was 3.7 ± 0.7 seconds, and the average after-flame time of the prototype shirt alone was 2.6 ± 0.4 second.

Table 7. 2. Instrumented manikin test results of garment ensemble with prototype shirt after the full-scale flame engulfment for 4 seconds.

Garment ensemble with shirt	Percent of burn area, (%)			After flame (sec.)	
	Second-degree	Third-degree	Total	Garment ensemble	Shirt
Prototype 1	17.88	5.92	23.80	4.4	2.4
Prototype 2	17.55	5.14	22.69	3.0	2.3
Prototype 3	21.14	6.52	27.66	3.8	3.1
Mean values and standard deviation	18.86 ± 1.98	5.86 ± 0.69	24.72 ± 2.61	3.7 ± 0.7	2.6 ± 0.4

Overall, similar observations were recorded for the garment ensemble with the prototype shirt after the full 4-second flame engulfment as those for the garment ensemble with the control shirt. The prototype and control shirts had major areas of discoloured fabric, notable thermal shrinkage of the outer layer fabric in the areas of the waist and arms, degraded fabric and char formation with some broken open parts and melted hook and loop closures on the cuffs. The three-dimensional warp-knitted fabric incorporated into the prototype shirt showed no visual damage in the yoke area or within the collar and cuffs. The average after-flame results were also similar in both garment ensembles. The garment ensemble with the prototype shirt had an average after-flame of 3.7 seconds for the whole garment ensemble and 2.6 seconds for the shirt alone, whereas the garment ensemble with the control shirt had an

average after-flame of 3.9 seconds for the whole garment ensemble and 2.4 seconds for the shirt alone.

Burn injuries were mainly concentrated in the legs, and arms where the garment ensemble with the prototype shirt had only one layer of fabric. Also, despite the presence of three-dimensional warp-knitted fabrics within the cuffs, the wrist area showed second and third-degree burns when the garment ensemble with the prototype shirt was fully engulfed in flames. Further improvement of design for sleeve, cuff and closure is needed. The research of [Rucker et al. \(2000\)](#) found that sleeves with FR cotton lining provided good thermal protection that led to minimal to no burns on the arms. Thus, the lining of sleeves with FR cotton fabric or incorporating additional layer of the outer fabric would be one of the suggestions for future shirt design improvement. Another suggestion would be to make a gusset closure instead of the current in-seam placket of the prototype shirt. A gusset closure provides an insert of fabric between the sides of sleeve opening that widens the cuff area and allows the hand to pass through. When the cuff is closed, the gusset fabric covers the manikin surface behind the sleeve opening and could help prevent burn injuries in the wrist area.

The test results generated by the instrumented manikin system for the garment ensemble with the prototype shirt and the garment ensemble with the control shirt are different. A statistical analysis was carried out to determine the significance of the differences. This data analysis is presented in the next section.

7.2.3 Comparison of thermal protection performance of garment ensembles with control and prototype shirts

This section addresses the sixth null hypothesis of the fourth objective of this research. The sixth null hypothesis states that there is no significant difference in thermal protection performance between the garment ensemble with the control shirt and the garment ensemble with the prototype shirt when tested by the flash fire instrumented manikin system at the full-scale level.

7.2.3.1 Summary of instrumented manikin test results

Table 7.3 and Figure 7.8 present comparisons of the percentages with second-degree, third-degree, and total burn area between garment ensembles with prototype shirts and control shirts. The full-scale, 4-second flame engulfment of the garment ensemble with the control shirt showed an average total predicted burn injury of 30.97 ± 2.94 % of the manikin surface that included 22.38 ± 2.99 % second-degree burn, and 8.59 ± 0.41 % third-degree burn. The full-scale, 4-second flame engulfment of the garment ensemble with the prototype shirt showed an average total predicted burn injury of 24.72 ± 2.61 % of the manikin surface that included 18.86 ± 1.98 % second-degree burn, and 5.86 ± 0.69 % third-degree burn.

Table 7.3 Summary table of the mean values of percentage of the manikin surface reaching the criteria for second or third degree burn when the garment ensembles were exposed to 4-seconds of flame engulfment.

Garment ensemble	Mean percentage of manikin surface and standard deviation, (%)		
	Second-degree	Third-degree	Total
Control	22.38 ± 2.99	8.59 ± 0.41	30.97 ± 2.94
Prototype	18.86 ± 1.98	5.86 ± 0.69	24.72 ± 2.61

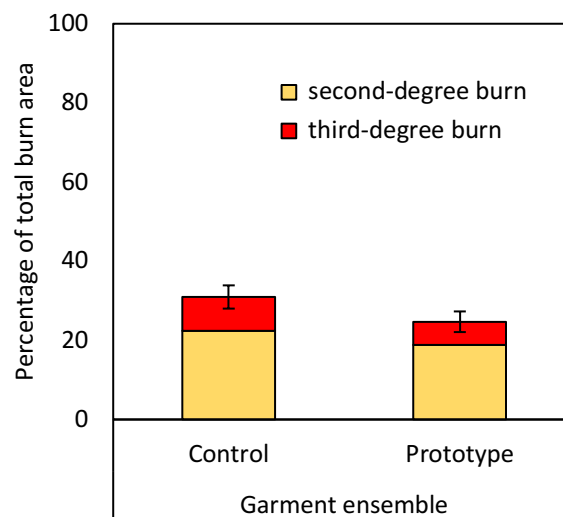


Figure 7.8 Bar chart shows mean percentage of manikin surface reaching second and third-degree burn when garment ensembles with control and prototype shirts were exposed to 4-seconds of flame engulfment.

The predicted second-degree, third-degree, and total burn in the percentage of surface manikin area, obtained for the garment ensemble with prototype shirt is less than the one obtained for the garment ensemble with control shirt.

7.2.3.2 Analysis of independent sample t-test

Independent samples, one-sided t-test allows for testing the sixth null hypothesis and determine whether the difference in the percentage of burns between garment ensembles with the control and prototype shirts is statistically significant.

Table 7.4 shows the comparison of mean values in percentage of burn area between garment ensembles with the control and the prototype shirts tested with instrumented manikin. Three garment ensembles with control shirts and three garment ensembles with prototype shirts were included in the statistical analysis. Statistical significance (α) was set at 0.05.

Table 7.4 Comparison of mean values in percentage of burn area between garment ensembles with control and prototype shirts tested with instrumented manikin.

Burn	Garment ensemble		Mean difference (I-J)	Sig.	95% CI for Difference	
	(I) Shirt	(J) Shirt			Lower Bound	Upper Bound
Second-degree	Control	Prototype	3.53	.082	-2.23	9.23
Third-degree	Control	Prototype	2.73	.002*	1.44	4.02
Total	Control	Prototype	6.26	.025*	-0.04	12.55

* Means are significantly different between garment ensembles with control and prototype shirts when subjected to independent samples t-test ($p < .05$).

Note. One-sided independent samples t-test was performed for each type of burn and garment ensemble.

The independent samples one-sided t-test shows that the mean difference in percentage of second-degree burn area is 3.53% with 95% CI (-2.23, 9.23) between the garment ensembles with control shirt and prototype shirt but is not statistically significant ($p = 0.082$). However, the mean difference in percentage of third-degree burn area of 2.73% with 95% CI (1.44, 4.02) between the garment ensembles with control shirt and prototype shirt is statistically significant ($p = 0.002$). The mean difference in percentage of total burn area of 6.26% with 95% CI (-0.04, 12.55) between the garment ensembles with control shirt and prototype shirt is also statistically significant ($p = 0.025$).

The amount of predicted second-degree burn was similar for some replications of the test for the garment ensembles with both the control and prototype shirts. The variability of second-degree burns obtained from test to test in the leg area also contributed to some similarities in the results of the garment ensembles with the control and prototype shirts. However, the garment ensembles tested with the prototype shirts consistently reduced the amount of third-degree burns and consequently total burns in the percentage of manikin surface area. There were distinctly less second-degree burns in the areas of the upper arms, upper back torso, neck, and less third-degree burns in the areas of arms and wrists.

Overall, there was strong evidence ($p = 0.025$) against the sixth null hypothesis. The incorporation of three-dimensional warp-knitted fabrics in the prototype shirt significantly decreased the total burn area of the manikin by 6.26% on average when fully engulfed in flames with the garment ensemble. Therefore, it can be concluded, that the new prototype shirt design with the incorporation of three-dimensional warp-knitted fabrics in the upper front and back torso, neck, and wrists improved the thermal protection performance of the garment.

7.2.4 Analysis of individual sensor response

This section introduces the selected individual sensor response in absorbed heat flux and its variation with time in areas prone to second-degree burns. Figure 7.9 shows the three-dimensional simulation of the instrumented manikin and the location

of the sensors covered by a shirt. The sensors of interest are located in the areas with no air gap between the garment ensemble and the manikin surface. These areas are highlighted in red since they are prone to burns when the garment ensemble with a control shirt is exposed to full-scale 4-second flame engulfment. The same areas are covered with the three-dimensional warp-knitted fabric incorporated into the prototype shirt. This artificially created an air gap between the garment ensemble and the manikin surface that provided thermal insulation and prevented burns.

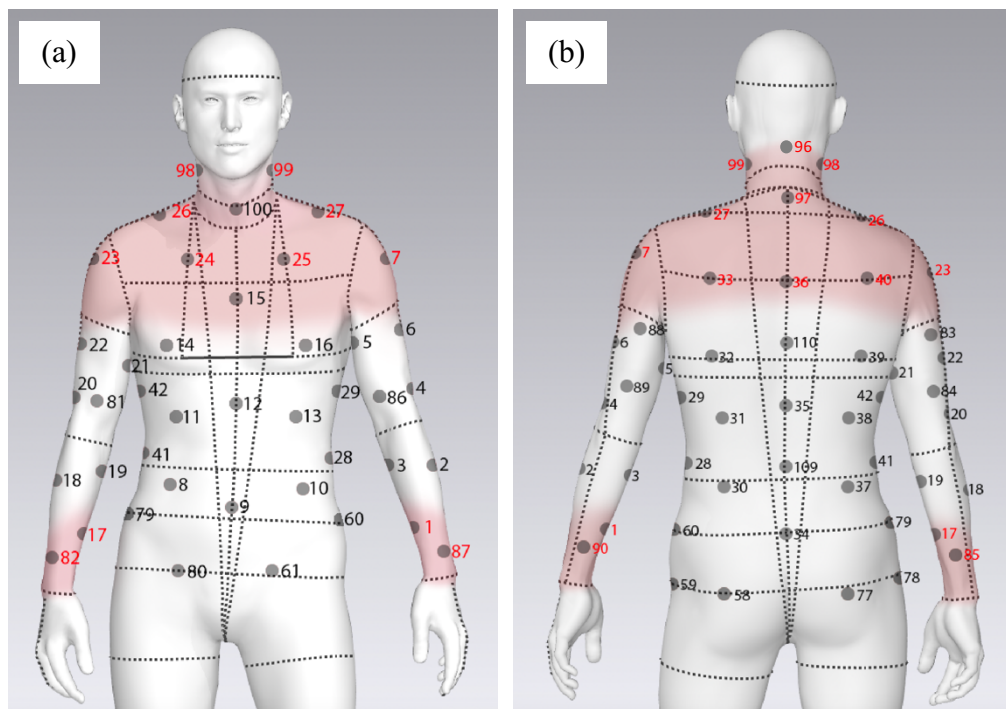


Figure 7.9 Location of sensors covered by the shirt and the areas prone to burn injury (shaded red) on the instrumented manikin: (a) front view, and (b) back view.

As described in Chapter 3, the thermal energy transferred through and from the garment ensemble to the manikin is measured by each sensor during the 4-second flame exposure and for 120 seconds after the exposure. Graphs of the absorbed heat flux and its variation with the time for each sensor of interest are generated by the software. Only 20 seconds of the absorbed heat flux data from the control and prototype shirts testing is presented on the graphs. These graphs show the differences in the thermal protection performance of control and prototype shirts and can be used to assess how the still air in the three-dimensional fabric incorporated into the

prototype shirt can prevent thermal energy from easily passing through the garment system. Detailed analysis conducted for each sensor response for the sensors located on the upper front and back torso, shoulders, upper arms, neck, and wrists is presented below. Sensors 15 and 100 were not included in the analysis. Seam allowances from the stapled seam of the t-shirt and multiple layers from shirt closures in the front centre covered sensors 15 and 100. Minimal to no thermal energy passed through the garment system in this location.

Figure 7.10 and Figure E.16 show average absorbed heat fluxes and their variations with time on the upper front torso of the manikin. This area is represented by sensor 25 on the left front and sensor 24 on the right front. Greater absorbed heat flux values, averaging 7.3 kW/m^2 (sensor 25) and 11.0 kW/m^2 (sensor 24) were recorded for the garment ensemble with the control shirt. Lower absorbed heat flux values, averaging 2.3 kW/m^2 (sensor 25) and 2.8 kW/m^2 (sensor 24) were recorded for the garment ensembles with prototype shirt. None of the absorbed heat fluxes recorded by sensors 25 and 24 reached second-degree or third-degree burns.

Interestingly, the right chest area represented by sensor 14 reached the second-degree burn criteria during the third replication of the test with the garment system that included the control shirt (Figure E.13). The maximum value of absorbed heat flux was 14.4 kW/m^2 (Figure E.23). It is important to emphasize that both the control and prototype shirts had the same patch pockets with flaps located in that area. The absorbed heat fluxes recorded by sensor 14 for the garment ensembles with the prototype shirt were slightly lower than those recorded for the control shirt. Since the flaps of the prototype shirt were directly attached to the yoke with the three-dimensional warp-knitted fabric, it can be suggested that this difference in the shirt construction contributed to the creation of a small air gap between the manikin surface and garment ensemble. This air gap could provide slightly more thermal insulation.

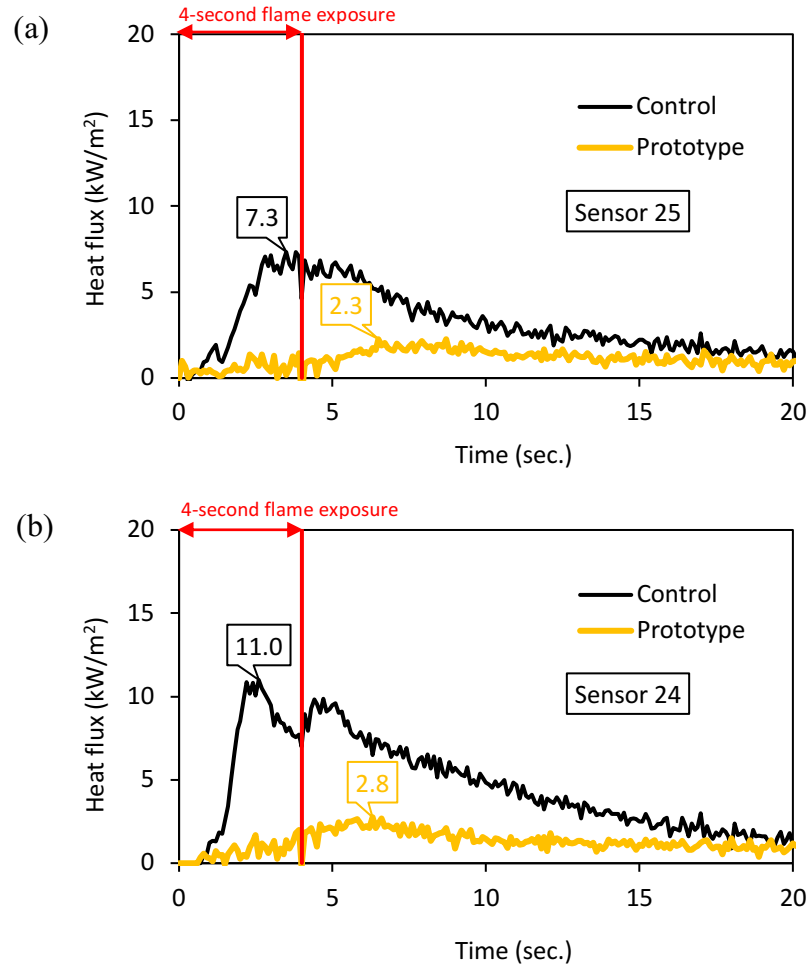


Figure 7.10 Average heat flux recorded by the skin simulant sensors caused by thermal energy passing through the garment ensemble with control and prototype shirts in different locations on the upper front torso area of the manikin: (a) left front, and (b) right front.

Figure 7.11 and Figure E.17 show averaged absorbed heat fluxes and their variation with the time on the upper back torso area of the manikin surface clothed with the garment ensembles with control and prototype shirts during the test. This area is represented by sensor 33 on the left back, sensor 36 on the centre back and sensor 40 on the right back. Greater absorbed heat flux values averaging 9.0 kW/m² (sensor 33), 7.3 kW/m² (sensor 36), and 16.8 kW/m² (sensor 40) were recorded for the garment ensembles with the control shirt. Much lower absorbed heat flux values averaging 2.2 kW/m² (sensor 33), 3.6 kW/m² (sensor 36) and 4.3 kW/m² (sensor 40) were recorded for the garment ensembles with prototype shirt.

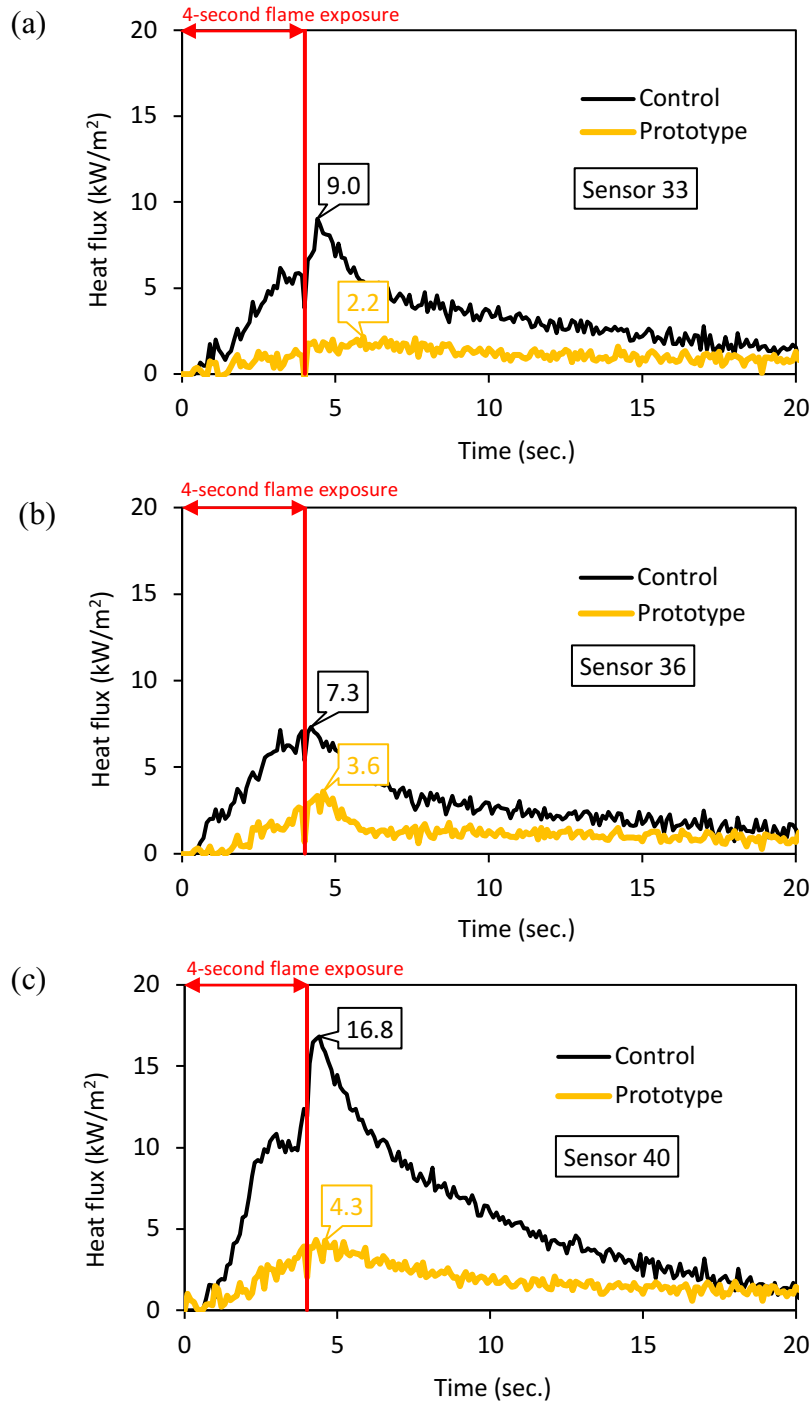


Figure 7.11 Average heat flux recorded by the skin simulant sensors caused by thermal energy passing through the garment ensemble with control and prototype shirts in different locations on the upper back torso area of the manikin: (a) left back, (b) centre back, and (c) right back.

During the testing of garment ensembles with control shirt number 2 and control shirt number 3, the absorbed heat flux values of sensor 40 reached 17.9 kW/m² and 18.8 kW/m² respectively (Figure 7.3, Figure E.13, and Figure E.17(c)). These absorbed heat flux values were high enough to reach second-degree burns in the right upper back area. During the testing of the garment ensemble with the prototype shirts, the highest value of absorbed heat flux recorded by the sensor 40 was 5.3 kW/m² for the prototype shirt number 3. None of the absorbed heat fluxes recorded by the sensor 40, as well as 36 and 33 reached second-degree or third-degree burns among the garment ensembles tested with the prototype shirts. The average difference between the highest absorbed heat flux values for the control and prototype shirts recorded by the sensor on the right side of the upper back torso area was approximately 12 kW/m² when the garment ensembles were tested.

Figure 7.12 and Figure E.18 show averaged absorbed heat flux and its variation with the time on the shoulder areas of the manikin surface clothed with the garment ensembles with control and prototype shirts during the test. This area is represented by sensor 27 on the left shoulder and sensor 26 on the right shoulder.

The shoulder areas were not severely affected by flame exposure. The rates of thermal energy were relatively low in that area. The maximum absorbed heat flux values of 4.0 kW/m² (sensor 27) and 2.9 kW/m² (sensor 26) on average were recorded for the garment ensembles with the control shirt. Nevertheless, the absorbed heat flux values recorded for the garment ensembles with the prototype shirt were even lower. They reached only 1.2 kW/m² (sensor 27) and 0.8 kW/m² (sensor 26) on average. None of the absorbed heat fluxes recorded by sensors 27 and 26 reached second-degree or third-degree burns for any garment ensemble tested.

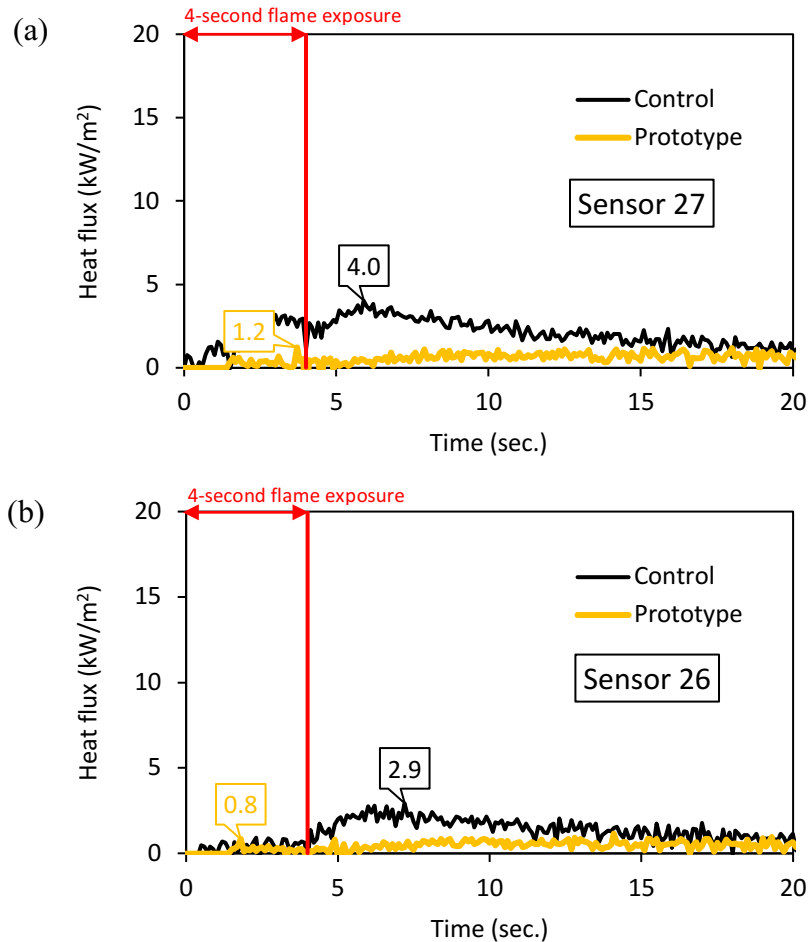


Figure 7.12 Average heat flux recorded by the skin simulant sensors caused by thermal energy passing through the garment ensemble with the control and prototype shirts in different locations on the shoulder area of the manikin: (a) left shoulder, and (b) right shoulder.

Figure 7.13 and Figure E.19 show averaged absorbed heat flux and their variation with the time on the upper arm areas of the manikin surface clothed with the garment ensembles with control and prototype shirts during the test. These areas are represented by sensor 7 on the left side and sensor 23 on the right side. Unlike the shoulder area, the upper arms were severely affected by flame exposure. The maximum absorbed heat flux values averaging 16.2 kW/m² (sensor 7) and 15.3 kW/m² (sensor 23) were recorded for the garment ensemble with the control shirt. Much lower absorbed heat flux values averaging 3.3 kW/m² (sensor 7) and

3.6 kW/m² (sensor 23) were recorded for the garment ensemble with the prototype shirt.

During testing of garment ensemble with the control shirt, the sensors that represent the upper arm areas recorded very high absorbed heat fluxes that led to predicted second-degree burns. The maximum absorbed heat flux values of 18.8 kW/m², 15.1 kW/m², and 16.1 kW/m² of sensor 7 reached second degree burns in the left upper arm area for all three replications of the test (Figure 7.3, also Figure E.12, Figure E.13, and Figure E.19(a)). The maximum absorbed heat flux value of 17.8 kW/m² of sensor 23 also reached the criteria for a second degree burn in the right upper arm area during the second replication of the test for the garment ensemble with control shirt (Figure 7.3, and Figure E.19(b)). During the testing of the garment ensemble with the prototype shirt, the highest value of absorbed heat flux recorded by sensors 7 and 23 was 4.4 kW/m² and 6.2 kW/m² for the second replication of the test (Figure E.19). None of the absorbed heat fluxes recorded by the sensor 7 or 23 reached the criteria for a second-degree or third degree burn during any of the three replications of the tests with the prototype shirts. The average difference between the highest absorbed heat flux values for the control and prototype shirts recorded by the sensors on the upper arm areas was approximately 12 kW/m² when the garment ensembles were tested.

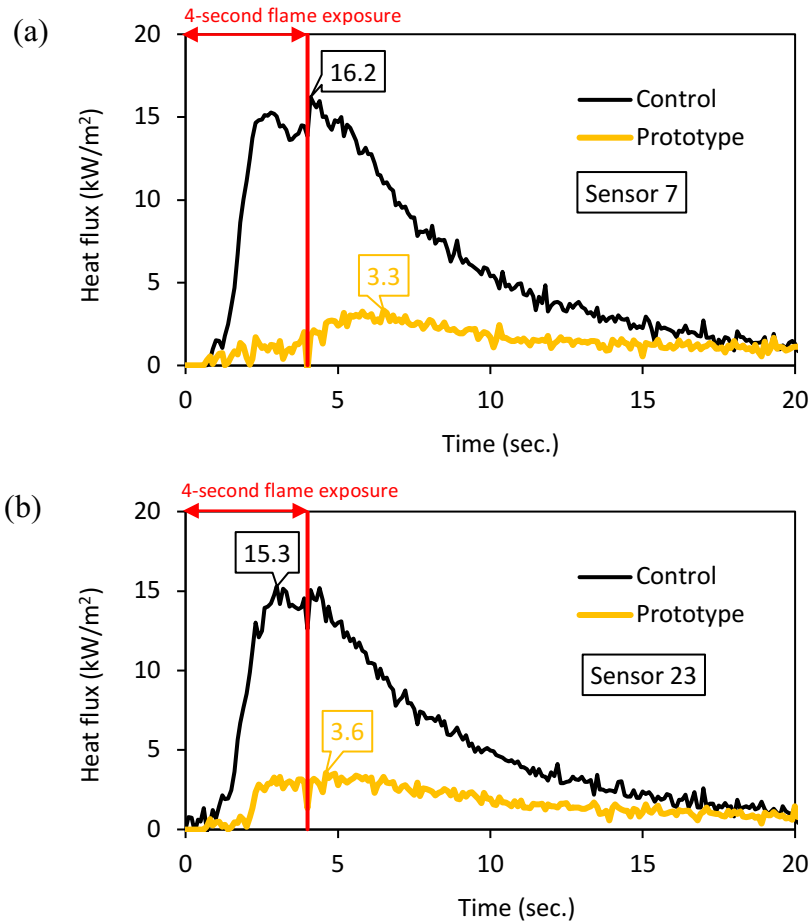


Figure 7.13 Average heat flux recorded by the skin simulant sensors caused by thermal energy passing through the garment ensemble with the control and prototype shirts in different locations on the upper arm area of the manikin: (a) left side, and (b) right side.

Figure 7.14 and Figure E.20 show averaged absorbed heat flux and their variation with the time on the neck area of the manikin surface clothed with the garment ensembles with control and prototype shirts during the test. This area is represented by sensor 99 on the left side, by sensor 97 at the centre back, and sensor 98 on the right side of the neck. Greater absorbed heat flux values averaging 35.3 kW/m² (sensor 99), 7.5 kW/m² (sensor 97), and 9.1 kW/m² (sensor 98) were recorded for the garment ensembles with the control shirt. Much lower absorbed heat flux values averaging 3.2 kW/m² (sensor 99), 1.1 kW/m² (sensor 97) and 1.3 kW/m² (sensor 98) were recorded for the garment ensembles with the prototype shirt.

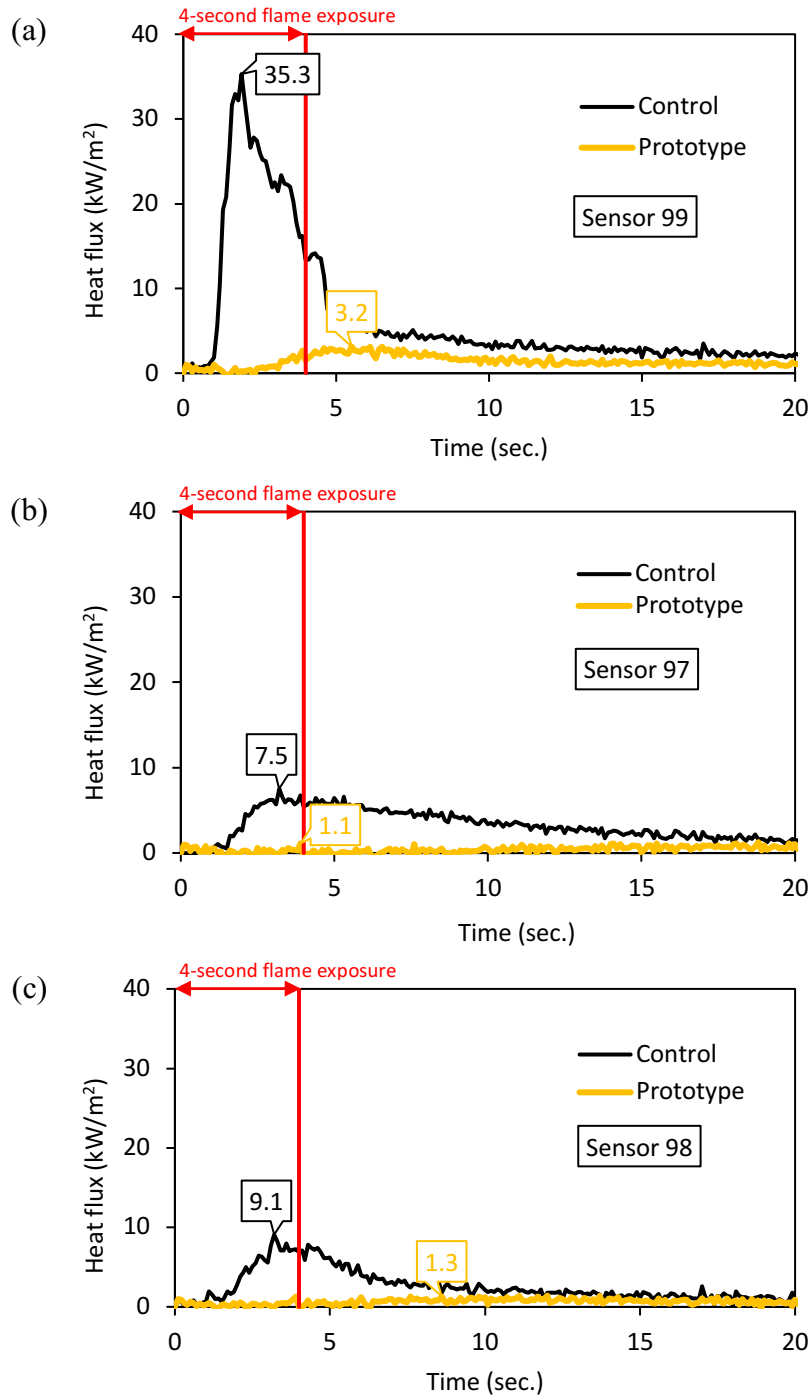


Figure 7.14 Average heat flux recorded by the skin simulant sensors caused by thermal energy passing through the garment ensemble with the control and prototype shirts in different locations on the neck area of the manikin: (a) left, (b) centre, and (c) right.

During the testing of the garment ensemble with control shirt, the absorbed heat flux values of sensor 99 reached 41.4 kW/m^2 , 31.6 kW/m^2 and 32.9 kW/m^2 (Figure 7.3, also Figure E.12, Figure E.13 and Figure E.20(a)). These absorbed heat flux values were high enough to reach second-degree burns on the left side of the neck area for all three replications of the test. During the testing of the garment ensemble with the prototype shirts, the highest value of absorbed heat flux recorded by sensor 99 was 4.2 kW/m^2 for the third replication of the test. None of the absorbed heat fluxes recorded by sensor 99 reached second-degree or third degree burns among the garment ensembles tested with the prototype shirts. The average difference between the highest absorbed heat flux values for the control and prototype shirts recorded by the sensor on the left side of the neck area was approximately 32 kW/m^2 when the garment ensembles were tested.

Interestingly, the back of the head-neck area represented by the sensor 96 reached second-degree and third degree burns when the garment ensemble with control shirt was tested (Figure 7.3, also Figure E.12 and Figure E.13). This same sensor reached second-degree or no burn when the garment ensemble with the prototype shirt was tested (Figure 7.7, also Figure E.14 and Figure E.15). The range of the highest values of absorbed heat flux recorded by sensor 96 was from 36.7 kW/m^2 to 78.8 kW/m^2 when the garment ensemble with control shirt was tested. Whereas the range of the highest values of absorbed heat flux recorded by sensor 96 was from 9.0 kW/m^2 to 40.5 kW/m^2 when the garment ensemble with the prototype shirt was tested. This sensor was partially covered during the test. Also, the collar of the prototype shirt, with the three-dimensional warp-knitted fabric, provided good thermal protection to the back of head-neck area when it covered sensor 96 during the test. So, the thermal energy was impeded by the collar and prevented the sensor from recording any burns.

Figure E.21 and Figure E.22 show averaged absorbed heat flux and their variation with the time on the wrist areas of the manikin surface clothed with the garment ensembles with control and prototype shirts during the test. These areas are represented by sensors 82, 90, 1 (left wrist), and 87, 85, 17 (right wrist).

As mentioned previously, the wrist areas were severely affected by the flame exposure. During the testing of the garment ensembles with both the control and prototype shirts, the sensors that represent the wrist areas recorded very high absorbed heat fluxes that led to predicted second-degree and third-degree burns in both shirt designs. The average maximum absorbed heat flux recorded by the sensors located on the wrists was approximately 50 kW/m^2 .

Overall, the analysis of individual sensor response showed that during the testing of the garment ensemble with the control shirt, the manikin sensors recorded higher values of absorbed heat flux in the areas of manikin surface that are prone to burns (e.g. upper front and back torso, upper arms, and neck) than the garment ensemble with the prototype shirt. The recorded higher values of absorbed heat fluxes frequently led to second or even third-degree burns predicted by instrumented manikin system these areas. In other words, high amounts of thermal energy, generated during the full-scale flame engulfment, could transfer through the control shirt and cotton t-shirt. Whereas, during the testing of garment ensembles with prototype shirt, the manikin sensors recorded much lower values of absorbed heat flux in the same areas of manikin surface. Since the manikin surface areas prone to burns were covered with three-dimensional warp-knitted fabrics in prototype shirts, none of the recorded absorbed heat fluxes reached second-degree or third degree burns when the garment ensembles were tested. Thus, it can be concluded that three-dimensional warp-knitted fabric incorporated in the prototype shirts impedes high amounts of thermal energy, generated during the full-scale flame engulfment, from transferring through the fabric system. The average difference between the highest absorbed heat flux values for the control and prototype shirts recorded by the sensors reached as high as 32 kW/m^2 when the garment ensembles were tested.

Additionally, the shoulder areas were not severely affected by flames. During the testing of the garment ensembles with the control and prototype shirts, the recorded absorbed heat fluxes for the shoulder areas were low and reached approximately 4.0 kW/m^2 and 1.0 kW/m^2 respectively. Unlike the shoulder areas, the wrist areas were severely affected by flames. The absorbed heat fluxes recorded by

the sensors were approximately 50 kW/m² and reached second-degree and third-degree burns during testing of each garment ensemble with the control or prototype shirts.

7.3 Summary

To sum up, three control shirts of wildland firefighters' protective clothing and three prototypes were tested with the whole garment ensemble by a flash fire instrumented manikin test system at the full-scale level. After the 4-second flame engulfment, the observations showed that both shirts had major areas of discoloured fabric, notable thermal shrinkage of the outer layer fabric, and char formation with some broken open parts. Predicted burn injuries were mainly concentrated on the legs, and arms where the garment ensemble with the control and prototype shirt had only one layer of fabric. Predicted burn injuries were also recorded in the areas of the upper front and back torso, upper arms, shoulders, and neck when the garment ensembles with the control shirts were tested. This finding is consistent with the results obtained previously by researchers ([Rucker et al., 2000](#)).

The prototype shirt design showed significant improvements in thermal protective performance when it was tested. It decreased the total burn area of the manikin surface by approximately 6% compared to the control shirt. Three-dimensional warp-knitted fabric substantially impeded high amounts of thermal energy, generated during the flame engulfment, from transferring through the fabric system in the areas of the upper front and back torso, upper arms, and neck. Moreover, there was no visual damage to the three-dimensional warp-knitted fabric after the flame engulfment exposure. However, this fabric placed in the cuffs, did not provide sufficient thermal protection in the wrist area. It showed second and third-degree burns when the prototype shirt was tested. Further improvements for the thermal protection of this area are needed, such as lining the sleeves with an additional fabric layer and constructing a gusset closure instead of the current in-seam placket that remains open even when the cuff is closed.

CHAPTER 8 SUMMARY, CONCLUSIONS, AND FUTURE WORK

8.1 Summary of research

The purpose of this research was to develop a prototype shirt for wildland firefighters' protective clothing with improved thermal protection without reducing thermal comfort. In order to maintain an air gap between the fabric and skin in areas where contact occurs, a three-dimensional warp-knitted fabric developed by (Keitch, 2014) was incorporated into the garment. The performance of the garment was evaluated to determine if an improvement in thermal protection was achieved. The research was completed by conducting the following four studies.

In the first study, the thermal protection of selected fabric systems representing the control shirt and the newly developed prototype shirt were assessed at the bench-scale level. Five fabric systems (OL-BL, OL-BL-S, OL-S-BL, OL-3D1-BL, and OL-3D2-BL) were tested under dry and wet base layer conditions. Three bench-scale tests were conducted with the following variations of heat exposure: (a) a flame heat source with a heat flux of 83 kW/m^2 , (b) a radiant heat source of 21 kW/m^2 , and (c) a combined flame and radiant heat source with a heat flux of 84 kW/m^2 . The data was collected as TPP, RHR, and CHTP ratings.

The second study was focused on the evaluation of the thermal comfort of selected fabric systems, also at the bench-scale level. Four fabric systems (OL-BL, OL(2)-BL, OL-3D1-BL, and OL-3D2-BL) were tested. Comfort properties were predicted using thermal resistance and evaporative resistance in a total heat loss (THL) calculation, together with air permeability. Data was collected as THL and air permeability values.

In the third study, the new shirt design of wildland firefighter' protective clothing with incorporation of three-dimensional warp-knitted fabric into contact areas was developed based on the design of a control garment which was the shirt currently worn by wildland firefighters in Alberta. Control and prototype shirts were constructed for evaluation of thermal protection at full-scale.

In the fourth study, the thermal protection assessment of the newly developed shirt prototype of wildland firefighters' protective clothing versus the control shirt was compared using a flash fire instrumented manikin test at the full-scale level. Three control shirts of wildland firefighters' protective clothing and three prototypes were tested. Each shirt was tested with the whole garment ensemble worn on top of a cotton t-shirt and briefs. The data was obtained in percentage of total predicted second-degree and third-degree burn injury of the manikin surface area.

8.2 Conclusions

The following conclusions apply to the specific fabric and garment systems used in this research. The first objective of this research was to assess the thermal protective performance of three-layer fabric systems compared with two-layer fabric systems representing the shirt and base layer garment of wildland firefighters' protective clothing. This objective was met, and the following conclusions were drawn:

- Three-dimensional warp-knitted fabrics incorporated between the outer layer and base layer in fabric systems OL-3D1-BL and OL-3D2-BL withstood high amounts of supplied thermal energy over longer periods of time before reaching predicted second-degree burn injury. Thus, they provided improved thermal protection over the fabric systems without the knit and greater protection than the fabric systems OL-BL-S and OL-S-BL with an air gap formed by a 6.4 mm spacer.
- The location of the spacer did not make a significant difference in the thermal protection when the two-layer fabric systems were tested in the flat specimen holders. The TPP and RHR ratings remained the same when the fabric systems OL-BL-S and OL-S-BL were tested. This observation was made for both wet and dry base layer conditions.
- The location of the spacer affected the thermal protection when the two-layer fabric systems were tested in the cylindrical specimen holder. The CHTP rating of fabric system OL-BL-S was significantly greater than the

CHTP rating of fabric system OL-S-BL. This observation was made for both wet and dry base layer conditions.

- Three-dimensional warp-knitted fabric incorporated between the outer layer and base layer in fabric systems OL-3D1-BL and OL-3D2-BL showed less thermal protection improvement when exposed to the radiant heat source in comparison to the exposure to the flame heat and combined flame and radiant heat sources. The thermal radiation was not blocked by the still air in the knit fabric as effectively as the convective energy from the flame exposure.
- Moisture content in the base layer of the fabric systems contributed to a decrease in the thermal protective performance of each fabric system in this research.

The second objective of this research was to evaluate the thermal comfort performance of three-layer fabric systems compared with two-layer fabric systems representing the shirt and base layer garments of wildland firefighters' protective clothing. This objective was met, and the following conclusions were drawn:

- Three-dimensional warp-knitted fabric incorporated between the outer layer and base layer in fabric systems OL-3D1-BL and OL-3D2-BL negatively influenced the thermal comfort by impeding the flow of heat and moisture vapour from the skin to the environment. In the prototype shirt design, only 25% of the shirt area includes the three-layer fabric system. Thus, the increase in thermal and evaporative resistance will mainly affect a small portion of the upper back torso which has a high sweat rate (Smith & Havenith, 2011), as well as areas of the upper front torso, shoulders, and upper arms which have a medium sweat rate.
- The lower back area which also has a high sweating rate will be covered with only one outer layer and base layer of fabric and this combination provided good heat and moisture vapour transmission in testing.

- The inclusion of the three-dimensional warp-knitted fabric between the outer and base layers positively influenced air permeability making the three-layer fabric systems more air permeable than two-layer fabric systems with either one or two outer layers and the base layer. In the proposed garment design, the inclusion of a three-dimensional warp-knitted fabric will allow wind from the environment to penetrate through the clothing system and will have a positive effect on thermal comfort.

The third objective of this research was to design and produce a shirt prototype for wildland firefighters protective clothing that incorporates a selected three-dimensional warp-knitted fabric in areas of the garment that are close to the skin and prone to second-degree burn injuries. This objective was met, and the following conclusions were drawn:

- The review of existing patented inventions showed that currently there are no wildland firefighters' protective shirt designs specifically focused on thermal protection in the areas that are prone to burn injuries.
- The patent of [Butzer and Coombs \(1995\)](#) disclosed a thermal protective overjacket that is worn on top of structural firefighters' protective clothing to provide additional thermal protection to similar areas of the body as the prototype shirt of this research.
- A novel prototype shirt design was developed to incorporate the three-dimensional warp-knitted fabric. Control and prototype shirts were successfully constructed which allowed for the next level of the research which was performing the full-scale flash fire instrumented manikin tests.

The fourth objective of this research was to assess the thermal protection performance of the control shirt of wildland firefighters' protective clothing and prototype shirt when tested by a flash fire instrumented manikin test system at the full-scale level. This objective was met, and the following conclusions were drawn:

- Similar to the findings of [Rucker et al. \(2000\)](#), predicted burn injuries were found in the contact areas of the control shirt and manikin surface when the garment ensemble was tested. These areas did not have an insulating air gap between the garment ensemble and manikin surface.
- The prototype shirt design showed significant improvements in thermal protection when it was exposed to full-scale flame engulfment for 4 seconds.
- The three-dimensional warp-knitted fabric substantially impeded high amounts of thermal energy, generated during the full-scale flame engulfment, from transferring through the fabric system in the contact areas of the garment and manikin surface.

8.3 Contributions and recommendations for future research

Contributions

In this thesis, the thermal protection of a wildland firefighter's garment was significantly improved through the use of a porous FR three-dimensional warp-knitted fabric, added to areas of the garment where the fabric was normally in direct contact with the skin and susceptible to burn injury. The three-dimensional warp-knitted fabric artificially maintained an air gap in the garment system and increased the protection provided by the garment to vulnerable areas of the body. The knitted fabric allowed a sufficient flow of heat and moisture vapour from the skin to the environment and high air permeability for cooling of the human body. Garment construction techniques were devised that allowed for the successful incorporation of the inflexible knit material into a shirt design closely matching the protective shirt design currently worn by wildland firefighters in Alberta. Other thermal protective

clothing, such as that worn by oil and gas workers, could benefit from the design ideas developed in this thesis for wildland fire fighters' shirts.

The additional data obtained by the thermocouples placed within the garments systems in the TPP and RHR tests has contributed to the understanding of heat transfer in multi-layer fabric systems and the effect of moisture on the thermal protection performance of protective clothing. This data can also potentially contribute to comparisons with heat transfer models in the research literature which only record temperatures measured with the copper disk sensor located behind the fabric. However, more detailed data analysis of graphs, obtained by additional thermocouples when the fabric systems were exposed to flame heat source and radiant heat source is still needed.

Recommendations for future work

The research showed successful proof of the design concept; however, there are areas that can be improved and investigated further:

- The greatest area of burn injury was on the arms in the manikin test, suggesting that additional improvements are still needed for the sleeves. An additional layer of the outer fabric could be used as a lining and constructing a gusset closure instead of the current in-seam placket that remains open even when the cuff is closed could be investigated.
- The prototype shirt should be tested in the field or in an exercise wear trial to understand its performance as regards fit and physiological comfort. Focus group interviews could also be carried out to understand the acceptance of the proposed new design by end users.
- Improvement to the pants design can also be investigated since burn injuries also occur on the legs.
- The effect of quilting on the thermal protective properties of three-dimensional warp-knitted fabric sewn to the outer layer can be evaluated through additional bench-scale testing.

- Additional testing such as test the assessment of steam protection (CGSB, 2017) of three-layer fabric systems in comparison with two-layer fabric systems can be conducted since fire fighters frequently encounter steam hazards.
- Additional interpretation of the testing data generated by this research will give a better understanding of heat transfer and the effects of moisture on clothing systems.

REFERENCES

- Ackerman, M., Batcheller, J., & Paskaluk, S. (2015). Off gas measurements from FR materials exposed to a flash fire. *AATCC Journal of Research*, 2(2), 1-12.
<https://doi.org/10.14504/ajr.2.2.1>
- Alberta ALIS (2021, March 5). Occupations in Alberta. Wildland firefighter. Working conditions. <https://alis.alberta.ca/occinfo/occupations-in-alberta/occupation-profiles/wildland-firefighter/>
- American Society for Testing and Materials. (2016). *ASTM D8007 Standard Test Method for Wale and Course Count of Weft Knitted Fabrics*. West Conshohocken, PA: American Society for Testing and Materials.
- American Society for Testing and Materials. (2017a) *ASTM F1868 Standard Test Method for Thermal and Evaporative Resistance of Clothing Materials Using a Sweating Hot Plate*. West Conshohocken, PA: American Society for Testing and Materials.
- American Society for Testing and Materials. (2018). *ASTM D3775 Standard Test Method for End (Warp) and Pick (Filling) Count of Woven Fabrics*. West Conshohocken, PA: American Society for Testing and Materials.
- American Society for Testing and Materials. (2018b). *ASTM D737 Standard Test Method for Air Permeability of Textile Fabrics*. West Conshohocken, PA: American Society for Testing and Materials.
- American Society for Testing and Materials. (2018c) *ASTM F1930 Standard Test Method for Evaluation of Flame-Resistant Clothing for Protection Against Fire Simulations Using and Instrumented Manikin*. West Conshohocken, PA: American Society for Testing and Materials.
- American Society for Testing and Materials. (2019a). *ASTM D123 Standard Terminology Relating to Textile*. West Conshohocken, PA: American Society for Testing and Materials.

American Society for Testing and Materials. (2019b). ASTM D1777 *Standard Test Method for Thickness of Textile Materials*. West Conshohocken, PA: American Society for Testing and Materials.

American Society for Testing and Materials. (2020a). ASTM F2700 *Standard Test Method for Unsteady-State Heat Transfer Evaluation of Flame-Resistant Materials for Clothing with Continuous Heating*. West Conshohocken, PA: American Society for Testing and Materials.

American Society for Testing and Materials. (2020b). ASTM F1939 *Standard Test Method for Radiant Heat Resistance of Flame-Resistant Clothing Materials with Continuous Heating*. West Conshohocken, PA: American Society for Testing and Materials.

American Society for Testing and Materials. (2020c). ASTM D1776 / D1776M *Standard Practice for Conditioning and Testing Textiles*. West Conshohocken, PA: American Society for Testing and Materials.

American Society for Testing and Materials. (2020d). ASTM D3776 *Standard Test Methods for Mass Per Unit Area (Weight) of Fabric*. West Conshohocken, PA: American Society for Testing and Materials.

American Society for Testing and Materials. (2020e). ASTM D 6193-16 *Standard Practice for Stitches and Seams*. West Conshohocken, PA: American Society for Testing and Materials.

American Society for Testing and Materials. (2022). ASTM F3538 *Standard Test Method for Measuring Heat Transmission Through Flame-Resistant Materials for Clothing in Flame Exposure Using a Cylindrical Specimen Holder*. West Conshohocken, PA: American Society for Testing and Materials.

- Barbeau, C., St-Arneault, E., & Bigonnesse, M. (2019) *Firefighter protective garment having a thermal barrier with spacers to increase dissipation of metabolic heat* (U.S. Patent No. 10245454B2). U.S. Patent and Trademark Office.
<https://patents.google.com/patent/US10245454B2>
- Barker, R. L., Ingram, J., Morton-Aslanis, J., & Deaton, A. S. (2020). Relationships between bench-scale measures of after-flame and thermal shrinkage and fire-resistant garment performance in fire manikin tests. In K. Lehtonen , B. P. Shiels, & R. B. Ormond (Eds.), *Performance of protective clothing and equipment: Innovative solutions to evolving challenges* (Vol. 11, pp. 1-17). West Conshohocken, PA: American Society for Testing and Materials.
<https://doi.org/10.1520/STP162420190086>
- Barwood, M. J., Davey, S., House, J. R., & Tipton, M. J. (2009). Post-exercise cooling techniques in hot, humid conditions. *European Journal of Applied Physiology*, 107, 385-396. <https://doi.org/10.1007/s00421-009-1135-1>
- Behnke, W. P. (1977). Thermal protective performance test for clothing. *Fire Technology*, 13, 6-12. <https://doi.org/10.1007/BF02338881>
- Bibeau, L. (2016). *Insulating garment for firefighter bunker gear* (Canadian patent No. 2919104C). Canadian Intellectual Property Office.
<https://patents.google.com/patent/CA2919104C>
- Budd, G.M., Brotherhood, J.R., Hendrie, A.L., Jeffery, S.E., Beasley, F.A., Costin, B.P., Zhien, W., Baker, M.M., Cheney, N.P. and Dawson, M.P.,(1997). Project Aquarius 6. Heat load from exertion, weather, and fire in men suppressing wildland fires. *International Journal of Wildland Fire*, 7(2), 119-131.
<https://doi.org/10.1071/WF9970119>
- Butler, B. W. (2014). Wildland firefighter safety zones: a review of past science and summary of future needs. *International Journal of Wildland Fire*, 23(3), 295-308.
<https://doi.org/10.1071/WF13021>

Butzer, M. J., Coombs, Ch. E. (1995). *Thermal protective overjacket* (U.S. Patent No. 5406648A). U.S. Patent and Trademark Office.

<https://patents.google.com/patent/US5406648A>

Carballo-Leyenda, B., Villa, J. G., López-Satué, J., & Rodríguez-Marroyo, J. A. (2017). Impact of different personal protective clothing on wildland firefighters' physiological strain. *Frontiers in Physiology*, *8*, 1–8.

<https://doi.org/10.3389/fphys.2017.00618>

Carballo-Leyenda, B., Villa, J. G., López-Satué, J., & Rodríguez-Marroyo, J. A. (2019). Characterizing wildland firefighters' thermal environment during live-fire suppression. *Frontiers in Physiology*, *10*, 1–8.

<https://doi.org/10.3389/fphys.2019.00949>

Canadian General Standards Board (2013). CAN/CGSB – 4.2 No. 78.1 *Textile Test Methods: Thermal Protective Performance of Materials for Clothing*. Ottawa, ON: Canadian General Standards Board.

Canadian General Standards Board (2014). CAN/CGSB –155.22 *Fireline Workwear for Wildland Firefighters*. Ottawa, ON: Canadian General Standards Board.

Canadian General Standards Board (2017). CAN/CGSB –155.20 *Workwear for Protection Against Hydrocarbon Flash Fire and Optionally Steam and Hot Fluids*. Ottawa, ON: Canadian General Standards Board.

Canadian General Standards Board (2019). CAN/CGSB – 4.2 No. 58 *Textile Test methods: Dimensional Change in Domestic Laundering of Textiles*. Ottawa, ON: Canadian General Standards Board.

Chen, Y. S., Fan, J., Qian, X., & Zhang, W. (2004). Effect of garment fit on thermal insulation and evaporative resistance. *Textile Research Journal*, *74*(8), 742-748.

<https://doi/pdf/10.1177/004051750407400814>

- Cheung, S. S., Petersen, S. R., & McLellan, T. M. (2010). Physiological strain and countermeasures with firefighting. *Scandinavian Journal of Medicine & Science in Sports*, 20, 103-116. <https://doi.org/10.1111/j.1600-0838.2010.01215.x>
- Coombs, Ch. E. (1985). *Protective garment* (U.S. Patent No. 4507806A). U.S. Patent and Trademark Office. <https://patents.google.com/patent/US4507806A>
- Chen, Y. S., Fan, J., Qian, X., & Zhang, W. (2004). Effect of garment fit on thermal insulation and evaporative resistance. *Textile research journal*, 74(8), 742-748. <https://doi/pdf/10.1177/004051750407400814>
- Crown, E. M., Ackerman, M. Y., Dale, J. D., & Tan, Y. B. (1998). Design and evaluation of thermal protective flightsuits. Part II: instrumented mannequin evaluation. *Clothing and Textiles Research Journal*, 16(2), 79-87. <https://doi.org/10.1177/0887302X9801600203>
- Crown, E. M., Ackerman, M. Y., Dale, J. D., & Rigakis, K. B. (1993). Thermal protective performance and instrumented mannequin evaluation of multi-layer garment systems. *AGARD Conference Proceedings 540 Aerospace Medical Panel Symposium: The Support of Air Operations under Extreme Hot and Cold Weather Conditions*, p. 14.8.
- Crown, E. M., Dale, J. D., & Bitner, E. (2002). A comparative analysis of protocols for measuring heat transmission through flame-resistant materials: capturing the effects of thermal shrinkage. *Fire and Materials*, 26(4-5), 207-213. <https://doi.org/10.1002/fam.797>
- Dale, J. D., Ackerman, M., Crown, B. M., Hess, D., Tucker, R., & Bitner, E. (2000). A study of geometry effects on testing single layer fabrics for thermal protection. In C. N. Nelson & N. W. Henry (Eds.), *Performance of protective clothing: issues and priorities for the 21st century, Seventh Volume, ASTM STP 1386* (pp. 393–408). West Conshohocken, PA: American Society for Testing and Materials.

- Dale, J. D., Crown, E. M., Ackerman, M. Y., Leung, E., & Rigakis, K. B. (1992). Instrumented mannequin evaluation of thermal protective clothing. In J. P. McBriarty & N. W. Henry (Eds.), *Performance of protective clothing, Fourth Volume, ASTM STP 1133* (pp. 717-733). Philadelphia: American Society for Testing and Materials.
- Das, A., & Alagirusamy, R. (2010a). Introduction to clothing comfort. In A. Das & R. Alagirusamy (Eds.), *Science in clothing comfort* (pp. 1–12). India: Woodhead Publishing.
- Das, A., & Alagirusamy, R. (2010b). Psychology and comfort. In A. Das & R. Alagirusamy (Eds.), *Science in Clothing Comfort* (pp. 13–30). India: Woodhead Publishing.
- DenHartog, E. A., Walker, M. A., & Barker, R. L. (2016). Total heat loss as a predictor of physiological response in wildland firefighter gear. *Textile Research Journal*, 86(7), 710-726. <https://doi.org/10.1177/0040517515596926>
- Diller, K. R. (1985). Analysis of skin burns. In R. C. Eberhart & A. Shitzer (Eds.), *Heat Transfer in Medicine and Biology: Analysis and Applications. Volume 2* (pp. 85–134). Boston, MA: Springer US.
- Edwards, C., & Marks, R. (1995). Evaluation of biomechanical properties of human skin. *Clinics in Dermatology*, 13(4), 375–380.
- Erni, S., Wang, X., Swystun, T., Taylor, S. W., Parisien, M. A., Robinne, F. N., Eddy, B., Oliver, J., Armitage, B., & Flannigan, M. D. (2024). Mapping wildfire hazard, vulnerability, and risk to Canadian communities. *International Journal of Disaster Risk Reduction*, 101, 104221. <https://doi.org/10.1016/j.ijdr.2023.104221>
- Flay, P., Hebert, M., & Bibeau, L. (2007). Fire insulating barrier material for a firefighter protective garment ((U.S. Patent No. 2007/0284558A1). U.S. Patent and Trademark Office. <https://patents.google.com/patent/US20070284558A1>

- Fu, M., Chen, W., Weng, W., Yuan, M., Luo, N., & Xu, X. (2018). Prediction of thermal skin burn based on the combined mathematical model of the skin and clothing. *The Journal of The Textile Institute*, 109(12), 1606–1612.
<https://doi.org/10.1080/00405000.2018.1437112>
- Grilliot, W. L., & Grilliot, M.I. (1991). *Firefighter's garments having minimum weight and excellent protective qualities* (U.S. Patent No. 5001783A). U.S. Patent and Trademark Office.<https://patents.google.com/patent/US5001783A>
- He, S., Huang, D., Qi, Z., Yang, H., Hu, Y., & Zhang, H. (2012). The effect of air gap thickness on heat transfer in firefighters' protective clothing under conditions of short exposure. *Heat Transfer Research*, 43(8).
<https://doi.org/10.1615/HeatTransRes.2012005913>
- Henriques, F. C. (1947). Studies of thermal injury, V: The predictability and the significance of thermally induced rate processes leading to irreversible epidermal injury. *Archives of Pathology*, 43(5), 489-502.
- Horrocks, A. R. (2016). Technical fibres for heat and flame protection. In A.R. Horrocks (Ed.) *Handbook of Technical Textiles* (pp. 237–270). Elsevier.
<https://doi.org/10.1016/B978-1-78242-465-9.00008-2>
- International Organization for Standardization. (2007). ISO 11079 *Ergonomics of the thermal environment. Determination and interpretation of cold stress when using required clothing insulation (IREQ) and local cooling effects*. Switzerland, Geneva: International Organization for Standardization.
- International Organization for Standardization. (2018). ISO 15384 *Protective clothing for firefighters — Laboratory test methods and performance requirements for wildland firefighting clothing*. Switzerland, Geneva: International Organization for Standardization.

- Jain, P., Barber, Q. E., Taylor, S., Whitman, E., Acuna, D. C., Boulanger, Y., Chavardès, R., D., Chen, J., Englefield, P., Flannigan, M., Girardin, M., P., Hanes, C.C., Little, J., Morrison, K., Skakun, R., S., Thompson, D., K., Wang, X., & Parisien, M. A. (2024). Canada under fire—drivers and impacts of the record-breaking 2023 wildfire season. *ESS Open Archive*, 1-44.
<https://doi.org/10.22541/essoar.170914412.27504349/v1>
- Kadolph, S. J. (2007). Textile fibres and their properties. In S.J. Kadolph (Ed.), *Textiles* (11th ed.) (pp. 31-56). Boston: Pearson
- Keitch, G. (2014). *Spacer textile* (European patent No. 2707529B1). European Patent Office. <https://patents.google.com/patent/EP2707529B1>
- Kim, Y., Lee, C., Li, P., Corner, B. D., & Paquette, S. (2002). Investigation of air gaps entrapped in protective clothing systems. *Fire and Materials*, 26(3), 121-126.
<https://doi.org/10.1002/fam.790>
- Kreith, F. (1965). *Principles of heat transfer*. International Textbook Company: Scranton.
- Lawson, L. K. (2002). *Effects of moisture on heat transfer through thermal protective fabric systems*. [Masters' thesis, University of Alberta]
<https://doi.org/10.7939/R3MK65K7N>
- Lawson, L. K., Crown, E. M., Ackerman, M. Y., & Douglas Dale, J. (2004). Moisture effects in heat transfer through clothing systems for wildland firefighters. *International Journal of Occupational Safety and Ergonomics*, 10(3), 227–238.
<https://doi.org/10.1080/10803548.2004.11076610>
- Lee, Y. M., & Barker, R. L. (1986). Effect of moisture on the thermal protective performance of heat-resistant fabrics. *Journal of Fire Sciences*, 4(5), 315-331.
<https://doi.org/10.1177/073490418600400502>

- Li, J., Gao, D., Li, K., Yang, Y., & Pan, Y. (2021). *Multifunctional emergency protective clothing for forest firemen* (China patent No. 213220621U). State Intellectual Property Office of the People's Republic of China.
<https://patents.google.com/patent/CN213220621U>
- Lu, Y., Li, J., Li, X., & Song, G. (2013). The effect of air gaps in moist protective clothing on protection from heat and flame. *Journal of fire sciences*, 31(2), 99-111.
<https://doi.org/10.1177/0734904112457342>
- Mah, T., & Song, G. (2010). Investigation of the contribution of garment design to thermal protection. Part 2: instrumented female mannequin flash-fire evaluation system. *Textile Research Journal*, 80(14), 1473-1487.
<https://doi.org/10.1177/0040517509358796>
- Mah, T. T. (2009). *Thermal protective garments for women: The contribution of garment design to thermal performance* [Master's thesis, University of Alberta]. Theses Canada. https://central.bac-lac.gc.ca/item?id=MR54968&op=pdf&app=Library&is_thesis=1&oclc_number=729988879
- Mäkinen, H., Smolander, J., & Vuorinen, H. (1988). Simulation of the effect of moisture content in underwear and on the skin surface on steam burns of fire fighters. In S. Z. Mansdorf, R. Sager & A. P. Neilsen (Eds.), *Performance of protective clothing: Second symposium* (pp. 415-421). West Conshohocken, PA: American Society for Testing and Materials. <https://doi.org/10.1520/STP26309S>
- Mao, N., & Russell, S. J. (2007). The thermal insulation properties of spacer fabrics with a mechanically integrated wool fiber surface. *Textile Research Journal*, 77(12), 914-922. <https://doi.org/10.1177/0040517507083524>
- Mokhtari Yazdi, M., & Sheikhzadeh, M. (2014). Personal cooling garments: a review. *The Journal of The Textile Institute*, 105(12), 1231-1250.
<https://doi.org/10.1080/00405000.2014.895088>

- Moritz, A. R., & Henriques, F. C. (1947). Studies of thermal injury, II: The relative importance of time and surface temperature in the causation of cutaneous burns. *The American Journal of Pathology*, 23(5), 695.
- National Fire Protection Association (2016). *NFPA 1977 Standard on Protective Clothing and Equipment for Wildland Firefighting*. Quincy, MA: National Fire Protection Association.
- National Fire Protection Association (2018). *NFPA 1971 Standard on Protective Clothing Ensembles for Structural Fire Fighting and Proximity Fire Fighting*. Quincy, MA: National Fire Protection Association.
- National Fire Protection Association (2023). *NFPA 2112 Standard on Flame-resistant Clothing for Protection of Industrial Personnel Against Short-Duration Thermal Exposures from Fire*. Quincy, MA: National Fire Protection Association.
- Navarro, K. M., Kleinman, M. T., Mackay, C. E., Reinhardt, T. E., Balmes, J. R., Broyles, G. A., ... & Domitrovich, J. W. (2019). Wildland firefighter smoke exposure and risk of lung cancer and cardiovascular disease mortality. *Environmental Research*, 173, 462-468.
<https://doi.org/10.1016/j.envres.2019.03.060>
- Palani Rajan, T., Ramakrishnan, G., & Kandhavadi, P. (2016). Permeability and impact properties of warp-knitted spacer fabrics for protective application. *The Journal of the Textile Institute*, 107(9), 1079-1088.
<https://doi.org/10.1080/00405000.2015.1084135>
- Pan, L., Lu, Y., Chen, X., & Huang, L. (2023). *High-strength forest fireproof garment and protection method thereof* (China patent No. 115569314B). State Intellectual Property Office of the People's Republic of China.
<https://patents.google.com/patent/CN115569314B>

- Petrilli, T., & Ackerman, M. (2008). *Tests of undergarments exposed to fire*. United States Department of Agriculture, Forest Service, Technology & Development Program. <https://www.fs.usda.gov/t-d/pubs/htmlpubs/htm08512348/index.htm#:~:text=Laboratory%20tests%20showed%20that%20firefighters,and%20stick%20to%20their%20skin>
- Reffeltrath, P. A. (2006). Heat stress reduction of helicopter crew wearing a ventilated vest. *Aviation, Space, and Environmental Medicine*, 77(5), 545-550.
- Reinhardt, T. E., & Ottmar, R. D. (2004). Baseline measurements of smoke exposure among wildland firefighters. *Journal of Occupational and Environmental Hygiene*, 1(9), 593–606. <https://doi.org/10.1080/15459620490490101>
- Rossi, R. M., & Zimmerli, T. (1996). Influence of humidity on the radiant, convective and contact heat transmission through protective clothing materials. In J. S. Johnson & S. Z. Mansdorf (Eds.), *Performance of protective clothing* (Vol.5, pp. 269–280). West Conshohocken, PA: American Society for Testing and Materials.
- Rucker, M., Anderson, E., & Kangas, A. (2000). Evaluation of standard and prototype protective garments for wildland firefighters. In C. N. Nelson & N. W. Henry (Eds.), *Performance of protective clothing: issues and priorities for the 21st century* (Vol. 7 STP 1386, pp. 546–556). West Conshohocken, PA: American Society for Testing and Materials. <https://doi.org/10.1520/STP14469S>
- Shu, Zh., Di, X., & Huang, H. (2012). *Forest fire-fighting flame-retarding clothes* (China patent No. 201220221345). State Intellectual Property Office of the People's Republic of China. <https://patents.google.com/patent/CN202569233U>
- Smith, C. J., & Havenith, G. (2011). Body mapping of sweating patterns in male athletes in mild exercise-induced hyperthermia. *European Journal of Applied Physiology*, 111(7), 1391-1404. <https://doi.org/10.1007/s00421-010-1744-8>

- Smith, W. R., Montopoli, G., Byerly, A., Montopoli, M., Harlow, H., & Wheeler III, A. R. (2013). Mercury toxicity in wildland firefighters. *Wilderness & Environmental Medicine*, 24(2), 141–145.
<https://doi.org/10.1016/j.wem.2013.01.004>
- Sol, J. A., West, M. R., Domitrovich, J. W., & Ruby, B. C. (2021). Evaluation of environmental conditions on self-selected work and heat stress in wildland firefighting. *Wilderness & Environmental Medicine*, 32(2), 149-159.
<https://doi.org/10.1016/j.wem.2021.02.004>
- Song, G. (2007). Clothing air gap layers and thermal protective performance in single layer garment. *Journal of industrial textiles*, 36(3), 193-205.
<https://doi.org/10.1177/1528083707069506>
- Sontag, M. S. (1985). Comfort Dimensions of Actual and Ideal Insulative Clothing for Older Women. *Clothing and Textiles Research Journal*, 4(1), 9–17.
<https://doi.org/10.1177/0887302X8500400102>
- Stoll, A. M., & Chianta, M. A. (1969). Method and rating system for evaluation of thermal protection. *Aerospace Medicine*, 40(11), 1232–1238.
- Stoll, A. M., & Greene, L. C. (1959). Relationship between pain and tissue damage due to thermal radiation. *Journal of Applied Physiology*, 14(3), 373–382.
<https://doi.org/10.1152/jappl.1959.14.3.373>
- Stull, J. O. (2000). Comparative thermal insulative performance of reinforced knee areas of firefighter protective clothing. In C. N. Nelson & N. W. Henry (Eds.), *Performance of protective clothing: Issues and priorities for the 21st century* (Vol.7, pp. 312–328). West Conshohocken, PA: American Society for Testing and Materials. <https://doi.org/10.1520/STP14454S>
- Tesoro, G. C. (1978). Chemical modification of polymers with flame-retardant compounds. *Journal of Polymer Science: Macromolecular Reviews*, 13(1), 283-353. <https://doi.org/10.1002/pol.1978.230130106>

- Tabachnick, B. G., & Fidell, L. S. (2007). Introduction. In B. G. Tabachnick and L. S. Fidell (Eds.) *Experimental designs using ANOVA* (pp. 1-28). Belmont, CA: Thomson/Brooks/Cole.
- Taylor, F.P., & Aldridge, D (1999). *Protective garment with apertured closed-cell foam liner* (U.S. Patent No. 5924134A). U.S. Patent and Trademark Office. <https://patents.google.com/patent/US5924134A>
- Torvi, D. A. (1997). *Heat transfer in thin fibrous materials under high heat flux conditions* [Doctoral dissertation, University of Alberta]. Era Education & Research Archive. <https://doi.org/10.7939/R3M03Z33Z>
- Torvi, D. A., Douglas Dale, J., & Faulkner, B. (1999). Influence of air gaps on bench-top test results of flame resistant fabrics. *Journal of Fire Protection Engineering*, 10(1), 1-12. <https://doi.org/10.1177/104239159901000101>
- Tyukavina, A., Potapov, P., Hansen, M. C., Pickens, A. H., Stehman, S. V., Turubanova, S., Parker, D., Zalles, V., Lima, A., Kommareddy, I., Song, X., Wang, L., & Harris, N. (2022). Global trends of forest loss due to fire from 2001 to 2019. *Frontiers in Remote Sensing*, 3, 825190. <https://doi.org/10.3389/frsen.2022.825190>
- Wang, M., Li, X., & Li, J. (2015). Correlation of bench scale and manikin testing of fire protective clothing with thermal shrinkage effect considered. *Fibers and Polymers*, 16(6), 1370–1377. <https://doi.org/10.1007/s12221-015-1370-5>
- Wang, Y. Y., Lu, Y. H., Li, J., & Pan, J. H. (2012). Effects of air gap entrapped in multilayer fabrics and moisture on thermal protective performance. *Fibers and Polymers*, 13, 647-652. <https://doi.org/10.1007/s12221-012-0647-1>
- Weiner, J. S. (1945). The regional distribution of sweating. *The Journal of Physiology*, 104(1), 32. <https://doi.org/10.1113/jphysiol.1945.sp004103>

- Withen, P. (2015). Climate change and wildland firefighter health and safety. *New Solutions: a Journal of Environmental and Occupational Health Policy*, 24(4), 577–584. <https://doi.org/10.2190/NS.24.4.i>
- Xavier Viegas, D. (1998). Forest fire propagation. *Philosophical Transactions of the Royal Society of London. Series A: Mathematical, Physical and Engineering Sciences*, 356(1748), 2907-2928. <https://doi.org/10.1098/rsta.1998.0303>
- Yin, Zh., Han, F., Yang, J., Zhang, Y., Wen, M., & Chen, H. (2020). *Novel forest fire prevention clothes* (China patent No. 211132764U). State Intellectual Property Office of the People's Republic of China. <https://patents.google.com/patent/CN211132764U>
- Ye, X., Hu, H., & Feng, X. (2008). Development of the warp knitted spacer fabrics for cushion applications. *Journal of Industrial Textiles*, 37(3), 213-223. <https://doi.org/10.1177/1528083707081592>

APPENDICES

APPENDIX A: MATERIALS AND METHODS

Evaluation of fabric physical properties

Fabric mass was determined for each fabric using analytical balances (Model M-310, Denver Instrument Company, Arvada, CO, US) according to ASTM D3776, option C (par. 9.3), five die-cut specimens were taken from different locations of each fabric sample with a total specimen area of approximately 100 cm² (ASTM, 2020d). The mass was measured for all five specimens, and calculations were applied to report mass in SI units (International System of Units) in g/m².

Fabric thickness was determined for each fabric using a thickness compression recovery tester (Custom Scientific Instruments Inc., Whippany, NJ, US) according to ASTM D1777, option 1, five die-cut specimens were taken from different locations of each fabric sample. The area of each specimen was 20% greater than the area of 645 mm² of the presser foot (ASTM, 2019b). The applied pressure was 1.0 kPa. Thickness values were obtained in inches then converted and reported in mm.

The *fabric count* measurements were performed for woven fabrics in both warp and weft directions. According to ASTM D3775 par. 9.4.2, a straight cut was made through the fabric and a ruler was placed on top of the fabric along the cut edge (ASTM, 2018). Five specimens from a woven fabric were randomly selected for the fabric count per distance in centimetres. The counting distance was one centimetre and was marked on each specimen. The numbers of yarns between two marks were obtained for each fabric and direction, and the average number of yarns per one centimetre of fabric was reported.

The count of wales and courses was performed for knitted fabrics, as directed in ASTM D8007 (ASTM, 2016). A ruler was placed on the top of the fabric along the width direction of the fabric for the wales count and along the length direction for the courses count. A pointer was moved along or across the fabric to aid in counting. The counting distance was one centimetre. Five areas were randomly selected for the knitted fabric counts, and the average number of wales and courses per one centimetre were reported.

Photomicrographs of fibres

Photomicrographs were obtained using a transmitted light microscope (Model CX31) with a digital camera (Model DP72) (Olympus Corp., Markham, ON, Canada).

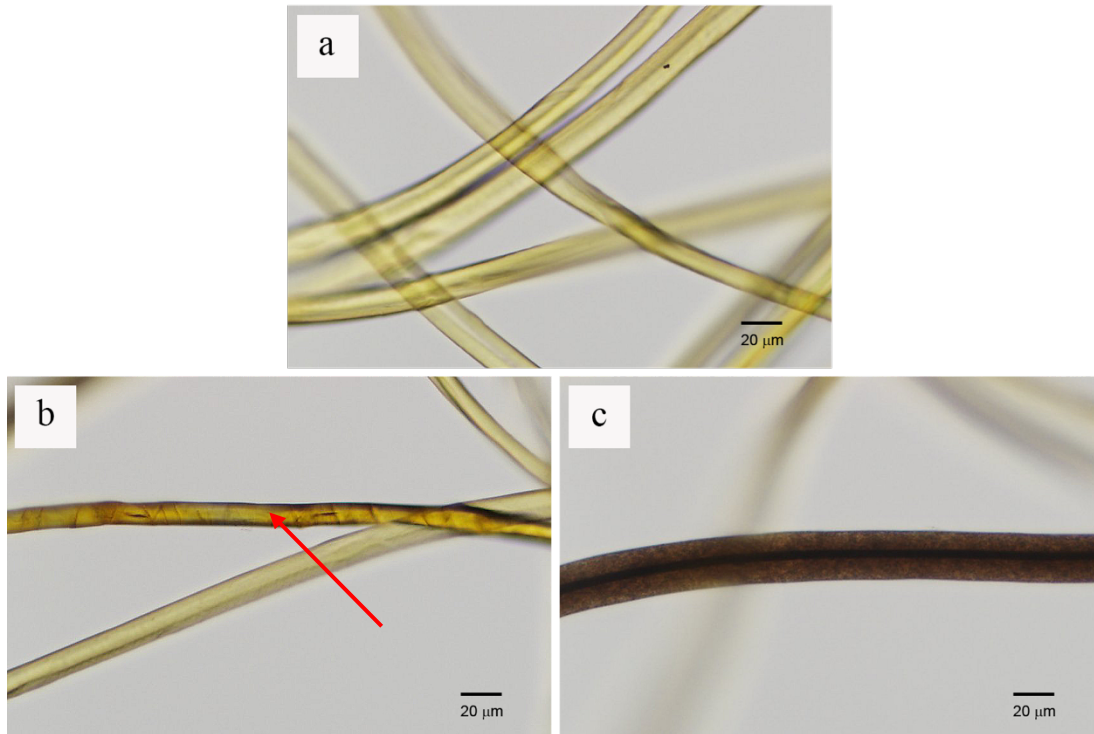


Figure A.1 Photomicrographs of fibres: (a) meta-aramid fibre, (b) para-aramid fibre, (c) anti-static fibre. (scale bar 20 μm)

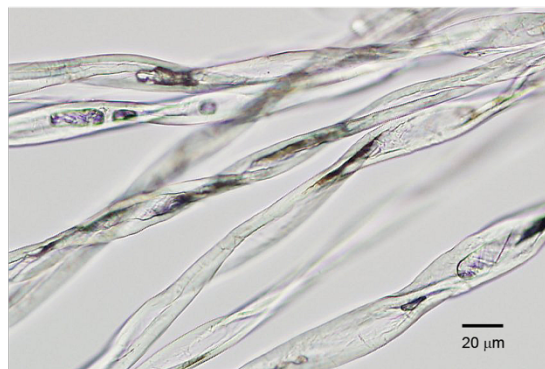


Figure A.2 Photomicrograph of cotton fibre. (scale bar 20 μm)

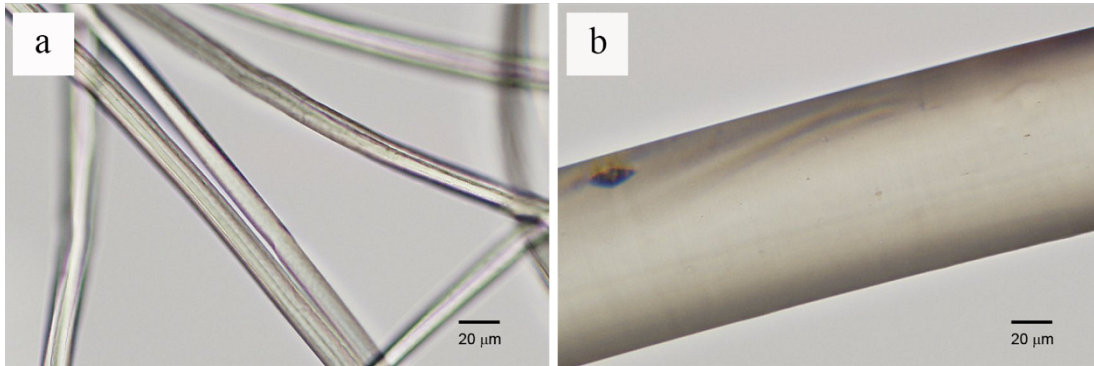


Figure A.3 Photomicrographs of fibres: (a) meta-aramid fibre, (b) monofilament PEEK fibre. (scale bar 20 μm)

Images of fabric surfaces

Images of the fabric structures were taken with a stereomicroscope with an integrated camera (Model EZ4W, Leica microsystems (Schweiz) AG, Heerbrugg, Switzerland).

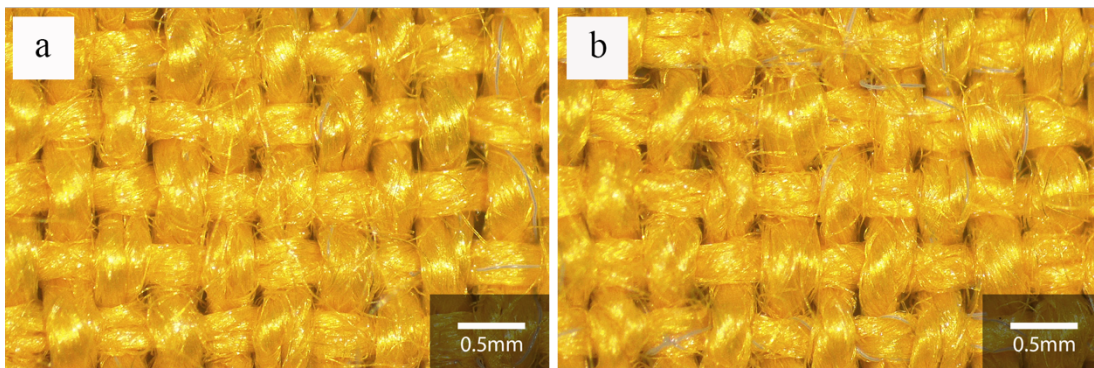


Figure A.4 Surface light stereomicroscope images of the outer layer fabric: (a) front, (b) back. (scale bar 0.5 mm)

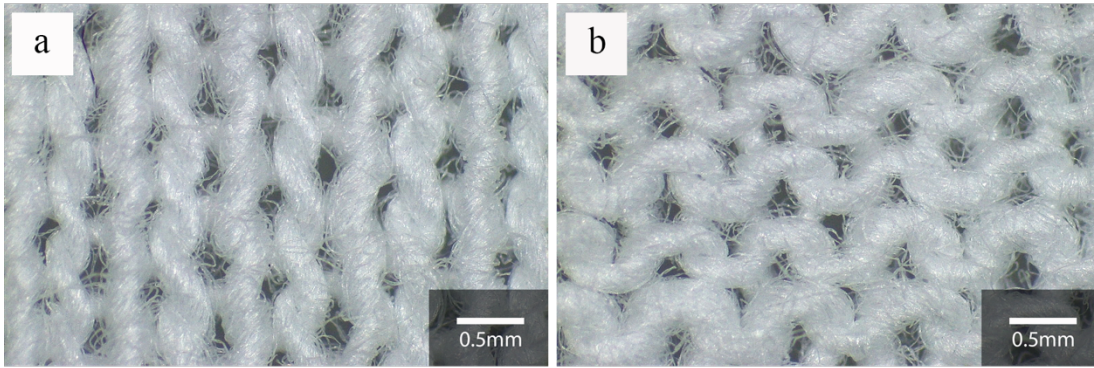


Figure A.5 Surface light stereomicroscope images of the base layer fabric: (a) front, (b) back. (scale bar 0.5 mm)

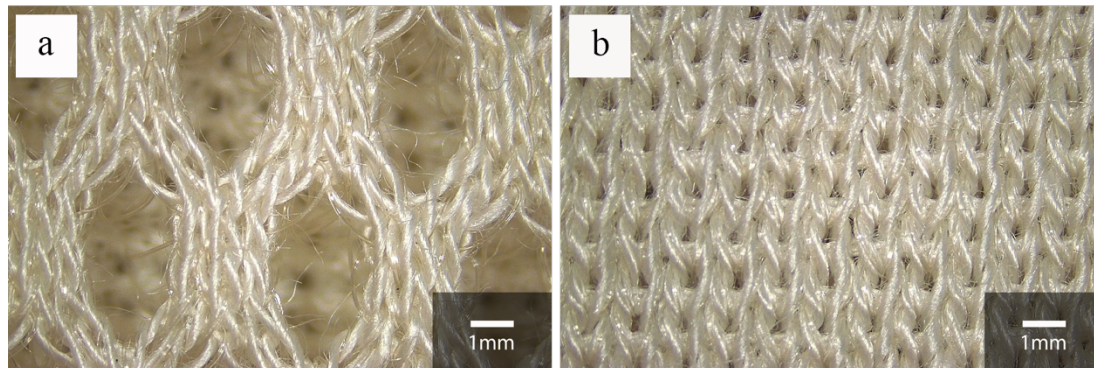


Figure A.6 Surface light stereomicroscope images of the three-dimensional warp knitted fabric (type 1): (a) front, (b) back. (scale bar 1 mm)

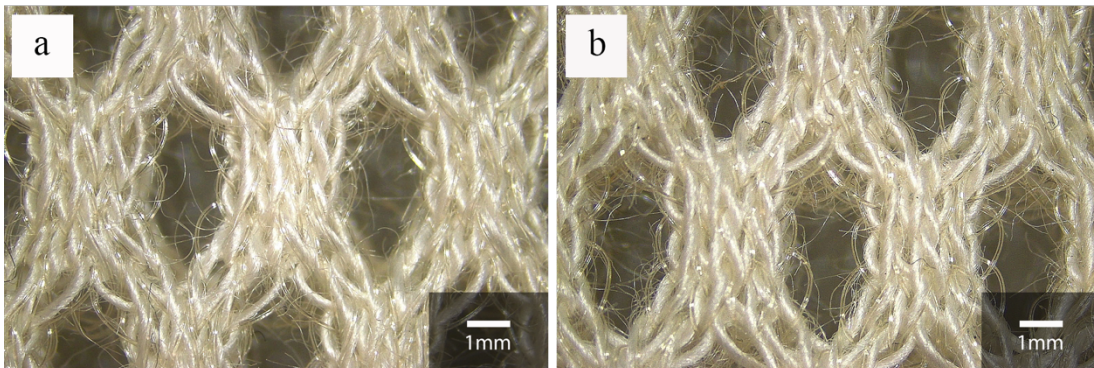


Figure A.7 Surface light stereomicroscope images of the three-dimensional warp knitted fabric (type 2): (a) front, (b) back. (scale bar 1 mm)

Instrumented manikin test settings

Table A.1 Body measurements of instrumented manikin (University of Alberta).

Measurement	cm	inches
Neck	39.5	15.5
Chest	101	39.75
Back width (armscye to armscye across shoulder blades)	40	15.5
Back width (shoulder cap to shoulder cap)	48	19
Waist	85	33.5
Hips (at fullest point)	99.5	39.25
Biceps circumference	31	12.25
Wrist circumference	18.5	7.5
Thigh circumference	54.5	21.5
Crotch (front waist to back waist)	68.5	27
Crotch (collar bone front to back base of neck)	152.5	60
Inseam (crotch to ankle bone)	74	29
Back length (base of neck to waist)	47	18.5
Outer arm length (base of neck to wrist)	68.5	31.5
Outer arm length (shoulder to wrist)	64	25.25
Underarm length	48	19

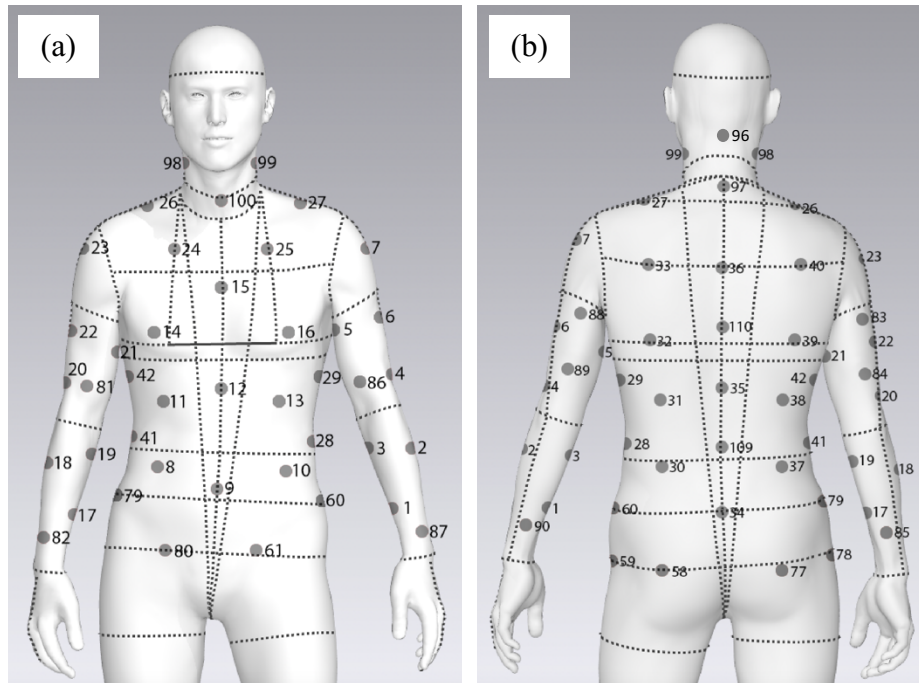


Figure A.8 Simulated instrumented manikin in CLO software and sensor location in the area covered by shirts: (a) front view, (b) back view.

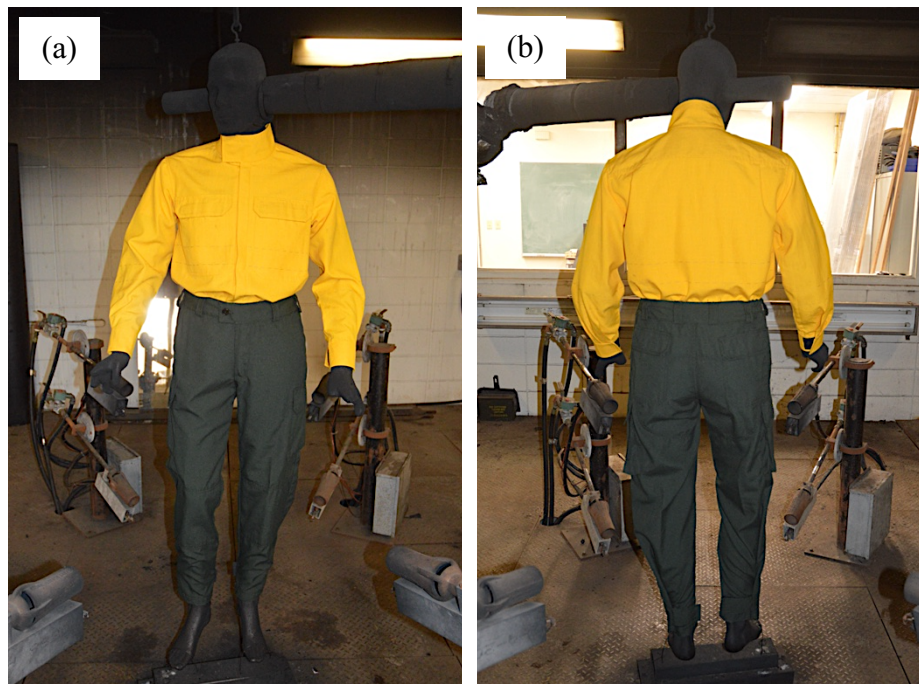


Figure A.9 Garment ensemble with the control shirt number 2: (a) front view, (b) back view.

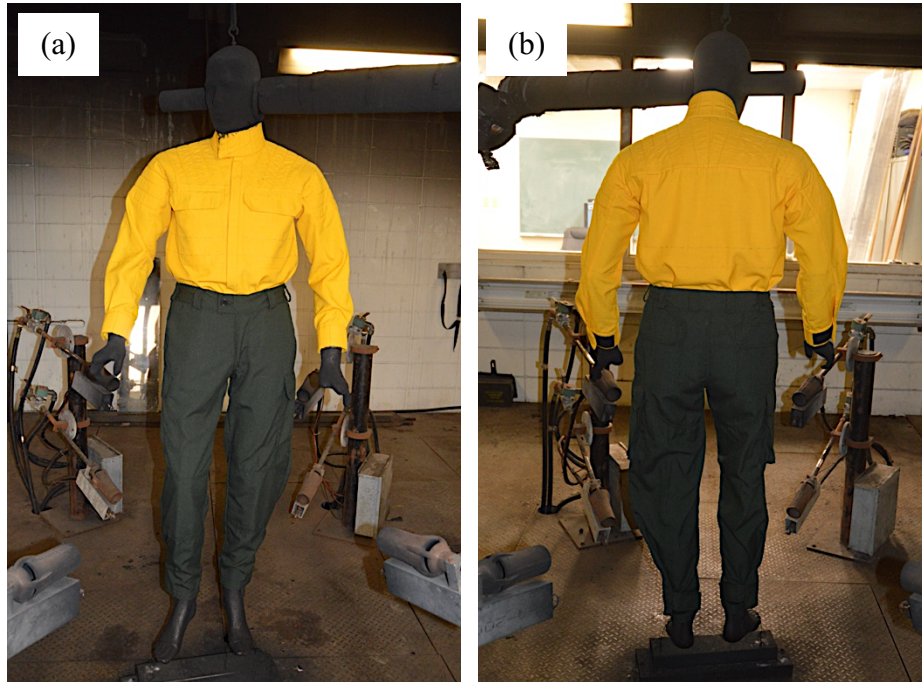


Figure A.10 Garment ensemble with the prototype shirt number 2: (a) front view, (b) back view.

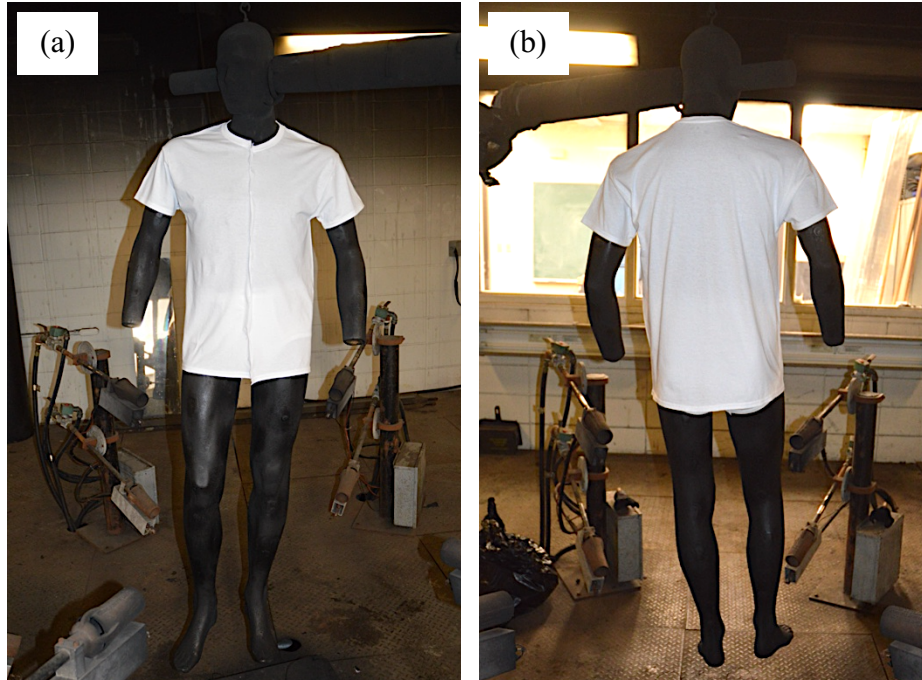


Figure A.11 Base layer comprised cotton t-shirt and briefs: (a) front view, (b) back view.

APPENDIX B: THERMAL PROTECTION TEST RESULTS

Raw data of thermal protection test results

Table B.1 Raw data of thermal energy and time to predicted second-degree burn for different fabric systems under dry and wet base layer conditions when exposed to a flame heat source.

Fabric system	Replica number	TPP rating results, under different base layer condition			
		Dry		Wet	
		Thermal energy, (J/cm ²)	Time to 2 nd -degree burn, (sec.)	Thermal energy, (J/cm ²)	Time to 2 nd -degree burn, (sec.)
OL-BL	1	44.4	5.3	40.2	4.8
	2	36.0	4.3	36.8	4.4
	3	43.5	5.2	38.5	4.6
	4	44.4	5.3	36.0	4.3
	5	45.2	5.4	38.5	4.6
OL-BL-S	1	72.9	8.7	56.9	6.8
	2	72.0	8.6	58.6	7.0
	3	72.0	8.6	57.8	6.9
	4	69.5	8.3	58.6	7.0
	5	69.5	8.3	62.0	7.4
OL-S-BL	1	71.2	8.5	64.5	7.7
	2	72.9	8.7	65.3	7.8
	3	73.7	8.8	66.2	7.9
	4	82.1	9.8	62.0	7.4
	5	72.0	8.6	66.2	7.9
OL-3D1-BL	1	169.1	20.2	150.7	18.0
	2	152.4	18.2	147.4	17.6
	3	150.7	18.0	161.6	19.3
	4	153.2	18.3	153.2	18.3
	5	161.6	19.3	154.1	18.4
OL-3D2-BL	1	119.7	14.3	108.0	12.9
	2	123.9	14.8	114.7	13.7
	3	112.2	13.4	111.4	13.3
	4	112.2	13.4	118.1	14.1
	5	112.2	13.4	118.1	14.1

Table B.2 Raw data of thermal energy and time to predicted second-degree burn for different fabric systems under dry and wet base layer conditions when exposed to a radiant heat source.

Fabric system	Replica number	RHR rating results, under different base layer condition			
		Dry		Wet	
		Thermal energy, (J/cm ²)	Time to 2 nd -degree burn, (sec.)	Thermal energy, (J/cm ²)	Time to 2 nd -degree burn, (sec.)
OL-BL	1	53.6	25.4	47.1	22.4
	2	51.4	23.8	43.9	20
	3	51.2	23.8	46.2	21.1
	4	49.5	23.1	46.1	21.2
	5	55.6	25.9	45.3	22
OL-BL-S	1	82.7	39.2	82.0	39
	2	82.4	38.2	75.9	34.6
	3	86.9	40.4	82.8	37.8
	4	94.9	44.3	86.6	39.8
	5	86.1	40.0	85.0	41.3
OL-S-BL	1	77.4	36.7	81.1	38.6
	2	72.7	33.7	66.7	30.4
	3	80.8	37.6	66.6	30.4
	4	80.5	37.6	72.2	33.2
	5	84.8	39.5	80.5	39.1
OL-3D1-BL	1	169.4	80.3	149.2	71
	2	148.9	69.0	142.9	65.1
	3	158.4	73.6	144.8	66.1
	4	151.4	70.7	139.7	64.2
	5	157.4	73.3	137.1	66.6
OL-3D2-BL	1	112.3	53.2	105.3	50.1
	2	110.3	51.1	104.3	47.5
	3	104.8	48.7	106.9	48.8
	4	113.1	52.8	105.3	48.4
	5	111.7	52.0	96.5	46.9

Table B.3 Raw data of thermal energy and time to predicted second-degree burn for different fabric systems under dry and wet base layer conditions when exposed to a combined flame and radiant heat source.

Fabric system	Replica number	CHTP rating results, under different base layer condition			
		Dry		Wet	
		Thermal energy, (J/cm ²)	Time to 2 nd -degree burn, (sec.)	Thermal energy, (J/cm ²)	Time to 2 nd -degree burn, (sec.)
OL-BL	1	30.0	3.5	29.1	3.4
	2	29.1	3.4	28.3	3.3
	3	29.1	3.4	30.7	3.6
	4	28.0	3.3	29.9	3.5
	5	30.5	3.6	28.2	3.3
OL-BL-S	1	52.2	6.1	50.6	5.9
	2	56.5	6.6	52.3	6.1
	3	56.5	6.6	48.7	5.7
	4	50.0	5.9	48.7	5.7
	5	55.1	6.5	47.8	5.6
OL-S-BL	1	41.9	4.9	44.6	5.2
	2	41.9	4.9	42.9	5.0
	3	41.1	4.8	41.8	4.9
	4	43.2	5.1	41.8	4.9
	5	41.5	4.9	42.7	5.0
OL-3D1-BL	1	125.8	14.7	116.6	13.6
	2	125.8	14.7	119.1	13.9
	3	126.7	14.8	118.7	13.9
	4	125.5	14.8	117.9	13.8
	5	125.5	14.8	117.0	13.7
OL-3D2-BL	1	96.7	11.3	90.8	10.6
	2	96.7	11.3	89.1	10.4
	3	94.2	11.0	89.7	10.5
	4	93.3	11.0	89.7	10.5
	5	95.0	11.2	88.0	10.3

Overall two-way ANOVA for thermal protection test results

Table B.4 Overall two-way ANOVA test for TPP rating results.

Source	SS	df	MS	F	Sig.
Intercept	396747.683	1	396747.683	21662.910	<.001
Base layer condition	533.241	1	533.241	29.116	<.001
Fabric system	84092.989	4	21023.247	1147.895	<.001
Base layer condition * Fabric system	183.987	4	45.997	2.511	.057
Error	732.584	40	18.315		
Total	482290.484	50			

Table B.5 Overall two-way ANOVA test for RHR rating results.

Source	SS	df	MS	F	Sig.
Intercept	435915.249	1	435915.249	18710.059	<.001
Base layer condition	708.252	1	708.252	30.399	<.001
Fabric system	57236.098	4	14309.024	614.162	<.001
Base layer condition * Fabric system	157.133	4	39.283	1.686	.172
Error	931.938	40	23.298		
Total	494948.671	50			

Table B.6 Table Summary table for overall two-way ANOVA test for CHTP rating results.

Source	SS	df	MS	F	Sig.
Intercept	228024.742	1	228024.742	112049.281	<.001
Base layer condition	152.928	1	152.928	75.148	<.001
Fabric system	59078.135	4	14769.534	7257.614	<.001
Base layer condition * Fabric system	141.250	4	35.313	17.352	<.001
Error	81.402	40	2.035		
Total	287478.458	50			

Percentage of thermal protection increase

Table B.7 Summary of differences in TPP rating values in percentage among three-layer and two-layer fabric systems.

Fabric system	Fabric system (for comparison)	Percentage of TPP rating differences under different base layer condition, (%)	
		Dry	Wet
OL-3D1-BL	OL-BL	269	304
	OL-BL-S	121	161
	OL-S-BL	112	137
OL-3D2-BL	OL-BL	172	200
	OL-BL-S	63	94
	OL-S-BL	56	76
OL-BL-S	OL-BL	67	55
OL-S-BL	OL-BL	74	70

Table B.8 Summary of differences in RHR rating values in percentage among three-layer and two-layer fabric systems.

Fabric system	Fabric system (for comparison)	Percentage of RHR rating differences under different base layer condition, (%)	
		Dry	Wet
OL-3D1-BL	OL-BL	200	212
	OL-BL-S	81	73
	OL-S-BL	98	94
OL-3D2-BL	OL-BL	111	127
	OL-BL-S	27	26
	OL-S-BL	39	41
OL-BL-S	OL-BL	66	80
OL-S-BL	OL-BL	52	61

Table B.9 Summary of differences in CHTP rating values in percentage among three-layer and two-layer fabric systems.

Fabric system	Fabric system (for comparison)	Percentage of CHTP rating differences under different base layer condition, (%)	
		Dry	Wet
OL-3D1-BL	OL-BL	329	303
	OL-BL-S	133	137
	OL-S-BL	200	175
OL-3D2-BL	OL-BL	225	206
	OL-BL-S	76	80
	OL-S-BL	127	109
OL-BL-S	OL-BL	84	69
OL-S-BL	OL-BL	43	46
OL-BL-S	OL-S-BL	29	15

Pairwise comparisons of dry and wet thermal protection results

Table B.10 Pairwise comparison of mean values of TPP rating for different fabric systems between dry and wet base layer conditions when exposed to a flame heat source.

Base layer condition	(I) Fabric system	(J) Fabric system	Mean difference (I-J)	Sig.	95% CI for Difference	
					Lower Bound	Upper Bound
OL-BL	dry	wet	4.6	.091	-0.8	10.2
OL-BL-S	dry	wet	12.4*	<.001	6.9	17.9
OL-S-BL	dry	wet	9.5*	<.001	4.1	15.0
OL-3D1-BL	dry	wet	4.0	.145	-1.4	9.5
OL-3D2-BL	dry	wet	2.0	.462	-3.5	7.5

* Means are significantly different between conditions of the base layer of each fabric system when subjected to a pairwise comparison of two-way ANOVA test ($p < .005$).
Note. Bonferroni correction was used for the alpha value adjustment for multiple comparisons. In total 10 multiple comparisons were conducted. Only 5 comparisons of interests were reported.

Table B.11 Pairwise comparison of mean values of RHR rating for different fabric systems between dry and wet base layer conditions when exposed to a radiant heat source.

Fabric system	(I) Base layer condition	(J) Base layer condition	Mean difference (I-J)	Sig.	95% CI for Difference	
					Lower Bound	Upper Bound
OL -BL	dry	wet	6.5**	.039	.4	12.7
OL-BL-S	dry	wet	4.1	.182	-2.0	10.3
OL-S-BL	dry	wet	5.8	.064	- .3	12.0
OL-3D1-BL	dry	wet	14.4*	<.001	8.2	20.5
OL-3D2-BL	dry	wet	6.7**	.033	.6	12.9

* Means are significantly different between conditions of base layer of each fabric system when subjected to a pairwise comparison of two-way ANOVA test ($p < .05$).

** Moderate evidence that means are different between conditions of fabric system when subjected to pairwise comparison of two-way ANOVA test ($p < .005$).

Note. Bonferroni correction was used for the alpha value adjustment for multiple comparisons. In total 10 multiple comparisons were conducted. Only 5 comparisons of interests were reported.

Table B.12 Pairwise comparison of mean values of CHTP rating for different fabric systems between dry and wet base layer conditions when exposed to a combined flame and radiant heat source.

Fabric system	(I) Base layer condition	(J) Base layer condition	Mean difference (I-J)	Sig.	95% CI for Difference	
					Lower Bound	Upper Bound
OL-BL	dry	wet	.1	.923	-1.7	1.9
OL-BL-S	dry	wet	4.5*	.001	2.6	6.3
OL-S-BL	dry	wet	-.8	.376	-2.6	1.0
OL-3D1-BL	dry	wet	8.0*	.001	6.2	9.8
OL-3D2-BL	dry	wet	5.7*	.001	3.9	7.5

* Means are significantly different between conditions of the base layer of each fabric system when subjected to pairwise comparison of two-way ANOVA test ($p < .005$).

Note. Bonferroni correction was used for the alpha value adjustment for multiple comparisons. In total 10 multiple comparisons were conducted. Only 5 comparisons of interests were reported.

Complementary graphs with the thermocouple response

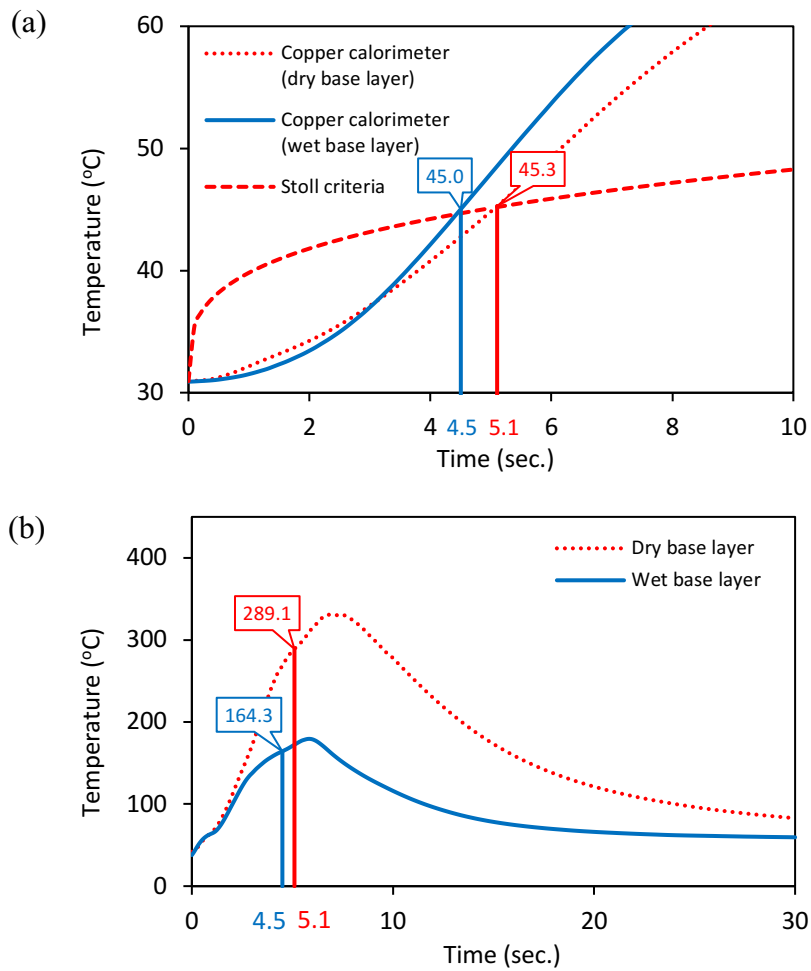


Figure B.1 Average temperature of the copper calorimeter, and thermocouples positioned at the base layer of fabric system OL-BL during the flame exposure test under dry and wet base layer condition: (a) copper calorimeter, and (b) thermocouple response.

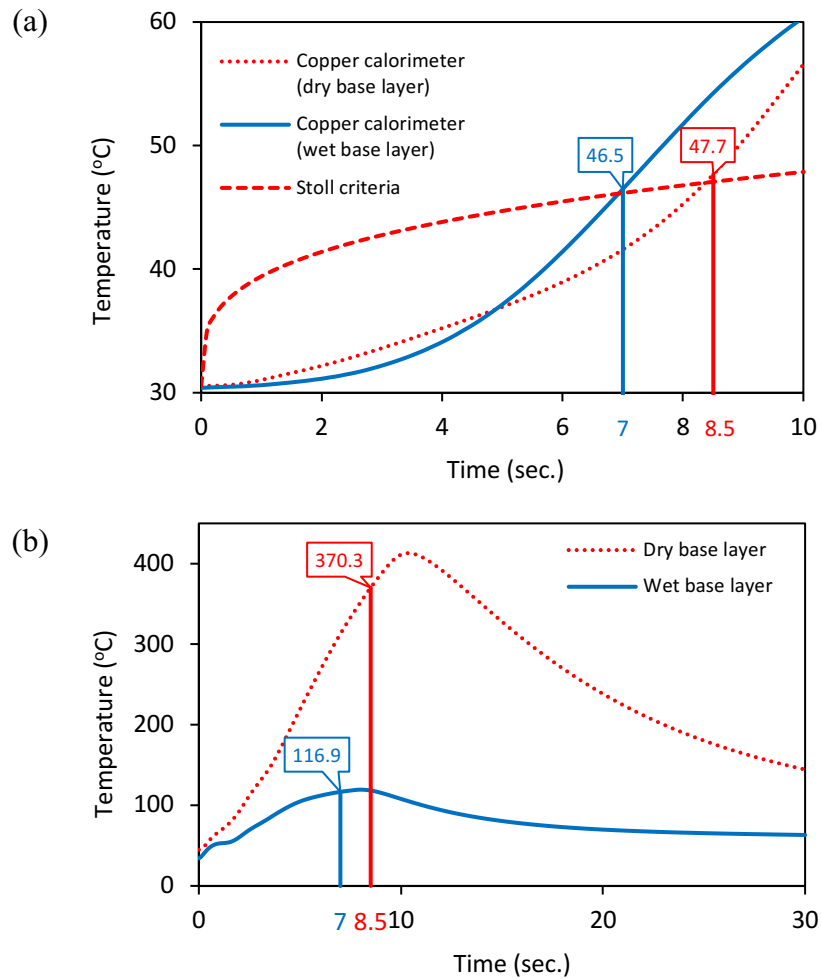


Figure B.2 Average temperature of the copper calorimeter, and thermocouples positioned at the base layer of fabric system OL-BL-S during the flame exposure test under dry and wet base layer condition: (a) copper calorimeter, and (b) thermocouple response.

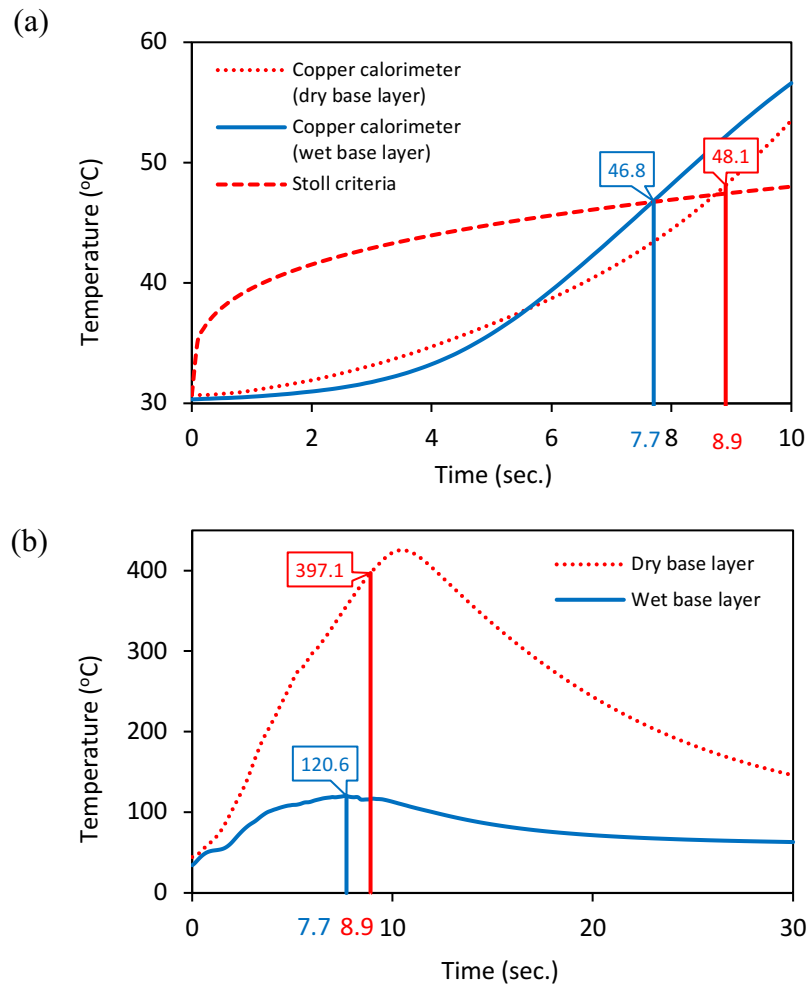


Figure B.3 Average temperature of the copper calorimeter, and thermocouples positioned at the base layer of fabric system OL-BL-S during the flame exposure test under dry and wet base layer condition: (a) copper calorimeter, and (b) thermocouple response.

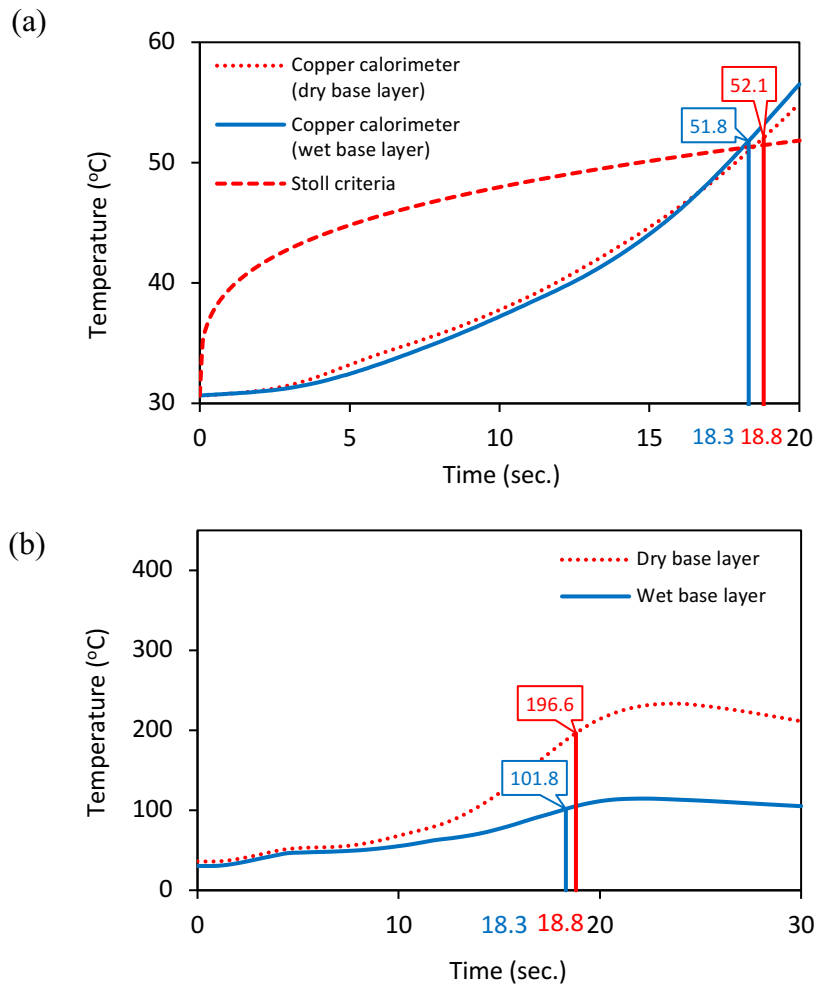


Figure B.4 Average temperature of the copper calorimeter, and thermocouples positioned at the base layer of fabric system OL-3D1-BL during the flame exposure test under dry and wet base layer condition: (a) copper calorimeter, and (b) thermocouple response.

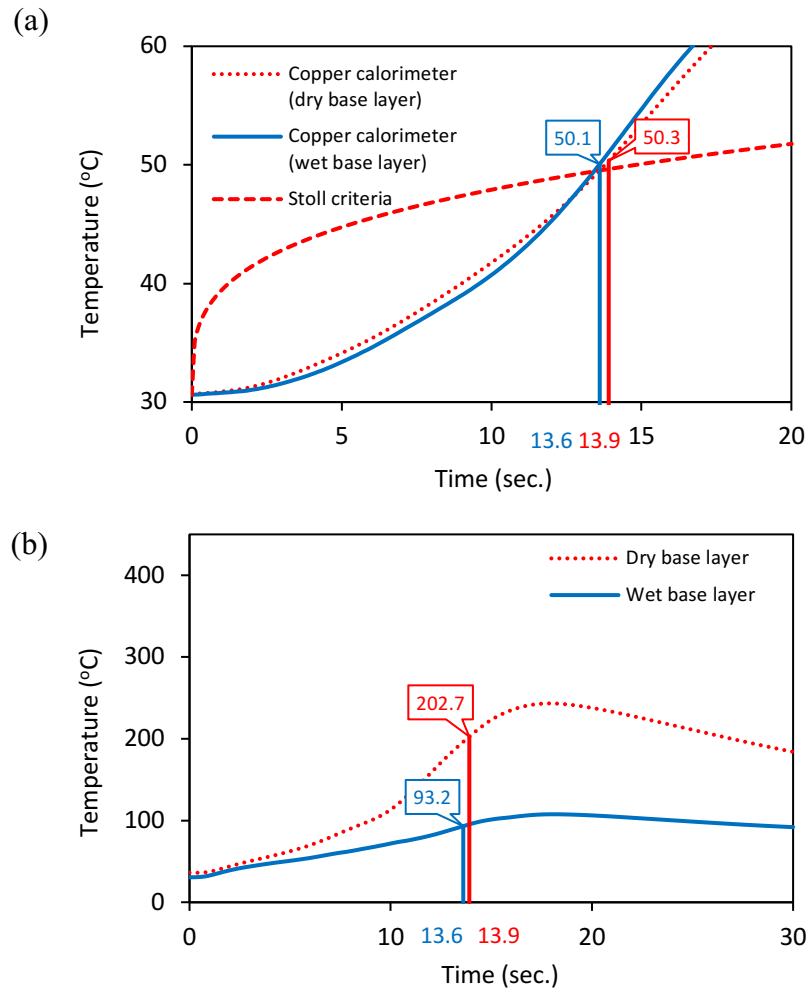


Figure B.5 Average temperature of the copper calorimeter, and thermocouples positioned at the base layer of fabric system OL-3D1-BL during the flame exposure test under dry and wet base layer condition: (a) copper calorimeter, and (b) thermocouple response.

APPENDIX C: COMFORT TEST RESULTS

Raw data of comfort test results

Table C.1 Raw data of intrinsic thermal and evaporative resistance values of bare plate, and different fabric systems.

Fabric system	Thermal resistance value, R_{ct} ($K \cdot m^2/W$)			Apparent evaporative resistance value, R_{et}^A ($kPa \cdot m^2/W$)		
	Replica number			Replica number		
	1	2	3	1	2	3
Bare plate		0.0535			0.0041	
OL	0.0208	0.0215	0.0218	0.0040	0.0027	0.0024
OL(2)	0.0352	0.0430	0.0408	0.0062	0.0058	0.0062
BL	0.0243	0.0252	0.0274	0.0028	0.0028	0.0025
3D1	0.0968	0.0990	0.1016	0.0144	0.0147	0.0146
3D2	0.0626	0.0678	0.0635	0.0076	0.0087	0.0097
OL-BL	0.0410	0.0451	0.0429	0.0062	0.0067	0.0059
OL(2)-BL	0.0581	0.0630	0.0623	0.0079	0.0078	0.0078
OL-3D1-BL	0.1283	0.1253	0.1295	0.0199	0.0197	0.0184
OL-3D2-BL	0.1075	0.1060	0.1150	0.0178	0.0171	0.0153

Note. Equation 3.6 from Chapter 3 was used to calculate the THL values of the individual fabrics and fabric system replicas. The averaged THL values of fabric systems are presented in the Table 5.1. The averaged THL value for the bare plate is 721 W/m^2 . The averaged THL value of individual fabrics OL, OL(2), BL, 3D1, and 3D2 are 709 W/m^2 , 499 W/m^2 , 729 W/m^2 , 270 W/m^2 , and 389 W/m^2 respectively.

Table C.2 Raw data of air permeability values of different fabric systems.

Replica number	Air permeability value (L/m ² · sec.)			
	Fabric system			
	OL-BL	OL(2)-BL	OL-3D1-BL	OL-3D2-BL
1	256.54	166.32	240.23	289.00
2	258.06	170.89	236.83	305.16
3	250.44	167.69	258.06	291.69
4	256.54	171.35	250.44	289.00
5	256.54	170.89	253.49	305.16
6	243.64	154.43	233.43	291.69
7	258.06	167.23	256.54	294.39
8	268.73	177.19	253.49	294.39
9	247.04	160.53	247.04	291.69
10	265.68	173.74	250.44	280.92

Overall two-way ANOVA for comfort test results

Table C.3 Overall one-way ANOVA test for THL results.

Source	SS	df	MS	F	Sig.
Intercept	1386520.083	1	1386520.083	14136.144	<.001
Fabric system	154344.250	3	51448.083	524.534	<.001
Error	784.667	8	98.083		
Total	1541649.000	12			

Table C.4 Overall one-way ANOVA test for air permeability results.

Source	SS	df	MS	F	Sig.
Intercept	2330302.611	1	2330302.611	41041.153	<.001
Fabric system	83387.721	3	27795.907	489.540	<.001
Error	2044.068	36	56.780		
Total	2415734.399	40			

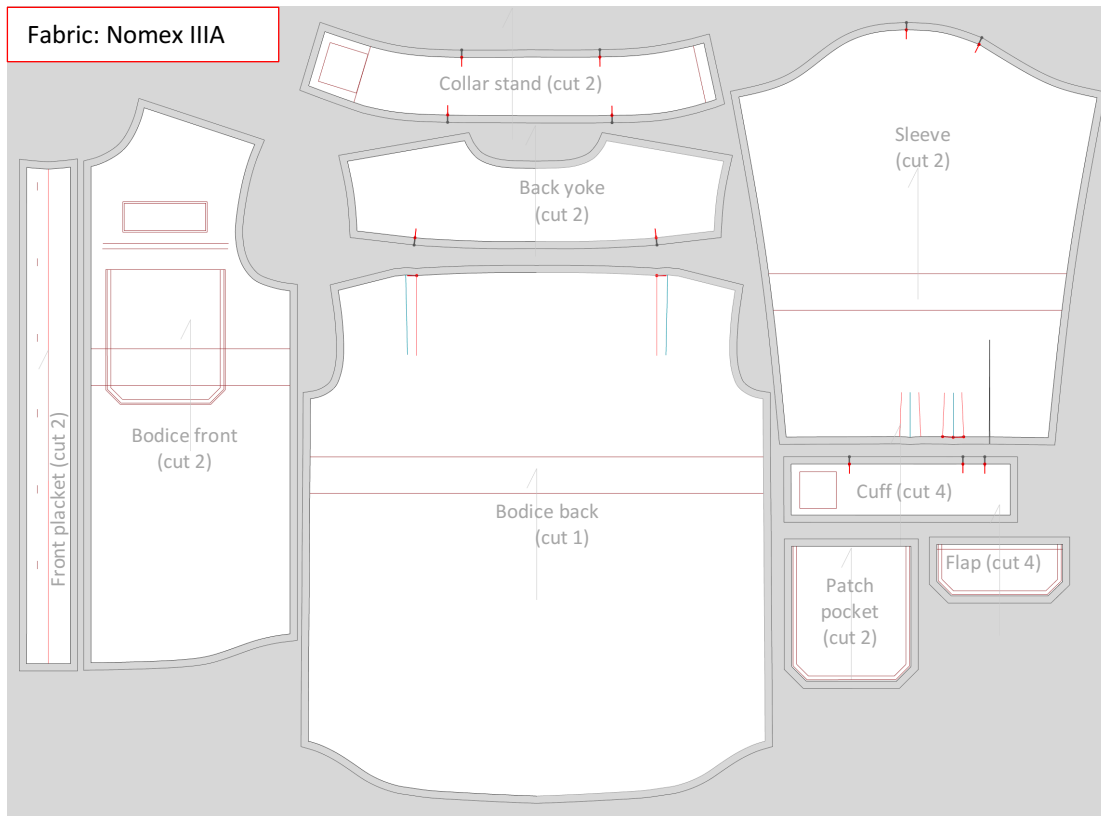
APPENDIX D: DESIGN AND CONSTRUCTION OF SHIRTS**Pattern pieces of shirts**

Figure D.1 Pattern pieces of control shirt.

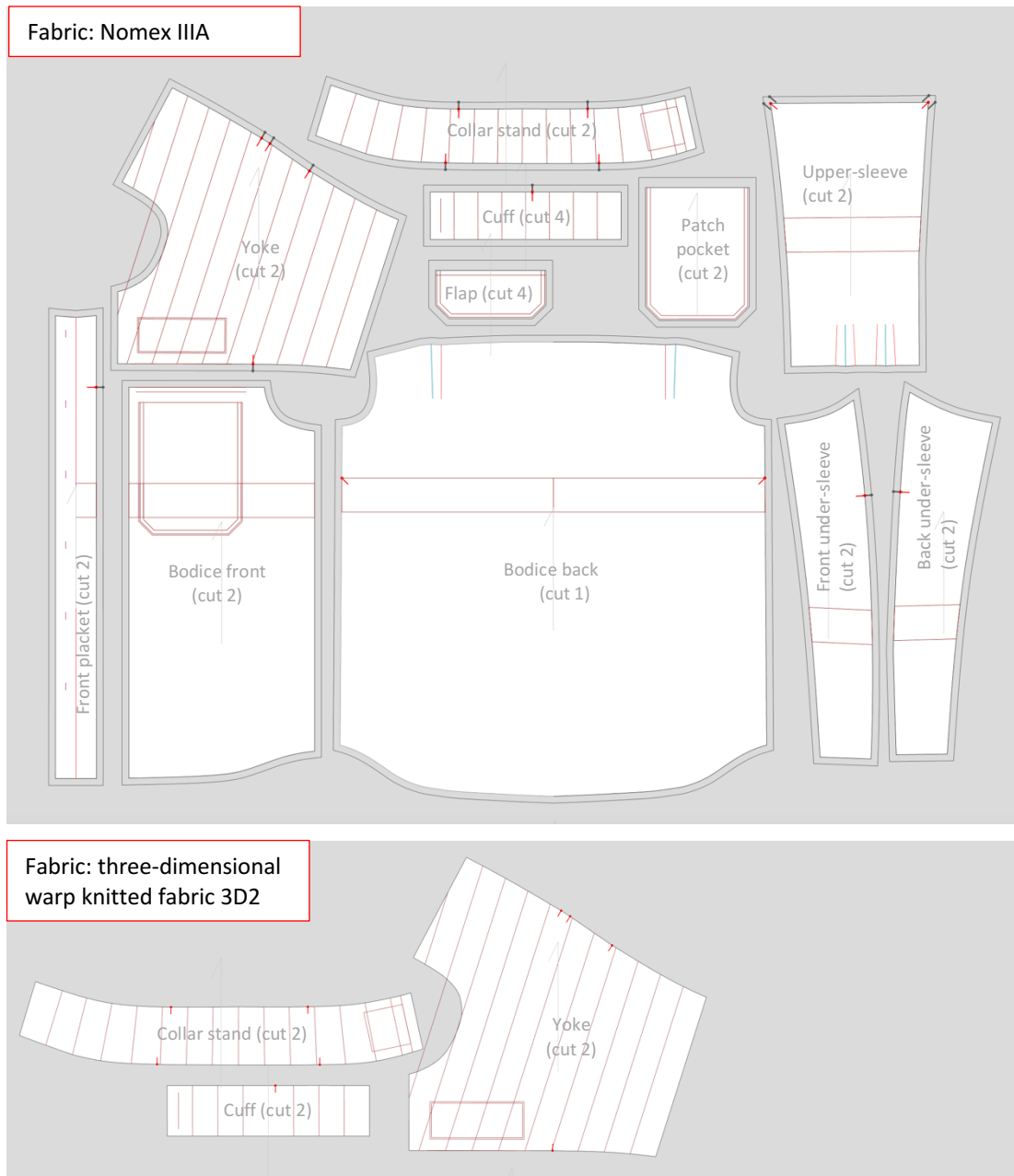


Figure D.2 Pattern pieces of prototype shirt.

Construction of shirts

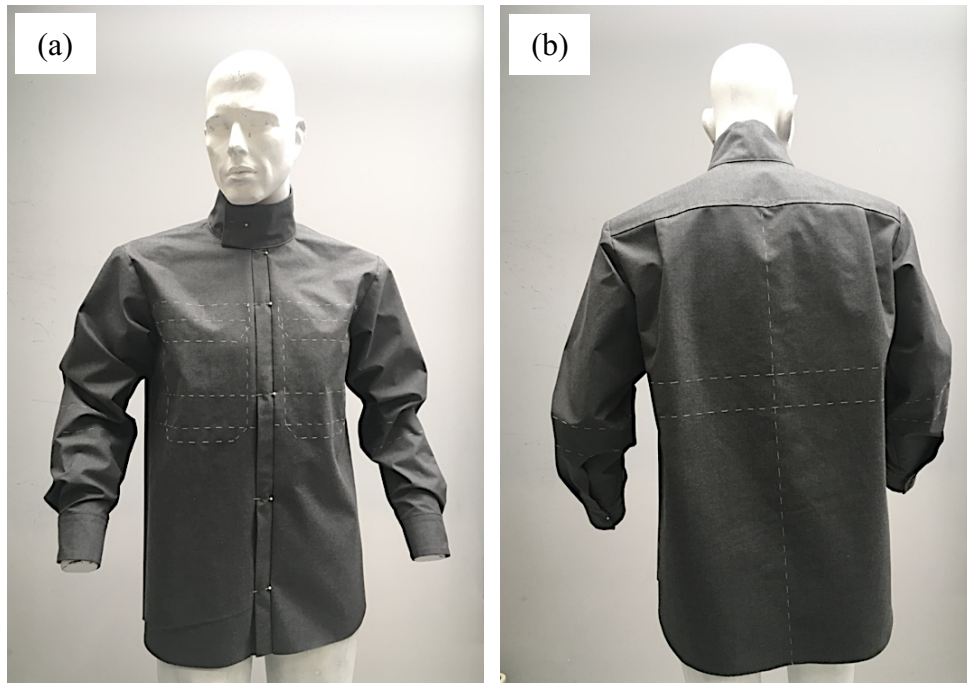


Figure D.3 Garment mock-up of control shirt: (a) front view, (b) back view.



Figure D.4 Garment mock-up of prototype shirt: (a) front view, (b) back view.



Figure D.5 Detailed view of prototype shirt: (a) yoke back, (b) yoke inner side, (c) collar with front closure, (d) patch pocket with flap, and sleeve cuff (e) closed (f) open.

Table D.1 Material consumption.

Material	Trademark	Quantity	
		Control	Prototype
Nomex® IIIA with moisture wicking finish (fabric width 152 cm)	Milliken & Company	157 cm	166 cm
Three-dimensional warp knitted fabric (fabric width 192 cm)	Heathcoat fabrics Spacetech® (code: N-02780-A01)	-	24 cm
Segmented adhesive reflective trim strip (strip width 5 cm)	3M™ Scotchlite™	200 cm	205 cm
Flame-resistant hook-and-loop (strip width 5 cm)	DuraGrip®	15 cm (hook) 33 cm (loop)	15 cm (hook) 33 cm (loop)
Stainless steel sew-on snaps (1.5 cm)	Nancelelor	7	7
Aramid thread (tex 60)	Anesafe (code: 1773489)	~800 m	~1000 m

Table D.2 Prototype shirt construction sequence.

Construction step	Seam type	Stitch type
1. Apply adhesive reflective trim strips horizontally onto shirt front and back pieces, patch pockets, and sleeves following the notches		
2. Construction of yoke		
<ul style="list-style-type: none"> • Attach bias binding to all the edges of the three-dimensional warp-knitted fabric layer 	SSaa-1	301
<ul style="list-style-type: none"> • Press seam allowances to the bias binding side 		
<ul style="list-style-type: none"> • Topstitch on the bias binding 2 mm away from the seamline 	LSq-2	301
<ul style="list-style-type: none"> • Baste or pin the yoke outerlayer together with the layer of three-dimensional fabric 		
<ul style="list-style-type: none"> • Stitch the yoke outerlayer together with the layer of three-dimensional fabric following evenly spaced 30 mm apart parallel lines 	SSv	301
<ul style="list-style-type: none"> • Remove basting stitches from yoke 		
<ul style="list-style-type: none"> • Serge centre back seams of the right and left pieces of yoke 		506
<ul style="list-style-type: none"> • Stitch two yoke pieces together along the centre back line 	SSa-1	301
<ul style="list-style-type: none"> • Press open the seam allowances of yoke 		
3. Construction of shirt front (applied to right and left shirt front pieces)		
3.1 Attaching the pocket to the shirt front		
<ul style="list-style-type: none"> • Serge top edge of the pocket 		506
<ul style="list-style-type: none"> • Fold and press top 30 mm seam allowance 		
<ul style="list-style-type: none"> • Attach hook-and-loop closure to the pocket (double topstitch around the loop portion of the strip) 	LSbj	301
<ul style="list-style-type: none"> • Fold and press 10 mm seam allowance 		
<ul style="list-style-type: none"> • Mark pocket positioning on the shirt front 		
<ul style="list-style-type: none"> • Pin and double topstitch* around the edges of patch pocket 	LSd-2	301

(continued)

Table D.2 Prototype shirt construction sequence (continued).

Construction step	Seam type	Stitch type
3.2 Preparing pocket flap for further attachment to shirt front		
<ul style="list-style-type: none"> • Fold flap along the top edge line with the wrong side out • Stitch along the edge (seam allowance 10 mm), leave a hole • Turn the flap correct side out and press • Double edgestitch* around the outer finished edges of the flap 	SSa-1	301
	SSe-3	301
4. Construction of the shirt back		
<ul style="list-style-type: none"> • Fold and press action pleats on the top of the shirt back • Baste action pleats on the top of the shirt back 		
5. Joining the shirt front, back, yoke, and sleeve pieces together		
5.1 Join yoke and upper-sleeve together		
<ul style="list-style-type: none"> • Stitch the upper sleeve to the yoke, serge the edge • Press seam allowance to the upper sleeve 	SSa-2	301 506
5.2 Join front pieces together (applied to right and left pieces)		
<ul style="list-style-type: none"> • Stitch the front under-sleeve and shirt front together along the armhole line, serge the edge • Stitch and serge the upper-sleeve, front under-sleeve, yoke, and shirt front along the front side sleeve seam and front yoke seam • Press seam allowance to the front under-seam and shirt front • Mark flap positioning under the yoke seam on the shirt front • Pin and double topstitch along the top edge of the flap 	SSa-2	301 506
	SSa-2	301 506
	LSd-2	301
(continued)		

Table D.2 Prototype shirt construction sequence (continued).

Construction step	Seam type	Stitch type
5.3 Joint back pieces together		
• Stitch back under-sleeve and shirt back together along the armhole line, serge the edge	SSa-1	301 506
• Serge back side sleeve seam allowances of the back under-sleeve and upper sleeve from the bottom to the notch that indicates the beginning of the in-seam placket		506
• Baste together under-sleeve and upper sleeve along the in-seam placket	SSa-1	301
• Stitch and serge the upper-sleeve, back under-sleeve, yoke, and shirt back along the back side sleeve seam and back yoke seam from right to left notch of the of the in-seam placket beginning	SSa-2	301 506
• Press seam allowance to the back under-seam and shirt back		
• Press open the seam allowances of in-seam placket		
• Topstitch on the both sides 2 mm away from the basting seam of in-seam placket	SSz-3	301
• Remove basting stitching from the in-seam placket		
5.4 Stitch and serge sleeve under seam and side seam of shirt front and back	SSa-2	301 506
5.5 Press seam allowance to the back under-sleeve and shirt back		
6. Construction and attachment of front plackets		
• Fold and press front placket along the long edge (wrong sides together)		
• Stitch and serge the long edge of front placket with yoke and shirt front piece	SSa-2	301 506
• Press seam allowance to the yoke and shirt front piece		
• Mark snaps' positioning of both front plackets		
• Attach snaps to the plackets		

(continued)

Table D.2 Prototype shirt construction sequence (continued).

Construction step	Seam type	Stitch type
7. Construction and attachment of cuffs		
• Baste or pin the outerlayer fabric of the outer cuff piece together with the layer of three-dimensional fabric		
• Stitch the outerlayer fabric of the outer cuff piece together with the layer of three-dimensional fabric following evenly spaced 30 mm apart parallel lines	SSv	301
• Remove basting stitches from the outer cuff piece		
• Stitch the outer cuff and inner cuff pieces together along the bottom seam correct sides together	SSa-1	301
• Press seam allowance to the inner cuff		
• Topstitch on the inner cuff piece 2 mm away from the seam	LSq-2	301
• Attach hook-and-loop closure to the correct sides of the cuff pieces (double topstitch around the loop portion of the strip to the correct side of the outer cuff piece, and double topstitch around the hook portion of strip to the correct side of the inner cuff piece)	LSbj	301
• Press 10 mm seam allowance of the top side of inner cuff piece		
• Stitch side seams of the outer and inner cuff pieces correct sides together	SSa-1	301
• Turn the cuff correct side out and press		
• Stitch the outer cuff piece and the sleeve correct sides together	SSa-1	301
• Stitch (in the ditch) the inner cuff piece in place when the correct side of the sleeve facing up	LScg-2	301
8. Construction and attachment of collar		
• Baste or pin the outerlayer fabric of the outer collar piece together with the layer of three-dimensional fabric		
• Stitch the outerlayer fabric of the outer collar piece together with the layer of three-dimensional fabric following evenly spaced 30 mm apart parallel lines	SSv	301
• Remove basting stitches from the outer collar piece		

(continued)

Table D.2 Prototype shirt construction sequence (continued).

Construction step	Seam type	Stitch type
<ul style="list-style-type: none"> Stitch the outer collar and inner collar pieces together along the top seam correct sides together Press seam allowance to the inner collar piece 	SSa-1	301
<ul style="list-style-type: none"> Topstitch on the inner collar piece 2 mm away from the seam 	LSq-2	301
<ul style="list-style-type: none"> Attach hook-and-loop closure to the correct sides of the collar (double topstitch around the loop portion of the strip to the correct side of the outer collar piece, and double topstitch around the hook portion of strip to the correct side of the inner collar piece) Press 10 mm seam allowance of the top side of inner collar piece 	LSbj	301
<ul style="list-style-type: none"> Stitch side seams of the outer and inner collar pieces correct sides together Turn the collar correct side out and press 	SSa-1	301
<ul style="list-style-type: none"> Stitch the outer collar piece and the yoke neckline edge correct sides together 	SSa-1	301
<ul style="list-style-type: none"> Stitch (in the ditch) the inner collar piece in place when the correct side of the yoke facing up 	LScg-2	301
<hr/>		
9. Hemming		
<ul style="list-style-type: none"> Serge and press 10 mm of seam allowance of the hem 		506
<ul style="list-style-type: none"> Edgestitch hem 7 mm away from the edge 	EFa	301

*Double top/edge stitching has two parallel stitches 2 and 10 mm away from the edge.

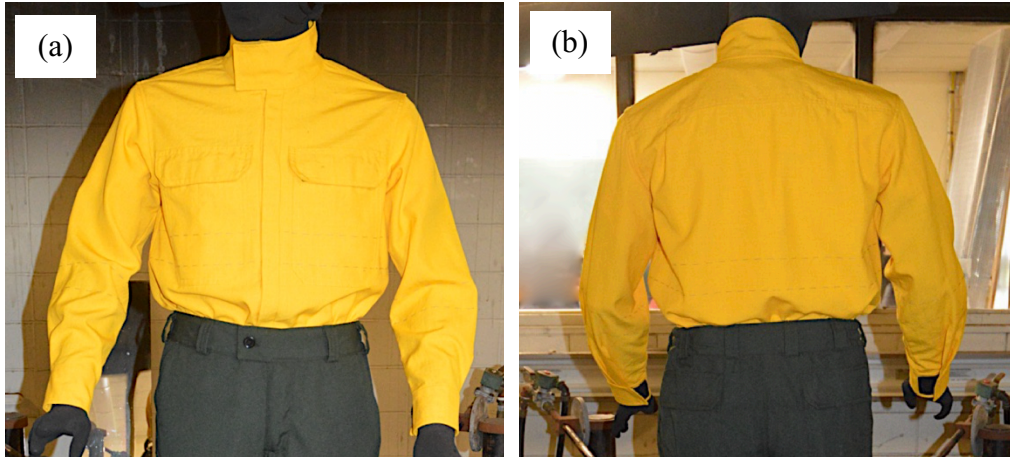
APPENDIX E: INSTRUMENTED MANIKIN TEST RESULTS**Shirt appearance before and after full-scale flame engulfment**

Figure E.1 Control shirt number 1 before the full-scale flame engulfment for 4 seconds: (a) front, and (b) back.

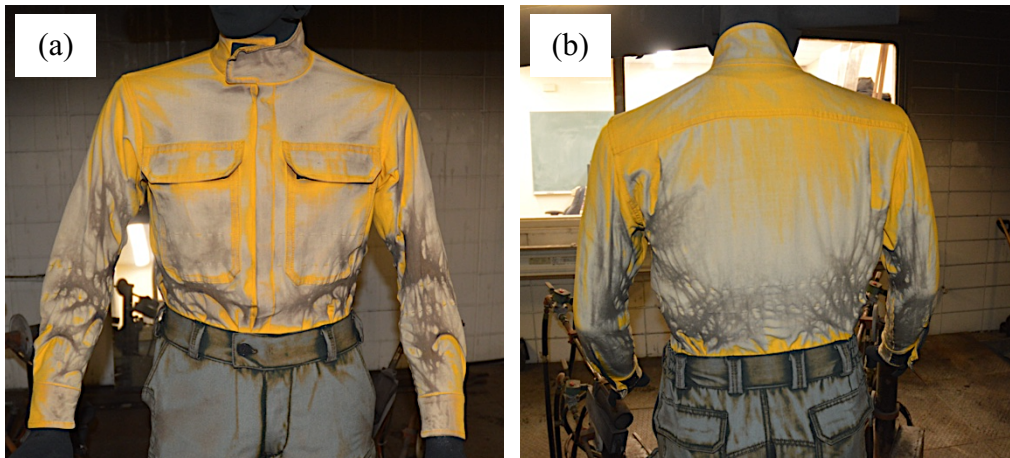


Figure E.2 Control shirt number 1 after the full-scale flame engulfment for 4 seconds: (a) front, and (b) back.

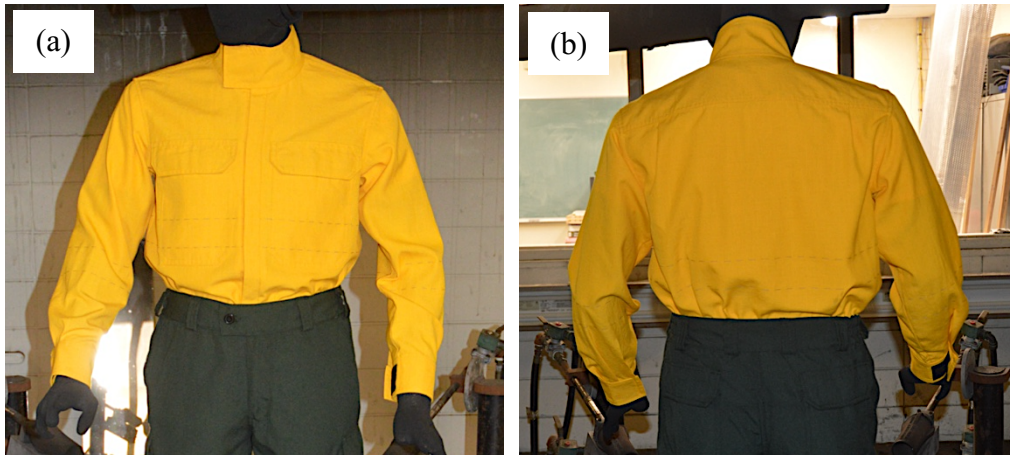


Figure E.3 Control shirt number 3 before the full-scale flame engulfment for 4 seconds: (a) front, and (b) back.

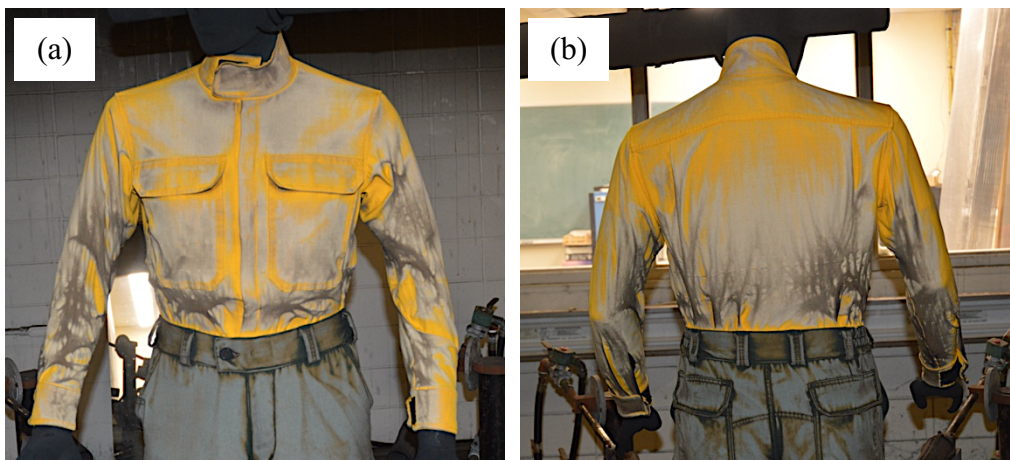


Figure E.4 Control shirt number 3 after the full-scale flame engulfment for 4 seconds: (a) front, and (b) back.



Figure E.5 Prototype shirt number 1 before the full-scale flame engulfment for 4 seconds: (a) front, and (b) back.



Figure E.6 Prototype shirt number 1 after the full-scale flame engulfment for 4 seconds: (a) front, and (b) back.

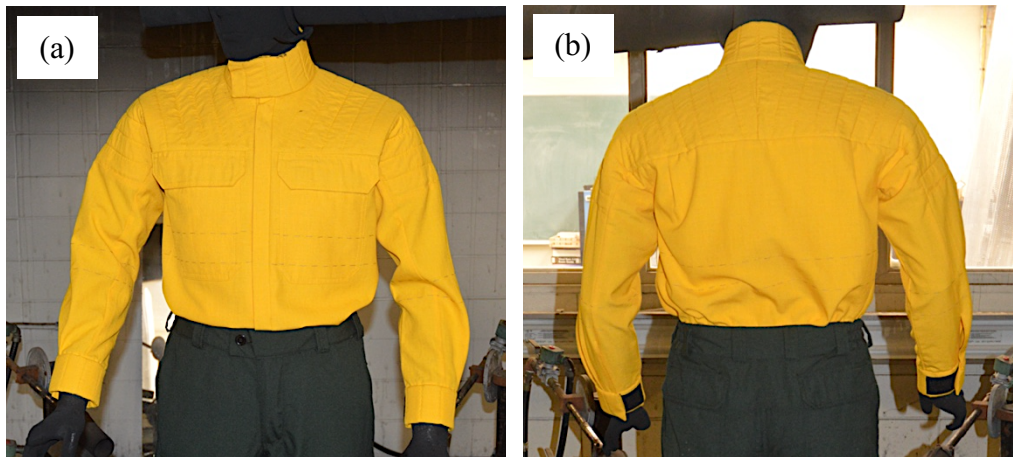


Figure E.7 Prototype shirt number 3 before the full-scale flame engulfment for 4 seconds: (a) front, and (b) back.



Figure E.8 Prototype shirt number 3 after the full-scale flame engulfment for 4 seconds: (a) front, and (b) back.

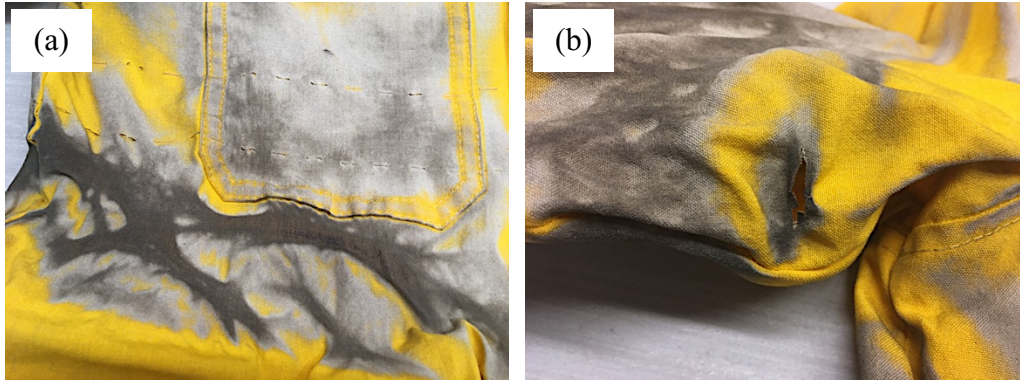


Figure E.9 Damage of the outer layer fabric of shirt after the full-scale flame engulfment for 4 seconds: (a) thermal shrinkage in the waist area, and (b) charring with broke open fabric on sleeve.

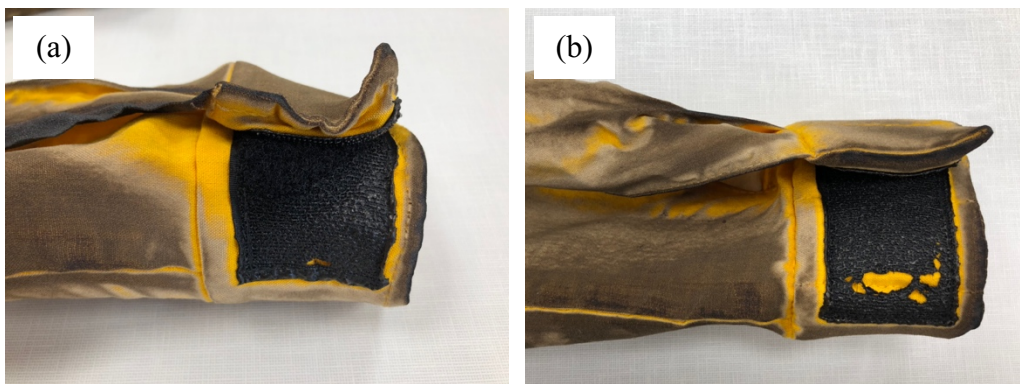


Figure E.10 Cuff hook and loop closure after the full-scale flame engulfment for 4 seconds: (a) control shirt, and (b) prototype shirt.

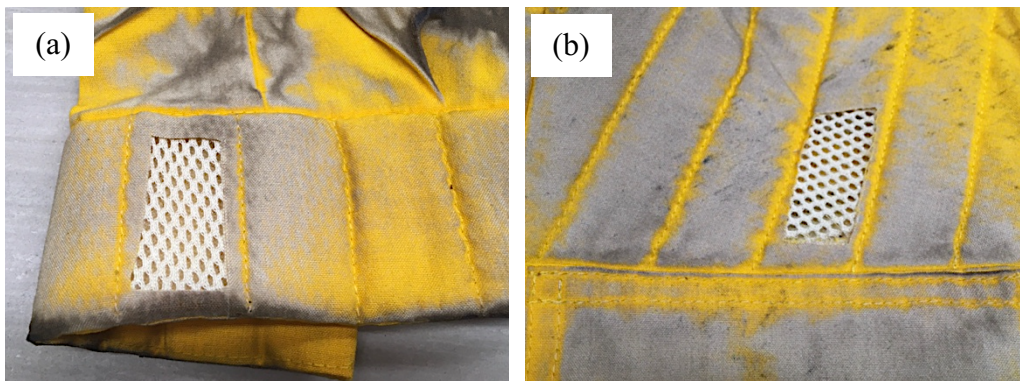


Figure E.11 Three-dimensional knitted fabric appearance after the full-scale flame engulfment for 4 seconds under the outer layer fabric of shirt prototype: (a) cuff, and (b) front yoke.

Burn injury pattern

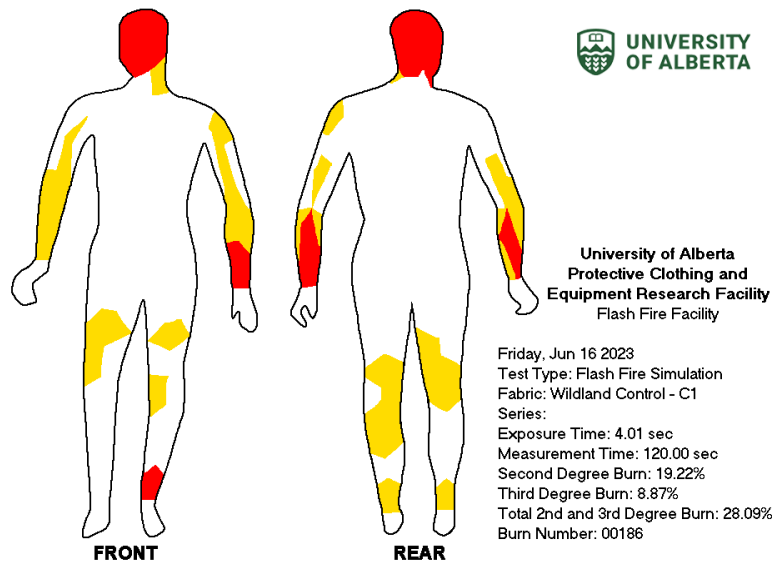


Figure E.12 Burn injury pattern generated by the instrumented manikin system when the garment ensemble with control shirt number 1 was engulfed in flames for 4 seconds.

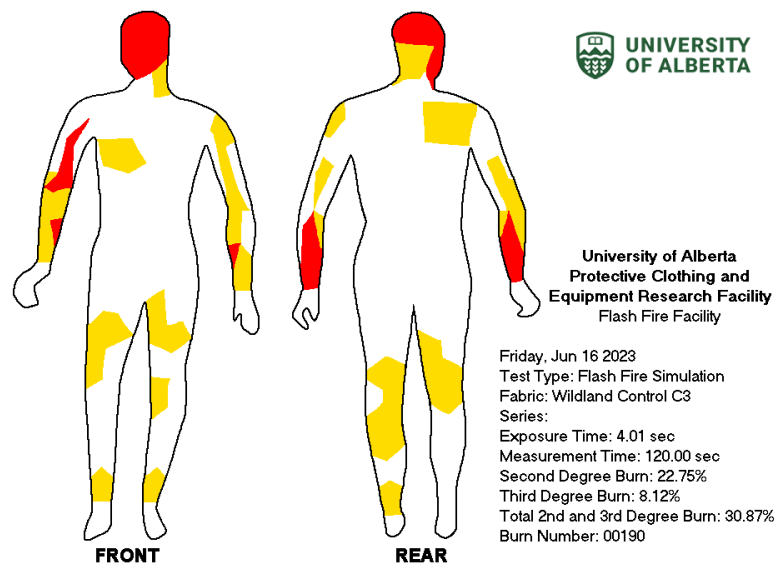


Figure E.13 Burn injury pattern generated by the instrumented manikin system when the garment ensemble with control shirt number 3 was engulfed in flames for 4 seconds.

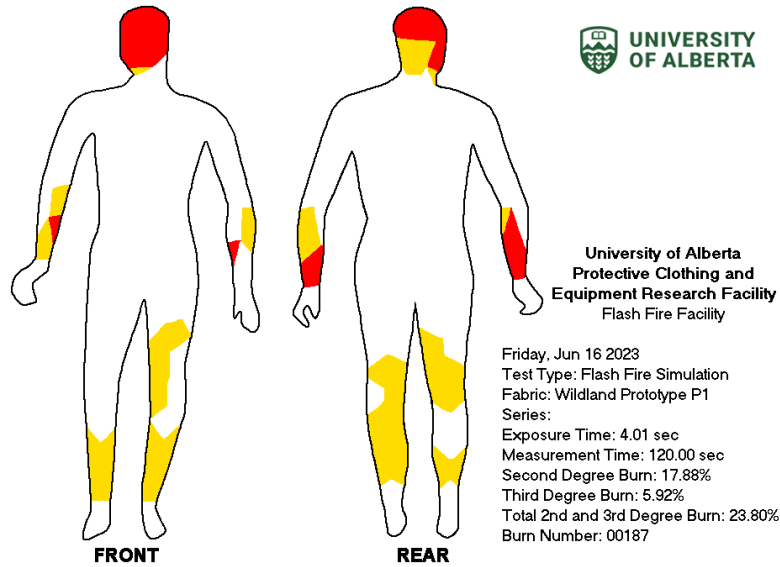


Figure E.14 Burn injury pattern generated by the instrumented manikin system when the garment ensemble with prototype shirt number 1 was engulfed in flames for 4 seconds.

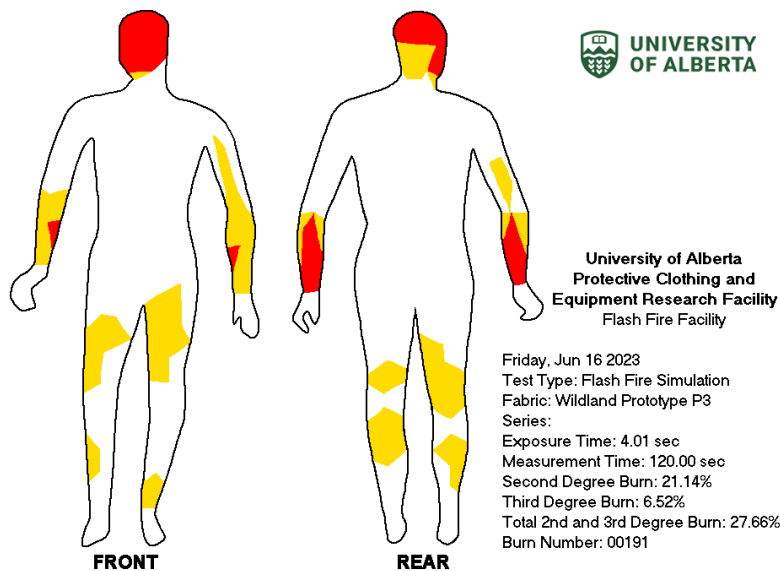


Figure E.15 Burn injury pattern generated by the instrumented manikin system when the garment ensemble with prototype shirt number 3 was engulfed in flames for 4 seconds.

Individual sensor response

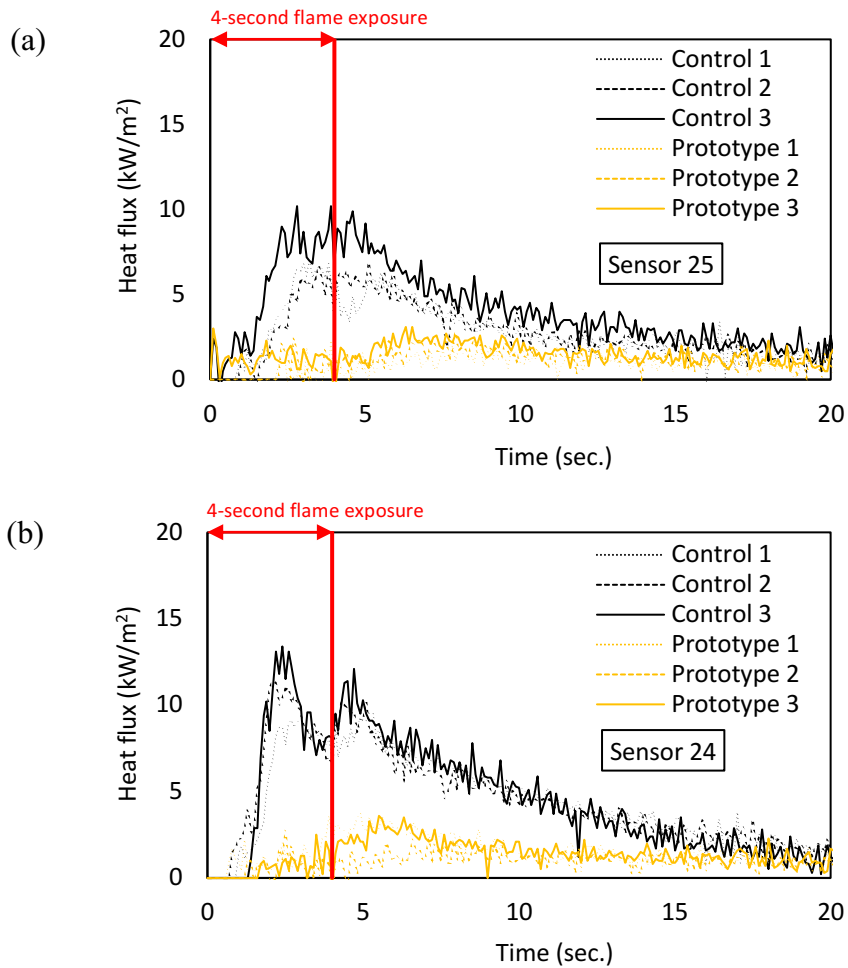


Figure E.16 Heat flux recorded by the skin simulant sensors caused by thermal energy passing through each garment ensemble with the control and prototype shirts in different locations on the upper front torso area of the manikin: (a) left front, and (b) right front.

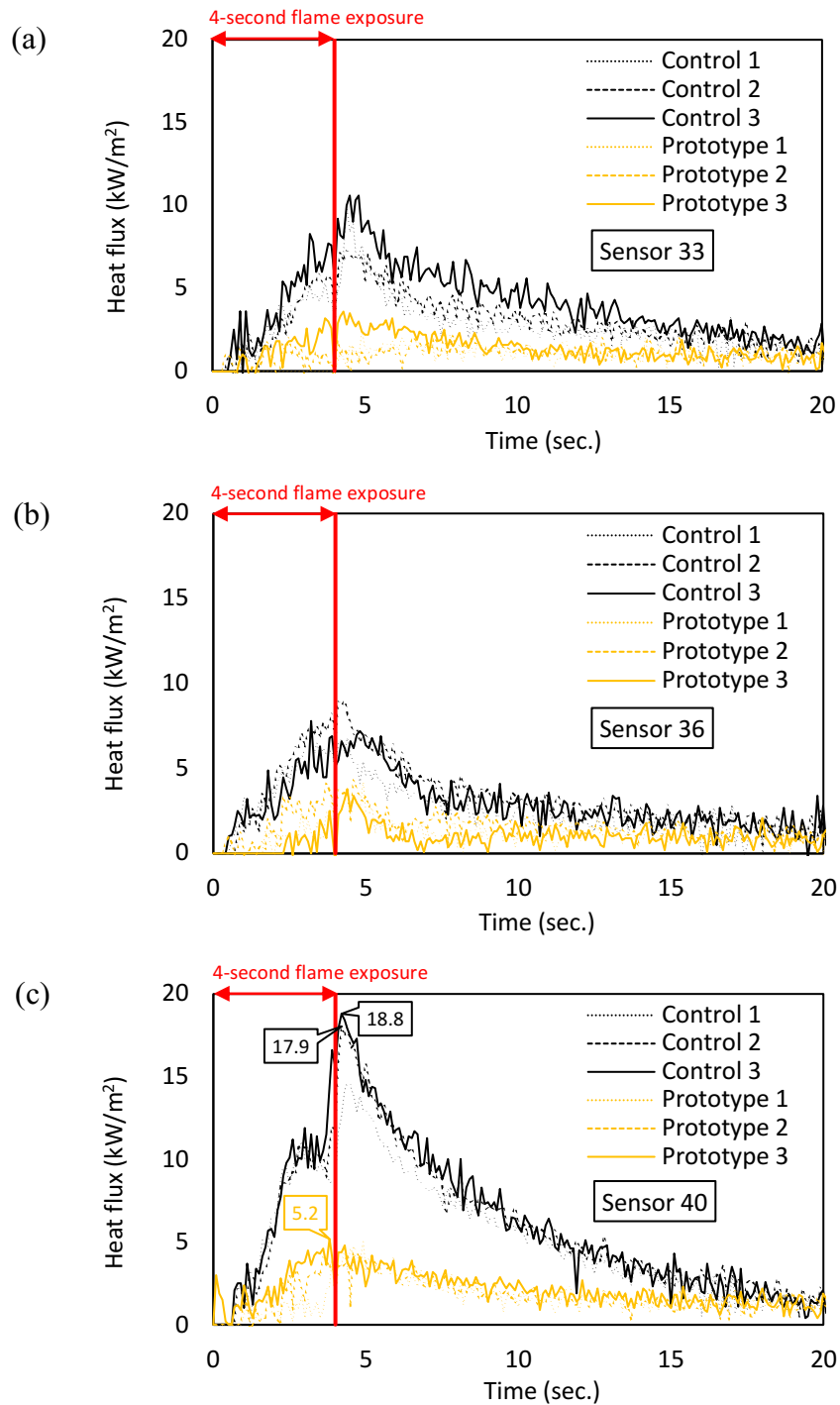


Figure E.17 Heat flux recorded by the skin simulant sensors caused by thermal energy passing through each garment ensemble with the control and prototype shirts in different locations on the upper back torso area of the manikin: (a) left side, (b) back centre, and (c) right side.

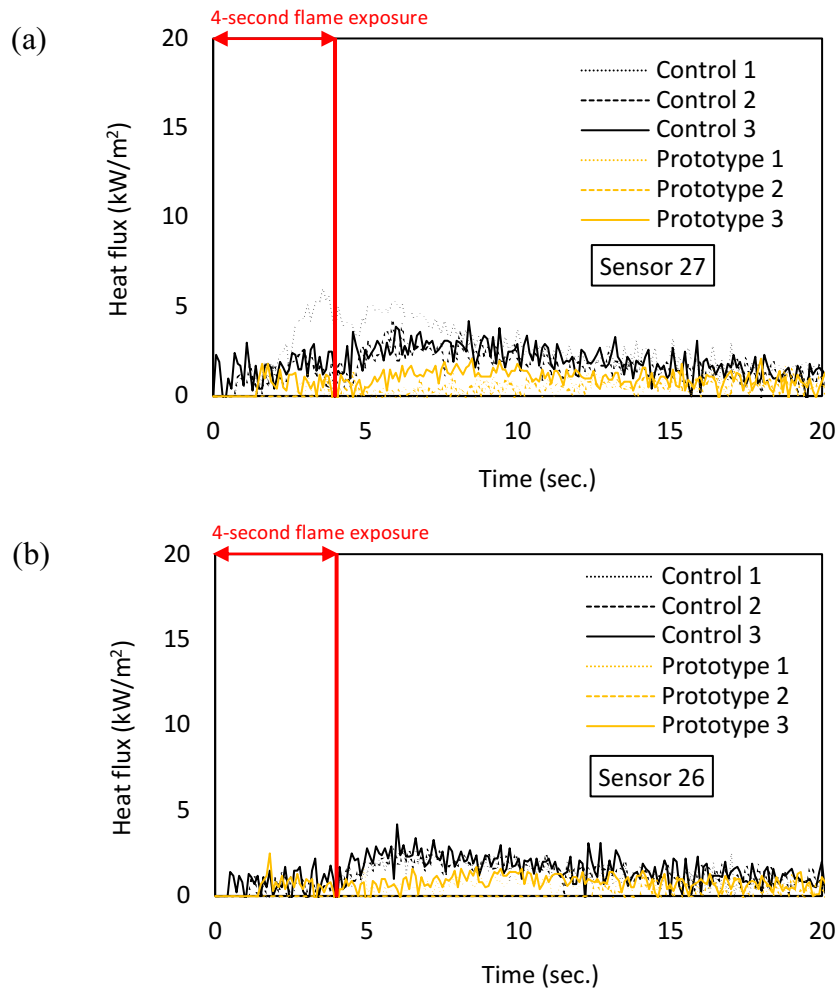


Figure E.18 Heat flux recorded by the skin simulant sensors caused by thermal energy passing through each garment ensemble with the control and prototype shirts in different locations on the shoulder area of the manikin: (a) left side, and (b) right side.

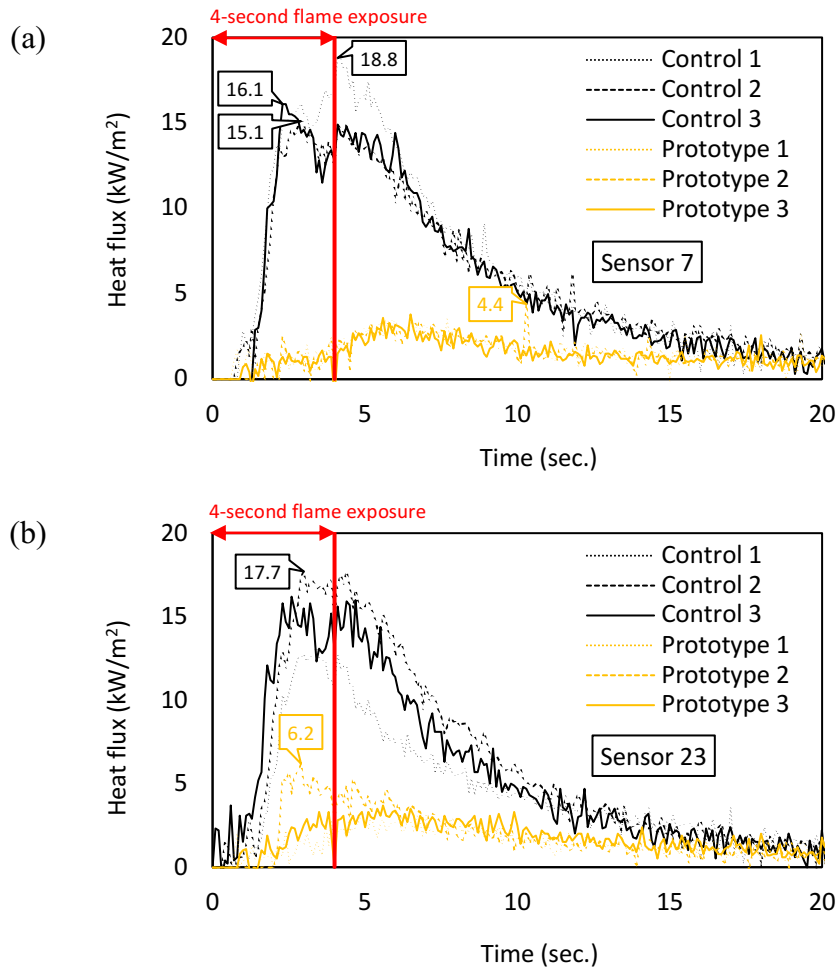


Figure E.19 Heat flux recorded by the skin simulant sensors caused by thermal energy passing through each garment ensemble with the control and prototype shirts in different locations on the upper arm areas of the manikin: (a) left side, and (b) right side.

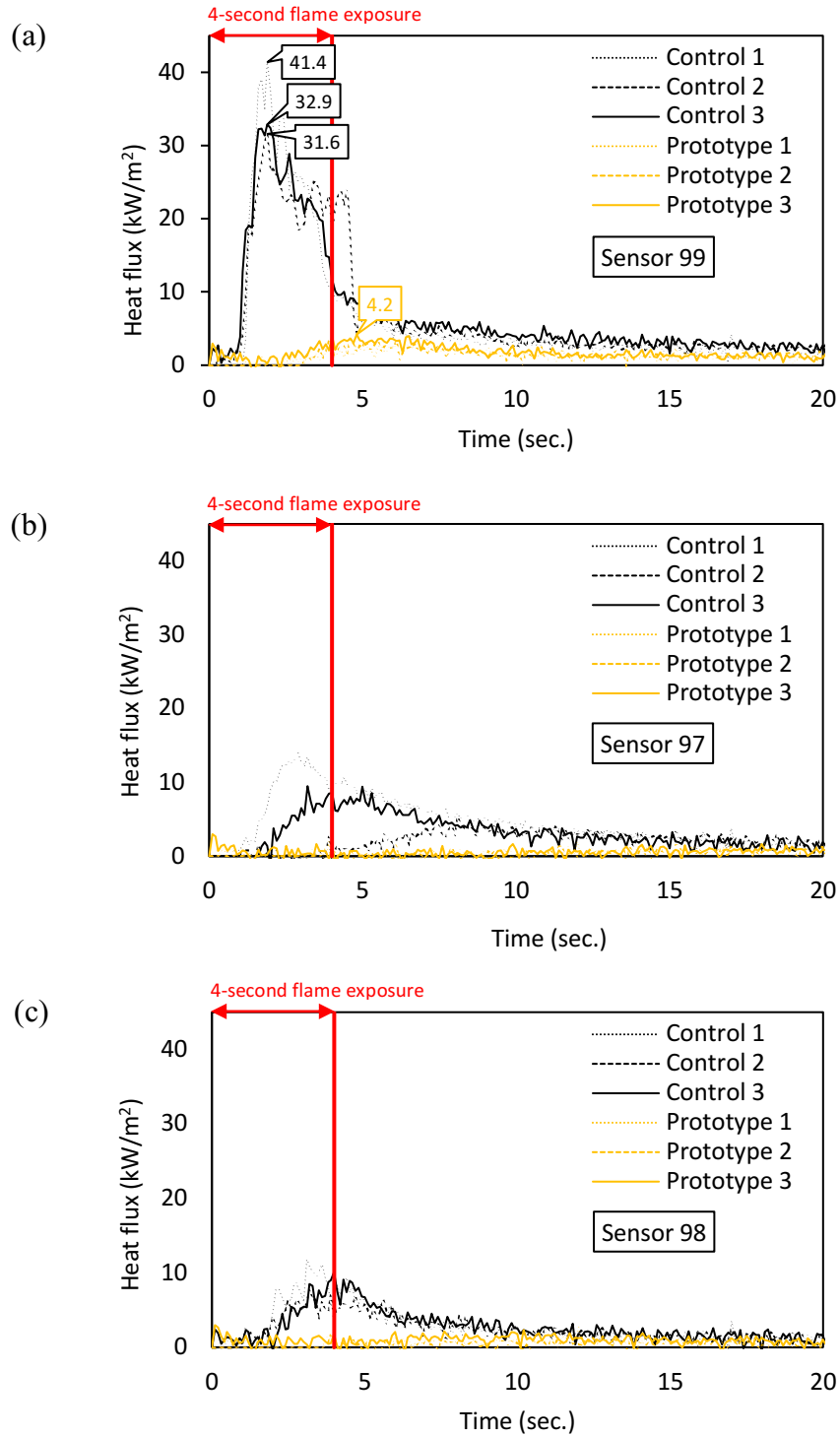


Figure E.20 Heat flux recorded by the skin simulant sensors caused by thermal energy passing through each garment ensemble with the control and prototype shirts in different locations on the neck area of the manikin: (a) left side, (b) back centre, and (c) right side.

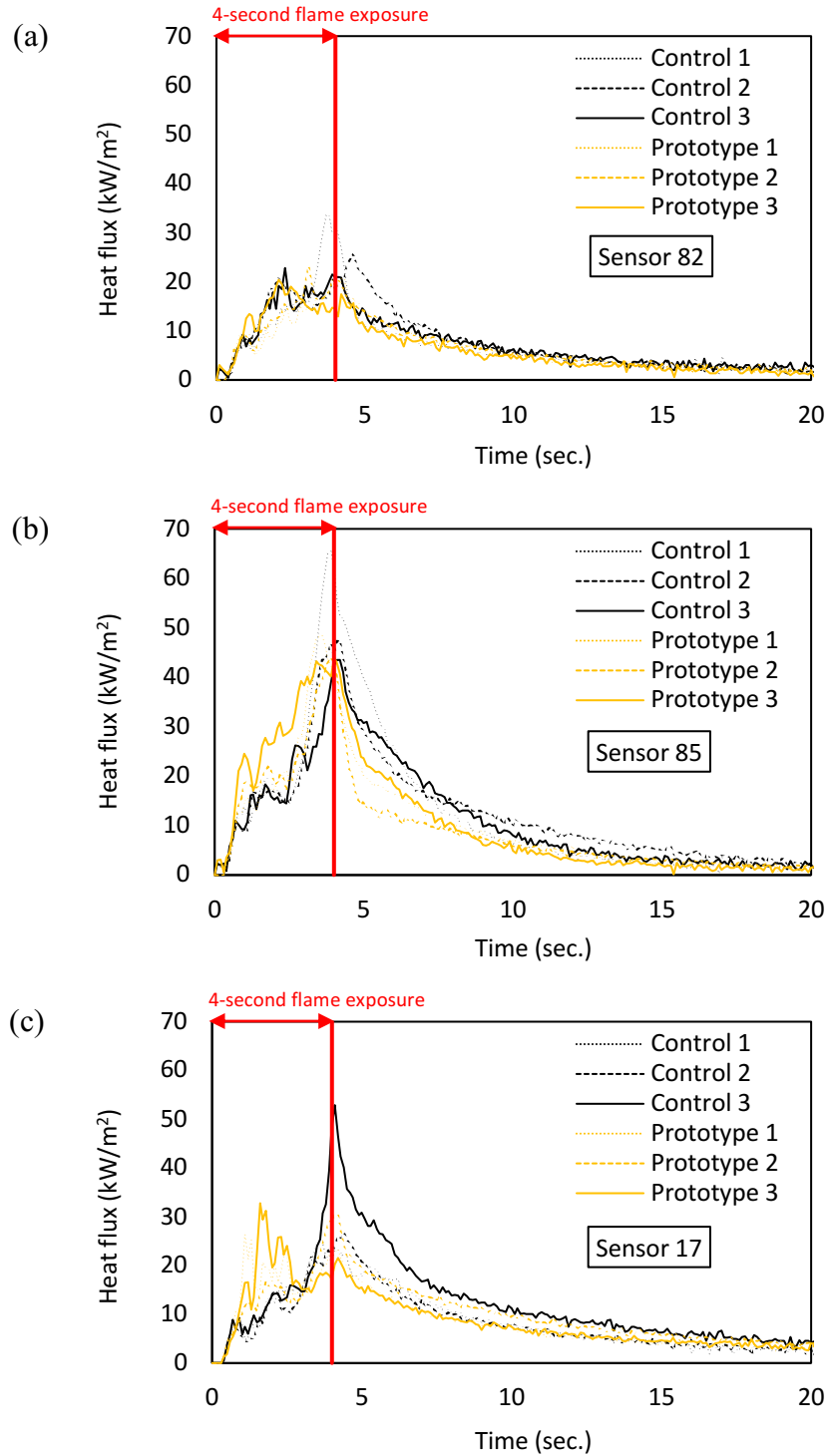


Figure E.21 Heat flux recorded by the skin simulant sensors caused by thermal energy passing through each garment ensemble with the control and prototype shirts in different locations on the right wrist area of the manikin: (a) front, (b) back, and (c) closure.

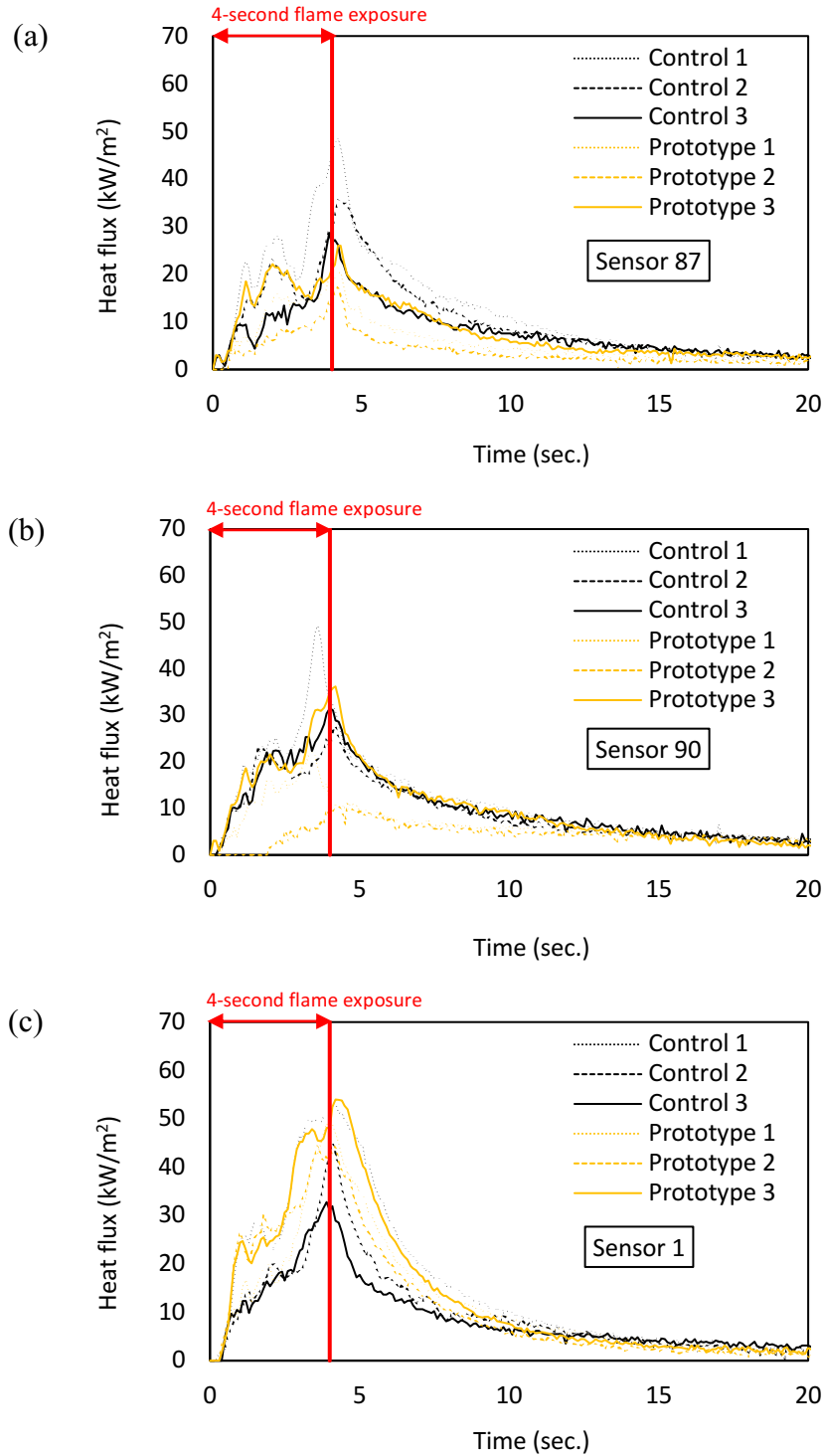


Figure E.22 Heat flux recorded by the skin simulant sensors caused by thermal energy passing through each garment ensemble with the control and prototype shirts in different locations on the left wrist area of the manikin: (a) front, (b) back, and (c) closure.

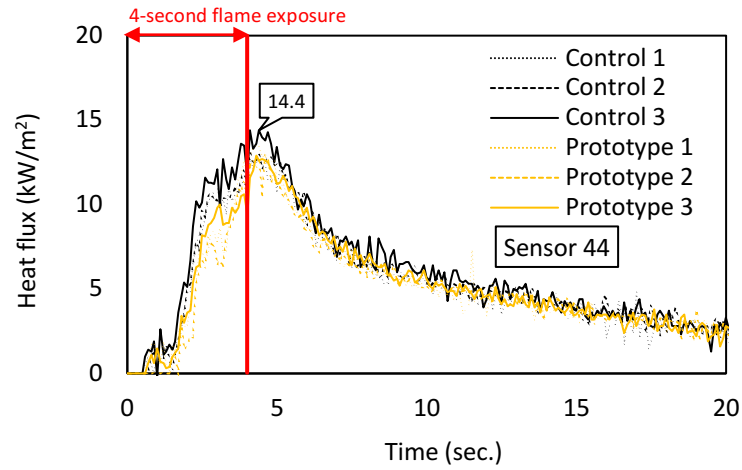


Figure E.23 Heat flux recorded by the skin simulant sensors caused by thermal energy passing through each garment ensemble with the control and prototype shirts in the location on the right chest area of the manikin.

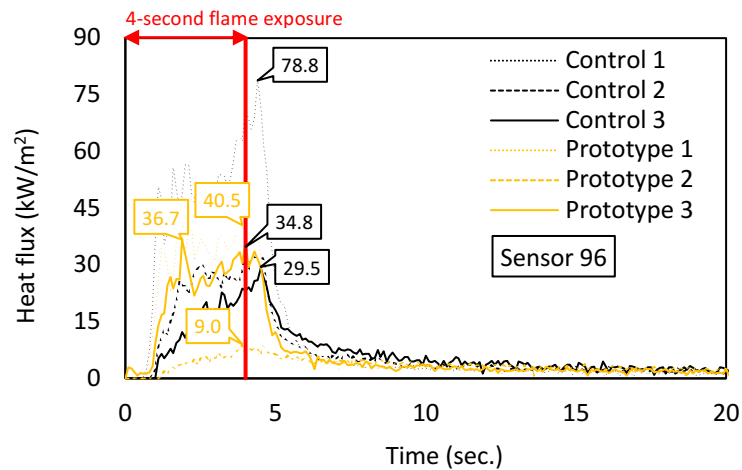


Figure E.24 Heat flux recorded by the skin simulant sensors caused by thermal energy passing through each garment ensemble with the control and prototype shirts in the location on the back neck-head centre area of the manikin.